CRACK SHEAR-SLIP IN

REINFORCED CONCRETE ELEMENTS

by

Derek Lai

A thesis submitted in conformity with the requirements

for the degree of Master of applied science

Graduate Department of Civil Engineering

University of Toronto

Thesis Title: Crack Shear-Slip in Reinforced Concrete Elements

Degree: Master of Applied Science

Year of Convocation: 2001

Full Name: Derek Lai

Name of Graduate Department: Department of Civil Engineering

Name of University: University of Toronto

ABSTRACT

A calculation procedure is developed for estimating crack shear stresses and crack slip displacements from average strain measurements made on reinforced concrete panels. Several series of previously tested panels are examined and crack shear-slip data are extracted. These data are compared against the predictions of previously developed crack slip models.

VecTor2 was used to analyse a series of panels, beams and shear walls subjected to shear and cyclic loads. Comparison with experimental results is made in terms of load-deformation response and ultimate strength. Good agreement with the experimental results is achieved.

Deficiencies in the analytical models are determined. Examples illustrating the similarity between the experimental and analytical results are also presented.

It is shown that rigorously accounting for crack slip displacements results in a better representation of various subtle aspects of behaviour, such as the failure mode and the capacity of elements to deform and redistribute load.

ACKNOWLEDGMENTS

First and foremost, I wish to thank my research supervisor, Professor Frank J. Vecchio, for his expertise, guidance and continuous support during the course of this project. I would like to take this opportunity and express to him all my gratitude.

Having the opportunity I would like to express my appreciation to my girlfriend Winnie for her support and encouragement throughout this endeavor.

Most of all, I wish to express my gratefulness to my family, Kam Chuen, Sau Chun, Cathy and Jessica for their moral support, understanding, and encouragement.

TABLE OF CONTENTS

LIST OF TABLES

LIST OF FIGURES

NOTATION

a = aggregate size

A_s = area of tension reinforcement, input of reinforcement area

B = crack stiffness matrix of the cracked concrete

C_s = influence of slippage on the cracks. $C_s = 0.55$ in the DSFM

$[D_c]$ = concrete stiffness matrices

$[D_s]_i$ = reinforcement stiffness matrices

e_{sh} = strain at the start of strain hardening in the reinforcement

E_c = modulus of elasticity of concrete

E_s = modulus of elasticity of steel

E_{sh} = strain hardening modulus

E_t = tangent modulus of concrete parallel to the crack direction

f'_{cl} = concrete post-cracking tensile stress associated with tension softening

f_{cl} = concrete principal tensile stress

f'_c = concrete cylinder strength

f_p = peak stress

f_{scri} = local reinforcement stresses

f_{si} = average stress

f'_t = concrete tensile strength

f_y = yield strength

f_{yi} = yield stress for the i-th reinforcement component

f_{yx} = yield strength of reinforcement in longitudinal direction

$f_{yy'}$ = yield strength of reinforcement in transverse direction

F = numerical constant = 0.1

F_{exp} = ultimate experimental strength

F_{pre} = predicted lateral load capacity

F_u = ultimate reinforcement stress

F_y = reinforcement yield stress

G = shear modulus for uncracked concrete

G_c = shear modulus of concrete

G_r = fracture energy parameter

L = characteristic length

n = number of reinforcement components

s = crack spacing

T = thickness of the material type

μ = shear retention factor

v_{ci} = crack shear stress

v_{cimax} = maximum crack shear stress

v_{co} = initial shear slip from Walraven test data

w = crack width

X = arbitrary variable

$\sigma_{x'}$ = concrete stress normal to the crack direction

$\sigma_{y'}$ = concrete stress parallel to the crack direction

λ = cracked shear constant

τ^c_{nt} = shear stress

δ_n = normal displacement

δ_s = shear displacement

δ_s^1 = slip displacement

δ_t = tangential displacement

$-\delta^c_n$ = compressive stress

Δ_s^e = experimental crack shear slip

Δ_s^t = theoretical crack shear slip

ε_0 = initial strain

ε_1 = principal tensile strain

ε_c = limit value after which aggregate interlock becomes zero

ε_{c1} = principal tensile strain

ε_{c2} = principal compressive strain

ε_{cx} = average strain in the x-direction

ε_{cy} = average strain in the y-direction

ε_p = peak strain

$\varepsilon_{s_i}^0$ = initial prestrain in the reinforcement

ε_{scri} = local reinforcement strains

ε_{sh} = strain at start of strain hardening

ε_{ts} = terminal strain

ε_u = ultimate strain

ε_x = longitudinal tensile strain

ε_{χ} = transverse tensile strain

$[\varepsilon_c]$ = stress-induced strains

$[\varepsilon^0]$ = elastic strain offsets

$[\varepsilon^p]$ = plastic offsets

$[\varepsilon^s]$ = shear slip strains

ρ_i = reinforcement ratio

ρ_x = reinforcement in x-direction

ρ_y = reinforcement in y-direction

τ = shear stress

γ_s^1 = crack slip shear strain

γ_{cxy} = shear strain

γ_{xy} = normal shear strain

θ_l = constant lag

θ_ε = inclination of principal compressive stress

θ_σ = inclination of principal compressive strain

θ_{ni} = the difference between the angle of orientation of the reinforcement (α_i) and the normal to the crack surface (θ)

α_i = angle of orientation of the reinforcement

CHAPTER 1

Introduction

1.1 Background

Reinforced concrete structures are widely accepted as a rational and economic form of multi-storey construction. In recent years, however, the rapid growth in the size and complexity of such structures has produced a situation in which, if further development is to be made with safety, a greater knowledge of their structural behaviour is necessary.

The complex interactions between the walls, floor slabs, service-cores and frames which comprise a reinforced concrete structure produce a response to loading of substantially greater stiffness and strength than has generally been predictable by approximate design methods. Attempts to apply more sophisticated and accurate methods of analysis have usually been abandoned due to the large amount of computation involved; however, this obstacle is being gradually overcome by the availability and application of more powerful electronic computers with more relevant programs. The need to account for the stiffening and strengthening effects of the interaction between the structural components is becoming increasingly acute with the continual demand to increase the height of new buildings.

In recent years, a growing research effort has been directed at the problems in this field. The subject is still in its infancy, however, and the results that have been published are widely scattered throughout the technical journals of the world. Thus, it appears, a need has arisen to bring together the design, construction, and research engineers concerned with reinforced concrete structures in order to review their existing knowledge, to discuss their outstanding problems, and, by so doing, to stimulate future design and research in this field.

1.2 Modified Compression Field Theory and Disturbed Stress Field Model

The formulation of the Modified compression Field Theory (MCFT) is the result of many years of research effort at the University of Toronto. Essentially, it was an enchancement of the compression field theory (Collins, 1978)) for concrete in shear and torsion. The MCFT (Vecchio and Collins 1982) is a model used for analyzing reinforced concrete subjected to two dimensional stress conditions. The model is based on a smeared crack approach with unique stress-strain relations, in which the cracked concrete is treated as an orthotropic material. The mathematical formulations of MCFT have shown good agreement with experimental results in most cases (Vecchio 1989, Adeghe 1986), and VecTor2 is one of the nonlinear finite element programs which incorporates this model to simulate the material behaviour.

The Disturbed Stress Field Model (DSFM) is an improved model for describing the behaviour of cracked reinforced concrete elements, representing a hybrid formulation between a fully rotating crack model and a fixed crack model. The DSFM builds on the concepts and formulations of the MCFT, treating cracked concrete as an orthotropic material with unique stress-strain relationships in compression and tension. Advancements in the formulation, relative to the MCFT, include a new consideration of the reorientation of the concrete stress and strain fields, removing the restriction that they be coincident, and an improved treatment of shear stresses on crack surfaces. An essential feature of the DSFM is to account for shear slip on crack surfaces in the element

compatibility relations. It is a prime objective of this thesis to investigate and develop improved formulations to model this crack shear-slip behaviour.

1.3 Objective of the study

This research was aimed at improving and corroborating the nonlinear analysis program VecTor2, and the underlying conceptual model DSFM (Disturbed Stress Field Model), with respect to crack slip modelling. More specifically, the objectives are listed as follows:

1. To determine an appropriate rotation lag formulation for the DSFM by investigating data from various concrete test panels.

2. To formulate a crack slip model, which can be incorporated into the analytical model, based on the data from various concrete panels.

3. Corroborate the models for structures under monotonic loading. Panels, beams and shear walls will be analyzed with MCFT and DSFM using various crack slip models.

4. Corroborate the models for structures under cyclic loading. Shear walls will be analyzed with MCFT and DSFM using various crack slip models.

1.4 Program VecTor2

VecTor2 is a two-dimensional nonlinear finite element program for plane stress analysis of reinforced concrete structures. VecTor2 utilizes the formulations of the MCFT and DSFM to model reinforced concrete using a smeared crack approach with unique stress-strain characteristics (Vecchio and Collins 1986).

The computation algorithm involves using a modified secant stiffness formulation in an iterative manner, modifying the calculated material stiffness matrices to reflect the

current state for each element. Iterations are performed until the convergence of the material stiffness matrices is achieved.

VecTor2 reads its input data from three different types of ASCII files (i) job file, (ii) structure file, and (iii) load case files. The user can use any text editor to create or alter these files. The job file allows the user to define the analysis to be performed. The structure file allows the user to input data relating to the structure mesh geometry and material properties. The load file allows the user to input data related to the applied loads.

By typing VT2 in DOS, the program Vector is invoked and the process becomes batch oriented. At this point, the finite element analysis program begins, performs the analysis, writes the results files, and returns to DOS after completing the analysis. To analyze a structure for a number of load stages, the user must make sure that sufficient disk space is available to store the results.

1.5 Chapter Layout

The research work carried out is presented in 7 chapters.

Chapter 2 presents a literature review of the aggregate interlock, shear stress, shear slip models, maximum shear stress formulations, MCFT and DSFM. It provides the background for concepts discussed in following chapters.

Chapter 3 presents the proposed models developed for this research. This chapter is primarily devoted to the derivation of the rotation lag formulations.

Chapter 4 presents the formulation of the shear slip model, based on the computational procedures of Maekawa and Walraven.

Chapter 5 presents the analyses of structures under monotonic loading.

Chapter 6 presents the analyses of structures under cyclic loading.

Chapter 7 presents conclusions derived from the research work and suggestions for future research.

CHAPTER 2

Literature Review

2.1 Introduction

It has long been recognized that cracks in concrete have a significant effect on the mechanical responses of reinforced concrete. The anisotropic properties of cracked reinforced concrete can directly give rise to shear forces in cracks; this is the case, for example, in beams without shear reinforcement, the shear resistance of which relies, for a considerable part, on the resistance of the crack faces to shear displacements (Fenwick, Paulay 1968) See Figure 2.1.

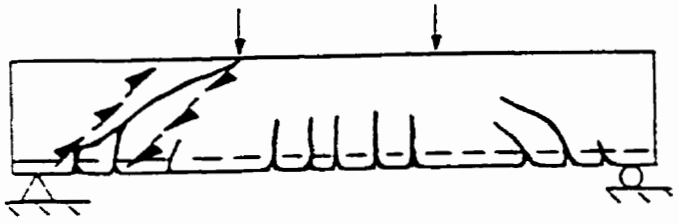

(a) Shear failure of beams.

Figure 2.1

When a crack is developed in a concrete mass, the surfaces of the crack are usually rough and irregular. When this crack forms along a continuous plane, a parallel displacement in this plane is possible and, therefore, projecting particles from one face of the crack come into contact with the matrix of the other face. Further movement is then restricted by the bearing and friction of the aggregate particles on the crack surface. Substantial shear forces can be transmitted across the crack interface. This is aggregate interlock action, and shear displacement (or shear slip) parallel to the direction of the crack is a prerequisite of shear transfer by aggregate interlock (Paulay 1968/1974). Sliding across the cracks is a major cause of shear deformation in reinforced concrete elements. (Soroushian et al. 1988)

There are two ways in which shear displacements may occur. The first is by the flexural rotation of the compression zone between adjacent concrete cantilevers. With this rotation, shear displacements are induced only if the cracks are curved. This is shown in Figure 2.2b, which shows the shear displacement δ_s and the crack width w. The second way in which shear displacements may occur is by bending within the concrete cantilevers, and this displacement is shown in Figure 2.2c.

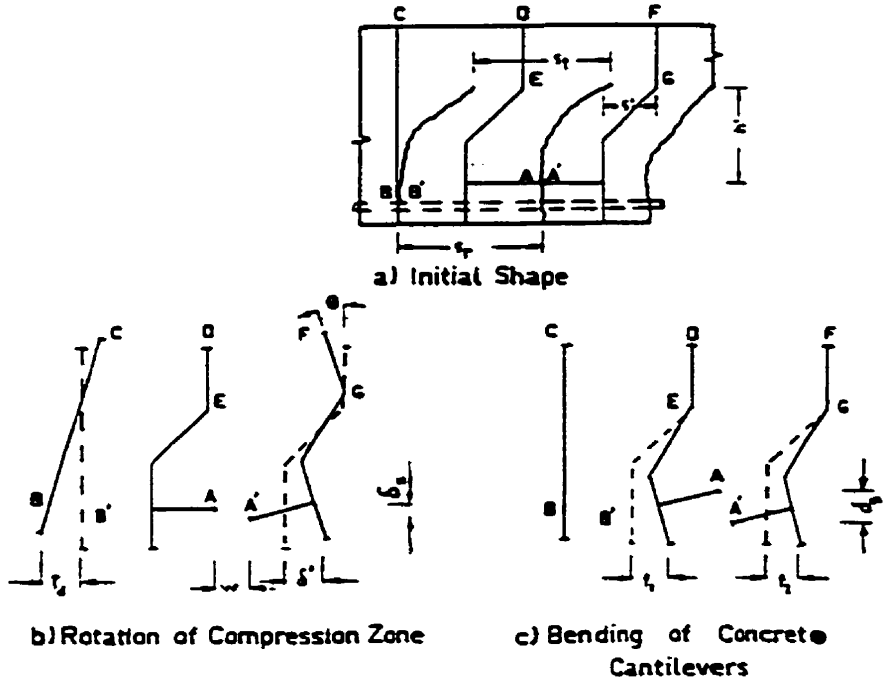

Figure 2.2

For the shear transfer across cracked planes crossed by reinforcement, the two major mechanisms in effect are the dowel action (shearing) of the reinforcement and the aggregate interlock. (Fardis and Buyukozturk 1979)

This chapter will focus on shear displacement (slip) along concrete cracks and aggregate interlock.

2.2 Behavioural Mechanism

When the tangential displacement (shear slip) δ_t occurs along a crack interface, the shear stress τ^c_{nt} working parallel to a crack is induced and is accompanied by the compressive stress $-\delta^c_n$ and the normal displacement δ_n (crack width) normal to the crack plane. These four parameters τ^c_{nt}, δ^c_n, δ_t, δ_n shown in Figure 2.3, thus define the deformational characteristics of a cracked concrete interface (Yoshikawa 1989).

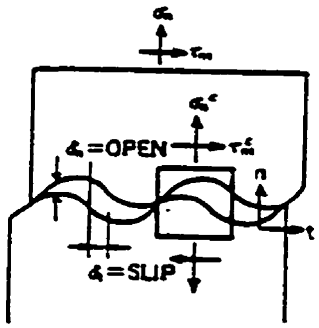

Figure 2.3

Slippage causes the irregular faces of the crack to separate slightly. Tensile stresses created in the rebar, if present, crossing the crack opening, induce clamping forces between the crack faces that in turn develop shear resistance (Fardis and Buyukozturk 1979).

The phenomenon of shear transfer is highly non-linear (Bazant and Gambarova 1980). The non-linear relations among the four parameters are qualitatively shown in Figure 2.4 for the two fundamental stress states, δ_n constant and δ^c_n constant.

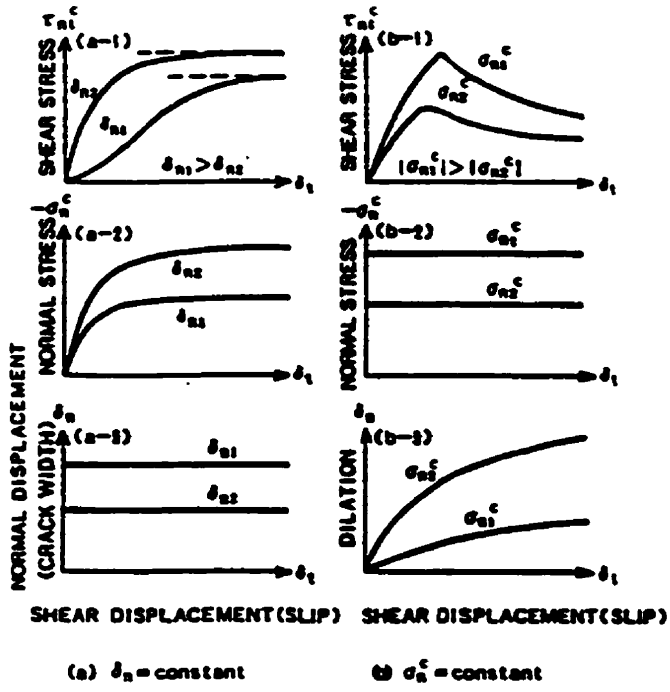

Figure 2.4

In the case where the crack width δ_n is constant, not only the shear stress τ^c_{nt} but also the normal compressive stress $-\delta^c_n$ is generated due to shear slip. Also, if the crack width δ_n is held constant, any relative displacement or slip δ_t between the opposite surfaces of a crack is always accompanied by relative normal displacement (i.e. crack dilatancy). Both phenomena may be called the coupling or cross effect which characterizes the mechanical behaviour of concrete with cracks (Yoshikawa 1989).

2.3 Brief description of the Models

In the past 20 to 25 years, quite a number of approaches have been introduced to model the effect of aggregate interlock and shear slip. Some of these approaches include:

(i) Reducing or modifying the shear modulus in the material crack stiffness matrix

-Lin and Scordelis 1975, Cedolin and Dei Poli 1977, Hu and Shnobrich 1990

(ii) The Rough Crack Model, which considers the crack faces as rough with stiff trapezoidal asperities.

-Bazant and Gambarova 1980

-Gambarova and Karakoc (improved) 1983

-Dei Poli, Prisco, and Gambarova (application) 1987, 1990, 1995 (model)

(iii) Two Phase Model

-Walraven and Reinhardt 1981, 1995

2.4 Reduction or Modification of Shear Modulus

Lin and Scordelis (1975) posed the following material property assumption for the cracked stiffness:

$$\begin{Bmatrix} \sigma_{x'} \\ \sigma_{y'} \\ \tau_{x'y'} \end{Bmatrix} = \begin{bmatrix} Ec & 0 & 0 \\ 0 & 0 & 0 \\ 0 & 0 & \lambda G \end{bmatrix} \begin{Bmatrix} \varepsilon_{x'} \\ \varepsilon_{y'} \\ \gamma_{x'y'} \end{Bmatrix} \tag{2.1}$$

in which x' and y' are parallel and perpendicular, respectively, to the cracks; G is the shear modulus for uncracked concrete; and λ is a cracked shear constant introduced to estimate the effective shear modulus due to dowel action and aggregate interlock.

Cedolin and Dei Poli, with a "smeared" representation of cracking and aggregate interlock action, tried to predict shear failures of beams through a finite element model. Crack propagation was taken into account by identifying the mechanism that sustains the load inside the cracked element and modifying accordingly its material matrix. Once the limiting value of tensile strain was reached, the element was considered unable to sustain any normal stresses in that direction. This method was used because it was simple but it gave rise to cracked regions rather than discrete cracks, which are not able to reproduce the capability of concrete between the cracks in carrying some stress; that is, tension stiffening effects. The authors noted that a gradual release of the normal stress in the direction normal to the crack could be done however. With this representation of cracking, the authors found that the only way to represent aggregate interlock was to give an appropriate value to the shear modulus G, in the material matrix. The authors posed

that a variation of G decreasing with the crack width was closest to the physical phenomenon. A simple linear dependence was assumed because of the lack of data:

$$G = F\left(1 - \frac{\varepsilon_1}{\varepsilon_0}\right); \qquad 0 \le \varepsilon_1 \le \varepsilon_c \tag{2.2}$$

$$G = 0; \qquad \varepsilon_1 \ge \varepsilon_c \tag{2.3}$$

F – numerical constant=0.1

ε_t – fictitious strain in the direction normal to the crack

ε_c – limit value after which aggregate interlock becomes zero

Hu and Schnobrich (1990) posed a nonlinear model for cracked reinforced concrete subjected to in plane shear and normal stresses. The model included the smeared crack representation, rotating crack approach, tension stiffening, stress degrading effect for concrete parallel to the crack direction, and shear retention of concrete on the crack surface. To take the shear stiffness of cracked concrete into account in the smeared crack model, a reduced shear modulus μG_c was used (with $0<\mu<1$). The corresponding material stiffness matrix is:

$$[C'] = \begin{bmatrix} 0 & 0 & 0 \\ 0 & E_t & 0 \\ 0 & 0 & \mu G_c \end{bmatrix} \tag{2.4}$$

where E_t is the tangent modulus of concrete parallel to the crack direction; G_c is the shear modulus of concrete; and μ is the shear retention factor. By implementing tension stiffening and shear retention effects, the matrix had the following form:

$$[C]_r = [T(\theta)]^T [C'][T(\theta)] + [G] \tag{2.5}$$

$$[T(\theta)] = \begin{bmatrix} c^2 & s^2 & sc \\ s^2 & c^2 & -sc \\ -2sc & 2sc & c^2 - s^2 \end{bmatrix} \qquad c = \cos\theta, s = \sin\theta \tag{2.6}$$

$$[G] = \frac{(\sigma_{x'} - \sigma_{y'})\cos^2 2\theta}{2(\varepsilon_x - \varepsilon_y)} \begin{bmatrix} s^2 & -s^2 & -sc \\ -s^2 & s^2 & sc \\ -sc & sc & c^2 \end{bmatrix} \qquad c = \cos 2\theta, s = \sin 2\theta \tag{2.7}$$

$\sigma_{x'}$ and $\sigma_{y'}$ are the tension-stiffening stress normal to the crack direction and the concrete stress parallel to the crack direction, respectively; θ is measured counterclockwise from the global x-axis to crack x'-axis.

In the above models, it seems that a true representation of what is going on at the crack interface is not provided, i.e. friction, normal stress, wedging action, etc. The reduction or variation of the shear modulus G is used to account for the aggregate interlock but each model seems to discount any major effect that aggregate interlock may have – i.e. choosing shear modulus reduction factors or shear retention factors just to stabilize the analysis and/or to maintain some non-zero value of shear stiffness in the matrix. It appears that Cedolin and Dei Poli were on the right track by mentioning the effect of increasing crack width on the shear stiffness.

2.5 Rough Crack Model

The crack faces are assumed to be rough, with trapezoidal asperities. The goal of the researchers, Bazant and Gambarova, was to focus on monotonic loading, and primarily on situations in which the failure occurs by tensile yielding of the reinforcement rather than compression or shear of the concrete (Bazant and Gambarova 1980).

Bazant and Gambarova (1980), posed the constitutive equations for a single crack considered by Walraven:

$$\begin{Bmatrix} d\sigma_{nn}{}^{c} \\ d\sigma_{nt}{}^{c} \end{Bmatrix} = \begin{bmatrix} B_{nn} B_{nt} \\ B_{tn} B_{tt} \end{bmatrix} \begin{Bmatrix} d\delta_n \\ d\delta_t \end{Bmatrix} \tag{2.8}$$

$$\sigma_{nn}{}^{c} = f_n(\delta_n, \delta_t);\ \sigma_{nt}{}^{c} = f_t(\delta_n, \delta_t) \tag{2.9}$$

$$B_{nn} = \partial f_n/\partial\delta_n,\ B_{nt} = \partial f_n/\partial\delta_t,\ Bt_n = \partial f_t/\partial\delta_n,\ B_{tt} = \partial f_t/\partial\delta_t \tag{2.10}$$

Some of the properties and assumptions of the Rough Crack model are:

i) Finite slip is impossible at zero relative normal displacements. The stress displacement relations for a rough crack exhibit a singularity at the initial state of zero relative displacements.

   i.e. $d\delta_t/d\delta_n = 0$ for $\delta_n = 0$

ii) The incremental stiffness matrix of cracked concrete is nonsymmetric and does not give parallel axes of stress and strain increments because a coupling of shear and normal component is present.

iii) When there is zero slip and a crack exists there is no compressive force on the crack face (i.e. for $\delta_t = 0$ and $\delta_n > 0$ we must have $\sigma_{nn}^c = 0$ because the crack surfaces cannot be in contact).

iv) For δ_t constant (constant slip), and increasing δ_n, the number of contact points decreases. Also, $|\sigma_{nn}^c|$ and $|\sigma_{nt}^c|$ must decrease as the opening increases, i.e.,

$$\frac{\partial|\sigma_{nn}^c|}{\partial\delta_n} = B_{nn} < 0; \frac{\partial|\sigma_{nt}^c|}{\partial\delta_n} = B_{tn} < 0; \qquad for \delta_t > 0 \tag{2.11}$$

Thus, the crack stiffness matrix is never positive definite, except for dt = 0. So, the crack response causes a tendency for instability; the response, however, is usually stabilized by the restraint provided by the reinforcement and the boundary conditions (Because $B_{nn} < 0$, and because B_{nt} and B_{tn} must be expected to be non-zero, the stress-displacement relations cannot be modelled by springs, not even nonlinear ones).

v) For δ_n constant (constant crack width), δ_t increases and Bnt > 0 and Btt > 0,

$$\frac{\partial|\sigma_{nn}^c|}{\partial\delta_t} = B_{nt} > 0; \frac{\partial|\sigma_{nt}^c|}{\partial\delta_t} = B_{tt}; \qquad for \delta_n > 0 \tag{2.12}$$

unless it slips so much and crack-teeth break off.

The following interface stresses were derived by Bazant and Gambarova (1980);

$$\sigma_{nn}^c = -\frac{a_1}{\delta_n}(a_2|\sigma_{nt}^c|)^p \qquad \sigma_{nt}^c = \tau_u r \frac{a_3 + a_4|r|^3}{1 + a_4 r^4} \tag{2.13}$$

$$r = \frac{\delta_t}{\delta_n} \qquad \tau_u = \tau_0 \frac{a_0}{a_0 + \delta_n^2} \tag{2.14}$$

$$p = 13.0\left(1 - \frac{0.231}{1 + 0.185\delta_n + 5.63\delta_n^2}\right) \tag{2.15}$$

$$\delta_n \geq 0 \quad a_0 = 0.01 D_a^2 \quad a_1 = 0.000534 N/mm \quad a_2 = 145 mm^2/N$$

$$a_3 = \frac{1}{\tau_0} 2.45 N/mm^2 \quad a_4 = 2.44\left(1 - \frac{1}{\tau_0} 4 N/mm^2\right); \qquad \tau_0 = 0.245 f'c$$

The formulations were updated by Karakoc and Gambarova (1987) as follows:

$$\sigma_{nn}{}^{c} = 0.62\frac{\delta_t}{(\delta_t{}^2 + \delta_n{}^2)^{0.25}}\sigma_{nt}{}^{c} \tag{2.16}$$

$$\sigma_{nt}{}^{c} = \tau_0\left(1-\sqrt{\frac{2\delta_n}{D_{max}}}\right)\frac{a_1 + a_2|r|^3}{1+a_2 r^4} \tag{2.17}$$

$\tau_0 = 0.25 f'c \quad a_1 = 2.45/\tau_0 \quad a_2 = 2.44(1\text{-}4/\tau_0)$

With the updated formulation, for evaluating confinement stress in terms of the shear stress, assuming the influence of shear slip, δ_t, is so dominant that the contribution of the crack opening, δ_n, can be neglected, $\sigma_{nn}{}^{c}$ can be expressed (very simplified),

$$\delta_{nn}{}^{c} = C_1(\delta_t)^{0.5} \tag{2.18}$$

$C_1 = 0.55$ to compensate for the disregard of δ_n. This simplified formulation can be used for predicting the results of test carried out at constant crack opening.

The equation (2.16) above predicts, when compared to experiments, for varying values of both d_n and δ_t, slightly lower values for confinement stress for lower values of the shear slip while it gives slightly higher values of δ_{nn} for considerable higher values of δ_t. This is because of the physical difference of the cracks kept at constant d_n when compared to the real situation (both δ_n and δ_t varying). When the δ_n is constant, after the engagement of the interface asperities, because of the initial dominant wedging action of the protruding particles, larger confinement stress is induced for smaller values of shear slip, as the crack width is not allowed to increase. However, as δ_t assumes larger values, the wedging action tends to lose its impact especially as the smaller and weaker asperities break off and become even (instead of sliding over one-another) again because δ_n is not allowed to increase; so, comparatively smaller δ_{nn} values are to be expected.

To account for this physical different behaviour,

$$\delta_{nn} = C_2(\delta_t)^{0.25}\sigma_{nt} \qquad C_2 = 0.75 \tag{2.19}$$

For a media characterized by parallel, regular and closely spaced cracks, the constitutive laws of the material may be obtained from the stress-displacement relations for the crack interface if the crack opening and the shear slip are smeared (i.e. continuously distributed). The relations between σ_{nn}, σ_{nt}, δ_n and δ_t can be expressed as previously noted:

$$\begin{Bmatrix} d\sigma_{nn}{}^{c} \\ d\sigma_{nt}{}^{c} \end{Bmatrix} = \begin{bmatrix} B_{nn} B_{nt} \\ B_{tn} B_{tt} \end{bmatrix} \begin{Bmatrix} d\delta_n \\ d\delta_t \end{Bmatrix} \tag{2.20}$$

Similarly, the incremental stress vector can be expressed in terms of the incremental strain vector as in the general form,

$$d\sigma = B d\varepsilon \tag{2.21}$$

B is the crack stiffness matrix of the cracked concrete.

A significant aspect of such formulations of interface stresses acting on the interface of a crack in a reinforced or plain concrete element in terms of the related displacement is that they can be used to express and update the constitutive laws of the concrete at each increment of load, and consequently can be employed in application especially as far as numerical methods such as the finite element method is concerned. Another application of the rough crack model follows.

Application to Thin-webbed Beams in Shear

In 1995, Prisco and Gambarova posed a model for the study of shear in thin-webbed reinforced and prestressed concrete beams. The limit analysis model was based on full yielding of the stirrups and impending collapse in shear compression for the inclined concrete struts on a fixed crack pattern. The rough crack model was adopted for aggregate interlock from studies by DeiPoli, Gambarova and Karakoc (1987) and Dei Poli, Prisco, and Gambarova (1990).

After the formation of diagonal cracks, a beam tends to behave like a plane truss: the longitudinal bars and the stirrups constitute the tension members, while the top flange and the inclined struts in the web are the compression members.

Some of the assumptions adopted were:

i) The faces of the inclined cracks are rough and interlocked; consequently, shear and normal stresses are transferred across the crack interface

ii) The average stress field in the web consists of a diagonal compression field, which is not aligned with the fixed cracks.

The aggregate interlock constitutive laws, in a slightly different format than previously presented in this thesis, from Karakoc are,

$$\sigma_{nn}{}^{c} = a_1 a_2 \frac{r}{\left(1+r^2\right)^{0.25}} \sqrt{\delta_n} \sigma_{nt}{}^{c} \tag{2.22}$$

$$\sigma_{nt}^{c} = \tau_0\left(1-\sqrt{\frac{2\delta_n}{D_{max}}}\right)r\frac{a_3+a_4|r|^3}{1+a_4r^4} \qquad (2.23)$$

$\tau_0 = 0.25f'c$ $\quad a_1a_2 = 0.62$ $\quad a_3 = 2.45/\tau_0$ $\quad a_4 = 2.44(1\text{-}4/\tau_0)$ $\quad r = \delta_t/\delta_n$

From these equations, it was found that the aggregate interlock contribution to the ultimate shear stress was,

$$\Delta\tau = \tau_0\left(1-\sqrt{\frac{2\delta_n}{D_{max}}}\right)r\frac{a_3+a_4|r|^3}{1+a_4r^4}\left(1-a_1a_2\frac{r}{(1+r^2)^{0.25}}\sqrt{\delta_n}\cot\phi\right) \qquad (2.24)$$

A simplified formulation with range of r between 0.6 - 1.0, D = 20, $\phi = \pi/4$ reduced the equation as follows:

$$\frac{\Delta\tau}{f'c} = 0.25r\frac{a_3+a_4|r|^3}{1+a_4r^4}\left(1-0.912\sqrt{\delta}+0.199\delta\right) \qquad (2.25)$$

2.6 The Two-Phase Model

The theory is based on the assumption that concrete can be conceived as a "two-phase" material which is composed of a collection of aggregate particles with high strength and stiffness (phase1), and a matrix material consisting of hardened cement paste with fine sand with lower strength and stiffness (phase 2), (Walraven and Reinhardt 1981). When the crack faces are subjected to a shear displacement, a wedging action is developed resulting in compressive stresses normal to the crack plane. Wedging action provides the link between normal and shear stresses on one hand, and crack opening and shear displacement (slip) on the other hand. The mechanism, according to Walraven, could only be adequately described if normal stress, shear stress, crack width, and shear displacement (slip) are all involved.

The theory of the stress-displacement relations for rough cracks was mentioned previously in this thesis when Bazant and Gambarova's model (1980) was described. Recall,

$$\begin{Bmatrix} d\sigma_{nn}^{c} \\ d\sigma_{nt}^{c} \end{Bmatrix} = \begin{bmatrix} B_{nn} & B_{nt} \\ B_{tn} & B_{tt} \end{bmatrix}\begin{Bmatrix} d\delta_n \\ d\delta_t \end{Bmatrix}$$

B_{nn}, B_{nt}, B_{tn}, B_{tt} are crack stiffnesses; δ_n is the crack opening; δ_t is the crack slip; σ_{nn}^{c} is the normal stress; and σ_{nt}^{c} is the shear stress.

These stress-displacement relations are analogous to stress-strain relations of incremental plasticity; they will give in general a path-dependent response which is expected in inelastic behaviour.

The formulation above was simplified to a less general formulation:

$$\sigma_{nn}^{c} = f_n(\delta_n, \delta_t); \; \sigma_{nt}^{c} = f_t(\delta_n, \delta_t) \tag{2.26}$$

which is analogous to the total strain (total deformation) theory of plasticity. It gives a response that is independent of the loading path in the (δ_n, δ_t) plane. It is assumed that the shear stress and normal displacement are functions only of the normal stress and shear displacements (only monotonic increase is considered). The crack stiffness coefficients are:

$$B_{nn} = \partial f_n/\partial \delta_n, \; B_{nt} = \partial f_n/\partial \delta_t, \; Bt_n = \partial f_t/\partial \delta_n, \; B_{tt} = \partial f_t/\partial \delta_t \tag{2.27}$$

The basic problem is the formulation of $\sigma_{nn}^{c} = f_n(\delta_n, \delta_t); \; \sigma_{nt}^{c} = f_t(\delta_n, \delta_t)$.

Walraven's fundamental model was developed based on a statistical analysis of the crack structure and associated contact areas between the crack faces as a function of the displacements δ_n and δ_t. Aggregate particles were simplified as spheres, which could be intersected by the crack plane at all depths with the same probability (see Figure 2.5).

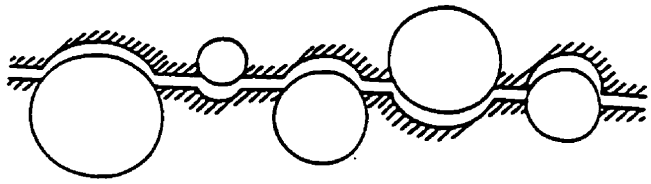

Figure 2.5

Since plastic deformations are expected to predominate (because of pore-volume reduction) over the elastic deformations, the stress-strain relation of the matrix material, consisting of hardened cement paste with aggregate particle < 0.25 mm, is assumed rigid plastic. The stress at which plastic deformation occurs is σ_{pu}. In Figure 2.6, a line of contact between opposite crack faces is shown. The projections of this line of contact on the X- and Y- directions are a_x and a_y. The shaded area represents that part of the matrix which has disappeared due to plastic deformation of the matrix. If the shear load on the plane of cracking is increased and crack opening is counteracted by restraining forces a mechanism will develop which can be described as follows: The contact areas tend initially to slide; as a result of sliding, the contact area is reduced so that too high contract

stresses occur. Hence, further plastic deformation occurs, until equilibrium of forces are obtained in the X- and Y- directions.

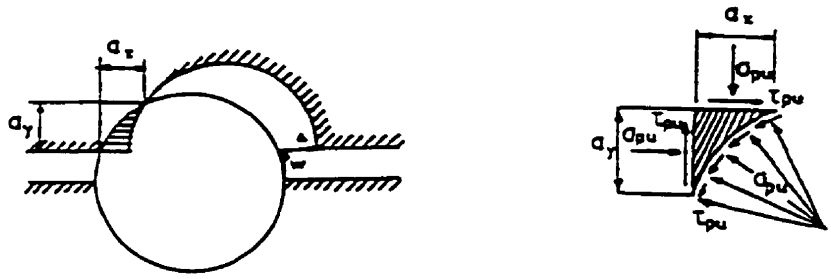

Figure 2.6

Briefly, the equilibrium conditions are:

$$\tau_{pu}=\mu\sigma_{pu} \tag{2.28}$$

$$\sum Fx = \sigma_{pu}\sum \bar{a}_y + \tau_{pu}\sum \bar{a}_x \tag{2.29}$$

$$\sum Fy = \sigma_{pu}\sum \bar{a}_x - \tau_{pu}\sum \bar{a}_y \tag{2.30}$$

where τ_{pu} is the shear stress at deformation of matrix;

Σa_x, Σa_y are the most probable average projected contact lengths over the crack length;

surface stresses are given by:

$$\sigma = \sigma_{pu}\left(\bar{A}_x - \mu\bar{A}_y\right) \tag{2.31}$$

$$\tau = \sigma_{pu}\left(\bar{A}_y + \mu\bar{A}_x\right) \tag{2.32}$$

where Ax, Ay are the most probable contact areas (= Σ(a)(l)).

Note: Quite an extensive analysis was done by the author to determine the values for Ax and Ay using statistical analysis; the final results will be presented here.

The interface stresses, proposed by Walraven and Reinhardt are:

$$\sigma_{nn}^{\ c} = -\frac{f_{cc}}{20}\left\{1.35\delta_n^{\ -0.63} + \left(0.191\delta_n^{\ -0.552} - 0.15\right)f_{cc}\right\}\delta_t \tag{2.33}$$

$$\sigma_{nt}^{\ c} = -\frac{f_{cc}}{30}\left\{1.8\delta_n^{\ -0.80} + \left(0.234\delta_n^{\ -0.707} - 0.20\right)f_{cc}\right\}\delta_t \tag{2.34}$$

where fcc is the concrete cube strength.

The model is based on the behaviour on particle level, taking into account the deformation of the hardened cement matrix and frictional forces between aggregate particles and matrix during sliding.

The Two-Phase model is the basis for the derivation of shear stress on crack surfaces for the Modified Compression Field Theory (Vecchio and Collins, 1986). In the MCFT, cracked concrete is treated as a new material with its own stress-strain relationships which are formulated in terms of average stresses and strains. Discrete cracks are considered by considering the local stress conditions at crack locations. Equilibrium requires shear stresses on a crack.

Based on Walraven's work, the following relationship was derived for shear stress on a crack (see Figure 2.7):

$$v_{ci} = 0.18 v_{ci\max} + 1.64 f_{ci} - 0.82 \frac{f_{ci}^{\,2}}{v_{ci\max}} \qquad (2.35)$$

$$\text{where } v_{ci\max} = \frac{\sqrt{-f'c}}{0.31 + \dfrac{24w}{(a+16)}}$$

where v_{ci} is the shear stress acting on the crack; v_{cimax} is the maximum shear stress that can be resisted on the crack; f_{ci} is the compressive stress on crack surface; f'c is the specified compressive strength of concrete; w is the average crack width (mm) and a is the aggregate size in millimeters.

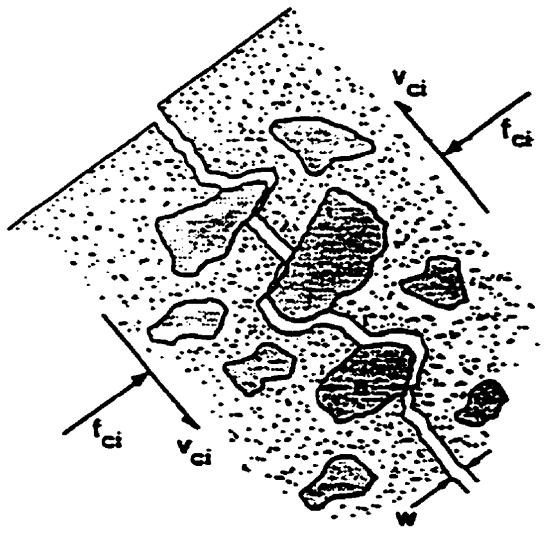

Figure 2.7

2.7 Modified Compression Field Theory

One of the simplifying assumption made by the MCFT is that the principal stress axes and principal strain axes coincide, or, the inclination of the cracks, θc, is equal to the inclination of the stress field, θ. In Figure 2.8(a), a comparison is shown. The data from the initial test series clearly showed that this was strictly not the case. The observed tendency was for the change in the principal stress direction to lag behind the change in the principal strain direction. Shown in Figure 2.8(b) are the angles of inclination for the stress and strain fields for Panel PV19. Prior to cracking, both fields were inclined at 45 degrees relative to the reinforcement directions. After first crack, there was an abrupt increase in the orientation of the principal strain direction but little change in the concrete stress field direction. Thereafter, both inclinations gradually moved higher, with a more or less constant difference (lag) between the two. After yielding of the transverse reinforcement, the reorientation of the stress field accelerated, with the inclination of the principal stresses following the pattern of the change in the principal strain direction. This behaviour was observed in most of the other test panels. Given that the pattern was one where the reorientation of directions of stress and strain seemed to be linked and not much different, and given the significant simplification it added to the computational aspects of the theory, it was decided to make the assumption that $\theta=\theta c$. It is this assumption that, in large part, gives rise to the inaccuracies of the MCFT for very lightly reinforced beams or elements.

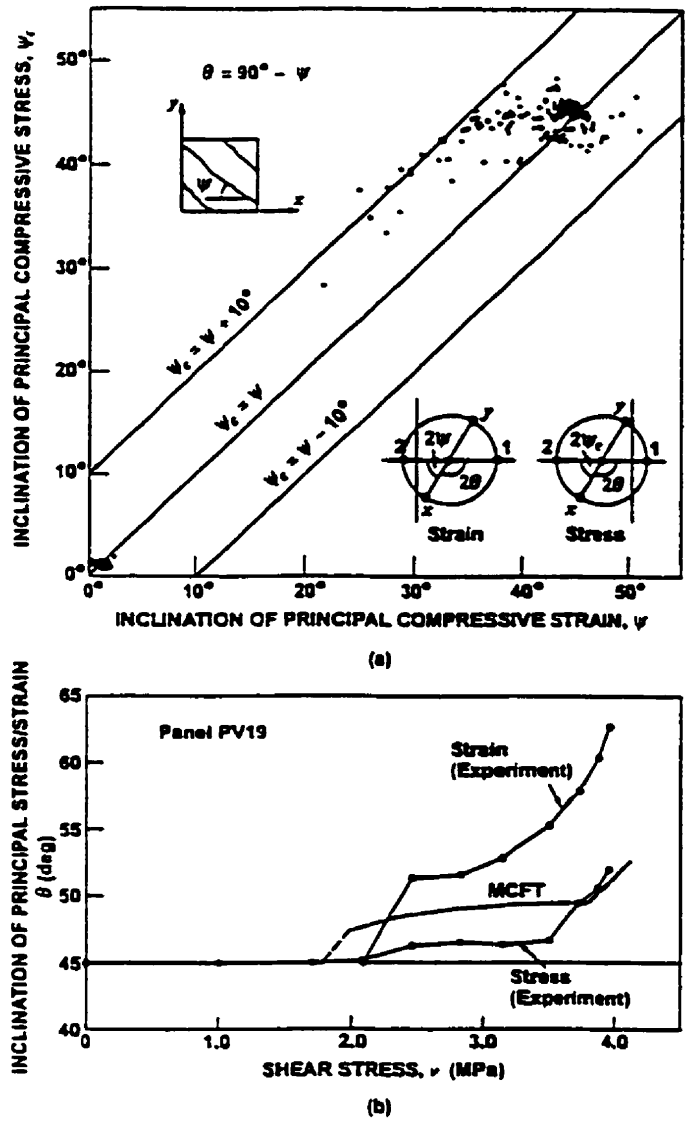

Figure 2.8

Another difficulty of the MCFT, as originally constituted, stems from the crack shear check. The cracks in the concrete are assumed to align with the average principal stress directions; hence, the average shear stresses in the directions orthogonal to the crack are necessary zero. However, at the crack surface, local stress conditions are different and can give rise to non-zero shear stresses on the crack surface (see Vecchio and Collins, 1986). The MCFT checks the magnitude of these local stresses; if they exceed a limit value, a reduction is made to the magnitude of the post-cracking average tensile stresses that can be sustained. In reality, the relationship between the concrete

tensile stresses and local shear stresses is not a direct one. Further, while shear stresses may be induced on the crack surface, the MCFT makes no allowance for discontinuous shear slip along the crack. Lastly, the crack shear check represents computational complexity that is disparate relative to the elegance and simplicity of the remainder of the formulation. The crack shear check has been the one aspect of the theory least well understood by others, and has often been ignored in their implementations of the MCFT.

2.8 Disturbed Stress Field Model

The Disturbed Stress Field Model (DSFM) was introduced by Vecchio (2000) as an alternative formulation for describing the behaviour of cracked reinforced concrete elements. The theory is an extension of the modified compression field theory (MCFT) (Vecchio and Collins 1986), with advancements made primarily with respect to modelling of shear slip along cracks. The impetus was to address the diminished accuracy seen from existing procedures under certain conditions, particularly for beams or wall elements containing no shear reinforcement. The new formulation combines aspects of rotating-crack and fixed-crack models, giving an improved representation of crack mechanisms and thereby resulting in increased accuracy.

Equilibrium conditions:

Equilibrium is used to relate the externally applied loads to the internal element forces. The element equilibrium condition is,

$$[\sigma] = [D_c][\varepsilon_c] + \sum_{i=1}^{n} [D_s]_i [\varepsilon_s]_i \tag{2.36}$$

where n is the number of reinforcement components, and $[D_c]$ and $[D_s]_i$ are concrete and reinforcement stiffness matrices, defined later. For the special case where the panel is orthogonally reinforced, and the reinforcement is aligned with the reference axes, the equilibrium equations become:

$$\sigma_x = f_{cx} + \rho_x \cdot f_{sx} \tag{2.37}$$

$$\sigma_y = f_{cy} + \rho_y \cdot f_{sy} \tag{2.38}$$

$$\tau_{xy} = v_{cxy} \tag{2.39}$$

The concrete stresses f_{cx}, f_{cy} and v_{cxy} can be conveniently determined from the principal stresses using the Mohr's circle of stress shown in Figure 2.9.

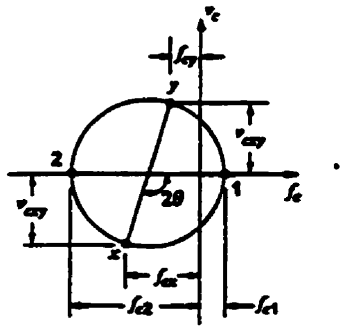

Figure 2.9

To ensure that the average tensile stress in the concrete can be transmitted across cracks, the following condition must be met:

$$f_{c1} \le \sum_{i=1}^{n} \rho_i (f_{yi} - f_{si}) \cdot \cos^2 \theta_{ni} \tag{2.40}$$

where ρ_i is the reinforcement ratio, f_{si} is the average stress, and f_{yi} is the yield stress for the i-th reinforcement component. The angle θ_{ni} is the difference between the angle of orientation of the reinforcement (α_i) and the normal to the crack surface (θ)

$$\theta_{ni} = \theta - \alpha_i \tag{2.41}$$

It is also important to note that the local increases in reinforcement stresses, at crack locations, lead to the development of shear stresses along the crack surfaces, v_{ci}. Equilibrium requirements give rise to the following relationship:

$$v_{ci} = \sum_{i=1}^{n} \rho_i (f_{scri} - f_{si}) \cos\theta_{ni} \cdot \sin\theta_{ni} \tag{2.42}$$

The local reinforcement stresses (f_{scri}) are determined from local reinforcement strains (ε_{scri}). The local reinforcement stresses are determined such as to satisfy the equilibrium condition that the average concrete tensile stresses must be transmitted across the cracks; that is:

$$\sum_{i=1}^{n} \rho_i (f_{scri} - f_{si}) \cos^2 \theta_{ni} = f_{c1} \tag{2.43}$$

Compatibility Relations:

Compatibility requires that any deformation experienced by the concrete must be matched by an identical deformation of the reinforcement. The relations establish a link between the external deformations and the element strains.

Relative to a reference x,y system, the measured strains would intrinsically contain both components of deformation. These measured or 'apparent strains' will be denoted as $[\varepsilon]=\{\varepsilon_x \quad \varepsilon_y \quad \gamma_{xy}\}$. The apparent inclination of the principal strain, θ_ε, would thus be calculated as:

$$\theta_\varepsilon = \frac{1}{2}\tan^{-1}\left[\frac{\gamma_{xy}}{\varepsilon_x - \varepsilon_y}\right] \tag{2.44}$$

The average shear slip strain can be defined as follows:

$$\gamma_s = \frac{\delta_s}{s} \tag{2.45}$$

The slip strain can be resolved into orthogonal components relative to the reference system: thus $[\varepsilon^s]=\{\varepsilon_x^s \quad \varepsilon_y^s \quad \gamma_{xy}^s\}$ where

$$\varepsilon_x^s = -\gamma_s/2\cdot\sin 2\theta \tag{2.46}$$

$$\varepsilon_y^s = \gamma_s/2\cdot\sin 2\theta \tag{2.47}$$

$$\gamma_{xy}^s = \gamma_s\cdot\cos 2\theta \tag{2.48}$$

By considering other effects, one obtains the following compatibility condition:

$$[\varepsilon]=[\varepsilon_c]+[\varepsilon^s]+[\varepsilon^0]+[\varepsilon^p] \tag{2.49}$$

where $[\varepsilon_c]$ are the stress-induced strains, $[\varepsilon^s]$ are the shear slip strains, $[\varepsilon^0]$ are the elastic strain offsets, and $[\varepsilon^p]$ are the plastic offsets.

Decoupling the two strain effects, the actual (net) strains within the continuum will be denoted as $[\varepsilon_c]=\{\varepsilon_{cx} \quad \varepsilon_{cy} \quad \gamma_{cxy}\}$. It is these strains that are to be employed in appropriate constitutive relations to determine the average stresses from the average strains for the concrete. For this purpose, the principal strains are determined from the net strains using the standard transformations:

$$\varepsilon_{c1},\varepsilon_{c2} = \frac{(\varepsilon_{cx}+\varepsilon_{cy})}{2} \pm \frac{1}{2}\left[(\varepsilon_{cx}-\varepsilon_{cy})^2+\gamma^2_{xy}\right]^{1/2} \tag{2.50}$$

$$\theta_\sigma = \frac{1}{2}\tan^{-1}\left[\frac{\gamma_{cxy}}{\varepsilon_{cx} - \varepsilon_{cy}}\right] \tag{2.51}$$

where ε_{c1} is the principal tensile strain, ε_{c2} is the principal compressive strain, ε_{cx} is the average strain in the x-direction, ε_{cy} is the average strain in the y-direction, γ_{cxy} is the shear strain, and θ_σ is the principal angle of stress and crack inclination.

The 'lag' in the rotation of the principal stresses in the continuum, relative to the rotation of the apparent principal strains, will be defined as:

$$\Delta\theta = \theta_\varepsilon - \theta_\sigma \tag{2.52}$$

In relating the apparent strain condition to the actual orientation of the stress and strain field within the continuum, the following relation is particularly useful:

$$\gamma_s = \gamma_{xy} \cdot \cos 2\theta_\sigma + (\varepsilon_y - \varepsilon_x) \cdot \sin 2\theta_\sigma \tag{2.53}$$

The reinforcement is assumed perfectly bonded to the concrete. Hence, the average strain in a reinforcement component is calculated from the total strains as follows:

$$\varepsilon_{s_i} = \frac{\varepsilon_x + \varepsilon_y}{2} + \frac{\varepsilon_x - \varepsilon_y}{2} \cdot \cos 2\alpha_i + \frac{\gamma_{xy}}{2} \sin 2\alpha_i + \varepsilon_{s_i}^0 \tag{2.54}$$

where α_i is the angle of orientation of the reinforcement and $\varepsilon_{s_i}^0$ is the initial prestrain in the reinforcement. The local strain in the reinforcement will be:

$$\varepsilon_{scr_i} = \varepsilon_{s_i} + \Delta\varepsilon_{1cr} \cdot \cos^2 \theta_{n_i} \tag{2.55}$$

Given nominal crack spacings in the reference x- and y-directions, s_x and s_y, the average crack spacing in the cracked continuum can be estimated as

$$s = \frac{1}{\frac{\sin\theta}{s_x} + \frac{\cos\theta}{s_y}} \tag{2.56}$$

The values s_x and s_y can be estimated from standard crack spacing formulations. Given the average crack spacing, the average crack width then can be calculated from the average tensile strain as follows:

$$w = \varepsilon_1 \cdot s \tag{2.57}$$

Constitutive Relations:

The compression response of cracked reinforced concrete is characterized by significant degress of softening arising from the effects of transverse cracking, as shown by Vecchio and Collins (1986). The principal compressive stress in the concrete f_{c2} is found to be a function of not only the principal compressive strain, but also of the coexisting principal tensile strain. The influence is captured by the reduction factor β_d, as follows:

$$\beta_d = \frac{1}{1 + C_s \cdot C_d} \leq 1.0 \tag{2.58}$$

In examing data collected from over 150 test panels (Vecchio and Collins 1993), the best correlations were obtained when the factor C_d was made a function of the ratio $\varepsilon_{c1}/\varepsilon_{c2}$, as follows:

$$C_d = 0.35\left(-\varepsilon_{c1} / \varepsilon_{c2} - 0.28\right)^{0.8} \tag{2.59}$$

The above is the preferred form for use in finite element formulations. However, for easier implementation into design procedures, accuracy is not much deteriorated when using a simpler form which is a function of ε_1 only. In updating the MCFT formulation, the following was proposed:

$$C_d = 0.27\left(\varepsilon_1 / \varepsilon_0 - 0.37\right) \tag{2.60}$$

The factor C_s accounts for the influence of slippage on the cracks. C_s is taken to be 0.55 in the DSFM. If slip on the cracks is not being explicitly taken into account in the element compatibility relations, as when using the MCFT formulation, then $C_s = 1.0$ is used.

The factor β_d is used to define both the peak stress (f_p) and the strain at peak stress (ε_p) in the compression response of the concrete. Hence, if using the $\varepsilon_1/\varepsilon_2$ formulation, then:

$$f_p = -\beta_d \cdot f'_c \tag{2.61}$$

$$\varepsilon_p = -\beta_d \cdot \varepsilon_0 \tag{2.62}$$

The compression response curve is described as:

$$f_{c2} = f_p\left[2(\varepsilon_{c2}/\varepsilon_p)-(\varepsilon_{c2}/\varepsilon_p)^2\right], \qquad \varepsilon_p < \varepsilon_{c2} < 0 \tag{2.63}$$

$$= f_p\left[1-\left(\frac{\varepsilon_{c2}-\varepsilon_p}{-2\varepsilon_0-\varepsilon_p}\right)^2\right], \qquad -2\varepsilon_0 < \varepsilon_{c2} < \varepsilon_p \tag{2.64}$$

For concrete in tension, prior to cracking, a linear relation is used; that is,

$$f_{c1} = E_c\varepsilon_{c_1} \qquad 0 < \varepsilon_{c_1} < \varepsilon_{cr} \tag{2.65}$$

$$E_c = 2\frac{f'_c}{\varepsilon_0} \tag{2.66}$$

$$\varepsilon_{cr} = \frac{f'_c}{E_c} \tag{2.67}$$

Recent experience with concretes made from Toronto-area aggregates suggest the following relationship for estimating the concrete tensile strength, f'_t:

$$f'_t = 0.65(f'_c)^{0.33} \tag{2.68}$$

Tension softening is particularly significant in concrete structures containing little or no reinforcement; for example, beams containing no web steel. Here, the concrete post-cracking tensile stress associated with tension softening, f^1_{c1}, is calculated as:

$$f^1_{c1} = f'_t\left[1-\frac{(\varepsilon_{c_1}-\varepsilon_{cr})}{\varepsilon_{ts}-\varepsilon_{cr}}\right] \tag{2.69}$$

where the terminal strain ε_{ts} is calculated from the fracture energy parameter G_f and characteristic length L as follows:

$$\varepsilon_{ts} = 2.0\frac{G_f}{f'_t \cdot L} \tag{2.70}$$

Here, G_f is taken as a constant value of 75N/m.

Post-cracking tensile stresses in the concrete also arise from interactions between the reinforcement and the concrete. In areas between cracks, load is transferred from the reinforcement to the concrete via bond stresses, producing significant levels of average tensile stress in the concrete. As previously done in the MCFT, these concrete tension stiffening stresses are modelled as follows:

$$f_{c1}^2 = \frac{f'_c}{1+\sqrt{C_t \varepsilon_{c_1}}} \tag{2.71}$$

For relatively small elements, $C_t = 200$ is used. For typical larger-scale elements, $C_t = 500$ is used.

The resulting average principal tensile stress in the concrete is the larger of the two values defined above. Hence,

$$f_{c1} = \max\left(f_{c1}^1, f_{c1}^2\right) \tag{2.72}$$

A trilinear stress-strain relation is used to model the response of reinforcement in tension or compression. Hence,

$$f_s = E_s \varepsilon_s \quad , \quad 0 < \varepsilon_s < \varepsilon_y \tag{2.73}$$

$$= f_y \quad , \quad \varepsilon_y < \varepsilon_s < \varepsilon_{sh} \tag{2.74}$$

$$= f_y + E_{sh}(\varepsilon_s - \varepsilon_{sh}) \quad , \quad \varepsilon_{sh} < \varepsilon_s < \varepsilon_u \tag{2.75}$$

$$= 0 \quad , \quad \varepsilon_s > \varepsilon_u \tag{2.76}$$

where f_y is the yield strength, E_s is the modulus of elasticity, E_{sh} is the strain hardening modulus, ε_y is the yield strain ($=f_y/\varepsilon_s$), ε_{sh} is the strain at start of strain hardening, and ε_u is the ultimate strain.

Slip Model:

The relationship initially adopted in the DSFM was that of Walraven (1981). Taking the stiffness portion of his formulation as follows:

$$\delta_s^1 = \frac{v_{ci}}{1.8w^{-0.8} + \left(0.234w^{-0.707} - 0.20\right) \cdot f_{cc}} \tag{2.77}$$

Once the slip displacement δ_s^1 has been found, Eq. (2.45) is used to determine the crack slip shear strain γ_s^1.

Another approach is to relate the changes in direction of the principal stresses to the changes in the direction of the apparent principal strains. Relative to the initial crack direction θ_{ic} (ie inclination of principal stresses/strains at first cracking), the rotation in the apparent principal strains ($\Delta\theta_\varepsilon$) is determined according to the prevailing load and material conditions at the current load stage:

$$\Delta\theta_\varepsilon = \theta_\varepsilon - \theta_{ic} \tag{2.78}$$

Allowing for the rotation lag, the change in inclination of the principal stress direction ($\Delta\theta_a$) can then be found:

$$\Delta\theta_\sigma = (\Delta\theta_\varepsilon - \Delta\theta_l) \quad \text{for } |\Delta\theta_\varepsilon| > \Delta\theta_l \tag{2.79}$$

$$= \Delta\theta_\varepsilon \quad \text{for } |\Delta\theta_\varepsilon| \le \Delta\theta_l \tag{2.80}$$

where the constant lag $\Delta\theta_l$ is taken as 5° for biaxially reinforced elements, 7.5° for uniaxially reinforced elements, and 10° for unreinforced elements. The inclination of the stress field at the current load stage is then calculated as:

$$\theta_\sigma = \theta_{ic} + \Delta\theta_\sigma \tag{2.81}$$

Then, using Eq. (2.53), the crack shear slip strain γ_s^2 can be determined.

In the DSFM, a hybrid formulation can be used. If done so, the crack slip shear strain is taken as the maximum of the values computed using each of the two methods; hence,

$$\gamma_s = \max(\gamma_s^1, \gamma_s^2) \tag{2.82}$$

CHAPTER 3

Rotation Lag Formulations/Data

3.1 General Trends

An original simplifying assumption of the MCFT was that the directions of the average principal strain remained coincident with the directions of the average principal stresses in the concrete. It was previously shown that this was strictly not the case. (See Figure 2.8a) The observed tendency was for the change in the principal stress direction to lag behind the change in the principal strain direction. Shown in Figure 2.8b are the angles of inclination for the stress and strain fields for Panel PV19, reinforced with ρ_x = 1.8% and ρ_y = 0.7% and subjected to pure shear (σ_x:σ_y:τ = 0:0:1).

Prior to cracking, both fields were inclined at 45° relative to the reinforcement directions. After first cracking, there was an abrupt increase in the inclination of the principal strain direction but little change in the concrete stress field direction. Thereafter, both inclinations gradually increased, with a relatively constant angle difference (lag) present. After yielding of the transverse reinforcement, the reorientation of the stress field accelerated in accordance with the pattern of the change in the principal strain direction.

In order to look for trends in the lag between principal stress and principal strain directions, data from panel tests were re-examined. The Vecchio panels (PV), Bhide panels (PB) and Aspiotis Panels (PHS and PA) were used for these analyses. The first inclination was to examine the change in the principal strain versus the change in the principal stress. Considered were 30 Vecchio panels (Vecchio and Collins, 1982), 16 Bhide panels (Bhide and Collins, 1987), and 12 Aspiotis panels (Aspiotis, 1993). Shown in Figure 3.1 to 3.3 are the plots of data extracted from the various panels. Figure 3.4 combines the data for all three series of panels.

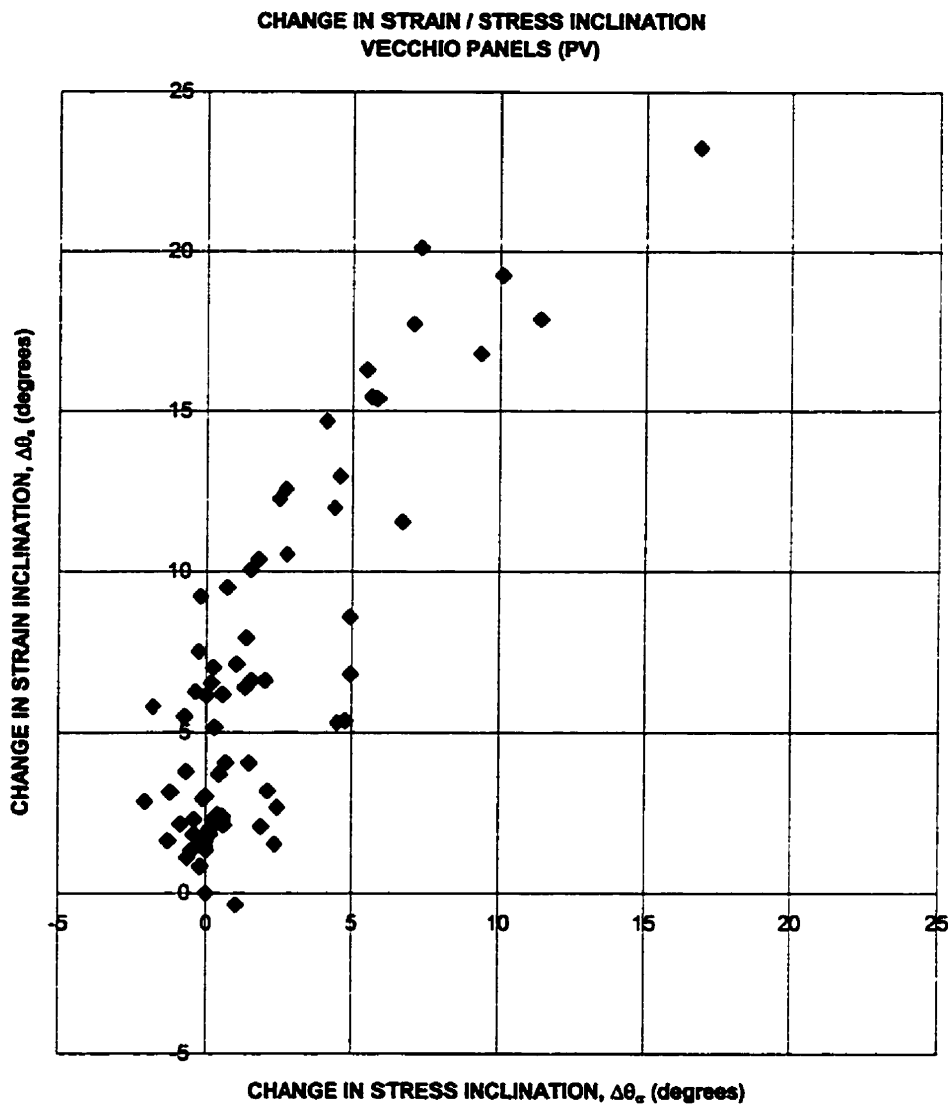
CHANGE IN STRAIN / STRESS INCLINATION
VECCHIO PANELS (PV)
CHANGE IN STRAIN INCLINATION, Δθε (degrees)
CHANGE IN STRESS INCLINATION, Δθσ (degrees)
25
20
15
10
5
0
-5
-5
0
5
10
15
20
25

Figure 3.1

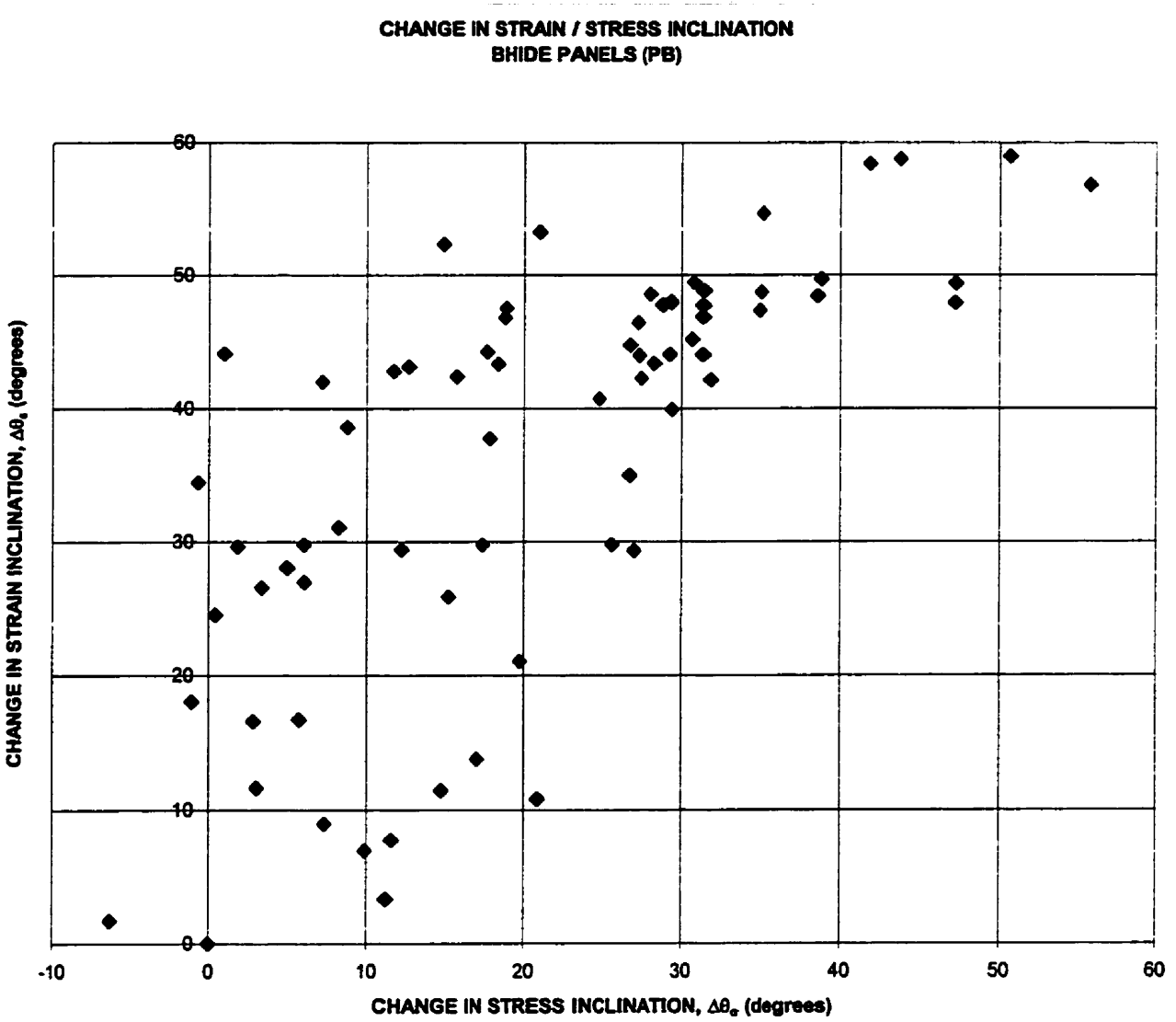
CHANGE IN STRAIN / STRESS INCLINATION
BHIDE PANELS (PB)
CHANGE IN STRAIN INCLINATION, Δθε (degrees)
CHANGE IN STRESS INCLINATION, Δθσ (degrees)
60
50
40
30
20
10
0
-10
0
10
20
30
40
50
60

Figure 3.2

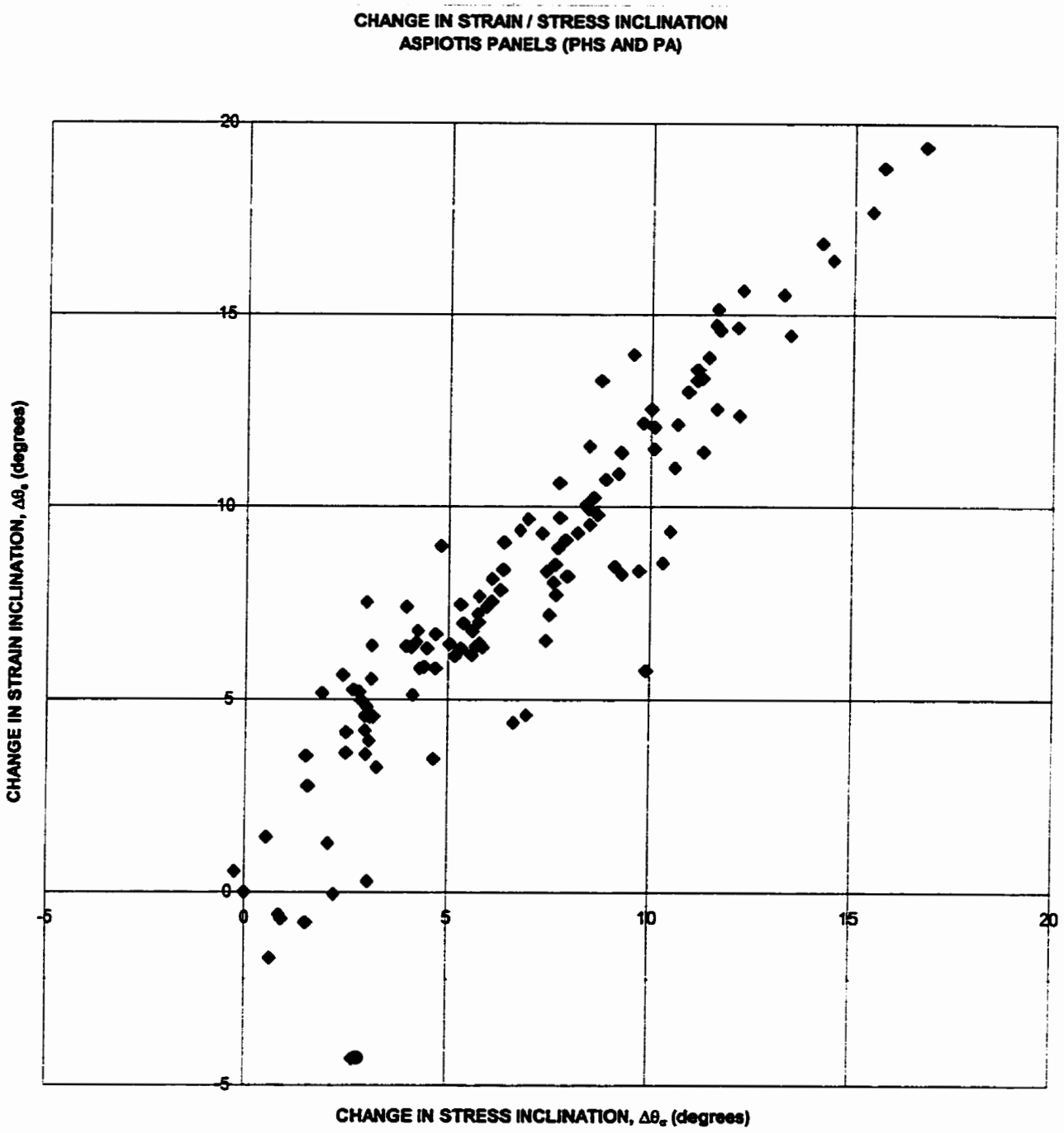
CHANGE IN STRAIN / STRESS INCLINATION
ASPIOTIS PANELS (PHS AND PA)
CHANGE IN STRAIN INCLINATION, Δθε (degrees)
CHANGE IN STRESS INCLINATION, Δθσ (degrees)
20
15
10
5
0
-5
-5
0
5
10
15
20

Figure 3.3

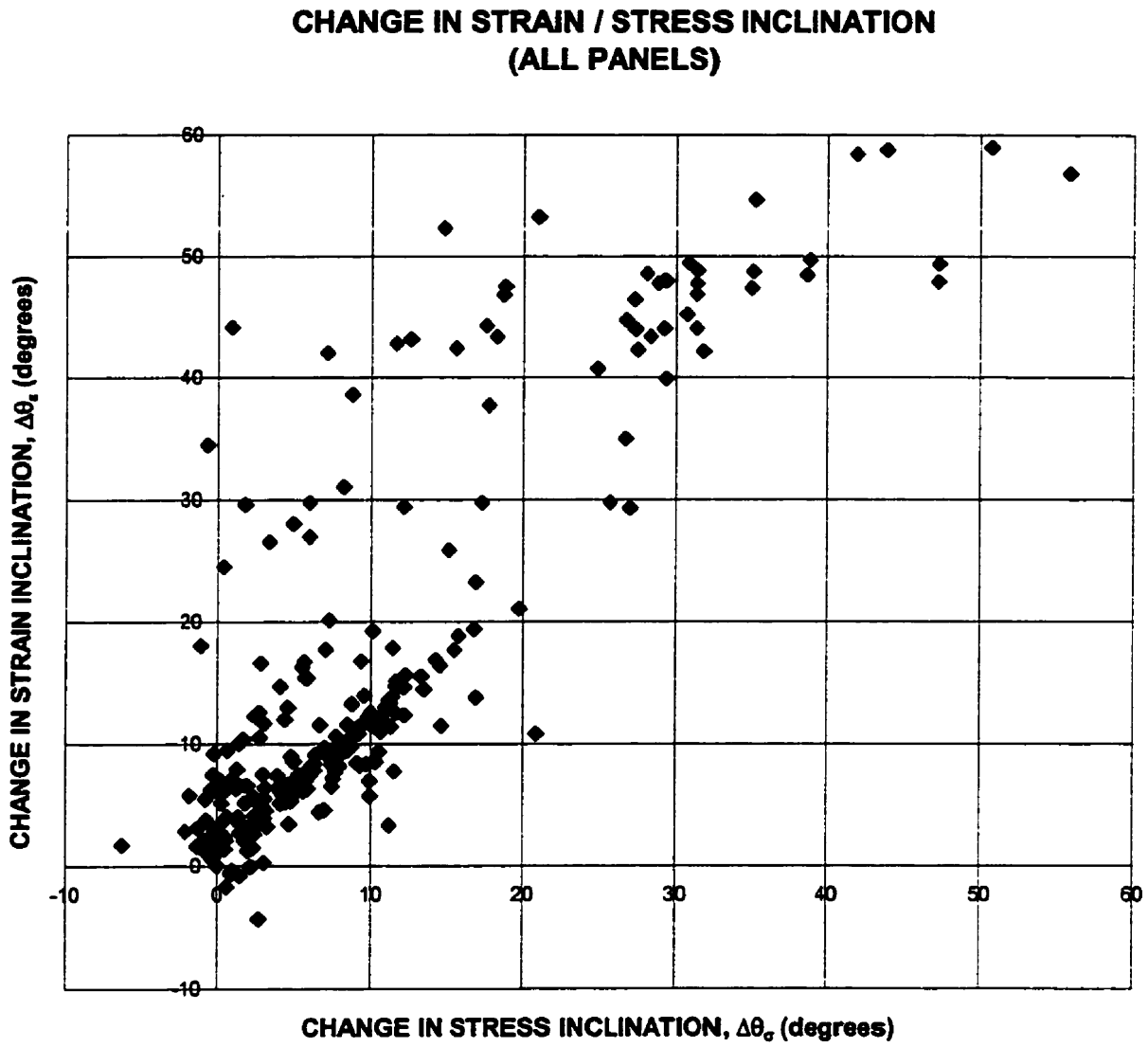
CHANGE IN STRAIN / STRESS INCLINATION
(ALL PANELS)
CHANGE IN STRAIN INCLINATION, Δθε (degrees)
CHANGE IN STRESS INCLINATION, Δθσ (degrees)
60
50
40
30
20
10
0
-10
-10
0
10
20
30
40
50
60

Figure 3.4

The Vecchio panels were biaxially reinforced in most cases, with dissimilar reinforcement ratio in both x and y directions. The principal stress lagged behind at about 5° to the principal strain. The Bhide tests were comprised primarily by uniaxial reinforced panels, with most of the panels reinforced in x-direction only. See Appendix A for details of the panels. The principal stress lagged behind at about 7.5° to the principal strain, and there was considerally more scatter in the results. In the Aspiotis panels, it was interesting to note that the change in principal stress remained approximately coincident with the change in the principal strain. The panels were biaxially reinforced with relatively heavy reinforcement in the x-direction and light reinforcement in the y-direction. Upon reviewing the three different types of panels together (Figure 3.4), no strong trends can be found.

Another way of looking at the change in the principal strain/stress was by grouping the panels according to the manner in which were reinforced. The panels used for uniaxial/biaxial reinforced analysis are shown in Table 3.1.

Table 3.1 Uniaxial/Biaxial Reinforced Panels

	Panel I.D.
Uniaxial reinforced panels	PV13, PB4, PB11, PB12, PB14, PB16, PB17, PB18, PB19, PB20, PB21, PB22, PB28, PB29, PB30, PB31, PB32, PHS1
Biaxial reinforced panels	PV1, PV2, PV3, PV4, PV5, PV6, PV7, PV8, PV9, PV10, PV11, PV12, PV14, PV16, PV18, PV19, PV20, PV21, PV22, PV23, PV24, PV25, PV26, PV27, PV28, PV29, PV30, PHS2, PHS3, PHS4, PHS5, PHS6, PHS7, PHS8, PHS9, PHS10, PA1, PA2

Figure 3.5 shows panels with uniaxial reinforcement, and Figure 3.6 shows panels with biaxial reinforcement.

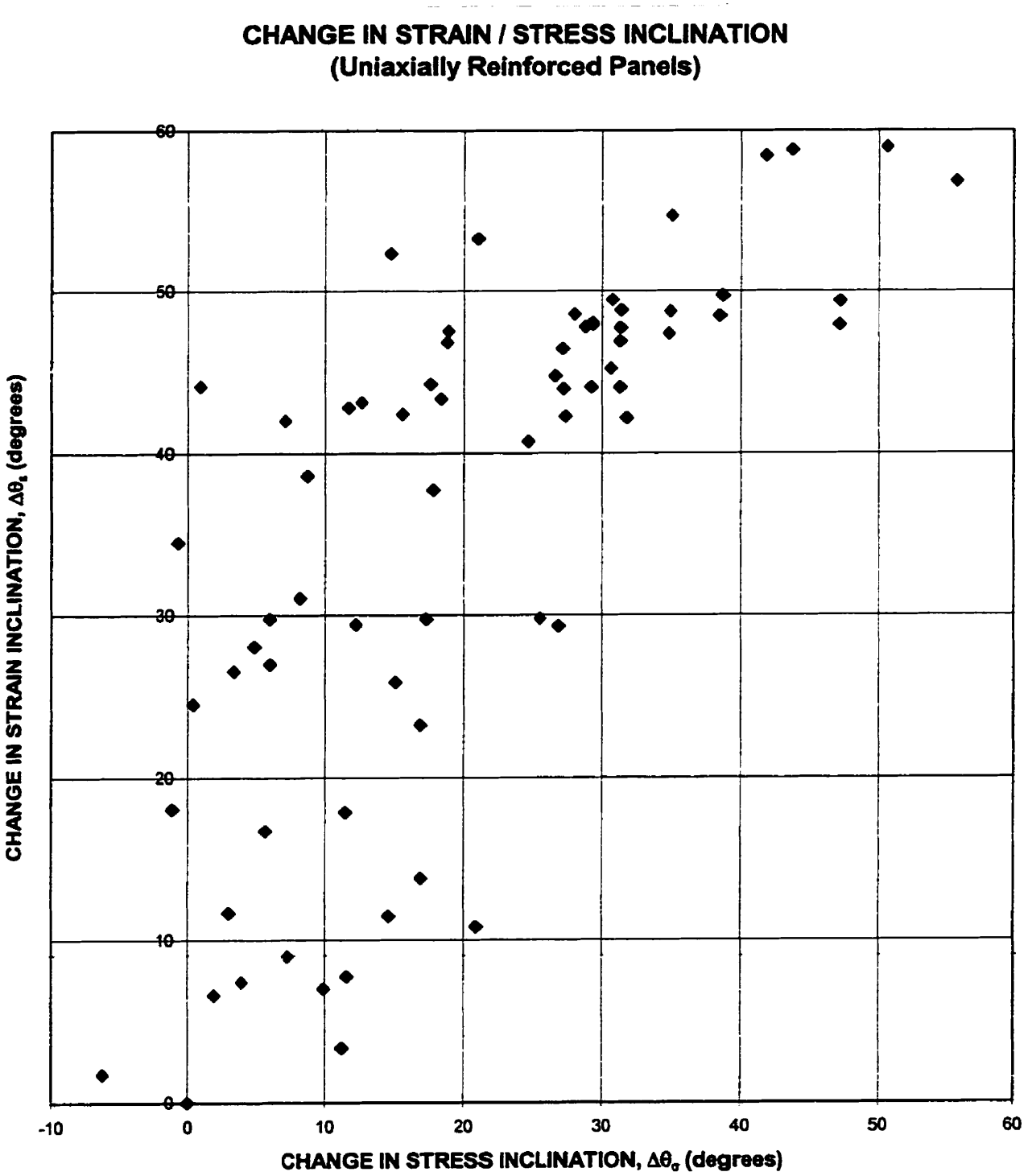
CHANGE IN STRAIN / STRESS INCLINATION
(Uniaxially Reinforced Panels)
CHANGE IN STRAIN INCLINATION, Δθε (degrees)
CHANGE IN STRESS INCLINATION, Δθσ (degrees)
60
50
40
30
20
10
0
-10
0
10
20
30
40
50
60

Figure 3.5

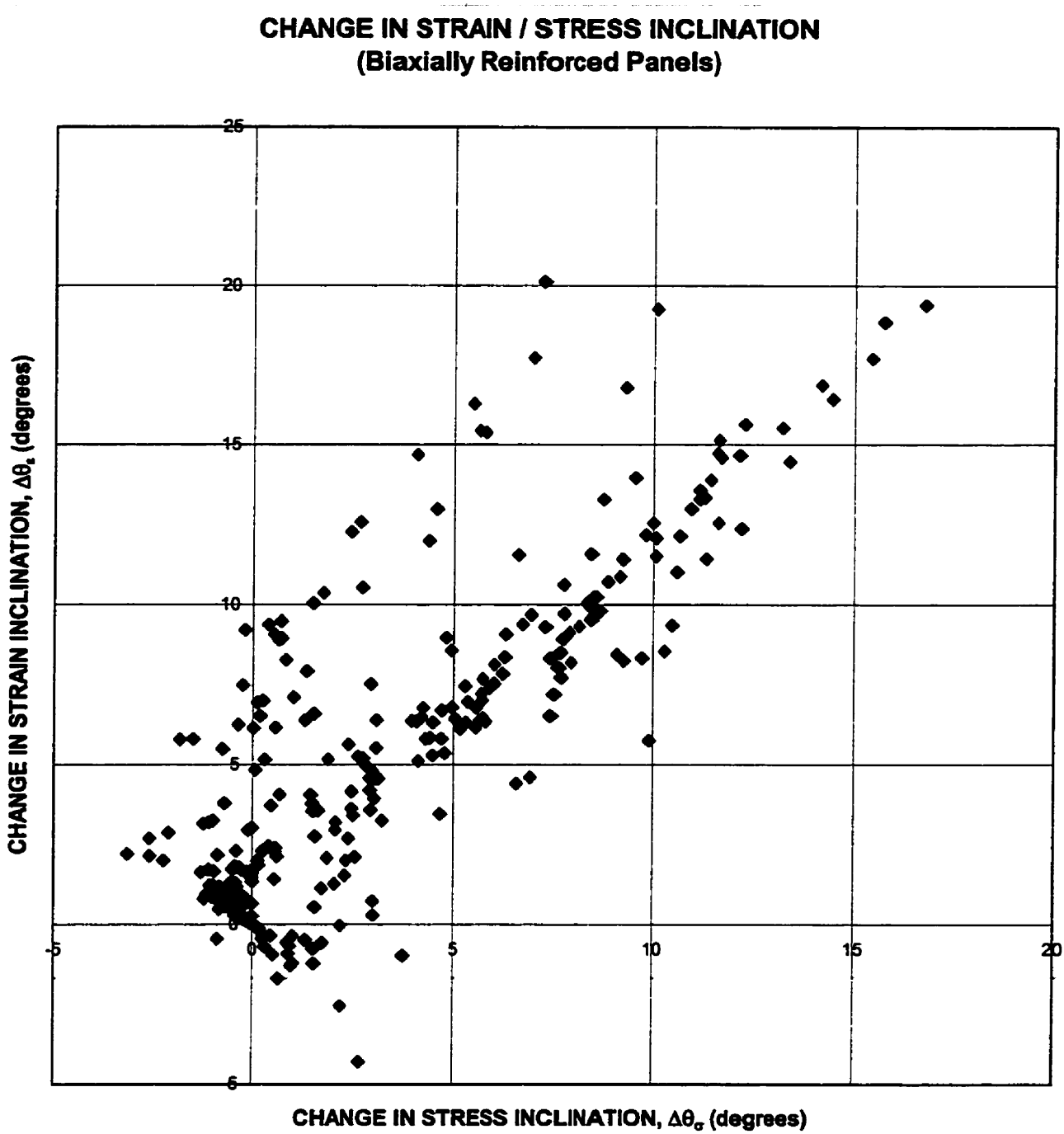
CHANGE IN STRAIN / STRESS INCLINATION
(Biaxially Reinforced Panels)
CHANGE IN STRAIN INCLINATION, Δθε (degrees)
CHANGE IN STRESS INCLINATION, Δθσ (degrees)
25
20
15
10
5
0
-5
0
5
10
15
20

Figure 3.6

For uniaxial reinforced panels, the principal stress lagged behind at about 7.5° to the principal strain. For biaxial reinforced panels, the principal stress lagged behind at about 5° to the principal strain.

The possible influencing factors which affected the change in the principal strain/stress angles included the reinforcement ratio (ρ_x, ρ_y), the yield strength of reinforcement (f_{yx}, f_{yy}), the strength of concrete (f'c) and the loading condition. Plots of ($\Delta\theta_\varepsilon$-$\Delta\theta_\sigma$) versus X are shown in Figures 3.7 to 3.10 for uniaxially reinforced and biaxially reinforced panels, respectively. X is an arbitrary variable and is defined as follows:

1. X=2-Nx-Ny for Figures 3.7 to 3.8, where

$$Nx = \frac{\rho_x (f_{yx} - f_{sx})}{0.4 f'c} \leq 1.0$$

$$Ny = \frac{\rho_y (f_{yy} - f_{sy})}{0.4 f'c} \leq 1.0$$

2. X= ($\rho_x f_{yx}$-$\rho_y f_{yy}$)/$\sqrt{f'c}$ for Figures 3.9 and 3.10.

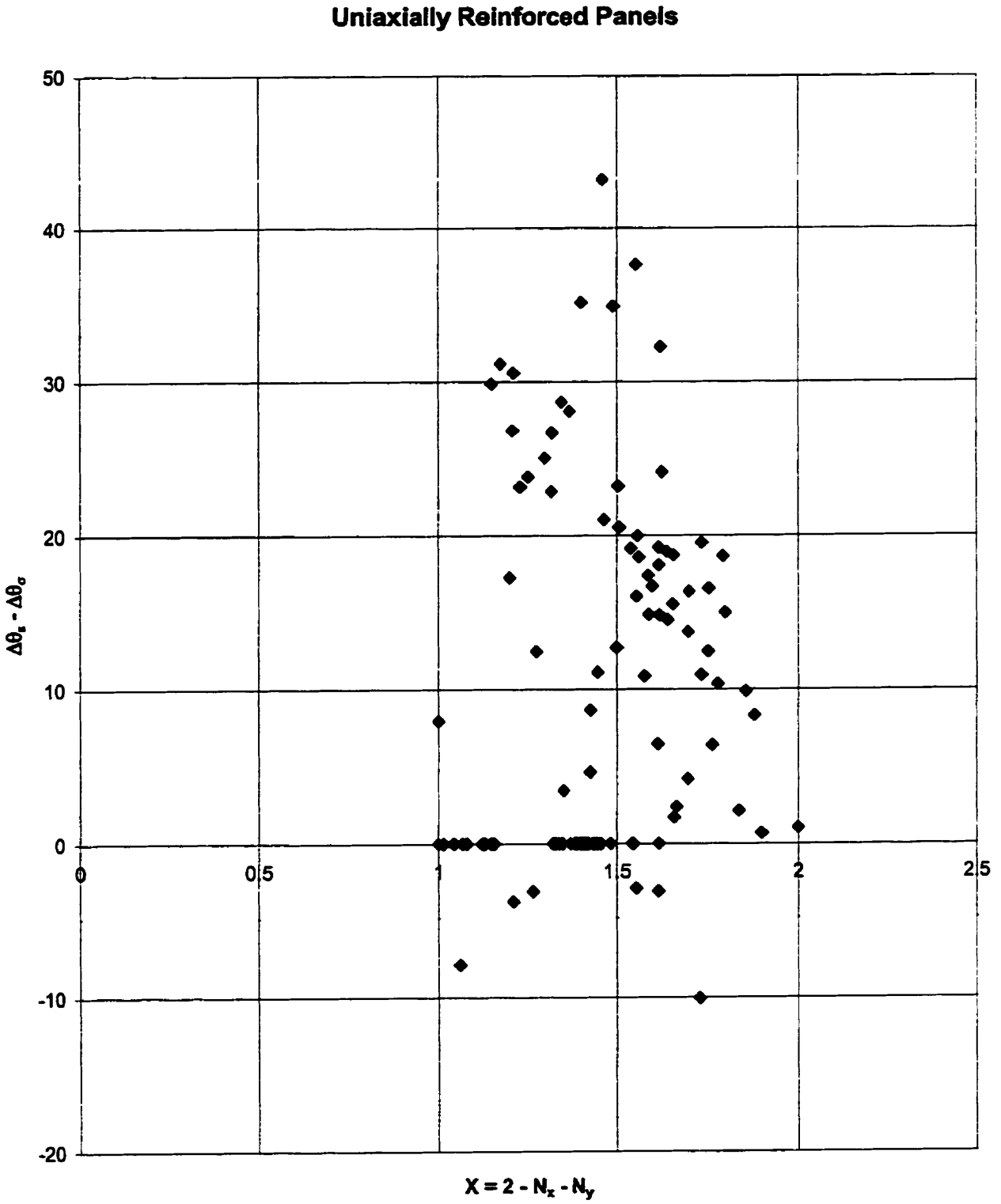
Uniaxially Reinforced Panels
50
40
30
20
10
0
-10
-20
0
0.5
1
1.5
2
2.5
$\Delta\theta_s - \Delta\theta_\sigma$
$X = 2 - N_x - N_y$

Figure 3.7

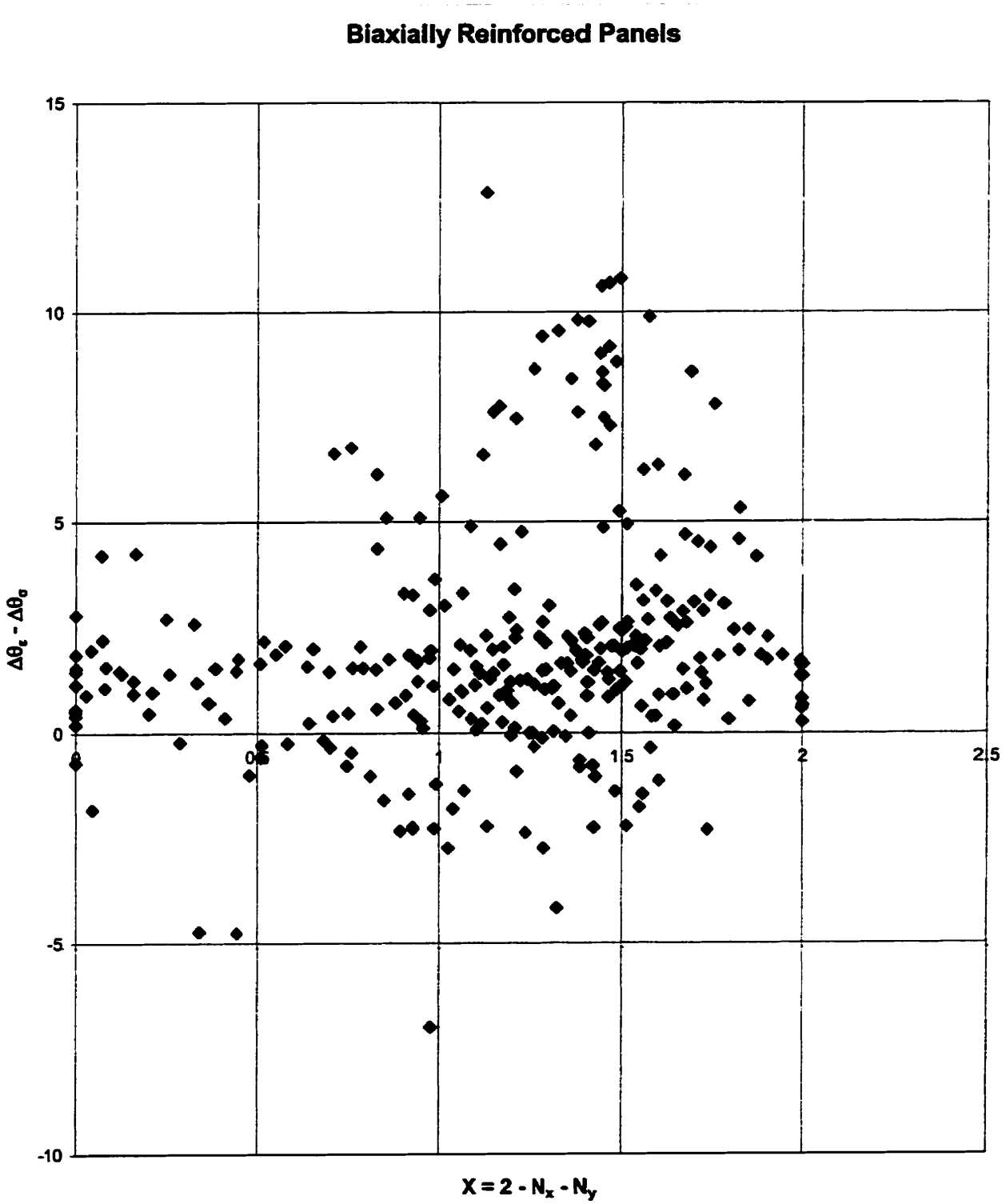
Biaxially Reinforced Panels
15
10
5
0
-5
-10
0
0.5
1
1.5
2
2.5
$\Delta\theta_t - \Delta\theta_\sigma$
$X = 2 - N_x - N_y$

Figure 3.8

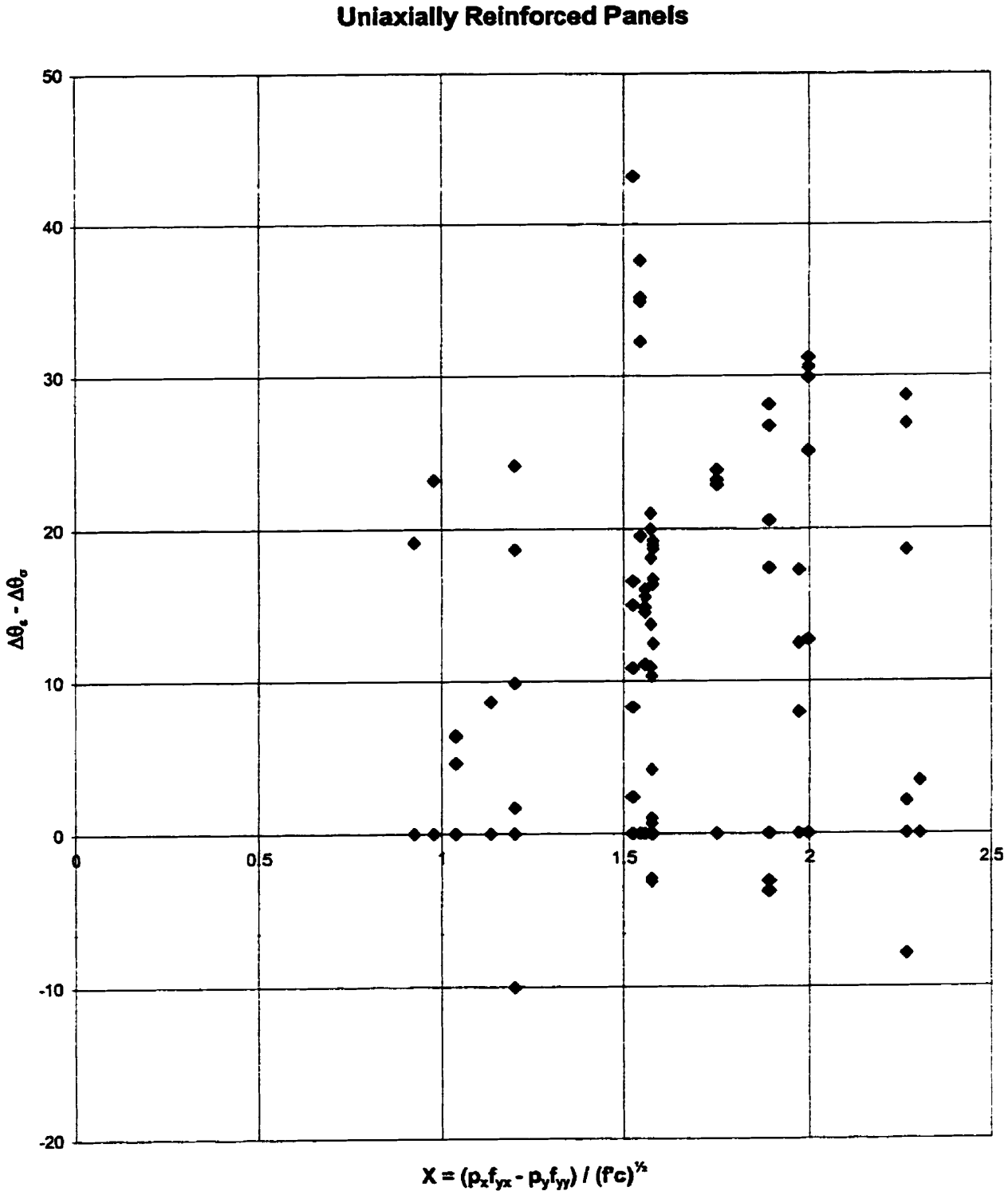
Uniaxially Reinforced Panels
50
40
30
20
10
0
-10
-20
0
0.5
1
1.5
2
2.5
$\Delta\theta_e - \Delta\theta_o$
$X = (p_x f_{yx} - p_y f_{yy}) / (f'c)^{1/2}$

Figure 3.9

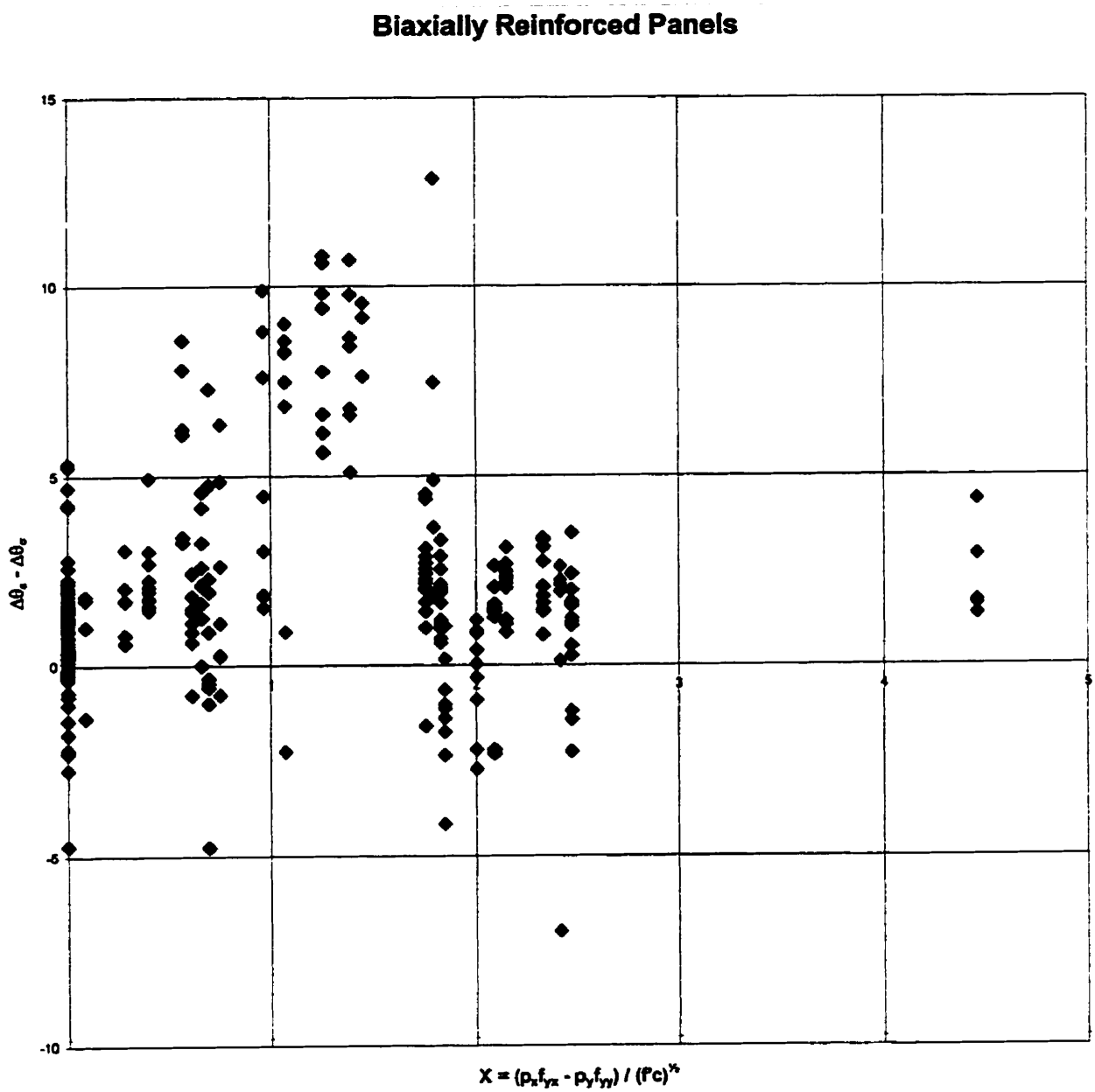
Biaxially Reinforced Panels
15
10
5
0
-5
-10
$\Delta\theta_e - \Delta\theta_o$
$X = (p_x f_{yx} - p_y f_{yy}) / (f'c)^{1/2}$

Figure 3.10

The analyses result showed a very scattered result. No strong correlation could be found between the rotational lag angle and the concrete/reinforcement material properties.

3.2 Conclusions

The inclinations of the principal stresses and principal strains are not necessarily equal. However, no strong trends were found from the analyses undertaken. As a rough approximation, the constant lag θ^l can be taken as 5° for biaxially reinforced elements, 7.5° for uniaxially reinforced elements, and 10° for unreinforced elements.

CHAPTER 4

Shear Slip Data

4.1 Introduction

In finite element analysis of cracked reinforced concrete, the development of nonlinear elastic procedures has generally progressed along two lines: rotating crack models and fixed crack models. With rotating crack models, it is assumed that a gradual reorientation occurs in the direction of cracks, as dictated by the loading or material response. Along with the change in crack direction, a gradual reorientation is assumed to occur in the principal stress and principal strain directions in the concrete. Conversely, with fixed crack models, crack directions remain fixed in the direction of first cracking. In some formulations, if the stress conditions dictate, discrete new cracks may form at alternate inclinations. An important aspect of the fixed crack approach is the determination of the shear stresses that necessarily develop on crack surfaces and the shear slips that occur as a result. Both the rotating crack and the fixed crack models have met with varying degrees of success. However, they do not work very well in all cases.

In the application of rotating crack models (e.g. MCFT), shear strength and stiffness are generally underestimated for panels containing heavy amounts of reinforcement in both directions, in panels subjected to high biaxial compressions in

addition to shear, or in panels where the reinforcement and loading conditions are such that there is no rotation of the principal stress or strain conditions. Conversely, shear strength and stiffness are generally overestimated for uniaxially reinforced panels or for panels containing very light reinforcement in the transverse direction. Reduced accuracy also has been observed in shear-critical beams containing very little or no transverse reinforcement (i.e., <0.05%). Here, the fully rotating crack model allows for a significant re-orientation of the stress-strain fields. In such beams, this may result in overestimated ductility, and over-predicted or under-predicted strengths, depending on the structural and loading details. The models proposed in this chapter attempts to redress the weaknesses in the above computational models.

4.2 Shear Slip Formulation - Experimental

Once again, 30 Vecchio panels (Vecchio and Collins 1982), 16 Bhide panels (Bhide and Collins 1987), 12 Aspiotis panels (Aspiotis 1993), and 3 Kirschner panels (Kirschner 1986) were considered. For each of these panels, crack shear slip response was examined. The shear slip data was calculated according to the following procedure:

1. a) For a given panel element, obtain

$$f'c, \rho_x, \rho_y, f_{yx}, f_{yy}, E_s, s$$

where f'c is the concrete cylinder strength, ρ_x, ρ_y are the reinforcement ratios in x, y-direction, f_{yx}, f_{yy} are the maximum yield strengths of steel in longitudinal, transverse direction, E_s is the modulus of elasticity, and s is the crack spacing.

b) From the experimental data, for a given load stage, extract:

$$\varepsilon_x, \varepsilon_y, \gamma_{xy}, \theta_\varepsilon, \theta_\sigma, f_{cl}, \varepsilon_1$$

where $\varepsilon_x, \varepsilon_y$ is the longitudinal, transverse tensile strain, γ_{xy} is the normal shear strain, $\theta_\varepsilon, \theta_\sigma$ are the inclination of principal compressive stress/strain, f_{cl} is the concrete principal tensile stress, and ε_1 is the principal tensile strain.

Note: $\theta_\varepsilon, \theta_\sigma$ are with respect to 1-direction for principal strains and principal stresses.

2. Find experimental crack shear slip, Δ_s^e:

i) $\gamma_x = \gamma_{xy} \cdot \cos 2\theta_\sigma + (\varepsilon_y - \varepsilon_x) \cdot \sin 2\theta_\sigma$

ii) $\Delta_s^e = \gamma_s \cdot s$ (s is assumed to be 50mm)

3. Find experiment crack shear stress, v_{ci}:

i) Given f_{c1}

ii) Estimate $\Delta\varepsilon_{1cr}$ (i.e. additional local strain at crack)

iii) Calculate local steel strains:

$$\varepsilon_{scrx} = \varepsilon_{sx} + \Delta\varepsilon_{1cr} \cdot \cos^2\theta_\sigma$$

$$\varepsilon_{scry} = \varepsilon_{sy} + \Delta\varepsilon_{1cr} \cdot \cos^2(90° - \theta_\sigma)$$

iv) Calculate local steel stresses:

$$f_{scrx} = \varepsilon_{scrx} \cdot E_s \le f_{yx}$$

$$f_{scry} = \varepsilon_{scry} \cdot E_s \le f_{yy}$$

v) Calculate resulting f_{c1}^*

$$f_{c1}^* = \rho_x (f_{scrx} - f_{sx}) \cos^2\theta_\sigma + \rho_y (f_{scry} - f_{sy}) \cos^2(90° - \theta_\sigma)$$

vi) Check $f_{c1}^* \rightarrow f_{c1}$; if not, go to (ii)

vii) $v_{ci} = \rho_x (f_{scrx} - f_{sx}) \cos\theta_\sigma \cdot \sin\theta_\sigma + \rho_y (f_{scry} - f_{sy}) \cos(\theta_\sigma - 90°) \cdot \sin(\theta_\sigma - 90°)$

The crack shear slip (Δ_s^e) and crack shear stress (v_{ci}) response was determined for each panel at each load stage.

In order to propose a new shear slip formulation, one must find a relationship between the experimental crack shear slip (Δ_s^e) and the various factors involved in the experiment. (i.e. v_{ci}, v_{cimax}, w, f'c)

Based on the experimental data, the following plots are constructed:

v_{ci} *vs.* Δ_s^e (see Figure 4.1)

v_{ci} / v_{cimax} *vs.* Δ_s^e (see Figure 4.2)

v_{ci} / v_{cimax} *vs.* Δ_s^e / w (see Figure 4.3)

Examining the v_{ci} *vs.* Δ_s^e (Figure 4.1), one observes that most of the shear stress data (v_{ci}) lie between 1MPa and 3MPa. The data is very scattered across the different panels. For example, the experimental slips of the Aspiotis (PA/PHS) panels are less

than 0.10 mm, the experimental slips of Vecchio (PV) and Kirschner (SE) panels are between 0 and 0.50 mm, while the experimental slips of Bhide (PB) panels are between 0 and 1.30 mm.

In Figure 4.2, $v_{ci}/v_{cimax} < 0.50$ in all panels. Notice that the plots only consider data after cracking. Data points are excluded from the plots when the cracks have not been formed and when the shear stress was very low (vci/vcimax < 0.10). The relationship observed seems to be somewhat linear.

Figure 4.3 is very similar to Figure 4.2, with the only difference being that the experimental shear slip was divided by the crack width, w (where $w = \varepsilon_1 \cdot s$). However, no strong trend can be found.

Crack Shear Slip Response

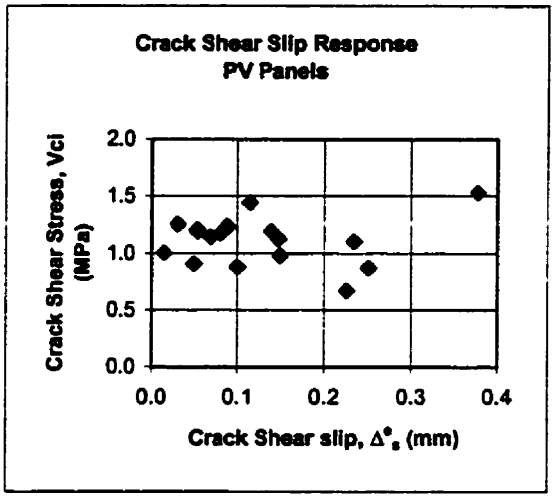

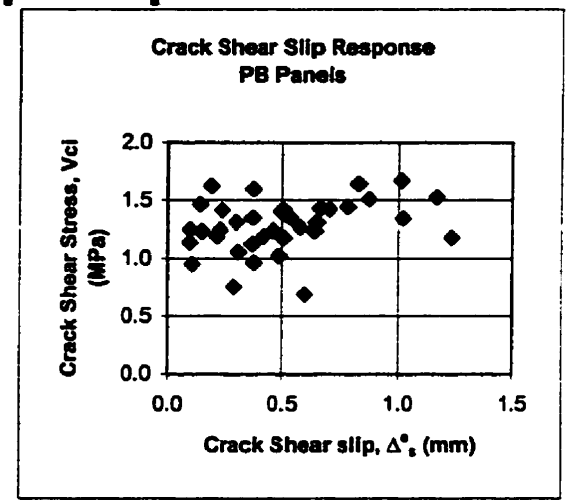

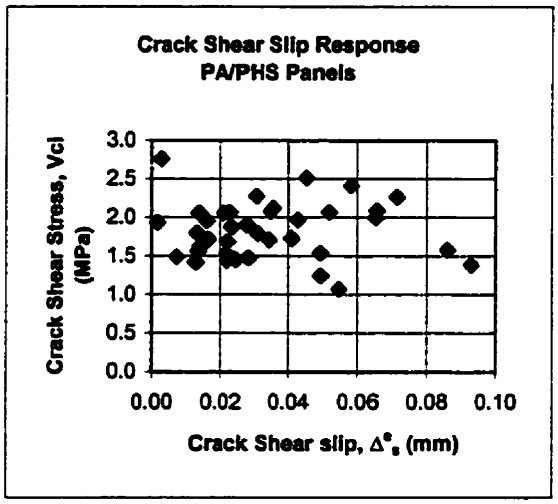

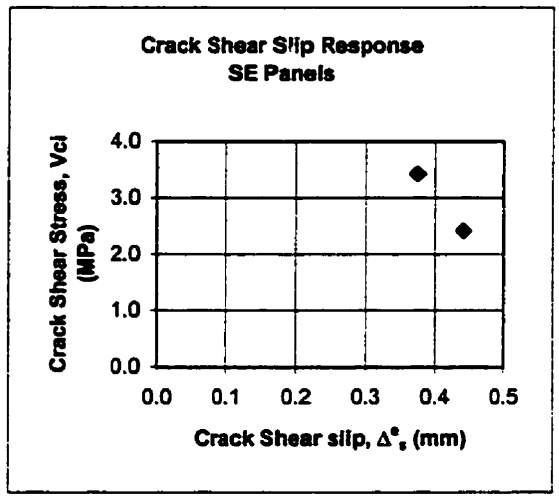

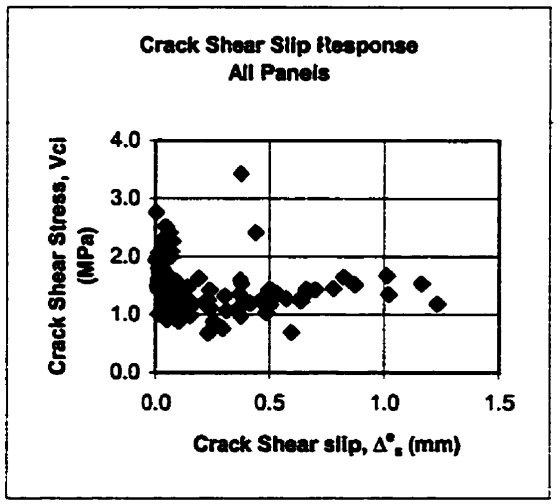

Figure 4.1 Vci vs. Δ^e_s

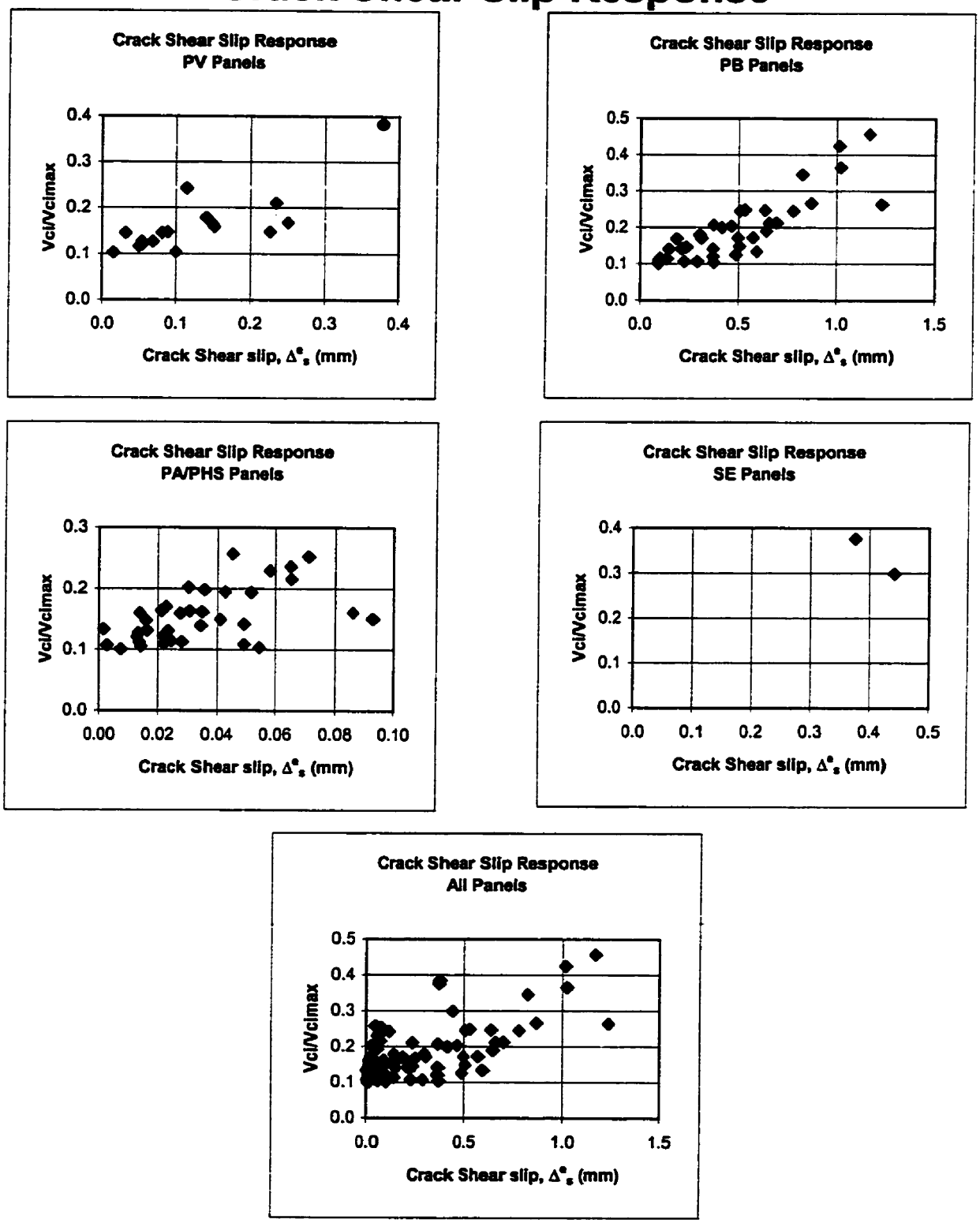

Figure 4.2 Vci/Vcimax vs. Δ^e_s

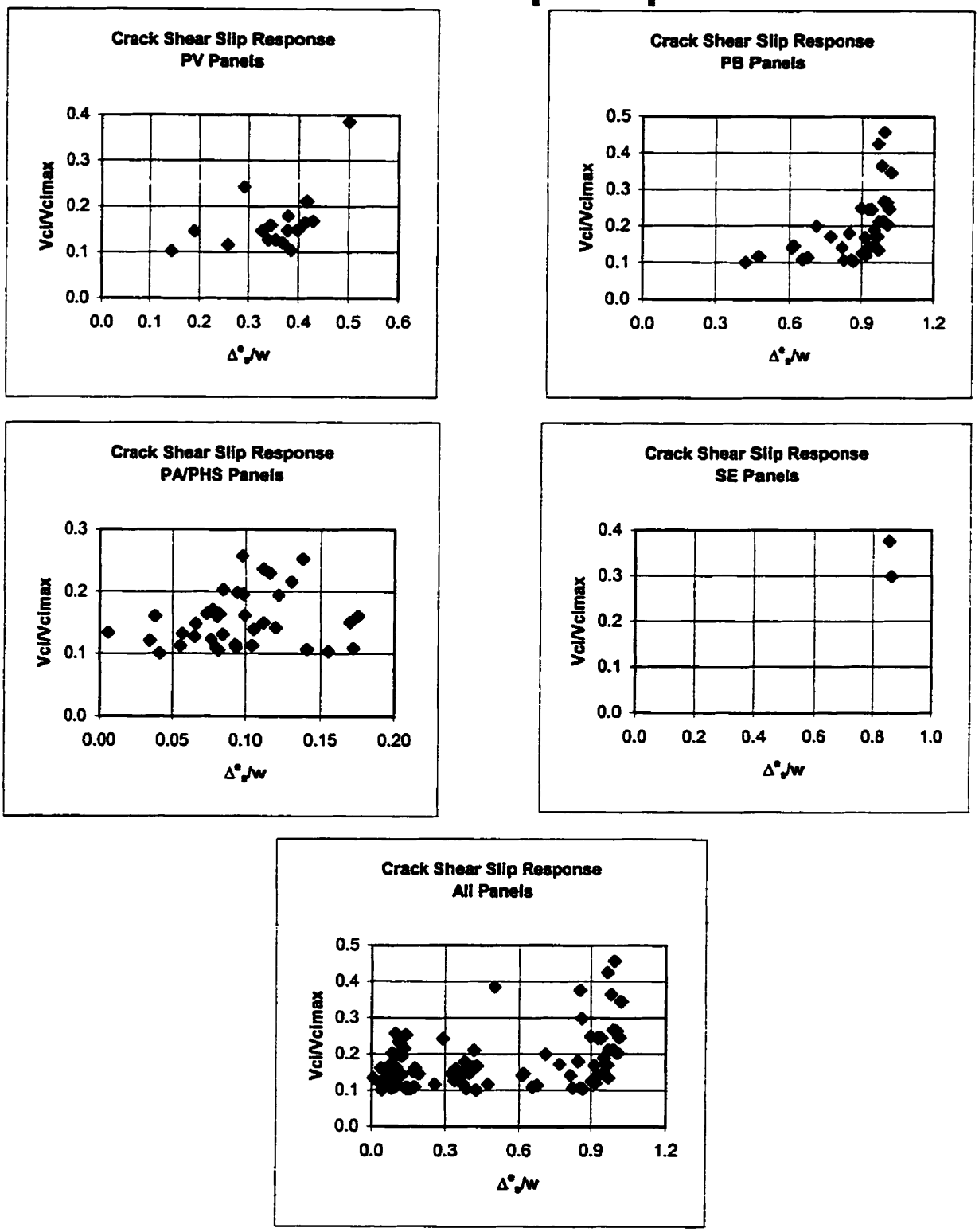

Figure 4.3 Vci/Vcimax vs. Δ^{e}_{s}/w

4.3 Shear Slip Formulation – Theoretical

In the shear slip formulation, various alternatives were considered for modelling crack shear slip. As discussed in the previous chapter, one alternative was to fix the degree of "lag" between the rotation of the stress field in the concrete and that of the strain field. A second alternative was to employ an explicit constitutive model to relate the amount of shear slip along the crack to the magnitude of the shear stress acting on the crack. In the DSFM formulation, a hybrid approach can be taken to combine the two.

For the stress-based approach, the relationships considered included those of Okamura and Maekawa (1991) and Walraven (1981). Also, an alternative formulation is proposed herein.

Model I: Maekawa

$$\Delta_s^t = 1.0w\sqrt{\frac{\psi}{1-\psi}}$$

where $\psi = \frac{v_{ci}}{v_{ci\max}}$.

Δ_s^t = theoretical slip displacement along the crack (mm); v_{ci} = shear stress acting on the crack (MPa); $v_{ci\max}$ = the maximum shear stress that can be resisted on the crack; w = average crack width (mm); a = aggregate size in mm.

For $v_{ci\max}$, the Vecchio-Collins (1986) relationship is used, as follows:

$$v_{ci\max} = \frac{\sqrt{f'c}}{0.31 + \frac{24w}{a+16}} \text{(MPa)}$$

Model II: Walraven – Model A

$$\Delta_s^t = \frac{v_{ci}}{1.8w^{-0.8} + (0.234w^{-0.707} - 0.20)\cdot f_{cc}}$$

where f_{cc} = concrete cube strength (MPa), approximately 1.2f'c.

Walraven – Model B

$$\Delta_s' = \frac{(v_{ci} + v_{co})}{[1.8w^{-0.8} + (0.234w^{-0.707} - 0.20) \cdot f_{cc}]}$$

where $v_{co} = \frac{f_{cc}}{30}$

Walraven Model B adds v_{co} to the stiffness portion of the formulation, where v_{co} is the initial shear slip from Walraven test data.

Model III: Lai/Vecchio – Model A

$$\Delta_s' = \Delta_s \sqrt{\frac{\psi}{1-\psi}}$$

where $\Delta_s = \frac{0.5 v_{ci\max}}{1.8w^{-0.8} + (0.234w^{-0.707} - 0.20) \cdot f_{cc}}$

$$\psi = \frac{v_{ci}}{v_{ci\max}}$$

$$v_{ci\max} = \frac{\sqrt{f'c}}{0.31 + \frac{24w}{a+16}}$$

Lai/Vecchio – Model B

$$\Delta_s' = 2\Delta_2 \sqrt{\frac{\psi}{1-\psi}}$$

where $\Delta_2 = \frac{0.2 v_{ci\max}}{1.8w^{-0.8} + (0.234w^{-0.707} - 0.20) \cdot f_{cc}}$

$$\psi = \frac{v_{ci}}{v_{ci\max}}$$

$$v_{ci\max} = \frac{\sqrt{f'c}}{0.31 + \frac{24w}{a+16}}$$

Note: The theoretical slip in Model B will be 80% of Model A.

Lai/Vecchio – Model C

$$\Delta_s^t = 2\Delta_2\sqrt{\frac{\psi}{1-\psi}}$$

where $\Delta_2 = \dfrac{(0.2v_{ci\max} + v_{co})}{1.8w^{-0.8} + (0.234w^{-0.707} - 0.20)\cdot f_{cc}}$

$$v_{co} = \frac{f_{cc}}{30}$$

$$\psi = \frac{v_{ci}}{v_{ci\max}}$$

$$v_{ci\max} = \frac{\sqrt{f'c}}{0.31 + \dfrac{24w}{a+16}}$$

Based on the theoretical data, the following plots were constructed for each of the model above.

Δ_s^e *vs.* Δ_s^t

Δ_s^e / Δ_s^t *vs.* $v_{ci} / v_{ci\max}$

The plots are given in Figures 4.4 to 4.15.

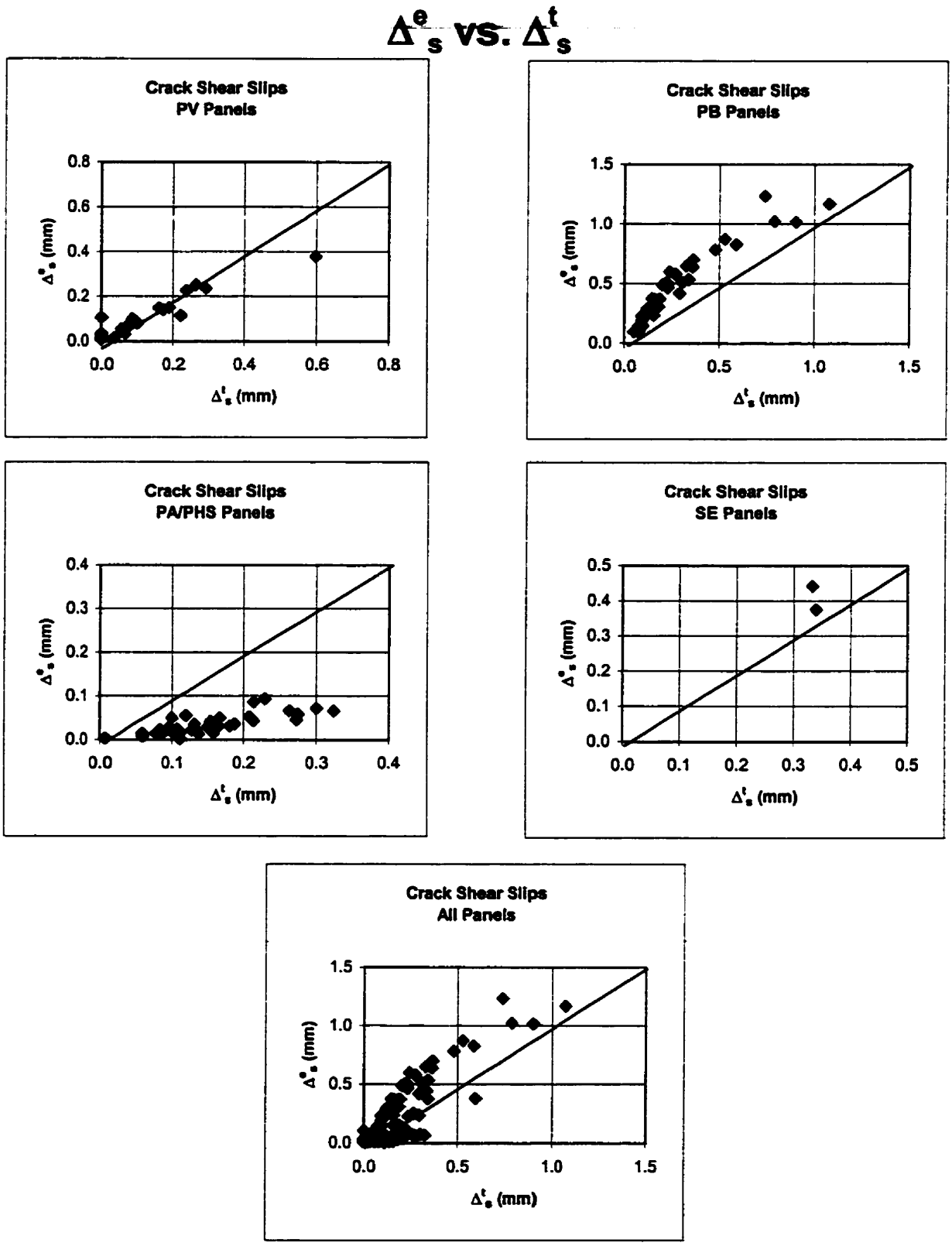

Figure 4.4 Model I: Maekawa

Δ^e_s/Δ^t_s vs. Vci/Vcimax

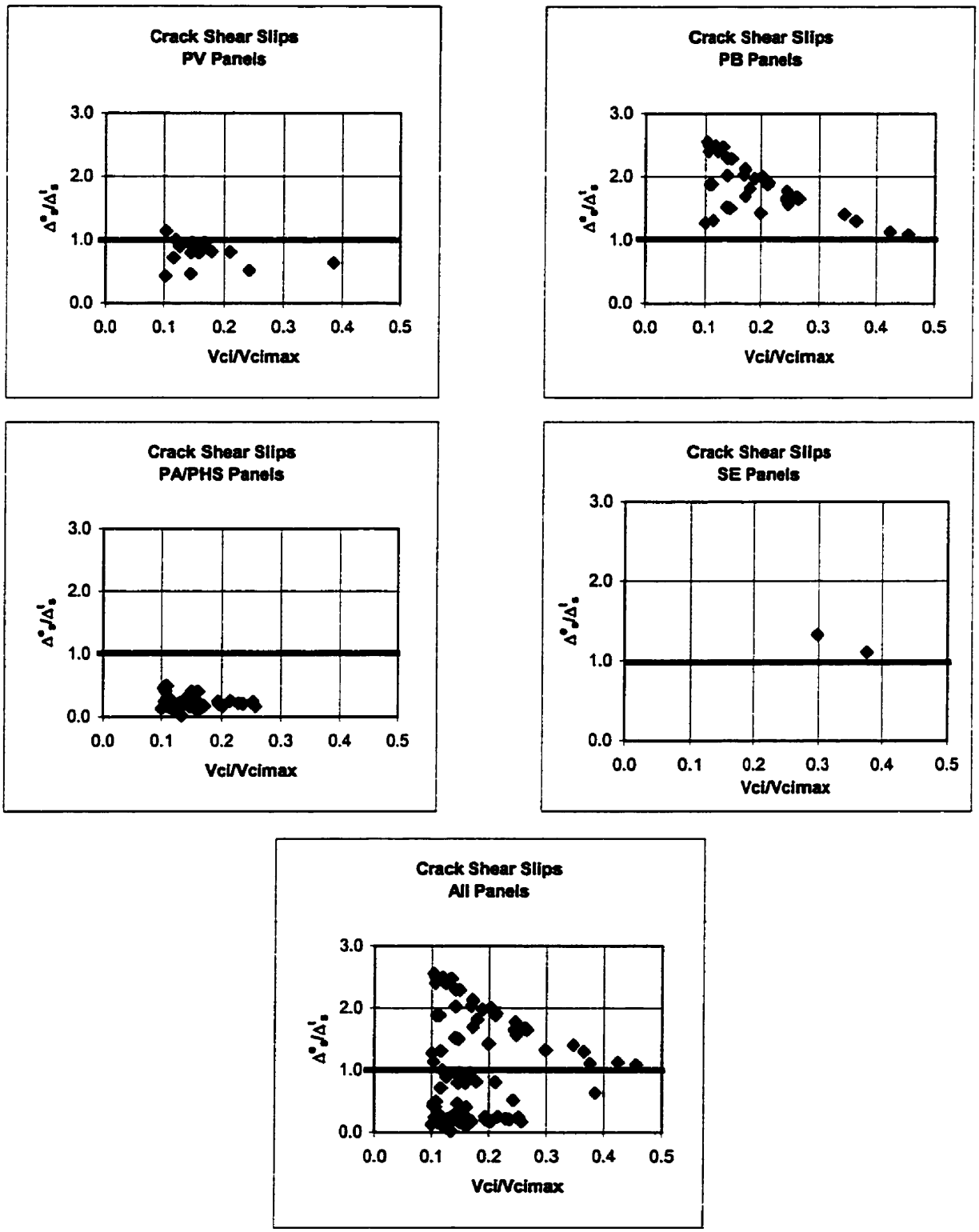

Figure 4.5 Model I: Maekawa

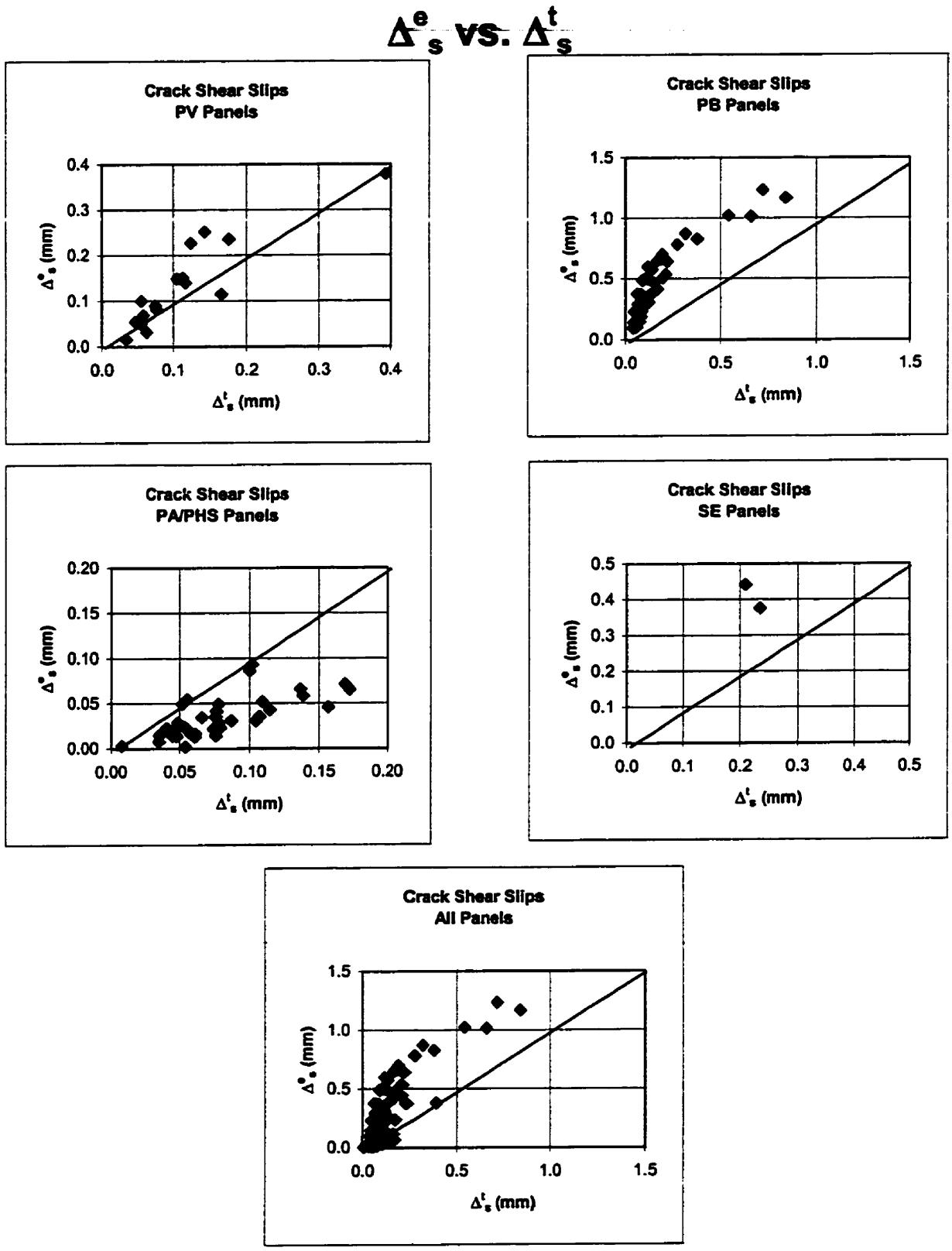

Figure 4.6 Model II: Walraven – Model A

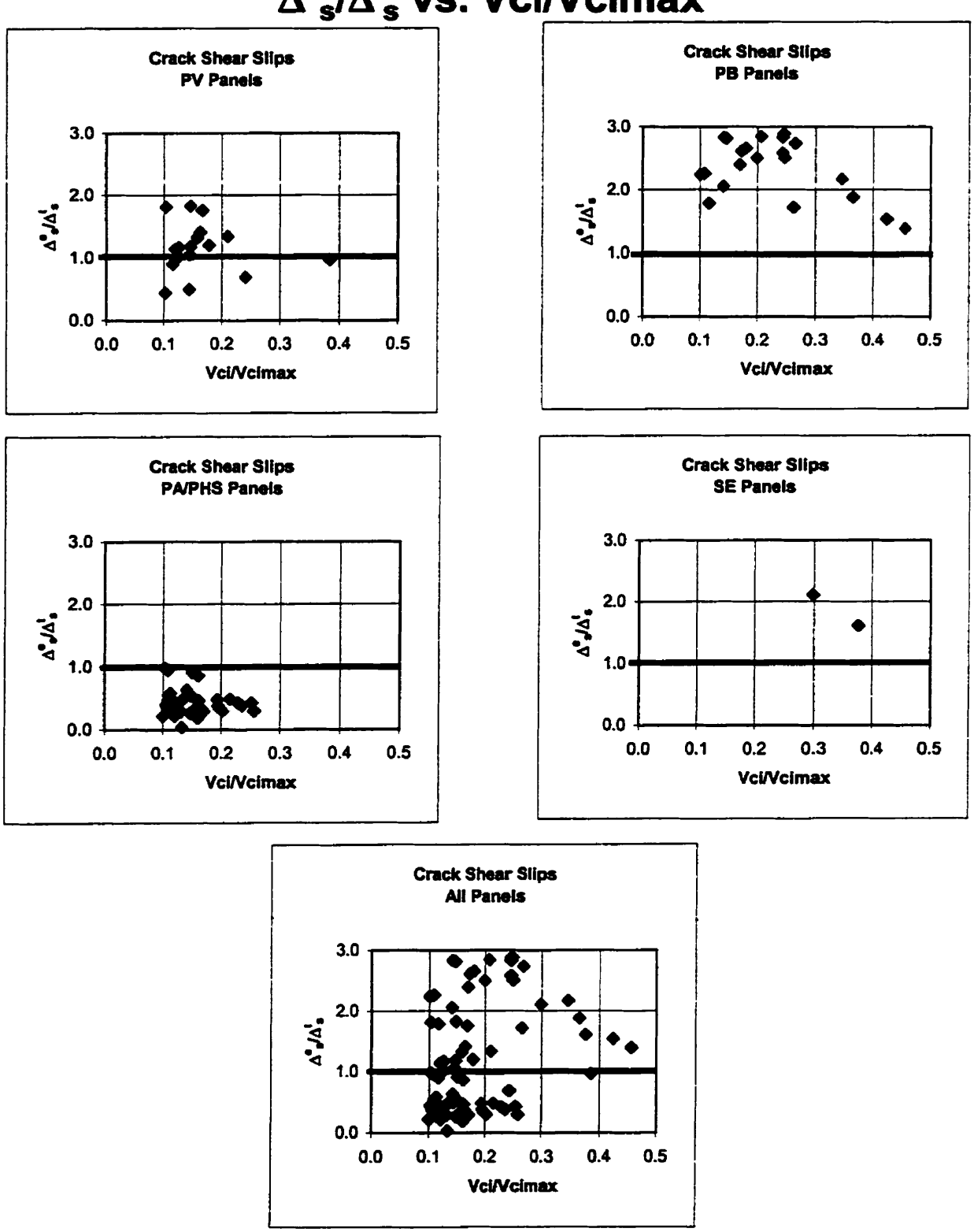

Figure 4.7 Model II: Walraven – Model A

Δ^e_s vs. Δ^t_s

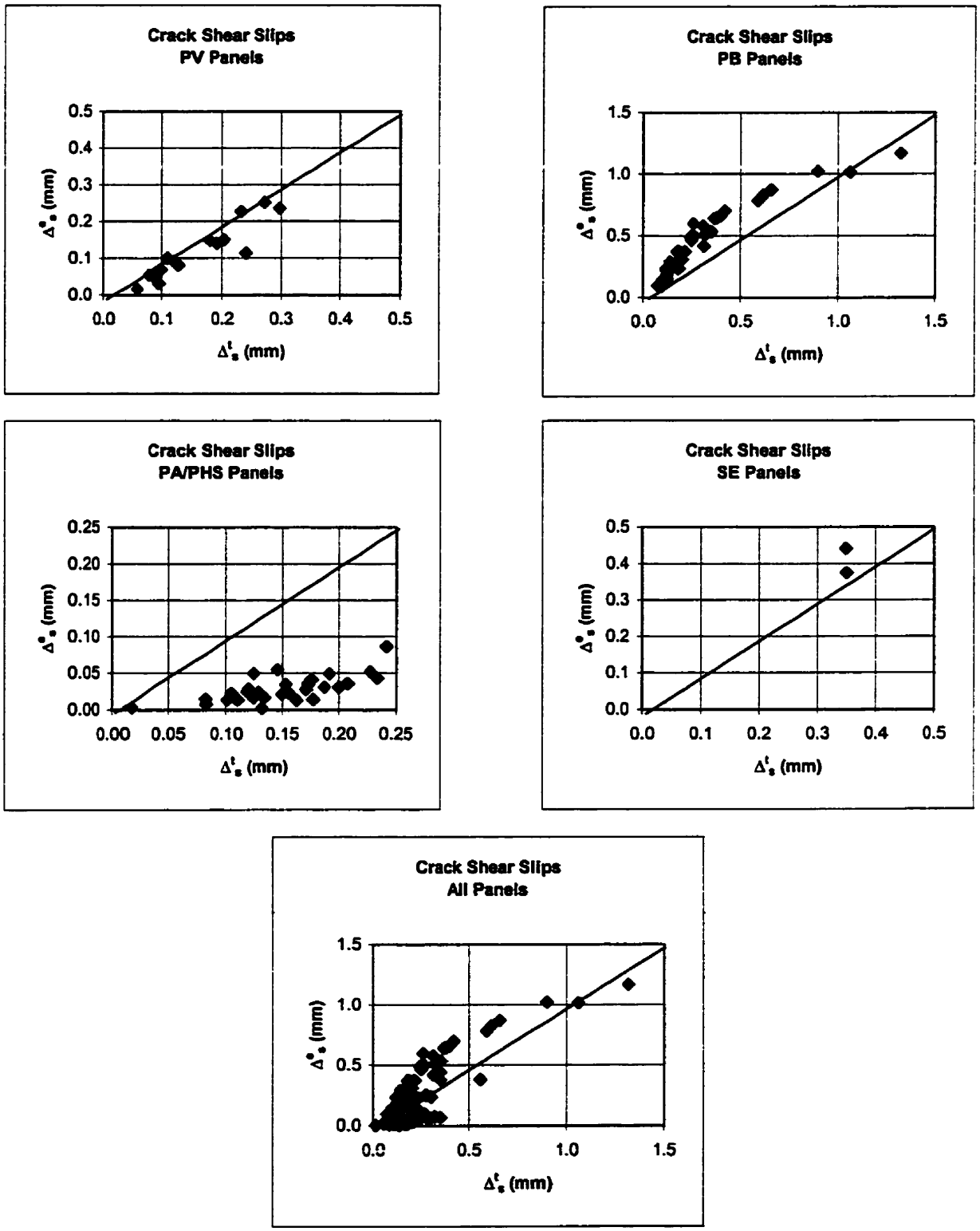

Figure 4.8 Model II: Walraven – Model B

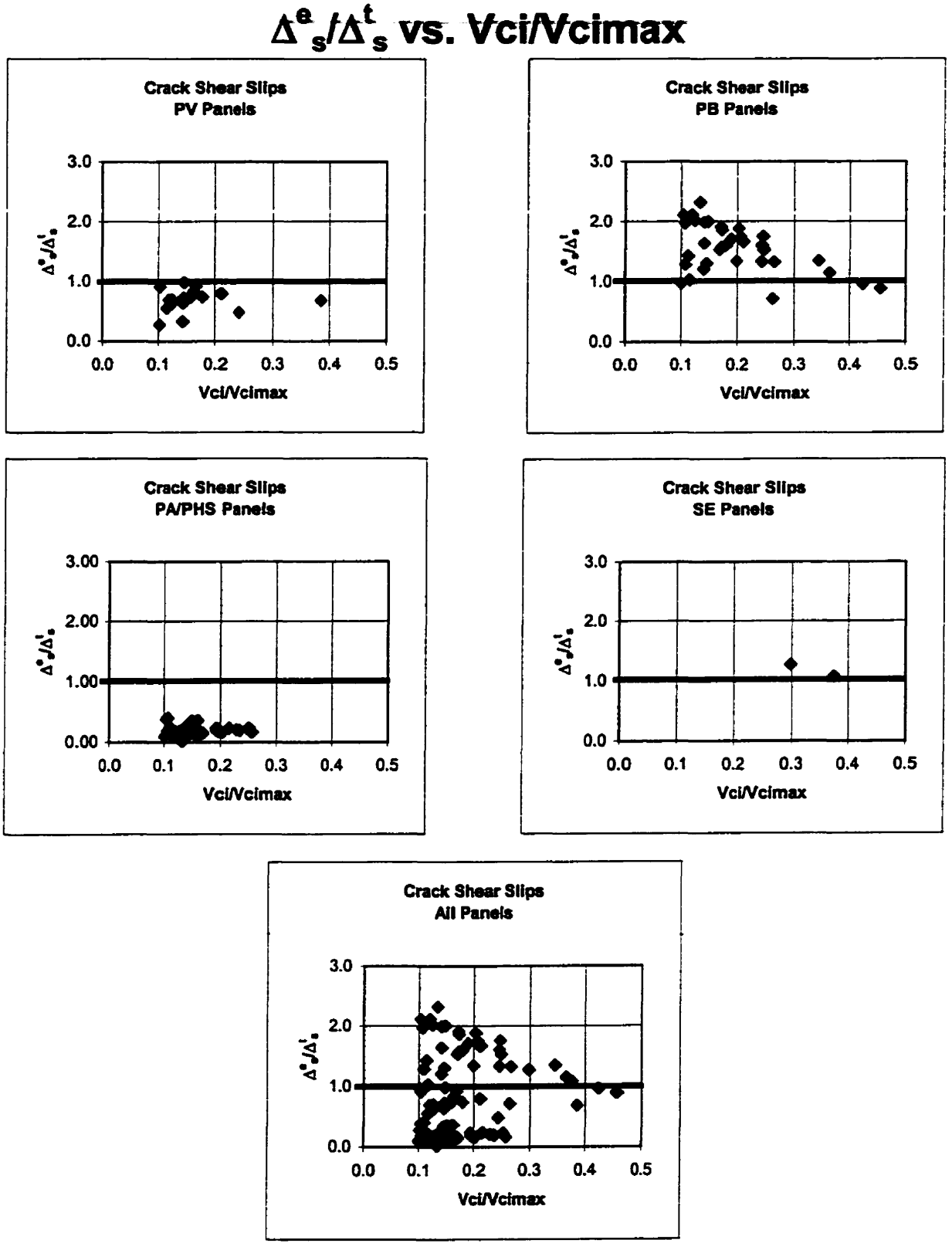

Figure 4.9 Model II: Walraven – Model B

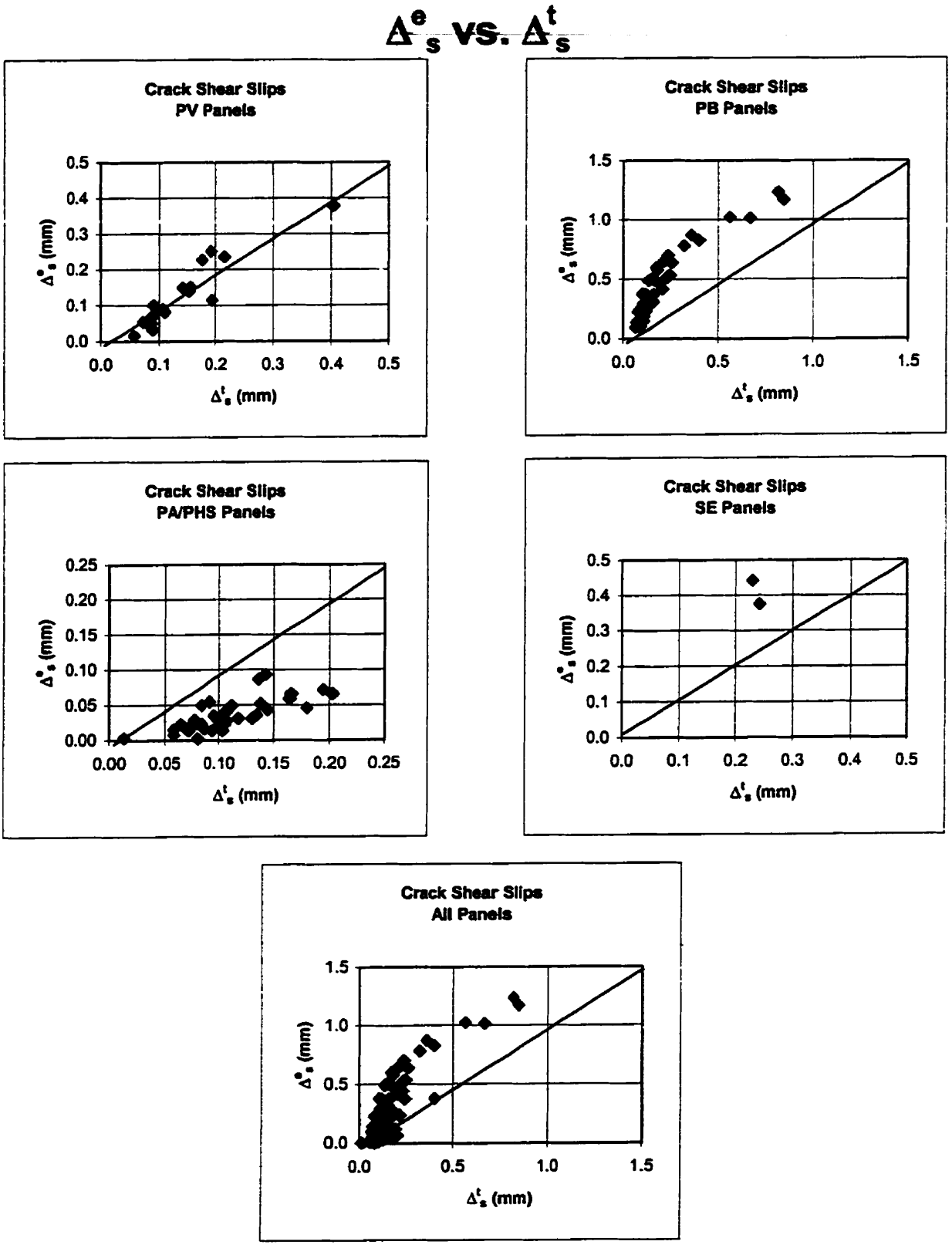

Figure 4.10 Model III: Lai/Vecchio – Model A

Δ^e_s/Δ^t_s vs. Vci/Vcimax

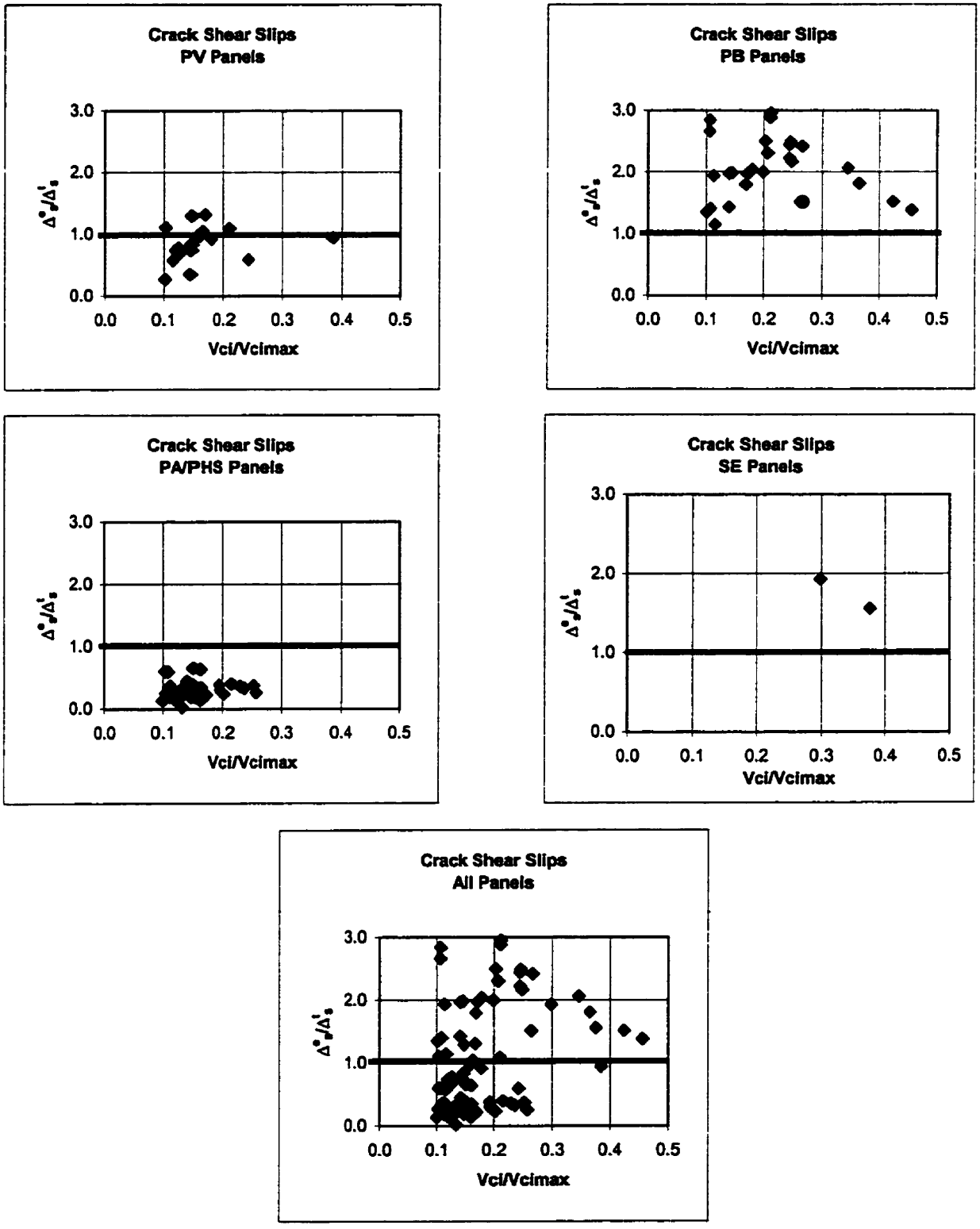

Figure 4.11 Model III: Lai/Vecchio – Model A

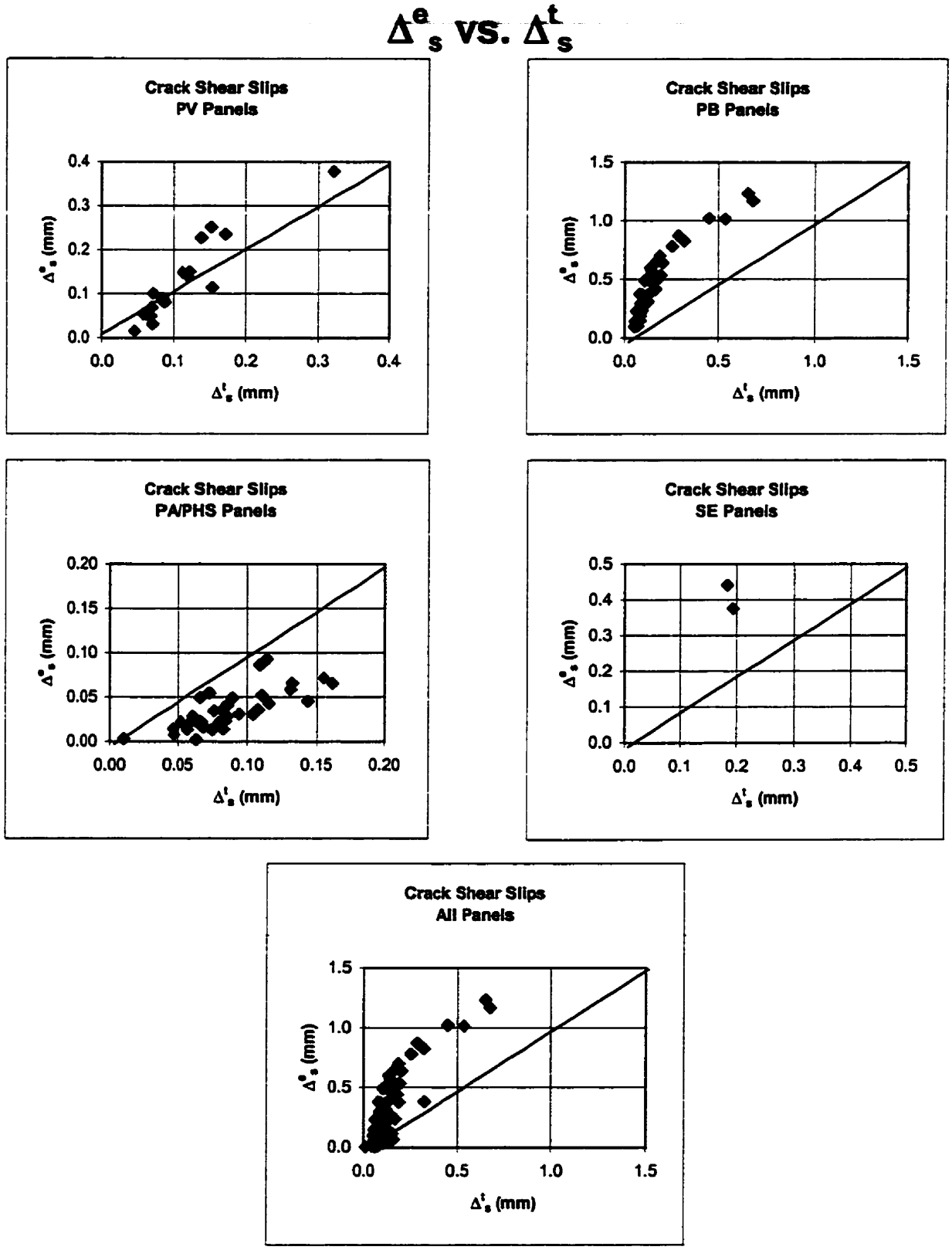

Figure 4.12 Model III: Lai/Vecchio – Model B

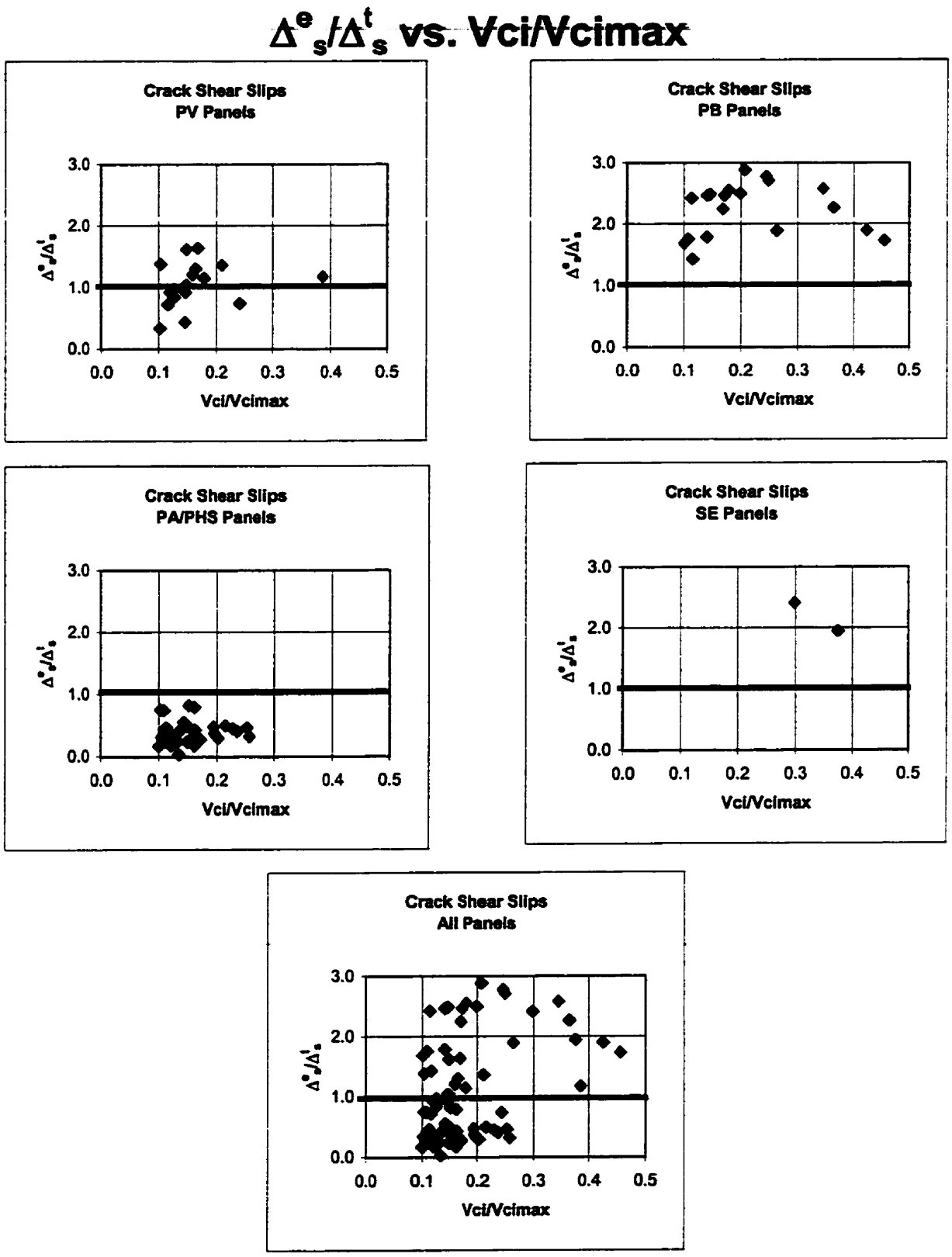

Figure 4.13 Model III: Lai/Vecchio – Model B

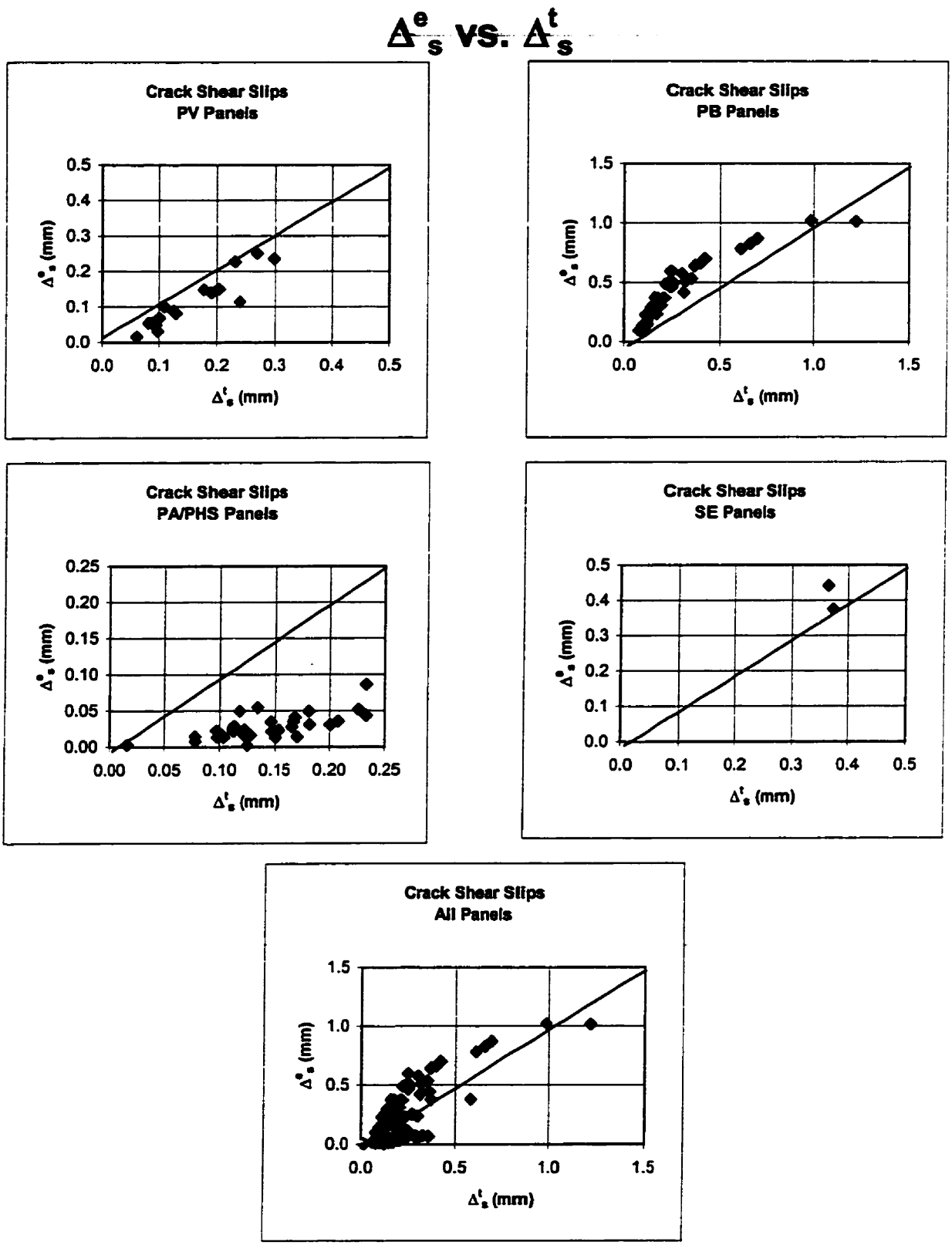

Figure 4.14 Model III: Lai/Vecchio – Model C

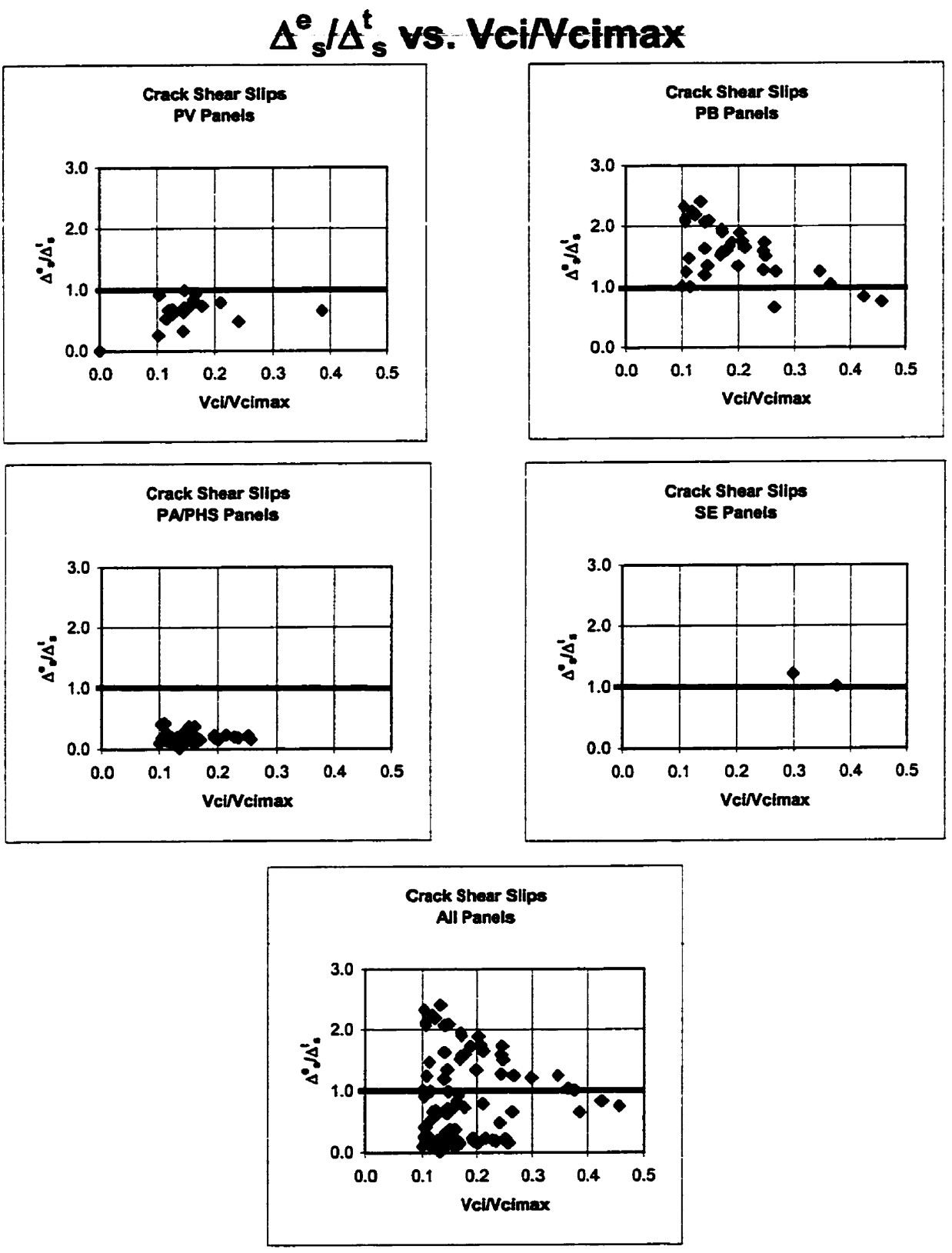

Figure 4.15 Model III: Lai/Vecchio – Model C

In the Maekawa model, the experimental slip was very well predicted for the PV panels. Experimental shear slip was under-estimated in the PB/SE panels, while it was over-estimated in the PA/PHS panels. (see Figure 4.4) These under- and over-estimated trends seemed to occur with all models. In Figure 4.5, the Δ_s^e / Δ_s^t *versus* $v_{ci} / v_{ci\max}$ correlation was constructed for the Maekawa model. It can be seen that Δ_s^e / Δ_s^t varies from 0 to 2.5 and $v_{ci} / v_{ci\max}$ varies from 0 to 0.5. The overall trends were fairly well represented by the Maekawa model.

With Walraven Model A, the experimental slip for the PV panels was not as well predicted as with Walraven Model B. The general shape for experimental shear slip versus theoretical shear slip (Δ_s^e *versus* Δ_s^t) in PB/SE/PA/PHS panels seemed to be very similar in both models, with Model B being closer to the 45-degree line. By looking at Δ_s^e / Δ_s^t in the Walraven models, Model A ranges from 0 to 6 and model B ranges from 0 to 4. Also, Model B shows a closer fit to $\Delta_s^e / \Delta_s^t = 1$. Hence, Model B is a better fit.

Out of the three Lai/Vecchio models for the PV panels, the experimental slip was best predicted with Models A and C. In fact, the experimental slip was very well predicted in these two models for the PV panels. The experimental slip was uder-estimated with all three models for the PB panels. Model C seems to have the best prediction out of the three models for the PB panels. An over-estimation for the experimental slip was seen on the PA/PHS panels with all models. Model B seems to have the best prediction in this case. Lai/Vecchio model C has the best prediction of experimental slip out of the three models. By looking at Δ_s^e / Δ_s^t *versus* $v_{ci} / v_{ci\max}$, it can be seen that $v_{ci} / v_{ci\max}$ varies from 0 to 0.5 for all 3 models. When looking at Δ_s^e / Δ_s^t in the Lai/Vecchio models, Models A and B range from 0 to 3.0 and Model C range from 0 to 2.5. Therefore, Model C data points have the closest fit to $\Delta_s^e / \Delta_s^t = 1$.

By comparing all the models, the Lai/Vecchio model seems to provide the best correlations. In chapter five and six, the various models discussed above will be implemented into the nonlinear finite element program VecTor2 to analyze the different structures under monotonic and cyclic loads.

CHAPTER 5

Analyses of Structures --- Monotonic Loading

5.1 Panel Elements

Three series of test panels were examined: the PV-, PB- and PA/PHS- series specimens. The PV-Series Panels, tested by Vecchio and Collins (1982), were the original panels on which the constitutive models of the MCFT were based. These panels were generally orthogonally reinforced, and subjected to various conditions of shear and normal stresses. The PB-Series panels were tested by Bhide and Collins (1989); these were generally uniaxially reinforced and subjected to various combinations of uniaxial tension and shear. The PA- and PHS-Series panels were tested by Vecchio, Collins and Aspiotis (1993). This last set involved panels constructed from high strength concrete, orthogonally reinforced ($\rho_y < \rho_x$), and subjected to various combinations of shear and normal stress. Specimen details are fully documented in the respective references; some relevant details are given in Table 5.1.

Table 5.1

Panel	f_c (MPa)	f_t (MPa)	ε_0 ($x10^3$)	ρ_x (%)	ρ_y (%)	f_{yx} (MPa)	f_{yy} (MPa)	Loading $\sigma_x:\sigma_y:v$
PV10	14.5	1.59	2.70	1.79	1.00	276	276	0:0:1
PV11	15.6	1.62	2.60	1.79	1.31	235	235	0:0:1
PV12	16.0	1.64	2.50	1.79	0.45	469	269	0:0:1
PV16	21.7	1.81	2.00	0.74	0.74	255	255	0:0:1
PV18	19.5	1.75	2.20	1.79	0.32	431	412	0:0:1
PV19	19.0	1.73	2.15	1.79	0.71	458	300	0:0:1
PV20	19.6	1.75	1.80	1.79	0.89	460	297	0:0:1
PV21	19.5	1.75	1.80	1.79	1.30	458	302	0:0:1
PV22	19.6	1.75	2.00	1.79	1.52	458	420	0:0:1
PV23	20.5	1.78	2.00	1.79	1.79	518	518	-0.39:-0.39:1
PV25	19.3	1.74	1.80	1.79	1.79	466	466	-0.69:-0.69:1
PV27	20.5	1.78	1.90	1.79	1.79	442	442	0:0:1
PV28	19.0	1.73	1.85	1.79	1.79	483	483	0.32:0.32:1
PA1	49.9	2.39	2.09	1.65	0.82	522	522	0:0:1
PA2	43.0	2.28	1.99	1.65	0.82	522	522	0:0:1
PHS1	72.2	2.71	2.68	3.23	0.00	606	0	0:0:1
PHS2	66.1	2.63	2.48	3.23	0.41	606	521	0:0:1
PHS3	58.4	2.52	2.44	3.23	0.82	606	521	0:0:1
PHS4	68.5	2.66	2.60	3.23	0.82	606	521	0.25:0.25:1
PHS5	52.1	2.43	2.58	3.23	0.41	606	521	0.25:0.25:1
PHS6	49.7	2.39	2.25	3.23	0.41	606	521	-0.25:-0.25:1
PHS7	53.6	2.45	2.10	3.23	0.82	606	521	-0.25:-0.25:1
PHS8	55.9	2.49	2.17	3.23	1.24	606	521	0:0:1
PHS9	56.0	2.49	2.68	3.23	0.41	606	521	-0.25:-0.25:1
PHS10	51.4	2.42	2.45	3.23	1.24	606	521	0.25:0.25:1
PB4	16.4	1.65	1.88	1.09	0.00	423	0	0.96:0:1
PB5	23.5	1.86	1.78	1.09	0.00	415	0	0.97:-1.03:1
PB6	17.6	1.69	1.86	1.09	0.00	425	0	1:0:1
PB7	20.2	1.77	2.15	1.09	0.00	425	0	1.89:0:-1
PB8	20.4	1.77	1.95	1.09	0.00	425	0	2.98:0:-1
PB10	24.0	1.88	1.88	1.09	0.00	433	0	5.94:0:-1
PB14	41.1	2.24	2.81	2.02	0.00	489	0	3.01:0:-1
PB16	41.7	2.25	3.23	2.02	0.00	502	0	1.96:0:-1
PB17	41.6	2.25	3.08	2.02	0.00	502	0	5.93:0:-1
PB19	20.0	1.76	1.91	2.20	0.00	402	0	1.01:0:-1
PB20	21.7	1.81	1.89	2.20	0.00	424	0	2.04:0:-1
PB21	21.8	1.82	1.80	2.20	0.00	402	0	3.08:0:-1
PB22	17.6	1.69	2.03	2.20	0.00	433	0	6.09:0:-1
PB28	22.7	1.84	2.01	0.00	2.20	0	426	0:1.98:1
PB29	41.6	2.25	2.60	2.02	0.00	496	0	0:2.02:-1
PB30	40.4	2.23	2.60	2.02	0.00	496	0	0:2.96:-1
PB31	43.4	2.28	3.00	2.02	0.00	496	0	0:5.78:-1
PB32	57.7	2.51	2.55	2.20	0.00	415	0	0:3.01:-1

Analyses were performed for all panels using both the MCFT and the DSFM. For the DSFM, separate analysis series were undertaken for each of the various slip model options: stress-based (Walraven, Maekawa and Lai/Vecchio derivative models), and hybrid-based (Hybrid I: Walraven + 5° lag, Hybrid II: Maekawa + 5° lag, Hybrid III: Lai/Vecchio + 5° lag). The computed shear capacities, and comparisons to the experimentally determined strengths, with and without the initial offset slip factor, are given in Table 5.2 and 5.3 for the 43 panels examined.

Table 5.2 Analyses with initial offset slip factor

Panel	f'c	f't	Ec	Vu-exp	Vu-theor/Vu-exp						
	(MPa)	(MPa)	(MPa)	(MPa)	0	1	2	3	4	5	6
Vecchio					No slip	Walraven	Maekawa	Lai	Hybrid I	Hybrid II	Hybrid III
PV10	14.5	1.59	10700	3.97	0.947	0.952	0.952	0.952	0.952	0.952	0.952
PV11	15.6	1.62	12000	3.56	1.011	1.034	1.039	1.034	1.034	1.034	1.034
PV12	16.0	1.64	12800	3.13	0.990	0.907	0.869	0.907	0.927	0.907	0.927
PV16	21.7	1.81	21700	2.14	0.935	1.000	1.000	1.000	1.000	1.000	1.000
PV18	19.5	1.75	17700	3.04	1.118	1.020	0.967	1.013	1.039	1.013	1.039
PV19	19.0	1.73	17700	3.95	1.033	1.003	0.982	1.003	1.013	0.992	1.003
PV20	19.6	1.75	21800	4.26	1.028	1.021	1.007	1.014	1.028	1.014	1.021
PV21	19.5	1.75	21700	5.03	1.002	1.103	1.026	1.085	1.074	1.074	1.074
PV22	19.6	1.75	19600	6.07	1.023	1.149	1.133	1.133	1.102	1.123	1.123
PV23	20.5	1.78	20500	8.87	0.807	0.915	0.915	0.915	0.915	0.915	0.915
PV25	19.3	1.74	21400	9.12	0.811	0.899	0.899	0.899	0.899	0.899	0.899
PV27	20.5	1.78	21600	6.35	1.018	1.184	1.184	1.184	1.184	1.184	1.184
PV28	19.0	1.73	20500	5.8	0.985	1.125	1.125	1.125	1.125	1.125	1.125
				Mean	0.978	1.024	1.008	1.020	1.022	1.018	1.023
				COV(%)	8.88	9.14	9.37	8.90	8.35	8.77	8.54

Table 5.2 (cont'd)

Panel	f'c	f't	Ec	Vu-exp	Vu-theor/Vu-exp						
	(MPa)	(MPa)	(MPa)	(MPa)	0	1	2	3	4	5	6
Aspiotis					No slip	Walraven	Maekawa	Lai	Hybrid I	Hybrid II	Hybrid III
PA1	49.9	2.39	47800	6.34	0.974	0.979	0.974	0.974	0.979	0.974	0.974
PA2	43.0	2.28	43200	6.22	0.993	0.993	0.993	0.993	0.993	0.993	0.993
PHS1	72.2	2.71	53900	2.95	0.985	0.917	0.917	0.917	0.917	0.917	0.917
PHS2	66.1	2.63	53300	6.66	0.965	0.865	0.769	0.865	0.874	0.884	0.879
PHS3	58.4	2.52	47900	8.19	1.099	1.065	0.962	1.060	1.079	1.109	1.069
PHS4	68.5	2.66	52700	6.91	1.009	0.944	0.870	0.940	0.949	1.009	0.949
PHS5	52.1	2.43	40400	4.81	0.905	0.818	0.762	0.812	0.830	0.849	0.824
PHS6	49.7	2.39	44200	9.89	0.882	0.926	0.906	0.894	0.870	0.870	0.870
PHS7	53.6	2.45	51000	10.26	1.099	1.222	1.216	1.210	1.152	1.158	1.146
PHS8	55.9	2.49	51500	10.84	0.986	1.052	1.046	1.046	1.024	1.035	1.024
PHS9	56.0	2.49	41800	9.37	0.999	0.948	0.825	0.942	0.958	0.989	0.958
PHS10	51.4	2.42	42000	8.58	0.993	1.025	0.932	1.025	0.988	1.011	0.993
				Mean	0.991	0.979	0.931	0.973	0.968	0.983	0.966
				COV(%)	6.39	10.75	13.44	10.81	9.40	9.49	9.25

Panel	f'c	f't	Ec	Vu-exp	Vu-theor/Vu-exp						
	(MPa)	(MPa)	(MPa)	(MPa)	0	1	2	3	4	5	6
Bhide					No slip	Walraven	Maekawa	Lai	Hybrid I	Hybrid II	Hybrid III
PB4	16.4	1.65	17500	1.16	1.080	0.957	0.957	0.950	0.957	0.957	0.957
PB5	23.5	1.86	26400	2.64	0.920	0.920	0.920	0.917	0.920	0.924	0.917
PB6	17.6	1.69	18900	1.15	1.099	0.974	0.974	0.967	0.974	0.974	0.974
PB7	20.2	1.77	18800	0.86	1.299	1.203	1.194	1.194	1.203	1.194	1.203
PB8	20.4	1.77	20900	0.80	1.188	1.138	1.131	1.125	1.138	1.131	1.125
PB10	24.0	1.88	25600	0.56	1.179	1.171	1.171	1.164	1.171	1.171	1.164
PB14	41.1	2.24	29200	1.54	0.984	0.867	0.828	0.857	0.857	0.828	0.857
PB16	41.7	2.25	25900	1.42	1.197	1.042	1.000	1.028	1.035	1.000	1.035
PB17	41.6	2.25	27100	1.22	0.984	0.905	0.866	0.892	0.892	0.866	0.892
PB19	20.0	1.76	20900	1.28	1.211	1.008	1.023	1.000	1.016	1.023	1.016
PB20	21.7	1.81	23000	1.42	1.310	1.141	1.141	1.141	1.148	1.148	1.155
PB21	21.8	1.82	24200	1.42	0.930	0.782	0.775	0.775	0.782	0.775	0.775
PB22	17.6	1.69	17400	1.03	1.025	0.870	0.854	0.862	0.870	0.854	0.862
PB28	22.7	1.84	22600	1.53	0.980	0.797	0.804	0.791	0.804	0.804	0.797
PB29	41.6	2.25	32000	1.49	1.121	0.980	0.940	0.966	0.973	0.946	0.966
PB30	40.4	2.23	31100	1.48	1.020	0.892	0.858	0.885	0.892	0.858	0.885
PB31	43.4	2.28	28900	1.15	1.050	1.023	0.932	0.960	0.953	0.932	0.953
PB32	57.7	2.51	45300	1.49	1.067	0.940	0.973	0.973	0.966	0.940	0.966
				Mean	1.091	0.978	0.963	0.969	0.975	0.963	0.972
				COV(%)	10.81	12.65	13.24	12.68	12.72	13.31	12.86
			Total:	**Mean**	**1.029**	**0.992**	**0.968**	**0.986**	**0.987**	**0.985**	**0.986**
				COV(%)	**10.53**	**11.06**	**12.28**	**11.07**	**10.64**	**11.01**	**10.74**

Table 5.3 Analyses without initial offset slip factor

Panel	f'c	f't	Ec	Vu-exp	Vu-theor/Vu-exp						
	(MPa)	(MPa)	(MPa)	(MPa)	0	1	2	3	4	5	6
Vecchio					No slip	Walraven	Maekawa	Lai	Hybrid I	Hybrid II	Hybrid III
PV10	14.5	1.59	10700	3.97	0.947	0.957	0.957	0.957	0.952	0.952	0.952
PV11	15.6	1.62	12000	3.56	1.011	1.034	1.034	1.034	1.034	1.034	1.034
PV12	16.0	1.64	12800	3.13	0.990	0.952	0.869	0.946	0.958	0.907	0.952
PV16	21.7	1.81	21700	2.14	0.935	1.000	1.000	1.000	1.000	1.000	1.000
PV18	19.5	1.75	17700	3.04	1.118	1.072	0.974	1.066	1.079	1.013	1.079
PV19	19.0	1.73	17700	3.95	1.033	1.038	0.982	1.023	1.038	0.992	1.028
PV20	19.6	1.75	21800	4.26	1.028	1.049	1.007	1.035	1.056	1.028	1.035
PV21	19.5	1.75	21700	5.03	1.002	1.109	1.080	1.091	1.056	1.074	1.074
PV22	19.6	1.75	19600	6.07	1.023	1.149	1.133	1.133	1.107	1.123	1.123
PV23	20.5	1.78	20500	8.87	0.807	0.915	0.915	0.915	0.915	0.915	0.915
PV25	19.3	1.74	21400	9.12	0.811	0.899	0.899	0.899	0.899	0.899	0.899
PV27	20.5	1.78	21600	6.35	1.018	1.184	1.184	1.184	1.184	1.184	1.184
PV28	19.0	1.73	20500	5.8	0.985	1.125	1.125	1.125	1.125	1.125	1.125
				Mean	0.978	1.037	1.012	1.031	1.031	1.019	1.031
				COV(%)	8.88	8.69	9.47	8.50	8.16	8.77	8.36

Panel	f'c	f't	Ec	Vu-exp	Vu-theor/Vu-exp						
	(MPa)	(MPa)	(MPa)	(MPa)	0	1	2	3	4	5	6
Aspiotis					No slip	Walraven	Maekawa	Lai	Hybrid I	Hybrid II	Hybrid III
PA1	49.9	2.39	47800	6.34	0.974	0.979	0.974	0.979	0.979	0.974	0.979
PA2	43.0	2.28	43200	6.22	0.993	0.993	0.993	0.993	0.993	0.993	0.993
PHS1	72.2	2.71	53900	2.95	0.985	0.917	0.917	0.917	0.917	0.917	0.917
PHS2	66.1	2.63	53300	6.66	0.965	0.903	0.769	0.898	0.913	0.884	0.908
PHS3	58.4	2.52	47900	8.19	1.099	1.133	0.962	1.109	1.113	1.109	1.109
PHS4	68.5	2.66	52700	6.91	1.009	0.977	0.870	0.972	0.977	1.009	0.977
PHS5	52.1	2.43	40400	4.81	0.905	0.849	0.762	0.862	0.849	0.849	0.849
PHS6	49.7	2.39	44200	9.89	0.882	0.938	0.906	0.898	0.906	0.870	0.898
PHS7	53.6	2.45	51000	10.26	1.099	1.228	1.216	1.210	1.169	1.158	1.164
PHS8	55.9	2.49	51500	10.84	0.986	1.052	1.046	1.046	1.041	1.035	1.035
PHS9	56.0	2.49	41800	9.37	0.999	1.060	0.825	1.004	1.009	0.989	1.004
PHS10	51.4	2.42	42000	8.58	0.993	1.025	0.932	1.021	1.016	1.011	1.016
				Mean	0.991	1.005	0.931	0.992	0.990	0.983	0.987
				COV(%)	6.39	10.41	13.44	9.90	9.12	9.49	9.05

Table 5.3 (cont'd)

Panel	f'c	f't	Ec	Vu-exp	Vu-theor/Vu-exp						
	(MPa)	(MPa)	(MPa)	(MPa)	0	1	2	3	4	5	6
Bhide					No slip	Walraven	Maekawa	Lai	Hybrid I	Hybrid II	Hybrid III
PB4	16.4	1.65	17500	1.16	1.080	0.983	0.957	0.983	0.990	0.957	0.983
PB5	23.5	1.86	26400	2.64	0.920	0.920	0.920	0.920	0.920	0.924	0.920
PB6	17.6	1.69	18900	1.15	1.099	1.009	0.974	1.002	1.009	0.974	1.009
PB7	20.2	1.77	18800	0.86	1.299	1.247	1.194	1.229	1.247	1.194	1.229
PB8	20.4	1.77	20900	0.80	1.188	1.156	1.131	1.144	1.150	1.131	1.144
PB10	24.0	1.88	25600	0.56	1.179	1.171	1.171	1.171	1.171	1.171	1.171
PB14	41.1	2.24	29200	1.54	0.984	0.896	0.828	0.877	0.867	0.828	0.867
PB16	41.7	2.25	25900	1.42	1.197	1.077	1.000	1.042	1.063	1.000	1.063
PB17	41.6	2.25	27100	1.22	0.984	0.931	0.866	0.911	0.892	0.866	1.106
PB19	20.0	1.76	20900	1.28	1.211	1.063	1.023	1.055	1.063	1.023	1.063
PB20	21.7	1.81	23000	1.42	1.310	1.190	1.141	1.204	1.197	1.148	1.211
PB21	21.8	1.82	24200	1.42	0.930	0.824	0.775	0.810	0.817	0.775	0.810
PB22	17.6	1.69	17400	1.03	1.025	0.909	0.854	0.893	0.901	0.854	0.893
PB28	22.7	1.84	22600	1.53	0.980	0.843	0.804	0.830	0.843	0.804	0.830
PB29	41.6	2.25	32000	1.49	1.121	1.013	0.940	1.000	0.993	0.946	0.993
PB30	40.4	2.23	31100	1.48	1.020	0.926	0.858	0.912	0.899	0.858	0.899
PB31	43.4	2.28	28900	1.15	1.050	1.002	0.932	0.981	0.953	0.932	0.960
PB32	57.7	2.51	45300	1.49	1.067	0.940	0.987	0.987	0.966	0.940	0.966
				Mean	1.091	1.006	0.964	0.997	0.997	0.963	1.007
				COV(%)	10.81	12.19	13.24	12.48	12.80	13.31	12.74
			Total:	**Mean**	**1.029**	**1.015**	**0.969**	**1.006**	**1.005**	**0.985**	**1.008**
				COV(%)	**10.53**	**10.56**	**12.35**	**10.55**	**10.46**	**11.02**	**10.47**

By comparing the models with initial offset slip factor, the Walraven model has the best correlation with a mean of 0.99 and a coefficient of variation (COV) of 11.1% for the ratio of theoretical to experimental shear strength. This is somewhat better than the estimates of capacity obtained from the MCFT, which produced a mean of 1.03 and a COV of 10.5%. The Lai/Vecchio, Hybrid I, II and III models all show similar results and are only slightly below the mean. The Maekawa model seems to slightly under-predicted the experimental results. Note in particular that the MCFT predictions for the PB-series panels were consistently high; on average, overestimating the strength of these uniaxially reinforced elements by 9%. Conversely, the other models under-estimated the strength of these panels by 2% to 4%. It should be noted, however, that several of the panels in this series failed at shear stresses at or marginally above the cracking load; hence accuracy

was significantly dependent on the estimate of the concrete tensile strength. For all the panels, the relationship used for tensile strength ($f'_t = 0.65(f'_c)^{1/3}$)

Looking at the results without the initial offset slip factor considered, the Lai/Vecchio and Hybrid I model have the best correlation with a mean of 1.01 and a coefficient of variation (COV) of about 10.5%. The MCFT and Maekawa model have the worst correlation compared to the other models, with the MCFT model overestimating the strength by 3%, and Maekawa underestimating the strength by 3%. When PB panels are examined, the Lai/Vecchio model has the best correlation with a mean of 1.00 and a coefficient of variation (COV) of 12.5%.

In general, analyses without the initial offset slip factor considered seem to produce the best correlations. The Lai/Vecchio model has the best correlation without the initial offset slip factor.

5.2 Shear Beams

For beams containing shear reinforcement of amounts equal to 0.2 percent or greater (Vecchio and Collins, 1988), the correlations obtained from MCFT and DSFM analyses will be essentially similar. However, for beam containing little or no shear reinforcement, or for beams simultaneously subjected to axial compression (and hence experiencing minimal cracking), the results from MCFT have shown reduced accuracy (Vecchio, 2000). Further, it is under such conditions that the results of the DSFM diverge from those of the MCFT. Hence, the corroboration studies presented here concentrate on these beam types.

Three series of beams were considered. Firstly, the set of eighteen beams tested by Podgorniak-Stanik (1998). This set is particularly challenging in terms of analytical modelling for the following reasons: the beams were large-scale, with the majority being 1000 mm deep, raising the prospect of size effects; the majority of the beams contained no shear reinforcement; and, several of the beams were constructed using high strength concrete. The second set modelled involved the twelve beams tested by Bresler and Scordelis (1963), often used as a benchmark. These beams were modelled because they cover a representative range of conditions in terms of reinforcement amounts, shear spans and failure modes. The third series of specimens considered involves a series of strip

beams, subjected to various combinations of axial compression and transverse shear, tested by Gupta (1998). This series will test the analytical procedures under conditions where cracking is minimal, and where capacity is governed by the formation of a single dominant crack. Pertinent details of the test specimens are given in Table 5.4; typical configurations are shown in Figure 5.1.

Table 5.4

Beam	b (mm)	h (mm)	d (mm)	Span (mm)	A_s/bd (%)	A_s'/bd (%)	ρ_y (%)	f'_c (MPa)	f'_t (MPa)	E_c (MPa)	ε_0 ($x10^3$)	f_{yx} (MPa)	f_{yy} (MPa)	Load Ratio N:V
BM100	300	1000	925	2700	0.76	0.14	0.079	46	2.33	37300	2.47	550	508	0:1
BM100D	300	1000	925	2700	1.05	0.43	0.079	46	2.33	37300	2.47	550	508	0:1
BN100	300	1000	925	2700	0.76	-	-	37	2.17	33500	2.21	550	-	0:1
BN100D	300	1000	925	2700	1.05	0.43	-	37	2.17	33500	2.21	550	-	0:1
UM100	300	1000	925	2700	0.76	0.14	0.079	42	2.26	35600	2.36	550	508	0:1
UM100D	300	1000	925	2700	1.05	0.43	0.079	42	2.26	35600	2.36	550	508	0:1
UN100	300	1000	925	2700	0.76	-	-	43	2.28	36100	2.39	550	-	0:1
UN100D	300	1000	925	2700	1.05	0.43	-	43	2.28	36100	2.39	550	-	0:1
WM100C	1000	1000	925	2700	1.40	1.40	0.038	41	2.24	35200	2.33	550	508	0:1
WM100D	1000	1000	925	2700	1.40	1.40	0.038	38	2.19	33900	2.24	550	508	0:1
BRL100	300	1000	925	2700	0.50	0.50	-	94	2.96	53300	3.53	550	-	0:1
BRH100	300	1000	895	2700	3.13	3.13	-	94	2.96	53300	3.53	550	-	0:1
BH100	300	1000	925	2700	0.76	0.76	-	99	3.01	54700	3.62	550	-	0:1
BH100D	300	1000	925	2700	1.05	1.05	-	99	3.01	54700	3.62	550	-	0:1
BH50	300	500	450	2700	0.81	0.81	-	99	3.01	54700	3.62	486	-	0:1
BH50D	300	500	450	2700	1.11	1.11	-	99	3.01	54700	3.62	486	-	0:1
BN50	300	500	450	2700	0.81	0.81	-	37	2.17	33500	2.21	486	-	0:1
BN50D	300	500	450	2700	1.11	1.11	-	37	2.17	33500	2.21	486	-	0:1

Table 5.4 (cont'd)

Beam	b (mm)	h (mm)	d (mm)	Span (mm)	A_s/bd (%)	A_s'/bd (%)	ρ_y (%)	f'_c (MPa)	f'_t (MPa)	E_c (MPa)	ε_0 ($x10^3$)	f_{yx} (MPa)	f_{yy} (MPa)	Load Ratio N:V
OA1	310	556	461	3658	1.81	1.81	-	22.6	1.84	26200	1.73	555	-	0:1
OA2	305	561	466	4572	2.27	2.27	-	23.7	1.87	26800	1.77	555	-	0:1
OA3	307	556	462	6401	2.74	2.74	-	37.6	2.18	33700	2.23	552	-	0:1
A1	307	561	466	3658	1.80	1.80	0.100	24.1	1.88	27000	1.79	555	326	0:1
A2	305	559	464	4572	2.28	2.28	0.101	24.3	1.88	27100	1.79	555	326	0:1
A3	307	561	466	6401	2.73	2.73	0.100	35	2.13	32600	2.15	552	326	0:1
B1	231	556	461	3658	2.43	2.43	0.147	24.8	1.90	27400	1.81	555	326	0:1
B2	229	561	466	4572	2.43	2.43	0.148	23.2	1.85	26500	1.75	555	326	0:1
B3	229	556	461	6401	3.06	3.06	0.148	38.8	2.20	34200	2.26	552	326	0:1
C1	155	559	464	3658	1.80	1.80	0.199	29.6	2.01	29900	1.98	555	326	0:1
C2	152	559	464	4572	3.66	3.66	0.202	23.8	1.87	26800	1.77	555	326	0:1
C3	155	554	459	6401	3.63	3.63	0.199	35	2.13	32600	2.15	552	326	0:1
PC1	489	375	188	1550	0.98	0.98	0.200	62.2	2.58	32100	2.50	487	520	0:1
PC2	489	375	188	1550	0.98	0.98	0.200	62.2	2.58	32100	2.50	487	520	4:1
PC3	406	375	188	1310	1.97	1.97	0.200	62.8	2.58	30000	2.70	450	520	4:1
PC4	375	365	183	1310	1.32	1.32	0.205	83.1	2.84	38800	2.60	487	520	0:1
PC5	375	365	183	1310	1.32	1.32	0.205	86.9	2.88	40200	2.60	487	520	8:1
PC6	375	365	183	1310	1.32	1.32	0.205	86.9	2.88	40200	2.60	487	520	4:1
PC7	375	365	183	1310	1.32	1.32	0.205	39.9	2.22	30800	1.90	487	520	0:1
PC8	375	365	183	1310	1.32	1.32	0.205	42.4	2.27	32000	1.90	487	520	4:1
PC9	375	365	183	1310	1.32	1.32	0.205	42.9	2.28	29200	2.10	487	520	8:1
PC10	625	365	183	1310	0.79	0.79	0.205	42.9	2.28	29200	2.10	487	520	4:1
PC11	625	365	183	1310	0.79	0.79	0.205	44.7	2.31	30000	2.10	487	520	8:1
PC12	375	365	183	1310	1.32	1.32	0.205	60	2.54	35500	2.20	487	520	0:1
PC13	375	365	183	1310	1.32	1.32	0.205	60	2.54	35500	2.20	487	520	4:1
PC14	375	365	183	1310	1.32	1.32	0.205	64.5	2.61	35900	2.30	487	520	8:1
PC15	375	365	183	1310	1.32	1.32	0.205	56.6	2.50	33900	2.20	487	520	20:1
PC16	375	365	183	1310	1.32	1.32	0.205	56.6	2.50	33900	2.20	487	520	4:1
PC17	375	365	183	1310	1.32	1.32	0.205	56.6	2.50	33900	2.20	487	520	8:1
PC18	625	365	183	1310	0.79	0.79	0.205	29.5	2.01	27100	1.80	487	520	4:1
PC19	625	365	183	1310	0.79	0.79	0.205	29.5	2.01	27100	1.80	487	520	8:1
PC20	625	365	183	1310	0.79	0.79	0.205	47.3	2.35	31200	2.10	487	520	6:1
PC21	625	365	183	1310	0.79	0.79	0.205	47.3	2.35	31200	2.10	487	520	4:1
PC22	375	365	183	1310	1.32	1.32	0.205	53.2	2.44	32400	2.20	487	520	0:1
PC23	375	365	183	1310	1.32	1.32	0.205	53.2	2.44	32400	2.20	487	520	3:1
PC24	375	365	183	1310	1.32	1.32	0.205	53.2	2.44	32400	2.20	487	520	1.5:1

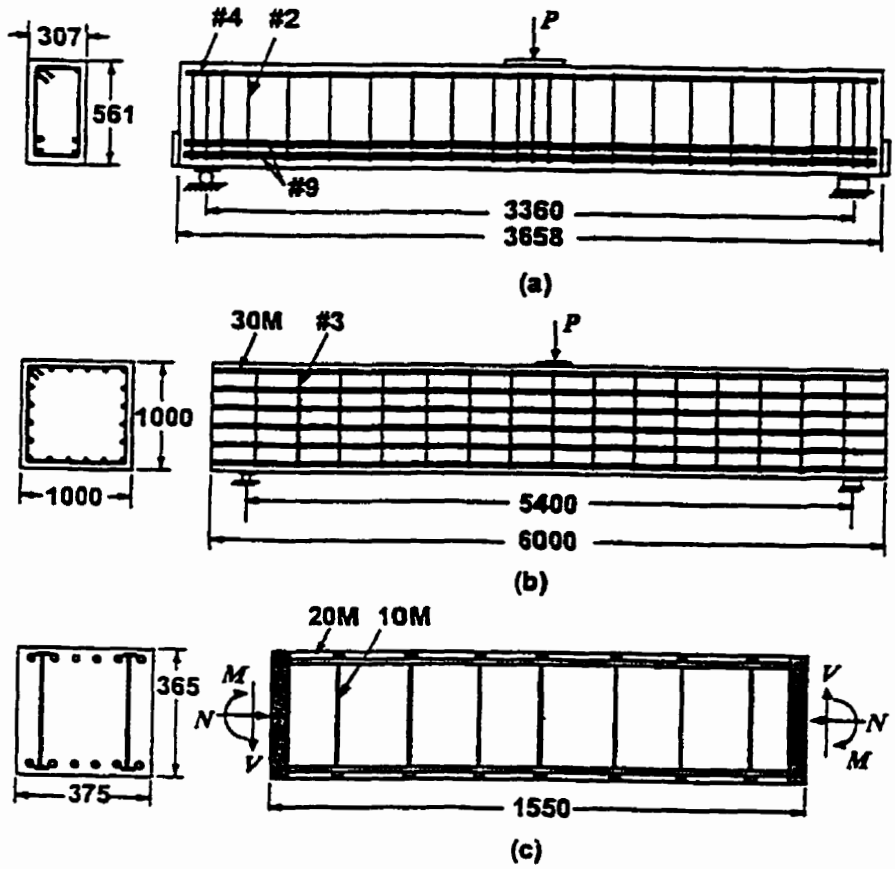

Figure 5.1 Details of test beams. (a) Bresler-Scordelis beams (b) Podgorniak-Stanik beams (c) Gupta Beams

The beams were modelled for finite element analyses using the typical meshes shown in Figure 5.2, taking advantage of symmetry to model one-half spans. The Podgorniak-Stanik beams were modelled with a 40 x 12 element mesh. With the Bresler and Scordelis beams, a mesh of 32 x 9 constant strain (8 d.o.f.) rectangular elements were used for the 7.32 m span beams; 39 x 9 elements for the 9.14 m span beams, and 40 x 9 elements for the 12.8 m span beams. The Gupta beams were modelled with a 18 x 10 element mesh. All material properties used were as given in Table 5.4; note that the concrete cracking stress was approximated using $0.65(f'_c)^{1/3}$. The Podgorniak-Stanik beams were subjected to displacement-controlled loading, with midspan displacement increments of 0.25 mm imposed. The Bresler-Scordelis beams and the Gupta beams were subjected to force-controlled loading, with shear load increments of 2.5 kN and 5.0 kN, respectively.

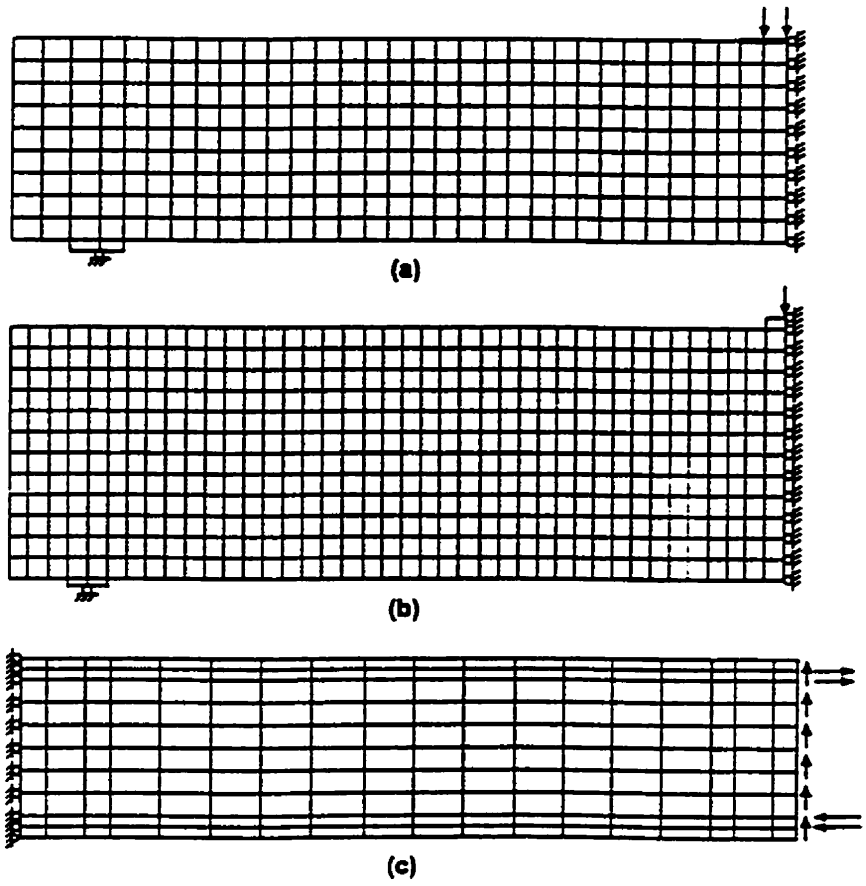

Figure 5.2 Typical finite element meshes. (a) Bresler-Scordelis beams (b) Podgorniak-Stanik beams (c) Gupta Beams

Table 5.5 Analyses without initial offset slip factor

Beam	$V_{u\text{-}exp}$ (kN)	$V_{u\text{-}theor}$ (kN)							$V_{u\text{-}theor}/V_{u\text{-}exp}$						
Podgorniak-Stanik		MCFT 0	Wal. 1	Maek. 2	Lai 3	Hy. I 4	Hy. II 5	Hy. III 6	MCFT 0	Wal. 1	Maek. 2	Lai 3	Hy. I 4	Hy. II 5	Hy. III 6
BM100	343	259	256	281	260	224	257	207	0.755	0.746	0.819	0.758	0.653	0.749	0.603
BM100D	462	470	430	428	428	493	426	464	1.017	0.931	0.926	0.926	1.067	0.922	1.004
BN100	192	181	177	191	177	152	180	156	0.943	0.922	0.995	0.922	0.792	0.938	0.813
BN100D	258	339	342	363	338	319	339	318	1.314	1.326	1.407	1.310	1.236	1.314	1.233
UM100	750	800	750	715	730	580	705	565	1.067	1.000	0.953	0.973	0.773	0.940	0.753
UM100D	910	1320	1000	1000	1000	1000	1035	1000	1.451	1.099	1.099	1.099	1.099	1.137	1.099
UN100	593	580	495	495	530	340	435	440	0.978	0.835	0.835	0.894	0.573	0.734	0.742
UN100D	637	970	870	960	835	790	965	785	1.523	1.366	1.507	1.311	1.240	1.515	1.232
WM100C	699	804	733	807	649	604	804	570	1.150	1.049	1.155	0.928	0.864	1.150	0.815
WM100D	834	1114	1070	1075	1042	789	1020	786	1.336	1.283	1.289	1.249	0.946	1.223	0.942
BRL100	164	190	167	176	162	147	191	141	1.159	1.018	1.073	0.988	0.896	1.165	0.860
BRH100	357	433	430	464	430	392	454	378	1.213	1.204	1.300	1.204	1.098	1.272	1.059
BH100	193	227	210	242	212	183	237	165	1.176	1.088	1.254	1.098	0.948	1.228	0.855
BH100D	281	431	413	489	413	430	453	423	1.534	1.470	1.740	1.470	1.530	1.612	1.505
BH50	132	149	134	152	131	126	140	119	1.129	1.015	1.152	0.992	0.955	1.061	0.902
BH50D	193	260	258	258	257	257	258	242	1.347	1.337	1.337	1.332	1.332	1.337	1.254
BN50	132	114	109	124	111	104	113	103	0.864	0.826	0.939	0.841	0.788	0.856	0.780
BN50D	163	192	205	209	204	191	212	195	1.178	1.258	1.282	1.252	1.172	1.301	1.196
								Mean	1.174	1.098	1.170	1.086	0.998	1.136	0.980
								COV(%)	18.56	19.01	20.87	18.55	24.75	21.60	23.84
Bresler-Scordelis															
OA1	167	155	150	150	150	140	145	140	0.931	0.901	0.901	0.901	0.841	0.871	0.841
OA2	178	130	120	120	115	110	115	110	0.730	0.674	0.674	0.646	0.618	0.646	0.618
OA3	189	155	140	138	135	138	138	140	0.820	0.741	0.728	0.714	0.728	0.728	0.741
A1	234	263	243	258	245	240	263	228	1.126	1.041	1.103	1.049	1.028	1.124	0.974
A2	245	230	205	205	205	210	205	210	0.941	0.838	0.838	0.838	0.859	0.838	0.859
A3	234	230	205	200	203	208	193	205	0.985	0.878	0.857	0.867	0.889	0.824	0.878
B1	222	230	215	220	220	230	223	218	1.036	0.968	0.991	0.991	1.036	1.002	0.980
B2	200	185	175	170	170	180	175	175	0.925	0.875	0.850	0.850	0.900	0.875	0.875
B3	178	208	180	173	178	178	178	185	1.169	1.011	0.969	0.997	0.997	0.997	1.039
C1	156	150	149	151	149	150	150	149	0.965	0.958	0.971	0.958	0.965	0.965	0.958
C2	162	145	140	135	140	140	140	140	0.895	0.864	0.833	0.864	0.864	0.864	0.864
C3	136	140	135	128	133	133	130	135	1.033	0.996	0.941	0.978	0.978	0.959	0.996
								Mean	0.963	0.896	0.888	0.888	0.892	0.891	0.885
								COV(%)	12.60	12.22	13.26	13.38	13.92	14.49	13.36

Table 5.5 (cont'd)

Gupta

PC1	437	420	420	400	420	415	395	425	0.961	0.961	0.915	0.961	0.950	0.904	0.973
PC2	863	770	730	705	750	715	700	720	0.892	0.846	0.817	0.869	0.829	0.811	0.834
PC3	845	630	600	580	590	575	575	575	0.746	0.710	0.686	0.698	0.680	0.680	0.680
PC4	401	385	345	335	340	320	315	315	0.960	0.860	0.835	0.848	0.798	0.786	0.786
PC5	679	885	875	850	865	855	845	850	1.303	1.289	1.252	1.274	1.259	1.244	1.252
PC6	668	670	630	605	625	615	605	610	1.003	0.943	0.906	0.936	0.921	0.906	0.913
PC7	387	290	285	285	285	275	270	270	0.749	0.736	0.736	0.736	0.711	0.698	0.698
PC8	497	490	490	475	480	485	465	475	0.986	0.986	0.956	0.966	0.976	0.936	0.956
PC9	516	610	610	610	615	620	620	620	1.182	1.182	1.182	1.192	1.202	1.202	1.202
PC10	726	830	785	765	770	775	755	770	1.143	1.081	1.054	1.061	1.067	1.040	1.061
PC11	754	1035	965	1040	1030	1045	1045	1005	1.373	1.280	1.379	1.366	1.386	1.386	1.333
PC12	490	335	325	325	320	310	305	310	0.684	0.663	0.663	0.653	0.633	0.622	0.633
PC13	680	590	560	540	545	540	525	540	0.868	0.824	0.794	0.801	0.794	0.772	0.794
PC14	686	765	765	750	755	760	755	750	1.115	1.115	1.093	1.101	1.108	1.101	1.093
PC15	358	390	390	390	390	390	390	390	1.089	1.089	1.089	1.089	1.089	1.089	1.089
PC16	945	935	935	930	930	930	930	935	0.989	0.989	0.984	0.984	0.984	0.984	0.989
PC17	707	740	740	740	760	740	740	740	1.047	1.047	1.047	1.075	1.047	1.047	1.047
PC18	832	695	660	650	685	655	635	640	0.835	0.793	0.781	0.823	0.787	0.763	0.769
PC19	751	725	720	735	720	750	750	750	0.965	0.959	0.979	0.959	0.999	0.999	0.999
PC20	715	955	930	910	940	900	890	895	1.336	1.301	1.273	1.315	1.259	1.245	1.252
PC21	767	735	720	720	710	710	700	695	0.958	0.939	0.939	0.926	0.926	0.913	0.906
PC22	443	320	310	305	305	290	290	290	0.722	0.700	0.688	0.688	0.655	0.655	0.655
PC23	603	490	455	445	450	445	430	440	0.813	0.755	0.738	0.746	0.738	0.713	0.730
PC24	528	495	455	445	450	445	430	440	0.938	0.862	0.843	0.852	0.843	0.814	0.833
								Mean	0.986	0.955	0.943	0.955	0.943	0.930	0.936
								COV(%)	19.18	19.90	21.02	20.86	21.88	22.48	21.60
							Total:	**Mean**	**1.043**	**0.989**	**1.006**	**0.984**	**0.950**	**0.990**	**0.940**
								COV(%)	**19.77**	**19.89**	**22.91**	**20.12**	**21.78**	**23.22**	**21.13**

Table 5.6 Analyses with initial offset slip factor

Beam	$V_{u\text{-}exp}$ (kN)	$V_{u\text{-}theor}$ (kN)		$V_{u\text{-}theor}/V_{u\text{-}exp}$	
Podgorniak-Stanik		Walraven 1	Lai 3	Walraven 1	Lai 3
BM100	343	246	259	0.717	0.755
BM100D	462	417	415	0.903	0.898
BN100	192	168	167	0.875	0.870
BN100D	258	328	328	1.271	1.271
UM100	750	605	585	0.807	0.780
UM100D	910	950	945	1.044	1.038
UN100	593	415	405	0.700	0.683
UN100D	637	805	800	1.264	1.256
WM100C	699	682	673	0.976	0.963
WM100D	834	926	922	1.110	1.106
BRL100	164	162	159	0.988	0.970
BRH100	357	403	409	1.129	1.146
BH100	193	205	205	1.062	1.062
BH100D	281	410	409	1.459	1.456
BH50	132	139	133	1.053	1.008
BH50D	193	258	258	1.337	1.337
BN50	132	107	104	0.811	0.788
BN50D	163	202	201	1.239	1.233
			Mean	1.041	1.034
			COV(%)	20.84	21.16
Bresler-Scordelis					
OA1	167	140	140	0.841	0.841
OA2	178	115	115	0.646	0.646
OA3	189	133	133	0.701	0.701
A1	234	208	205	0.889	0.878
A2	245	190	190	0.777	0.777
A3	234	193	193	0.824	0.824
B1	222	190	190	0.856	0.856
B2	200	165	165	0.825	0.825
B3	178	170	170	0.955	0.955
C1	156	143	140	0.916	0.900
C2	162	135	135	0.833	0.833
C3	136	128	128	0.941	0.941
			Mean	0.834	0.831
			COV(%)	11.02	10.84

Table 5.6 (cont'd)

Gupta

PC1	437	420	425	0.961	0.973
PC2	863	710	720	0.823	0.834
PC3	845	580	590	0.686	0.698
PC4	401	340	350	0.848	0.873
PC5	679	860	850	1.267	1.252
PC6	668	615	595	0.921	0.891
PC7	387	285	285	0.736	0.736
PC8	497	475	465	0.956	0.936
PC9	516	605	595	1.172	1.153
PC10	726	755	775	1.040	1.067
PC11	754	975	995	1.293	1.320
PC12	490	320	320	0.653	0.653
PC13	680	535	530	0.787	0.779
PC14	686	745	735	1.086	1.071
PC15	358	390	390	1.089	1.089
PC16	945	940	930	0.995	0.984
PC17	707	740	750	1.047	1.061
PC18	832	635	675	0.763	0.811
PC19	751	750	720	0.999	0.959
PC20	715	880	905	1.231	1.266
PC21	767	700	690	0.913	0.900
PC22	443	310	310	0.700	0.700
PC23	603	445	460	0.738	0.763
PC24	528	375	370	0.710	0.701
			Mean	0.934	0.936
			COV(%)	20.69	20.62
		Total:	**Mean**	**0.947**	**0.946**
			COV(%)	**20.86**	**20.85**

The typical load-deformation responses of BM100, BM100D, BN100, BN100D are shown on Figure 5.3-5.6. Note that BM100 and BM100D contained shear reinforcement; BN100 and BN100D did not. The computed responses for the Podgorniak-Stanik beams showed more scatter (Table 5.5, Table 5.6). From Figures 5.3-5.6 and Tables 5.5-5.6, it can be seen that most models had a tendency to overestimate strengths, but the accuracy in each model was somewhat improved compared to the MCFT model. The Hybrid I formulation has good correlation with a mean of 1.00 but a COV of 24.8%. The failure mechanism determined from the DSFM typically provided a better representation than the MCFT. The typical load-deformation responses shown in Figures 5.3-5.6 indicate good correlation between the experimental behaviour and that calculated using the DSFM. The computed responses obtained using the MCFT, also

shown in Figures 5.3–5.6, provide equally good correlation for this representative set of beams.

The behaviour of the Bresler-Scordelis beams was modelled reasonably well, although the tendency was to underestimate the load capacity (see Table 5.5, Table 5.6). For the Bresler-Scordelis beams, the MCFT had the best correlation with a mean of 0.96 and a COV of 12.6%. The other models all had a mean of about 0.90 and a COV of about 14.0%. The main challenge of the Bresler-Scordelis beams was that with beams containing no shear reinforcement (OA1, OA2, OA3), the computed shear capacity of the beams was highly dependent on the concrete cracking stress. However, the computed responses obtained here provided good correlation for these beams. The typical load-deformation responses shown in Figures 5.7-5.10 indicate good correlation between the experimental behaviour and that calculated using the DSFM. The computed responses obtained using the MCFT provided equally good correlation for this representative set of beams.

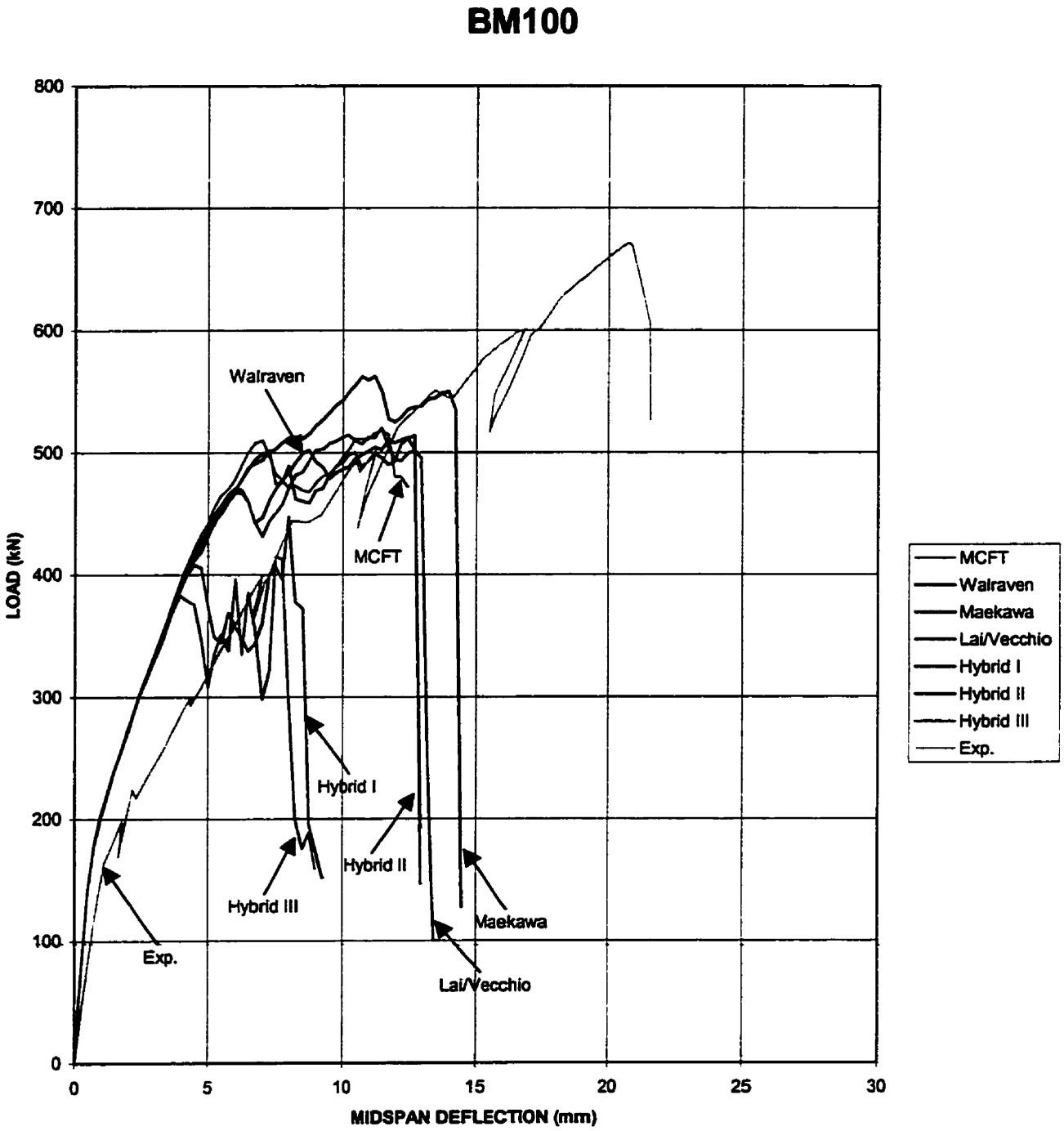
BM100
LOAD (kN)
MIDSPAN DEFLECTION (mm)
0
100
200
300
400
500
600
700
800
0
5
10
15
20
25
30
Walraven
MCFT
Hybrid I
Hybrid II
Hybrid III
Exp.
Maekawa
Lai/Vecchio
MCFT
Walraven
Maekawa
Lai/Vecchio
Hybrid I
Hybrid II
Hybrid III
Exp.

Figure 5.3

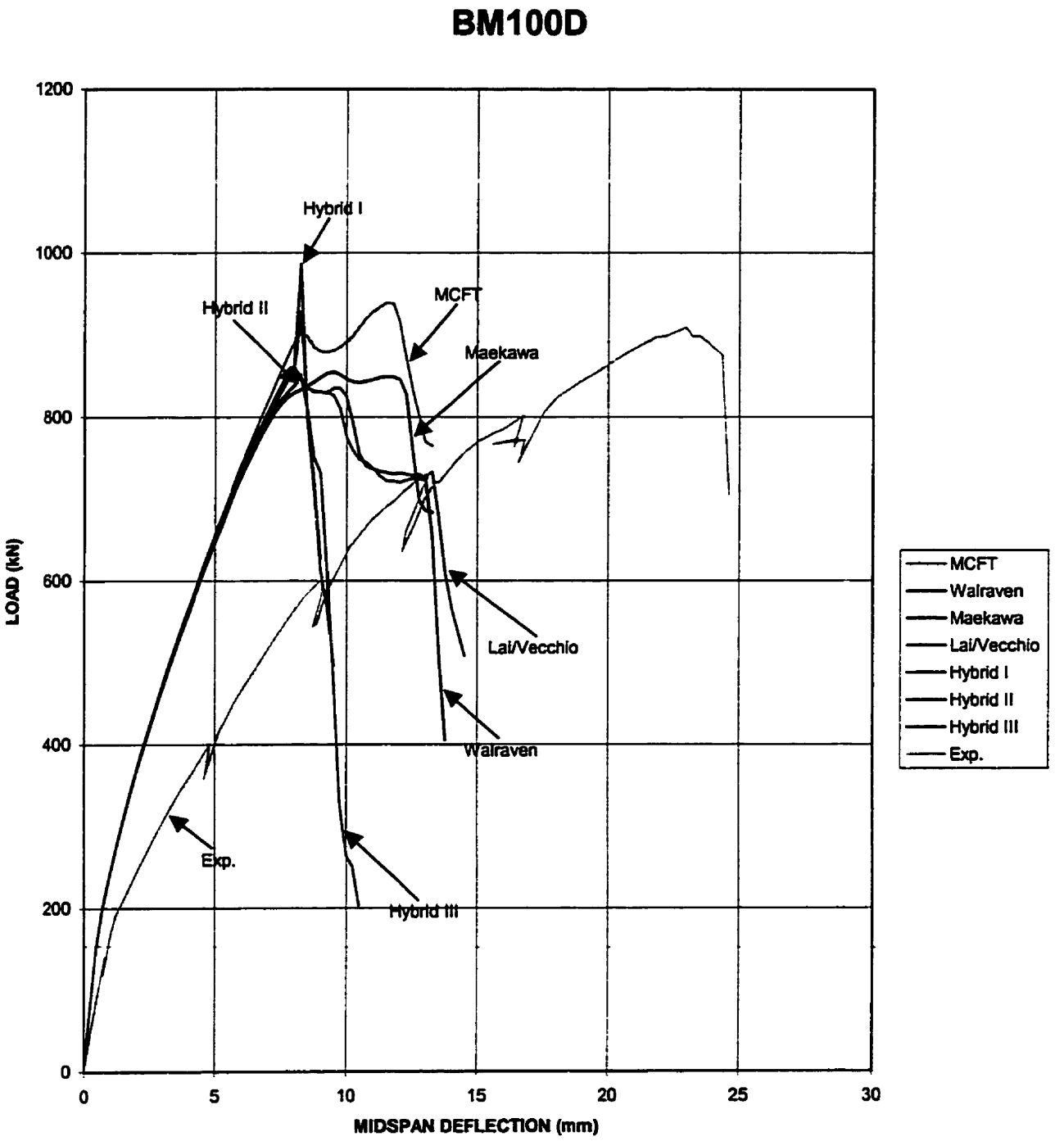
BM100D
LOAD (kN)
MIDSPAN DEFLECTION (mm)
0
200
400
600
800
1000
1200
0
5
10
15
20
25
30
Hybrid I
Hybrid II
MCFT
Maekawa
Lai/Vecchio
Walraven
Exp.
Hybrid III
MCFT
Walraven
Maekawa
Lai/Vecchio
Hybrid I
Hybrid II
Hybrid III
Exp.

Figure 5.4

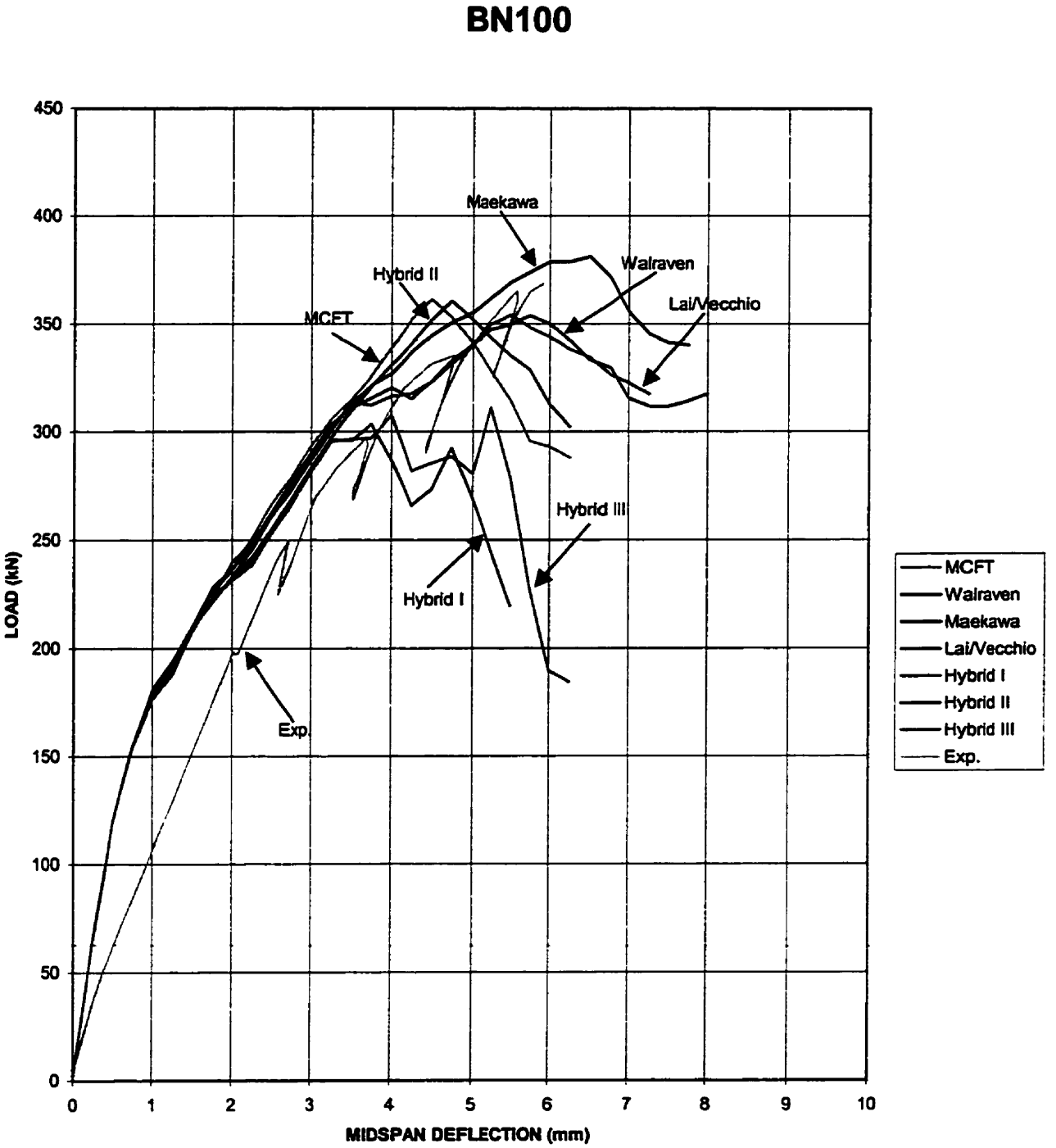
BN100
LOAD (kN)
MIDSPAN DEFLECTION (mm)
0
50
100
150
200
250
300
350
400
450
0
1
2
3
4
5
6
7
8
9
10
Maekawa
Hybrid II
Walraven
Lai/Vecchio
MCFT
Hybrid III
Hybrid I
Exp.
MCFT
Walraven
Maekawa
Lai/Vecchio
Hybrid I
Hybrid II
Hybrid III
Exp.

Figure 5.5

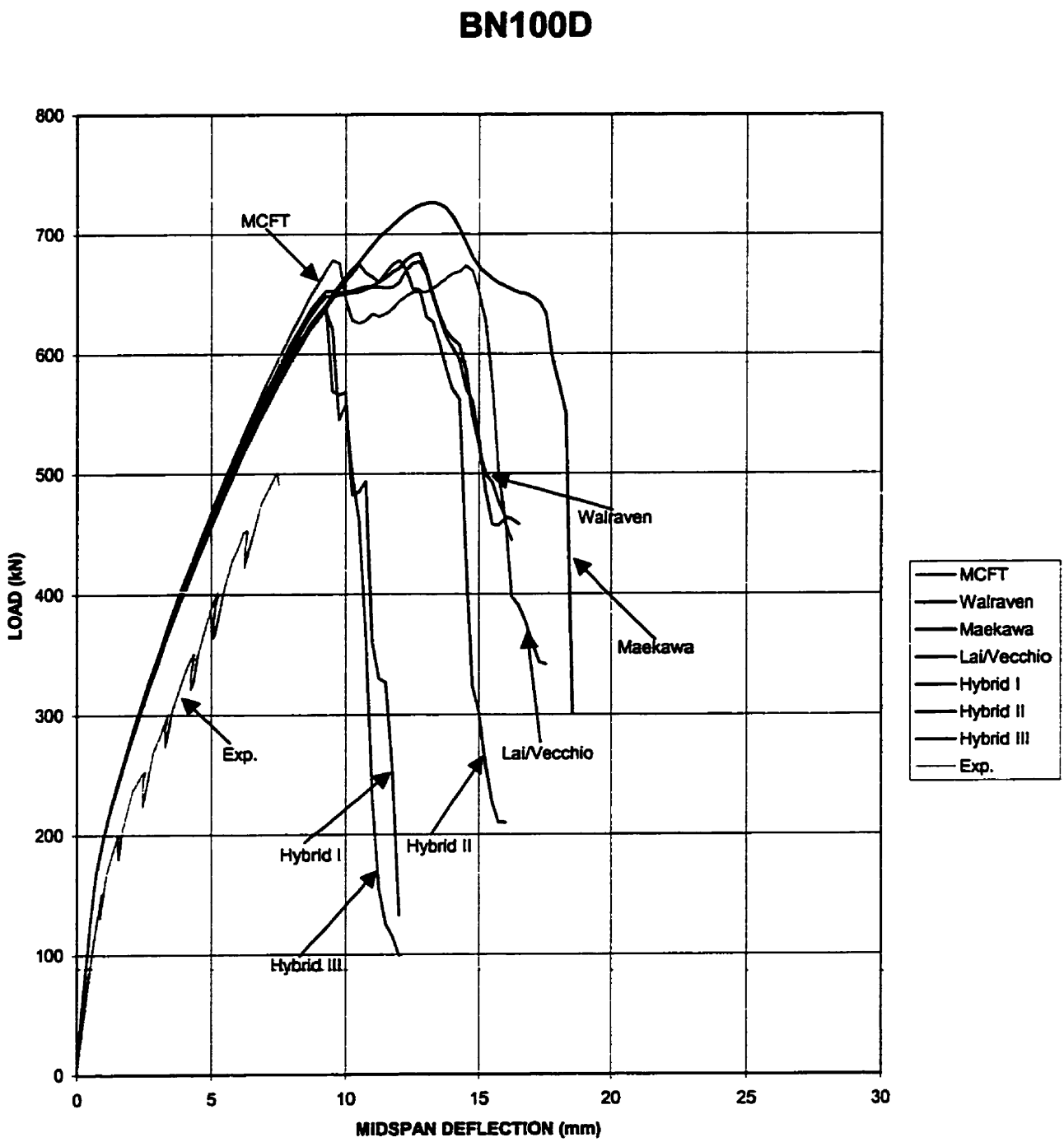
BN100D
LOAD (kN)
MIDSPAN DEFLECTION (mm)
0
100
200
300
400
500
600
700
800
0
5
10
15
20
25
30
MCFT
Walraven
Maekawa
Lai/Vecchio
Exp.
Hybrid I
Hybrid II
Hybrid III
MCFT
Walraven
Maekawa
Lai/Vecchio
Hybrid I
Hybrid II
Hybrid III
Exp.

Figure 5.6

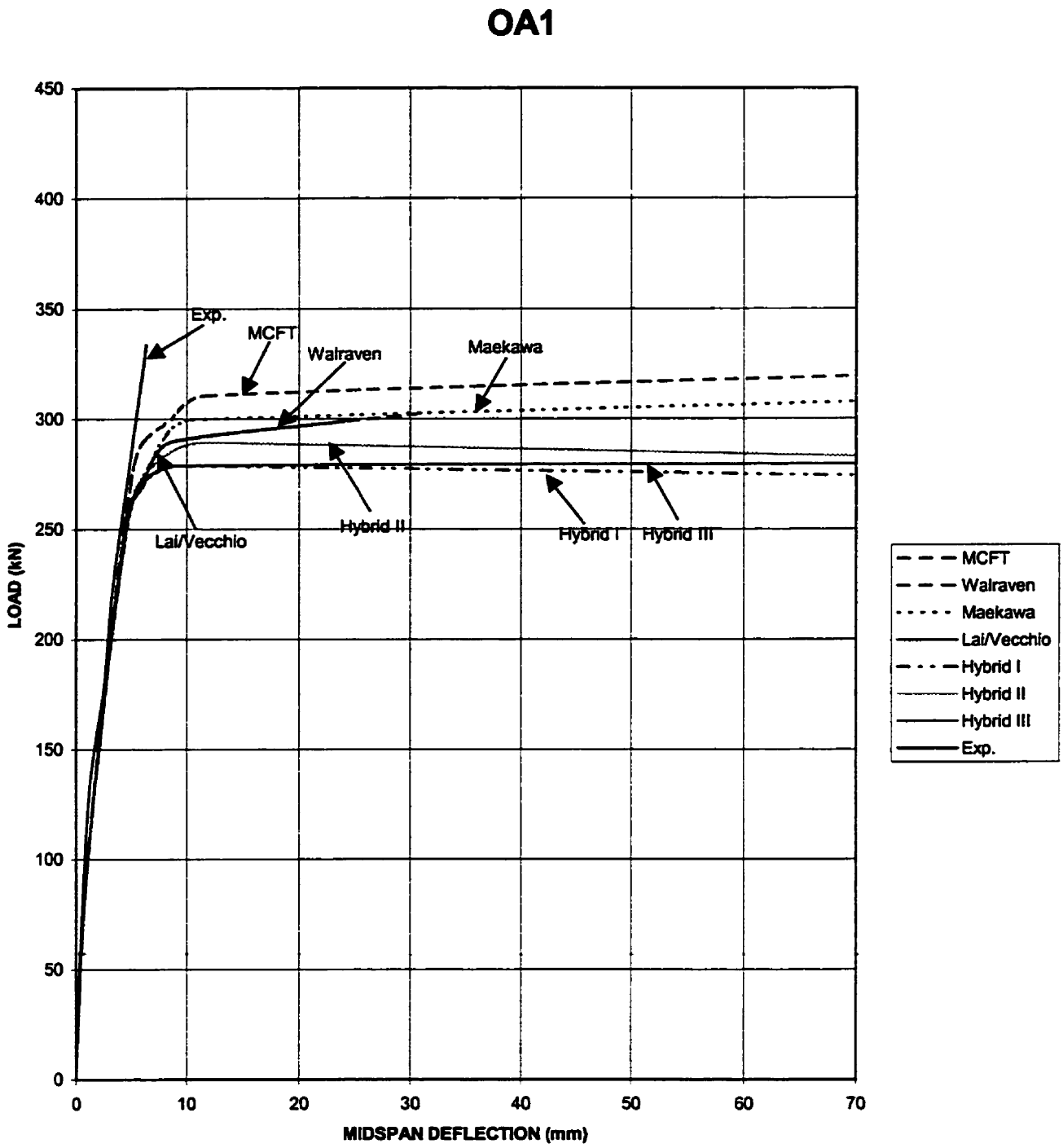
OA1
LOAD (kN)
MIDSPAN DEFLECTION (mm)
0
50
100
150
200
250
300
350
400
450
0
10
20
30
40
50
60
70
Exp.
MCFT
Walraven
Maekawa
Lai/Vecchio
Hybrid II
Hybrid I
Hybrid III
MCFT
Walraven
Maekawa
Lai/Vecchio
Hybrid I
Hybrid II
Hybrid III
Exp.

Figure 5.7

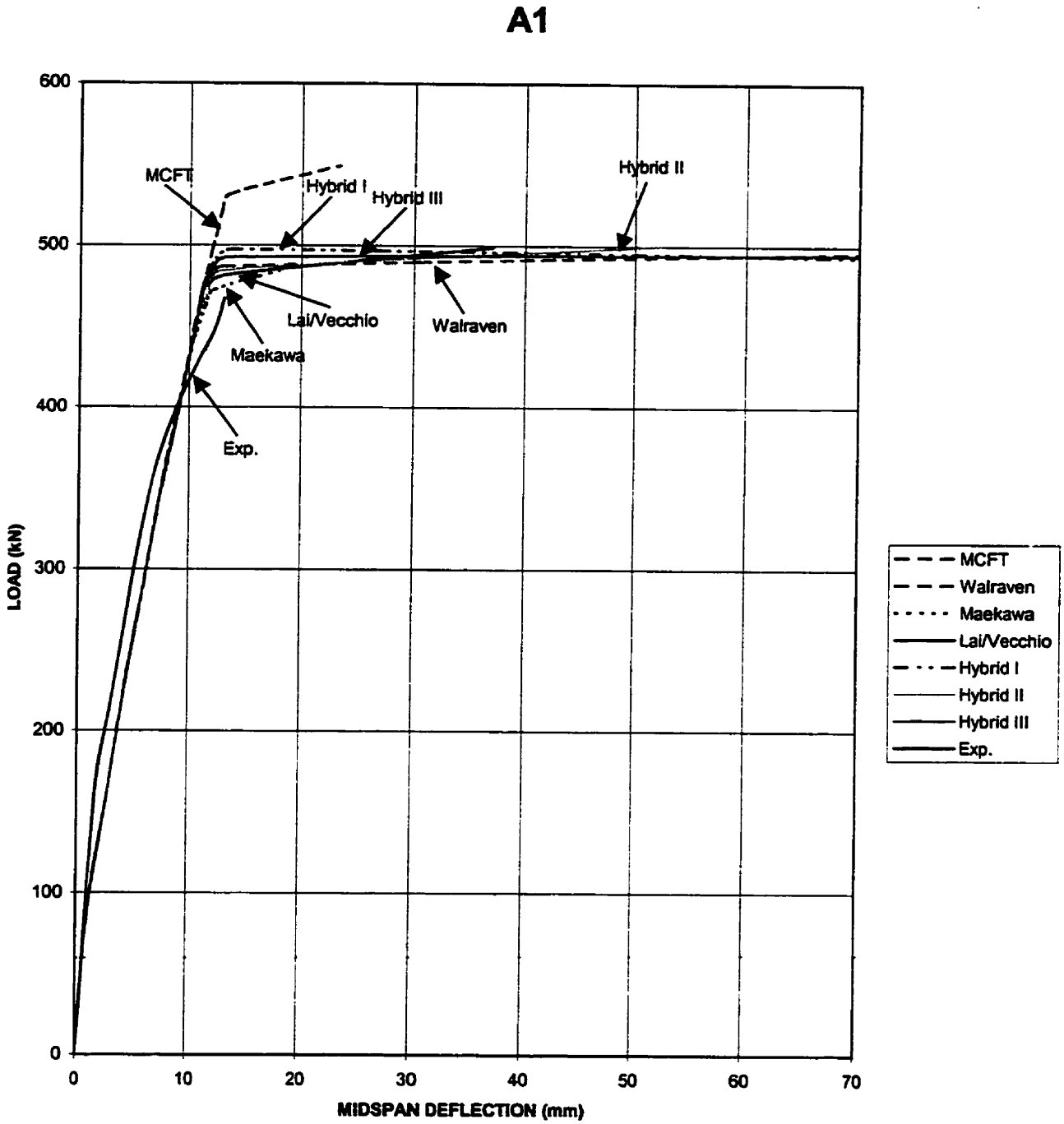
A1
600
500
400
300
200
100
0
LOAD (kN)
0
10
20
30
40
50
60
70
MIDSPAN DEFLECTION (mm)
MCFT
Hybrid I
Hybrid III
Hybrid II
Lai/Vecchio
Walraven
Maekawa
Exp.
MCFT
Walraven
Maekawa
Lai/Vecchio
Hybrid I
Hybrid II
Hybrid III
Exp.

Figure 5.8

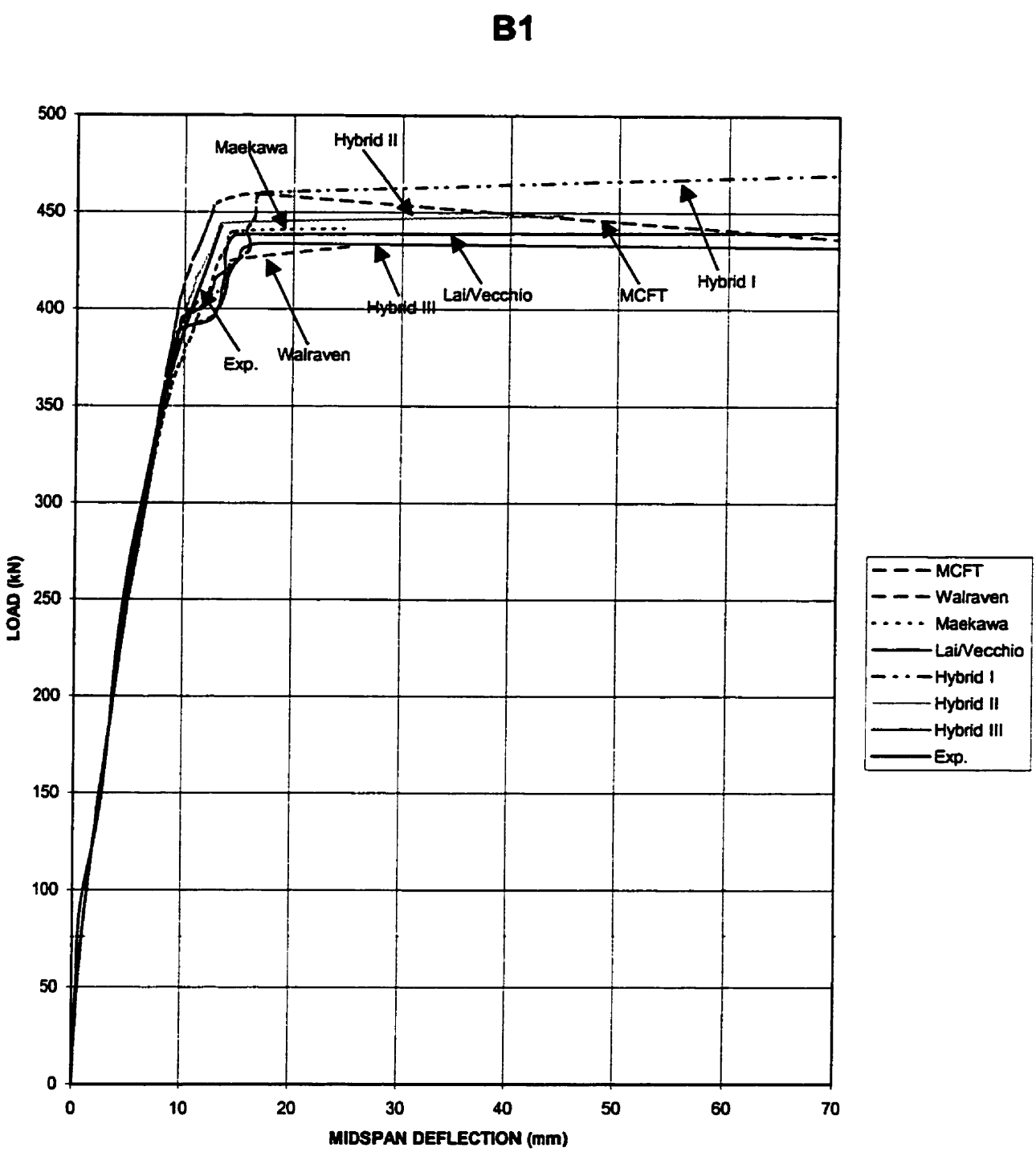
B1
LOAD (kN)
MIDSPAN DEFLECTION (mm)
0
50
100
150
200
250
300
350
400
450
500
0
10
20
30
40
50
60
70
Maekawa
Hybrid II
Hybrid I
Lai/Vecchio
MCFT
Hybrid III
Exp.
Walraven
MCFT
Walraven
Maekawa
Lai/Vecchio
Hybrid I
Hybrid II
Hybrid III
Exp.

Figure 5.9

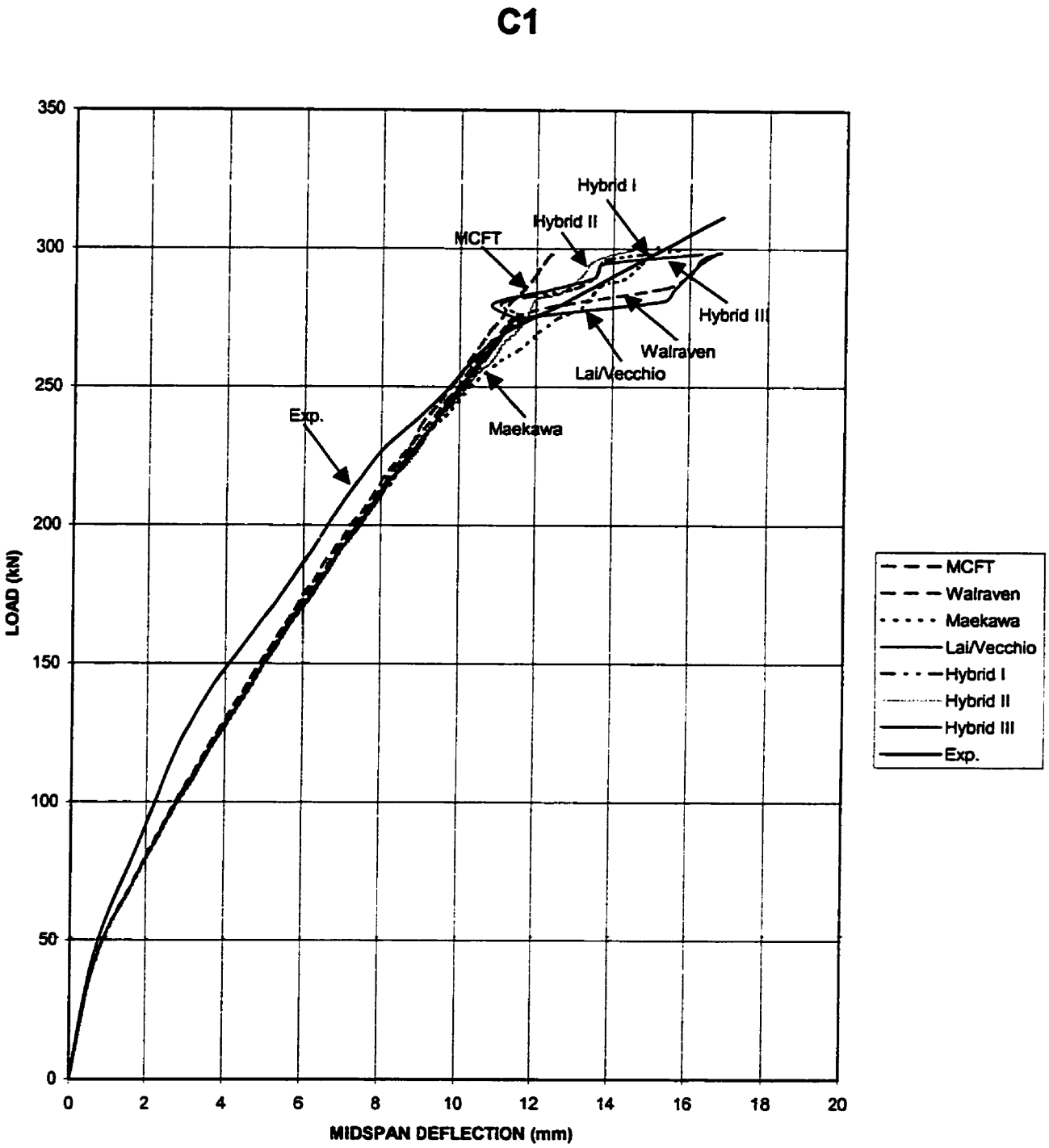
C1
350
300
250
200
150
100
50
0
LOAD (kN)
0
2
4
6
8
10
12
14
16
18
20
MIDSPAN DEFLECTION (mm)
Hybrid I
Hybrid II
MCFT
Hybrid III
Walraven
Lai/Vecchio
Exp.
Maekawa
MCFT
Walraven
Maekawa
Lai/Vecchio
Hybrid I
Hybrid II
Hybrid III
Exp.

Figure 5.10

The behaviour of the Gupta beams was typically dominated by the formation of a principal crack, with failure ensuing shortly thereafter. With increasing ratios of compression to shear, behaviour became more brittle and somewhat more dependent on the ability of cracks to realign and form direct struts. The Lai/Vecchio model, in better modelling the delayed rotation of the cracks, resulted in improved predictions of strength and response, with a mean of 0.96 and a COV of 20.9%. Direct measurements of the beam deflections were not obtained because of the test set-up used. However, the ability of the other model which incorporated the DSFM to represent rebar strains and concrete surface strains was found to be reasonably good at all stages of loading.

Although only the Walraven and Lai/Vecchio models were employed for analyses with initial slip offset considered, the combined results showed a tendency to under-estimate capacity compared to analyses without any initial slip offset. In conclusion, the analyses tend to have better accuracy if the initial offset factor is not included.

For the three sets of beams combined, the results without initial offset is compared, and the ratio of calculated to observed shear capacity obtained using the Lai/Vecchio model has a mean of 0.98 and a coefficient of variation of 20.1%. This is measurably better than the mean of 1.04 and a COV of 19.8% obtained using the MCFT, and very close to 0.99, 19.9% and 0.99, 23.2% obtained using Walraven and Hybrid II, respectively.

5.3 Shear Walls

To gauge the accuracy of the analysis procedures under more common conditions, two series of shear walls tested by Lefas et al. (1990) were studied. The test program consisted of 13 large-scale walls tested under various conditions of axial and lateral load. The wall geometries were of two types; the Type I walls were relatively squat with a height-to-width ratio of 1.0, and the Type II walls were more slender with a height-to-width of 2.0 (see Figure 5.11). In both cases, the walls were of rectangular cross section but contained a more heavily reinforced concealed column in the edge (flange) regions. The web regions of the walls were generally reinforced in the vertical and horizontal

directions in accordance with ACI 318 specifications. Percentages of reinforcement, and concrete and steel material properties, are given in Table 5.7.

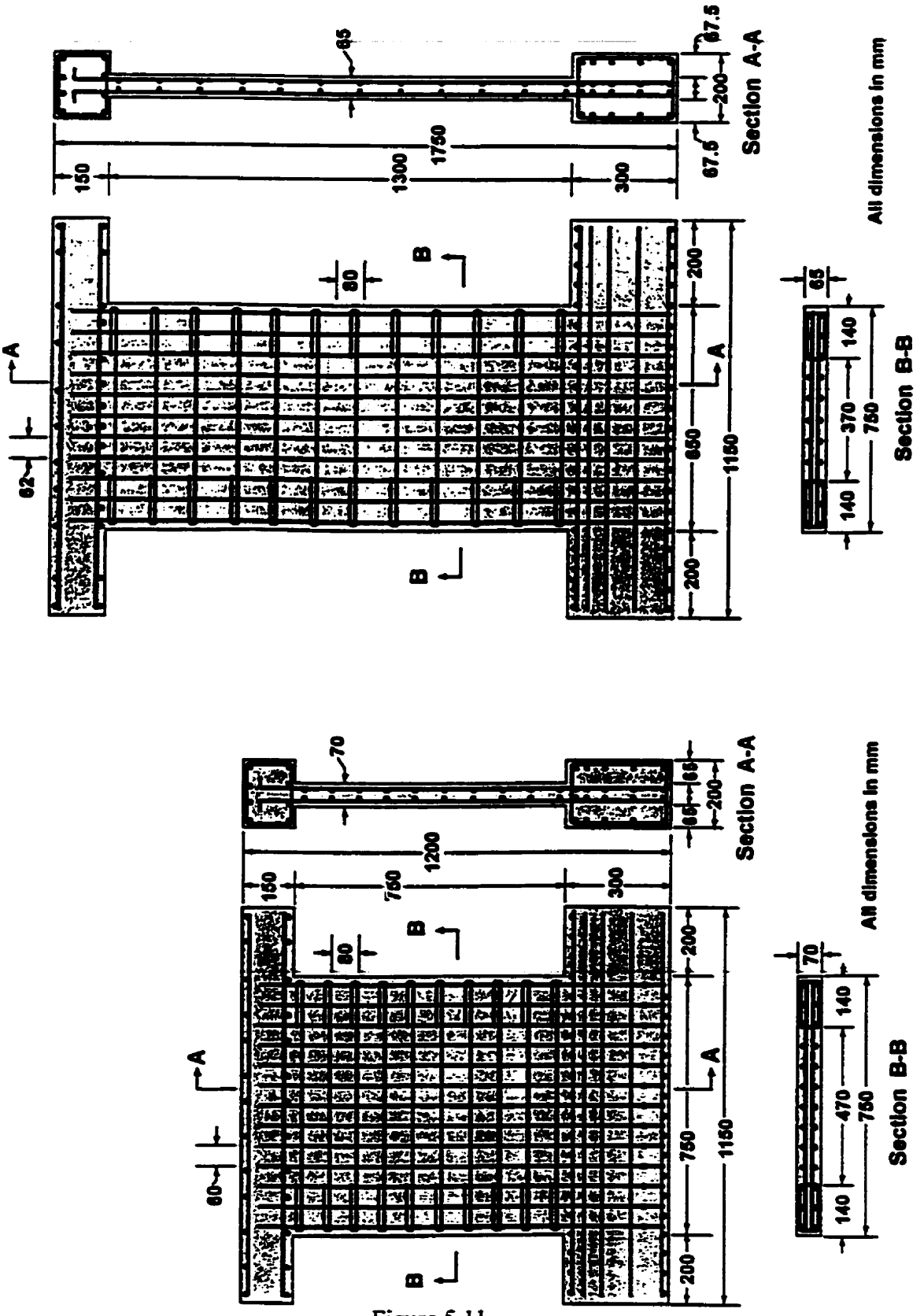
65
67.5
200
67.5
Section A-A
All dimensions in mm
150
1300
1750
300
80
B
A
200
650
1150
200
82
65
140
370
750
140
Section B-B
70
65
65
200
1200
150
750
300
80
200
750
1150
200
60
70
140
470
750
140

Figure 5.11

Table 5.7

Concrete

Wall	Type	Axial Load (kN)	f'_c (MPa)	f'_t (MPa)	ε_c (MPa)
SW11	I	0	37.8	2.20	33350
SW12	I	230	38.8	2.23	33750
SW13	I	355	39.3	1.94	29350
SW14	I	0	30.4	1.97	29900
SW15	I	185	31.3	2.00	30300
SW16	I	460	37.4	2.20	33150
SW17	I	0	34.9	2.12	32050
SW21	II	0	30.9	2.00	30150
SW22	II	182	36.6	2.16	32800
SW23	II	343	34.5	2.10	31850
SW24	II	0	34.9	2.12	32050
SW25	II	325	32.6	2.04	30950
SW26	II	0	21.8	1.67	25300

*$\nu_0 = 0.15$ assumed for all walls.

Reinforcement

	Zone	T (mm)	ρ_x (%)	f_{yx} (MPa)	ρ_y (%)	f_{yy} (MPa)	ρ_z (%)	f_{yz} (MPa)
Type I Walls	Web	70	1.095*	520	2.138	470	-	-
	Flange	70	1.095*/0.448	520/420	3.076	470	1.200	420
Type II Walls	Web	65	0.820**	520	2.090	470	-	-
	Flange	65	0.820**/0.336	520/420	3.312	470	0.900	420

* 0.365 in wall SW17
** 0.410 in wall SW26
ρ = reinforcement ratio
f_y = yield stress

The walls were subjected to constant axial loads combined with monotonically increasing lateral load applied through the top spreader beam. The walls exhibited a strong, ductile behaviour, developing strengths greater than expected. Lefas et al

reported the development of triaxial compressive stress conditions at the base of the walls and in the concealed columns, and attributed the high shear resistance of the walls to this.

Finite element analyses were undertaken for the two series of walls tested. A 340-element mesh was used to represent the Type I walls, and a 536-element mesh was used for the Type II walls (see Figure 5.12). The axial load was represented by constant-value nodal forces applied to the top spreader beam; the lateral loading was applied in the form of imposed horizontal displacement of the spreader beam. Note that no attempt was made to model base rotation due to rebar slip.

The analysis results are given in Table 5.8. Given in Figure 5.13 - Figure 5.16 are representative observed and computed load-deformation plots for each wall type, one with no axial load, SW11 and SW21, and one with the highest level of axial load, SW16 and SW23. The strengths of the walls were computed accurately and with a low degree of scatter; the ratio of the calculated to observed strength for the 13 walls had a mean of 1.02 to 1.04 and a coefficient of variation of 5.2% to 6.0%. The results show very little difference between each model. In most situations involving orthogonally reinforced structures containing above minimum levels of reinforcement, such is likely to be the case. The predicted failure modes involved crushing of concrete at the compression toe region coupled with a sliding shear failure along the base in some cases; this corresponded well with the observed failures reported by Lefas et al. The computed deflections and ultimate ductility showed some variance relative to the observed responses, but generally were accurately represented as well.

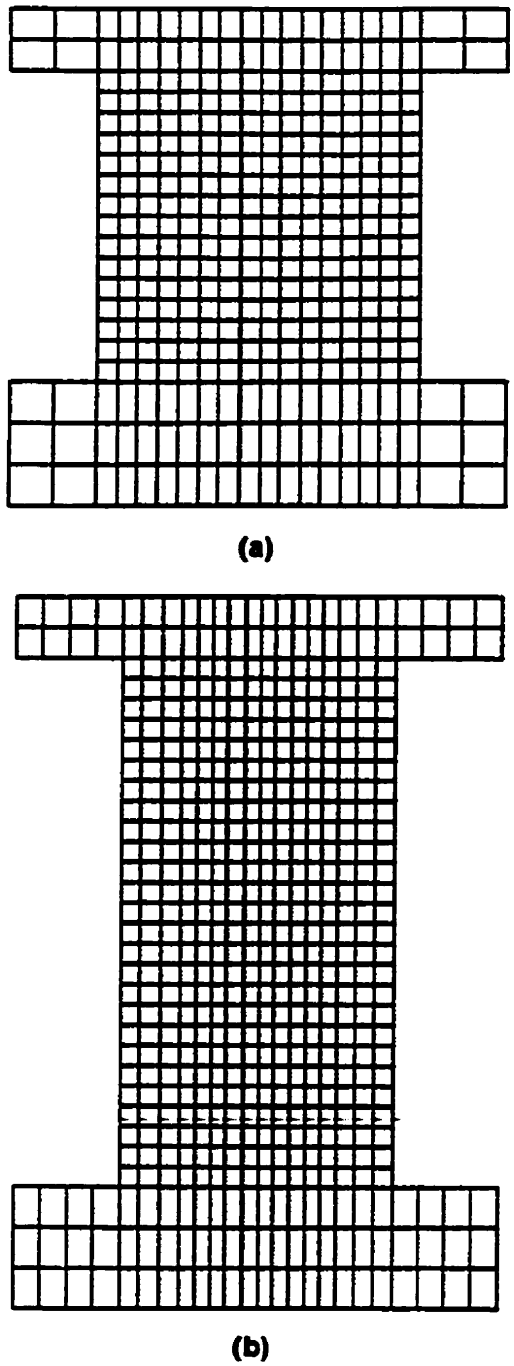

Figure 5.12 Finite element meshes for shear walls. (a) Type I walls. (b) Type II walls.

Table 5.8 (without initial offset slip factor)

Wall	$V_{u\text{-}exp}$ (kN)	$V_{u\text{-}theor}$ (kN)							$V_{u\text{-}theor}/V_{u\text{-}exp}$						
		MCFT 0	Wal. 1	Mae. 2	Lai 3	Hy. I 4	Hy. II 5	Hy. III 6	MCFT 0	Wal. 1	Mae. 2	Lai 3	Hy. I 4	Hy. II 5	Hy. III 6
SW11	260	281	287	286	284	280	280	280	1.081	1.104	1.100	1.092	1.077	1.077	1.077
SW12	340	337	346	345	346	341	343	343	0.991	1.018	1.015	1.018	1.003	1.009	1.009
SW13	330	360	367	365	366	367	367	367	1.091	1.112	1.106	1.109	1.112	1.112	1.112
SW14	265	268	277	275	272	268	268	268	1.011	1.045	1.038	1.026	1.011	1.011	1.011
SW15	320	302	310	309	309	310	309	308	0.944	0.969	0.966	0.966	0.969	0.966	0.963
SW16	355	371	374	372	374	376	374	376	1.045	1.054	1.048	1.054	1.059	1.054	1.059
SW17	247	254	260	254	258	258	255	257	1.028	1.053	1.028	1.045	1.045	1.032	1.040
SW21	127	123	126	124	125	123	123	123	0.969	0.992	0.976	0.984	0.969	0.969	0.969
SW22	150	153	154	154	155	153	153	154	1.020	1.027	1.027	1.033	1.020	1.020	1.027
SW23	180	173	174	171	173	171	168	165	0.961	0.967	0.950	0.961	0.950	0.933	0.917
SW24	120	125	127	127	127	125	125	125	1.042	1.058	1.058	1.058	1.042	1.042	1.042
SW25	150	168	169	169	168	169	167	168	1.120	1.127	1.127	1.120	1.127	1.113	1.120
SW26	123	118	119	119	119	119	118	118	0.959	0.967	0.967	0.967	0.967	0.959	0.959
								Mean	1.020	1.038	1.031	1.033	1.027	1.023	1.023
								COV(%)	5.40	5.29	5.51	5.21	5.51	5.58	5.95

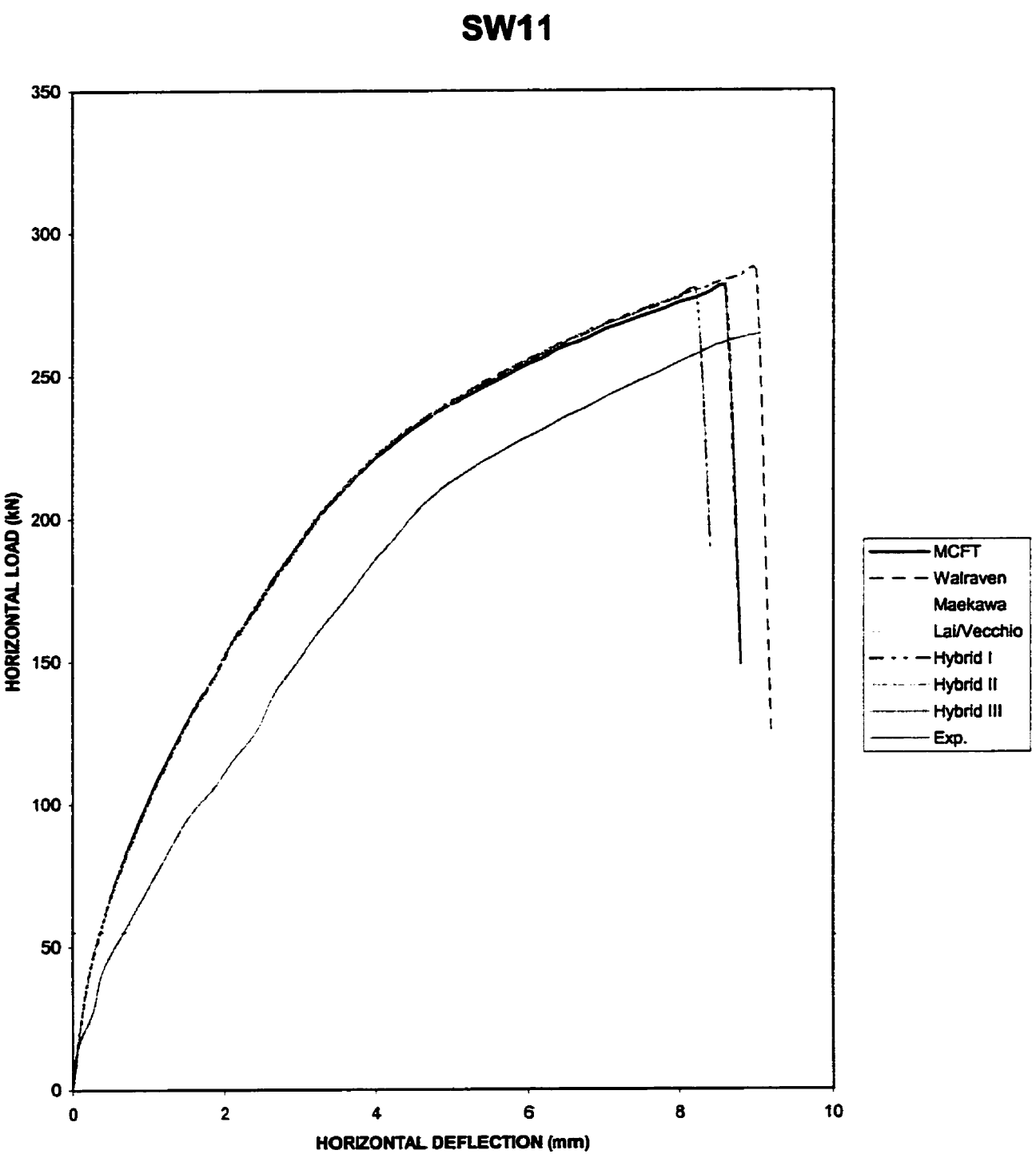
SW11
HORIZONTAL LOAD (kN)
350
300
250
200
150
100
50
0
0
2
4
6
8
10
HORIZONTAL DEFLECTION (mm)
MCFT
Walraven
Maekawa
Lai/Vecchio
Hybrid I
Hybrid II
Hybrid III
Exp.

Figure 5.13

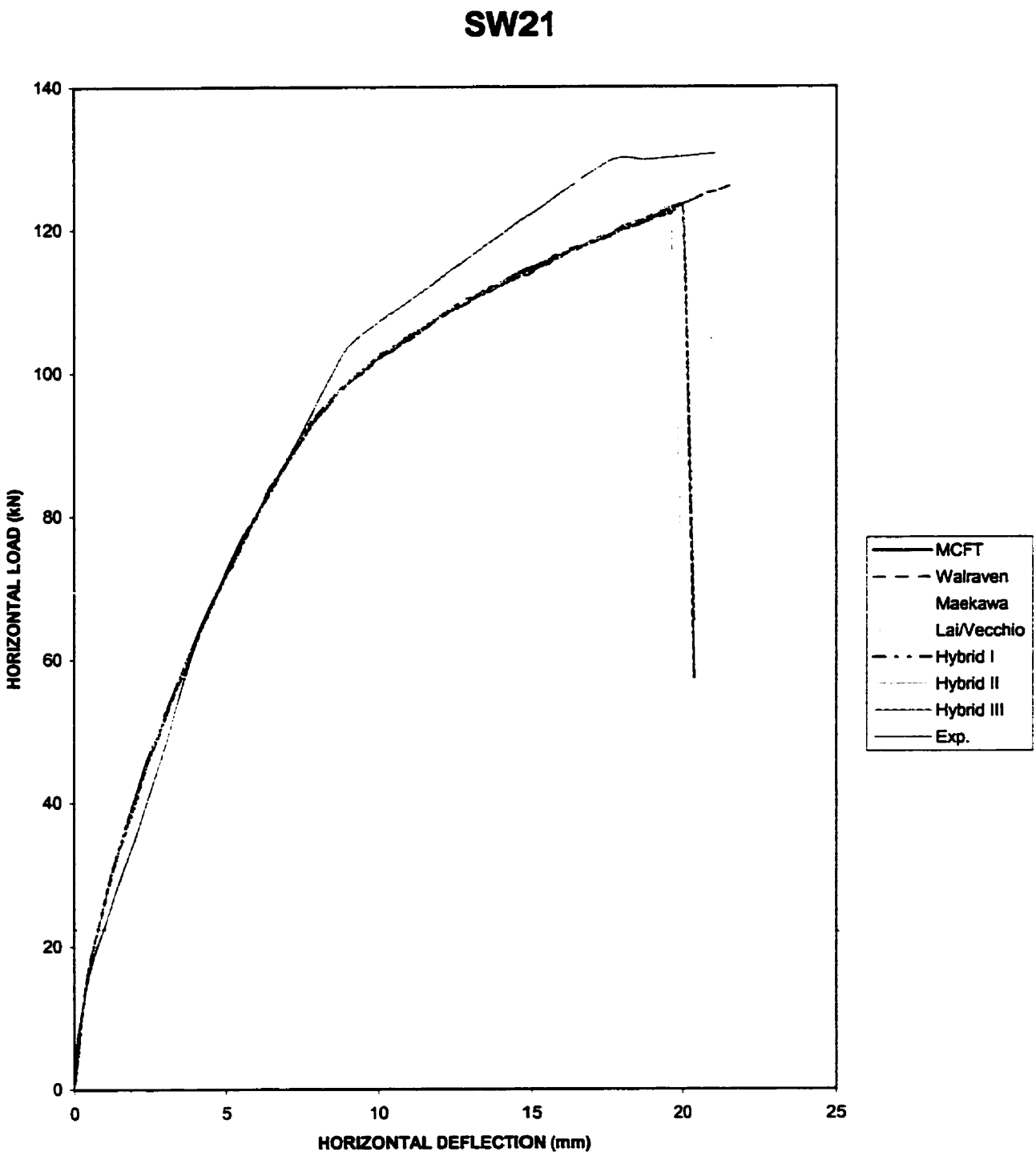
SW21
HORIZONTAL LOAD (kN)
HORIZONTAL DEFLECTION (mm)
0
20
40
60
80
100
120
140
0
5
10
15
20
25
MCFT
Walraven
Maekawa
Lai/Vecchio
Hybrid I
Hybrid II
Hybrid III
Exp.

Figure 5.14

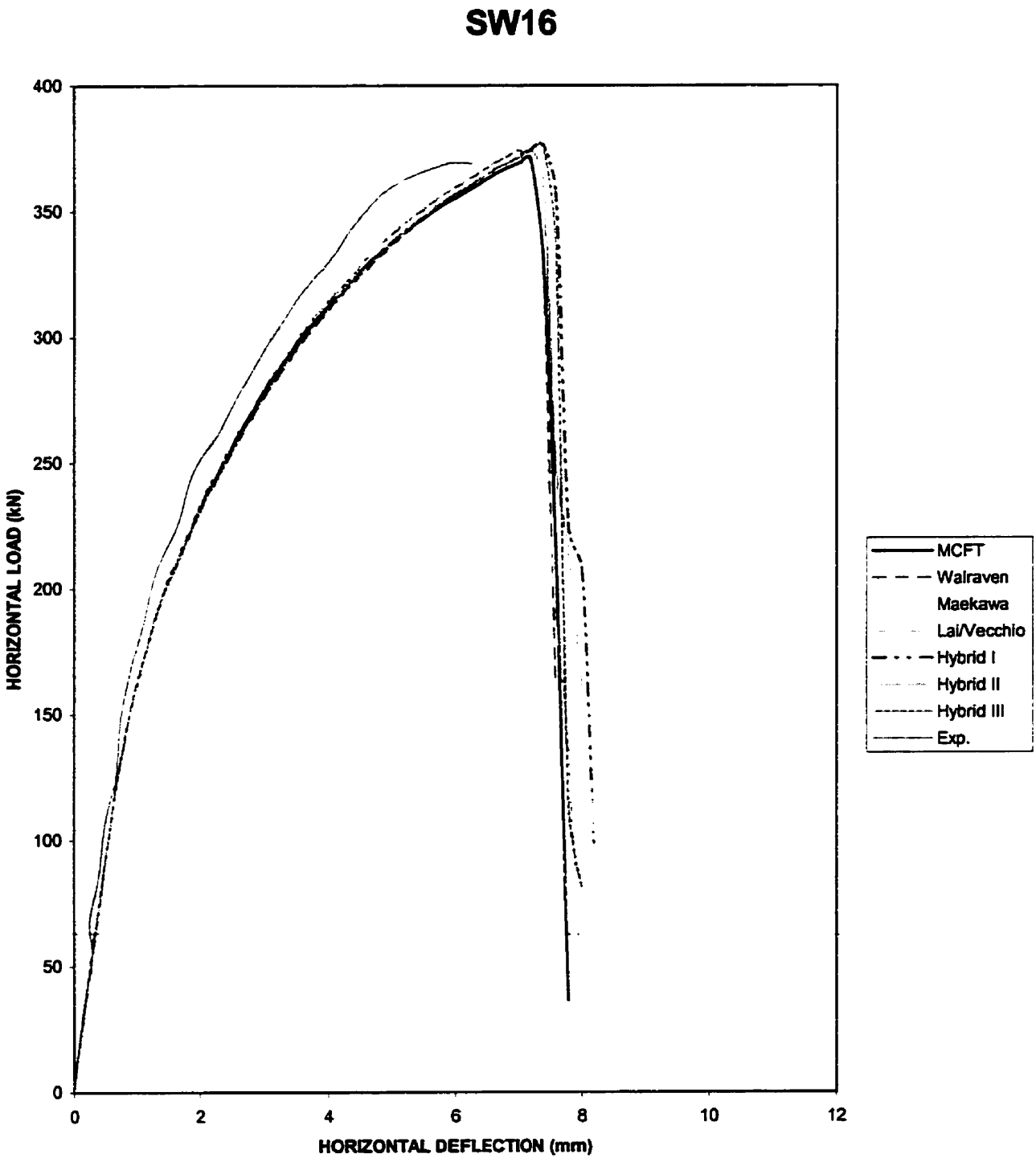
SW16
HORIZONTAL LOAD (kN)
HORIZONTAL DEFLECTION (mm)
0
50
100
150
200
250
300
350
400
0
2
4
6
8
10
12
MCFT
Walraven
Maekawa
Lai/Vecchio
Hybrid I
Hybrid II
Hybrid III
Exp.

Figure 5.15

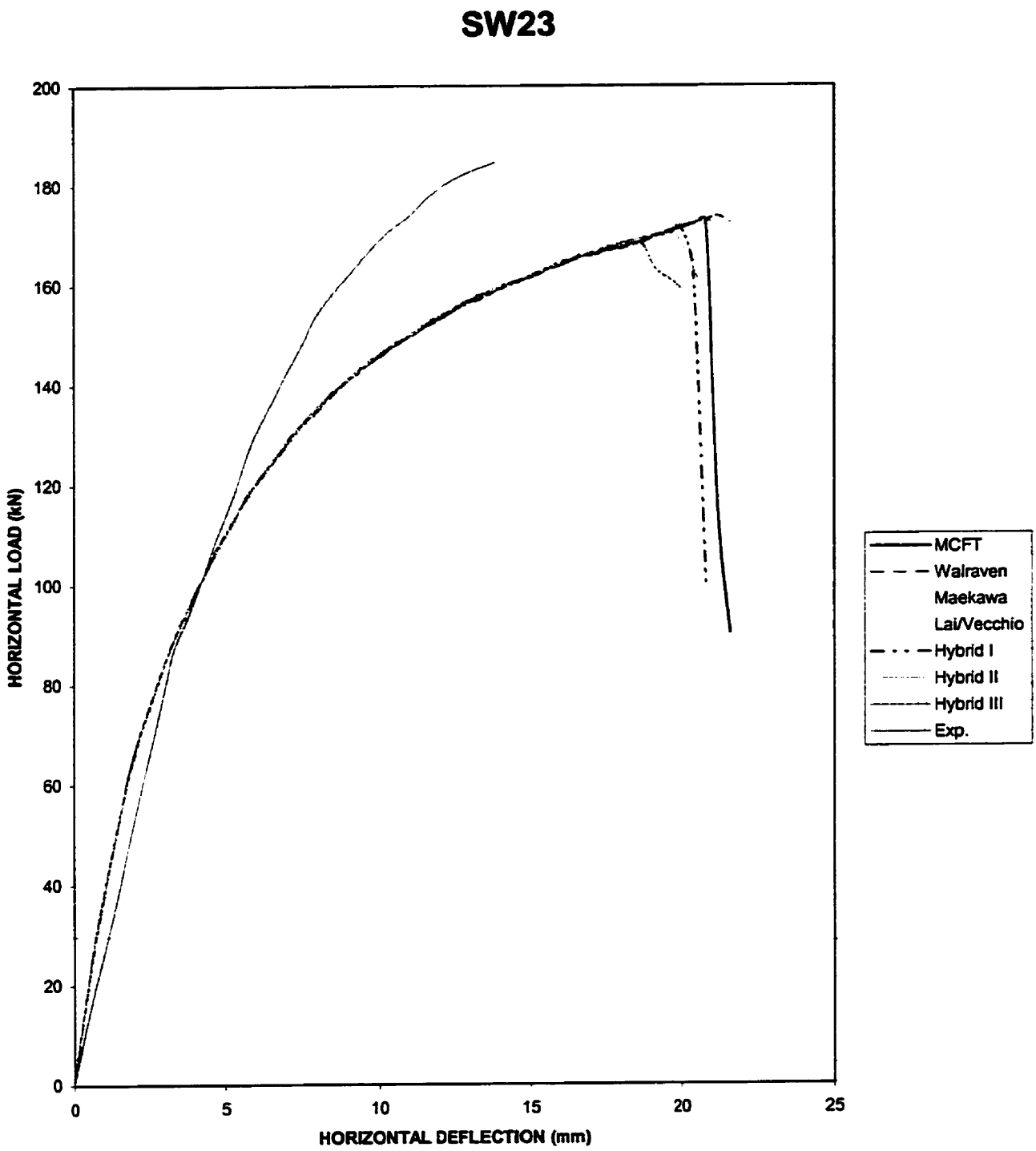
SW23
HORIZONTAL LOAD (kN)
HORIZONTAL DEFLECTION (mm)
0
20
40
60
80
100
120
140
160
180
200
0
5
10
15
20
25
MCFT
Walraven
Maekawa
Lai/Vecchio
Hybrid I
Hybrid II
Hybrid III
Exp.

Figure 5.16

5.4 Conclusions

The accuracy of the proposed formulation was tested by examining correlations with the test results from panels, beams and shear walls. It should be noted that most of the test specimen considered were difficult cases due to the nature of the reinforcement, cross section or loading details. The DSFM was generally found to provide accurate calculations of strength, load-deformation response, and failure mode. By comparison, the Lai/Vecchio model produced the best correlation for the panels, the DSFM models had the best correlation for the beams. For the shear walls, all the models produced close results compared to the experimental values. Analyses without the initial offset slip factor considered seem to produce the best correlations for panels and beams. As for the shear walls, the application of the initial offset slip factor has no effect on the results.

CHAPTER 6

Analyses of Structures --- Cyclic Loading

6.1 Description of Tests

The test specimens selected in this study were specifically chosen to examine the cyclic response of reinforced concrete walls and to corroborate the results obtained from the analytical procedures. The series of tests considered consists of four shear walls (B1, B2, B7, B8) with the same geometric properties, but with different web reinforcement, concrete confinement and axial load. These four walls were tested at the Portland Cement Association (Oesterle 1976).

The experimental investigation of B1, B2, B7, B8 involved cyclic displacements imposed along the axis of the web wall of the structure. The first two cycles consisted of displacements of 50.4 mm, incremented by 25.4 mm, with two complete cycles in each direction imposed at each displacement level.

The wall geometry and the nominal dimensions for the PCA walls are shown in Figure 6.1. The material properties are given in Table 6.1. The arrangement of vertical and horizontal reinforcement for the two types of wall are given in Table 6.2.

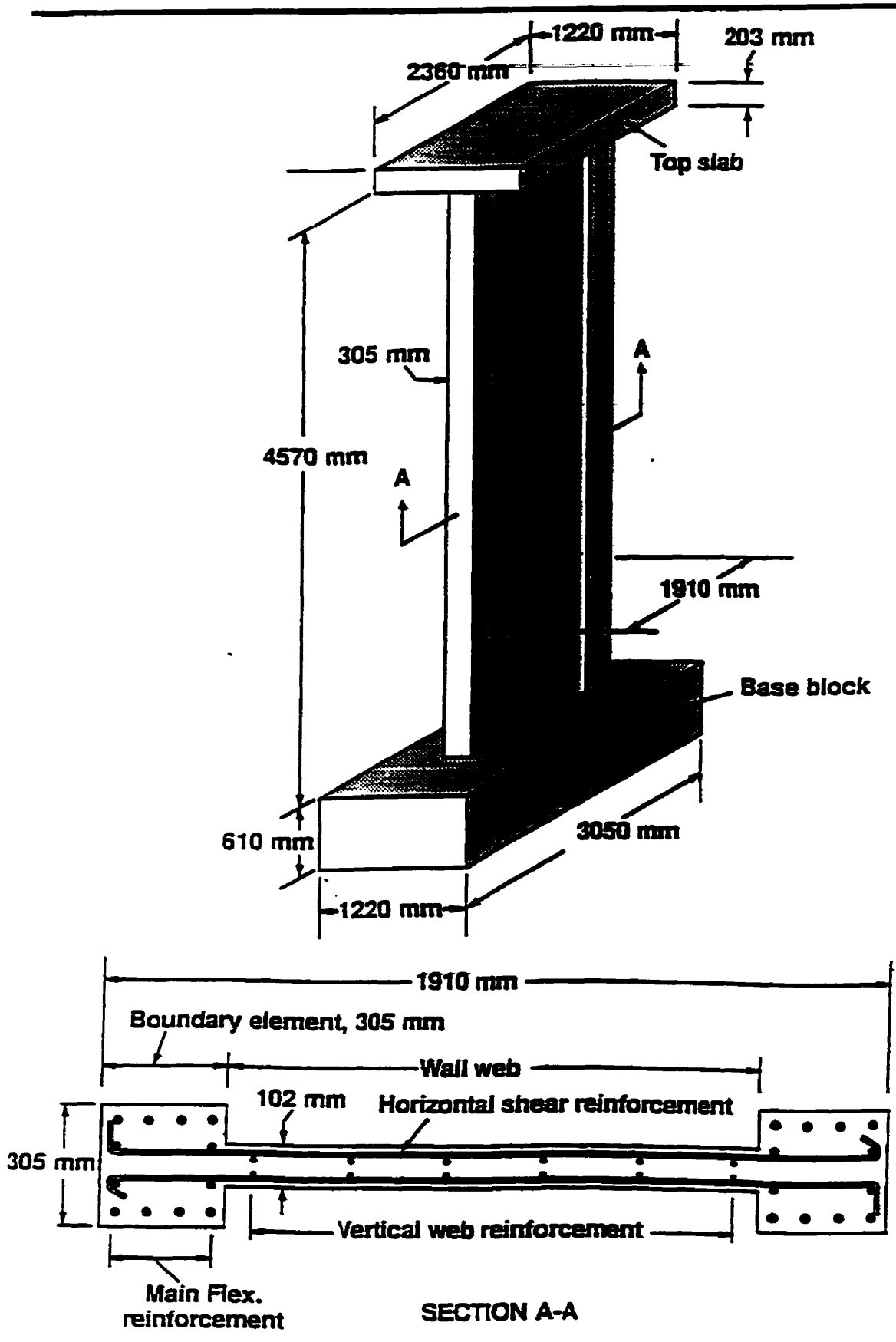

Figure 6.1 Nominal Dimensions of PCA walls

6.2 Analytical Modelling of Walls

The mesh layouts used in analyzing the PCA walls are shown in Figure 6.2. The PCA walls were modelled using first order rectangles and were divided into three different material zones on the basis of thickness, direction, and the amount of reinforcement.

The PCA walls were modelled with a mesh of 252 reinforced concrete elements. A total of 80 elements were used for the flanges: 4 elements in the horizontal direction and 20 elements in the vertical direction. For the web wall, a total of 160 elements were used: 8 in the horizontal direction and 20 in the vertical direction. The top slab was modelled with a total of 12 elements lying in the horizontal direction. The analysis consisted of many cycles and was performed from 80 to 244 load stages with a displacement increment of 5 mm.

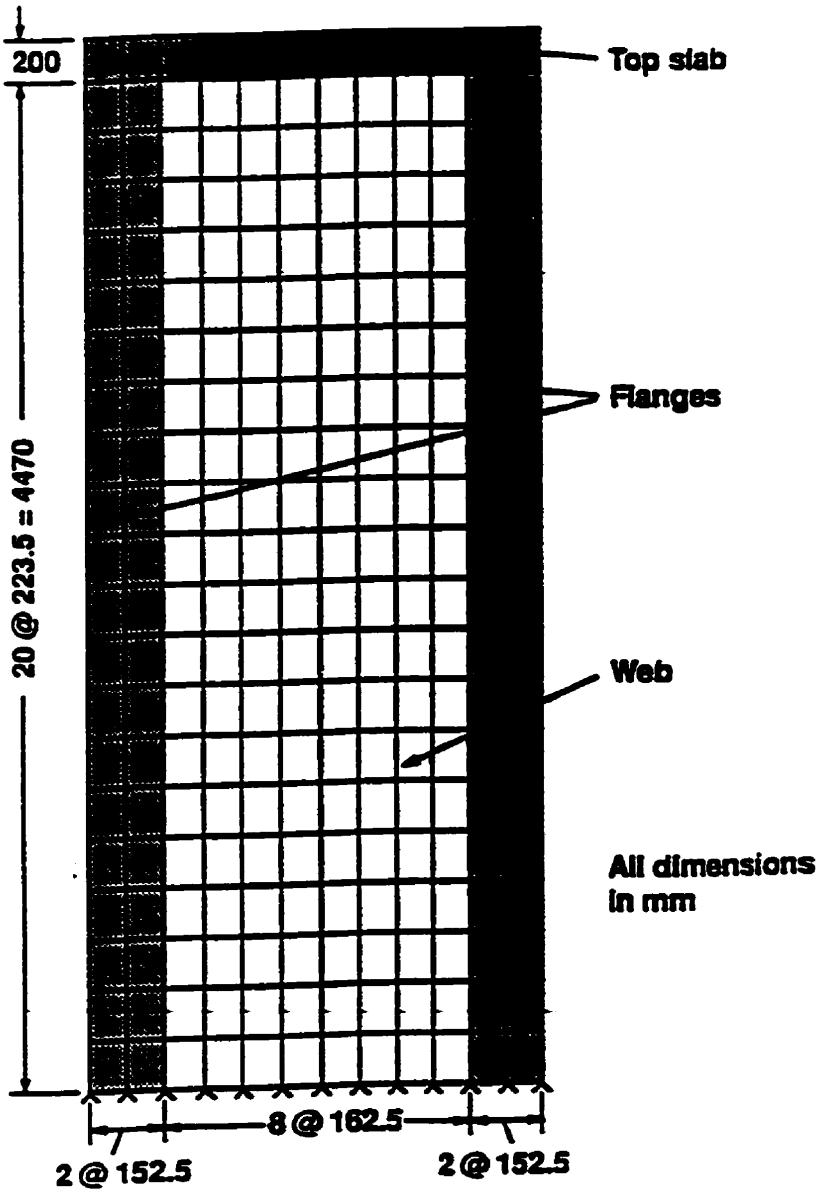

Figure 6.2 Mesh layout of PCA walls

Table 6.1 gives the material properties of the walls as used in the analysis. Table 6.2 gives the reinforcement percentages used in modeling of shear walls.

Table 6.1 Material Properties and Axial Load

Concrete

SPECIMEN	*MAT TYPE*	f'_c *(MPa)*	f'_t *(MPa)*	E_c *(MPa)*	*T (mm)*	*Axial Load (kN)*
B1	1	53	2.42	32300	102	0
	2	53	2.42	32300	305	0
	3	99.9	9.99	60000	1220	0
B2	1	53.7	2.42	32700	102	0
	2	53.7	2.42	32700	305	0
	3	99.9	9.99	60000	1220	0
B7	1	49.4	2.42	30100	102	1193
	2	49.4	2.42	30100	305	1193
	3	99.9	9.99	60000	1220	1193
B8	1	42	2.42	25600	102	1193
	2	42	2.42	25600	305	1193
	3	99.9	9.99	60000	1220	1193

Table 6.2 Reinforcement Percentages for PCA Shear Walls

Steel

SPECIMEN	*MAT TYPE*	*DIR (deg)*	A_s *(%)*	F_y *(MPa)*	F_u *(MPa)*	E_s *(MPa)*	E_{sh} *(MPa)*	e_{sh} *(me)*
B1	1	0	0.31	521	730	200000	2000	3.0
	1	90	0.29	521	730	200000	2000	3.0
	2	0	0.31	521	730	200000	2000	3.0
	2	90	1.11	450	710	200000	2000	2.5
	3	0	5.00	600	900	200000	2000	5.0
	3	90	5.00	600	900	200000	2000	5.0
B2	1	0	0.63	533	750	200000	2000	3.0
	1	90	0.29	533	750	200000	2000	3.0
	2	0	0.63	433	750	200000	2000	3.0
	2	90	3.67	410	650	200000	2000	2.5
	3	0	5.00	600	900	200000	2000	5.0
	3	90	5.00	600	900	200000	2000	5.0
B7	1	0	0.63	490	750	200000	2000	3.0
	1	90	0.29	490	750	200000	2000	3.0
	2	0	0.63	490	750	200000	2000	3.0
	2	90	3.67	458	650	200000	2000	2.5
	2	400	0.38	490	750	200000	2000	3.0
	3	0	5.00	600	900	200000	2000	5.0
	3	90	5.00	600	900	200000	2000	5.0
B8	1	0	1.38	482	750	200000	2000	3.0
	1	90	0.29	454	750	200000	2000	3.0
	2	0	1.38	482	750	200000	2000	3.0
	2	90	3.67	447	650	200000	2000	2.5
	2	400	0.41	454	750	200000	2000	3.0
	3	0	5.00	600	900	200000	2000	5.0
	3	90	5.00	600	900	200000	2000	5.0

A total of 28 series of analyses were performed using VecTor2. The main emphasis was placed on determining the influence derived from the various crack shear-slip models. The element slip model used for the various series of analyses are shown in Table 6.3.

Table 6.3 Element Slip Modelling

SPECIMEN	*ANALYSIS SERIES*	*ELEMENT SLIP DISTORTIONS MODEL*
B1	B1-0	MCFT
	B1-1	Walraven
	B1-2	Maekawa
	B1-3	Lai/Vecchio
	B1-4	Hybrid I
	B1-5	Hybrid II
	B1-6	Hybrid III
B2	B2-0	MCFT
	B2-1	Walraven
	B2-2	Maekawa
	B2-3	Lai/Vecchio
	B2-4	Hybrid I
	B2-5	Hybrid II
	B2-6	Hybrid III
B7	B7-0	MCFT
	B7-1	Walraven
	B7-2	Maekawa
	B7-3	Lai/Vecchio
	B7-4	Hybrid I
	B7-5	Hybrid II
	B7-6	Hybrid III
B8	B8-0	MCFT
	B8-1	Walraven
	B8-2	Maekawa
	B8-3	Lai/Vecchio
	B8-4	Hybrid I
	B8-5	Hybrid II
	B8-6	Hybrid III

6.3 Load-Deformation Relationship

In general, the analytical results were in close agreement with the experimental results. Load-deformation response and ultimate strength were well predicted. However, failure was usually not achieved until an extra displacement cycle was imposed.

A series of plots showing the experimental and theoretical lateral load versus lateral deflection responses are given in Figures 6.3 to 6.34. It can be seen that the ultimate strengths and load-deformation responses were accurately simulated.

The experimental load-deformation response of PCA Wall B1 is shown in Figure 6.3.

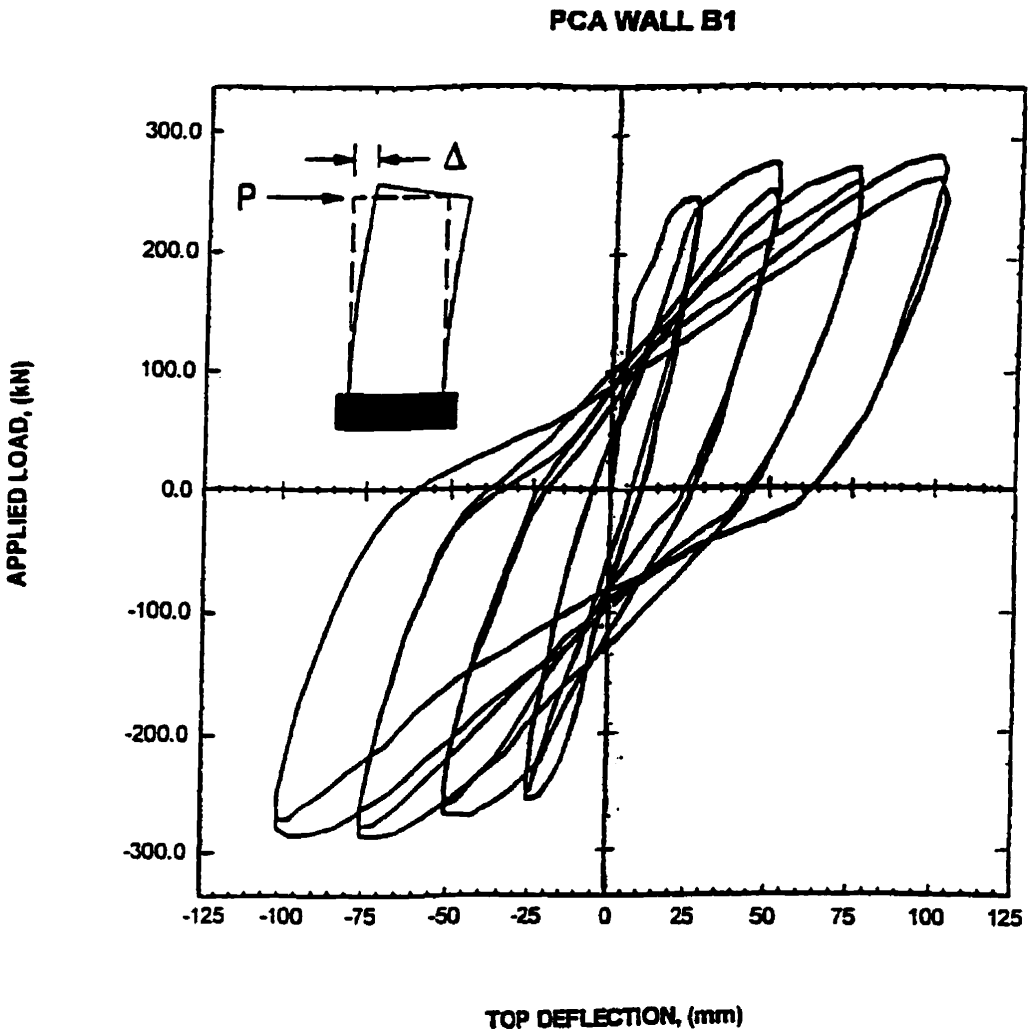

Figure 6.3 Experimental load-deformation response for PCA Wall B1

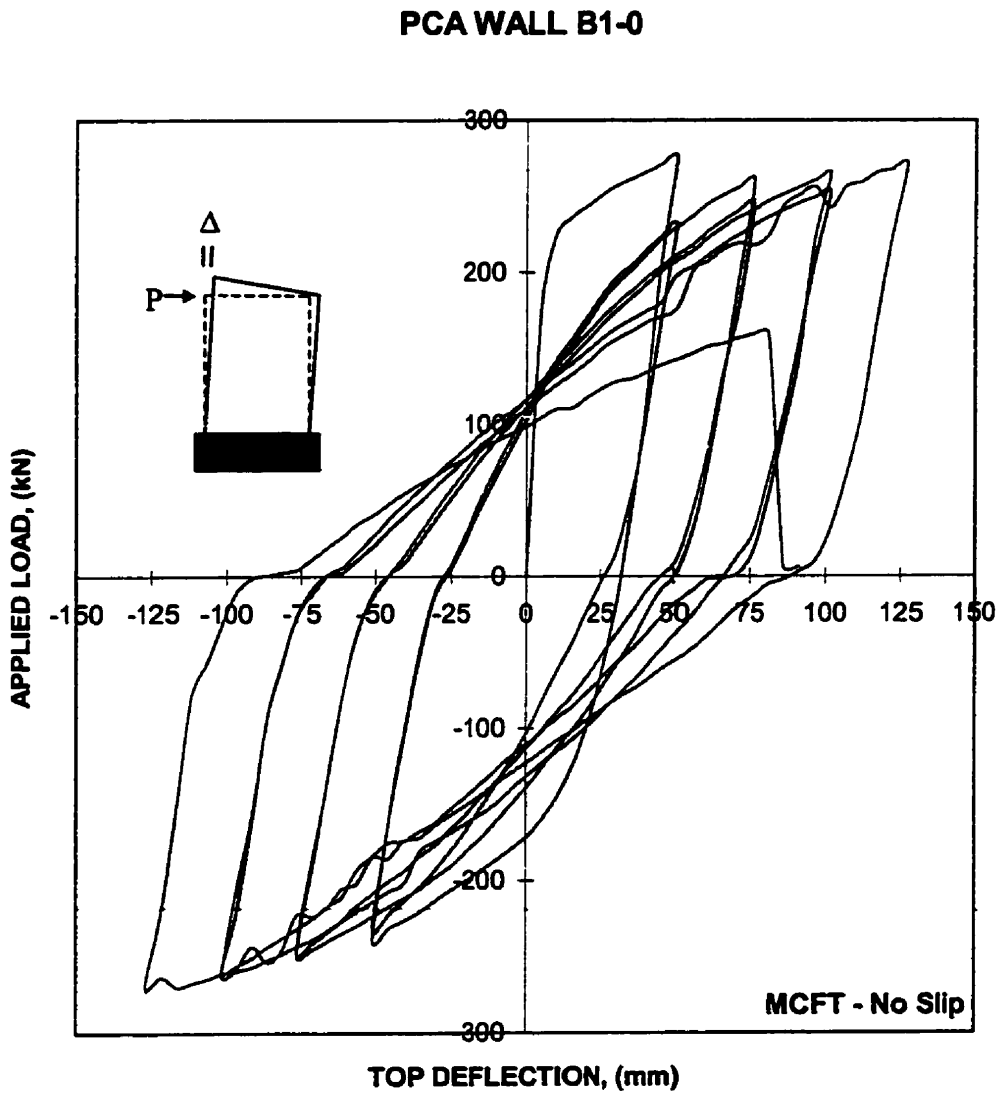

Figure 6.4 Analytical load-deformation response for PCA Wall B1-0 predicted by VecTor2

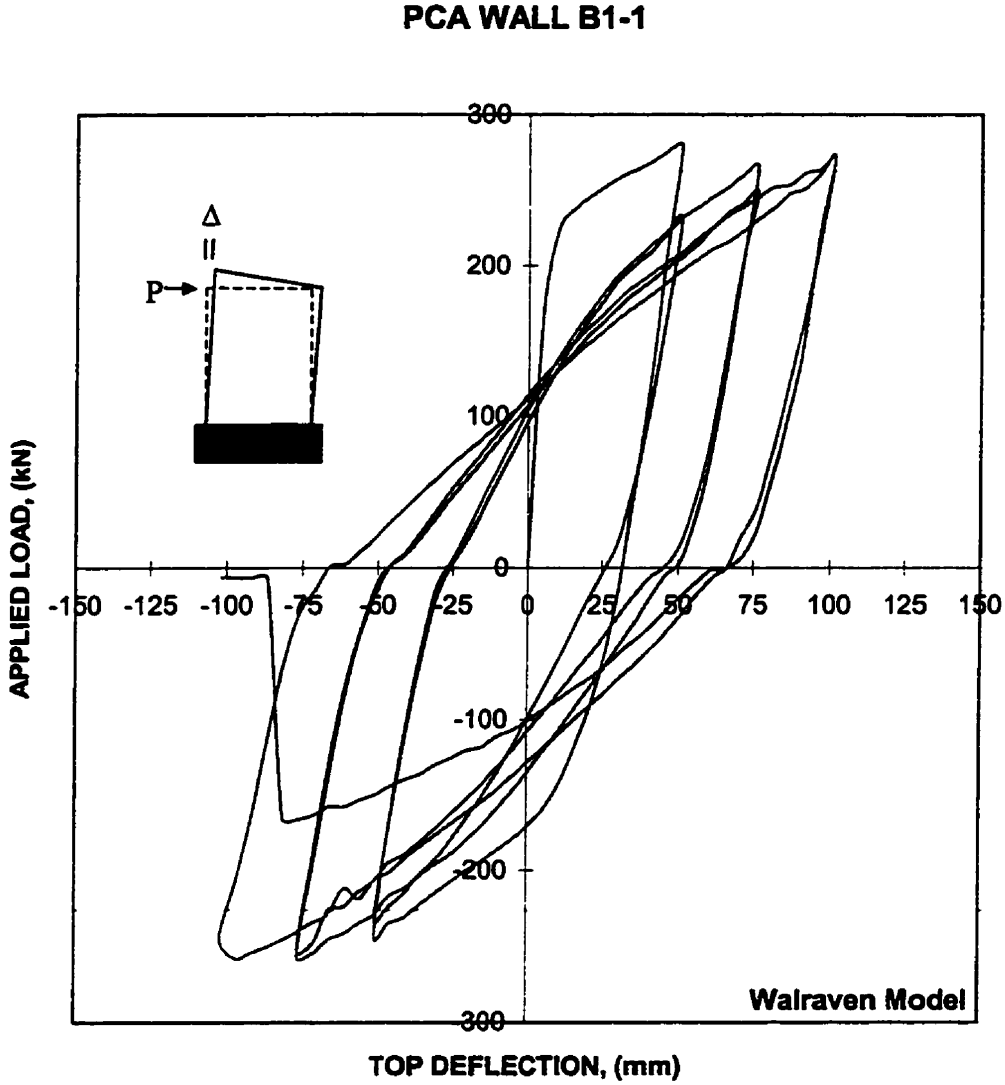

Figure 6.5 Analytical load-deformation response for PCA Wall B1-1 predicted by VecTor2

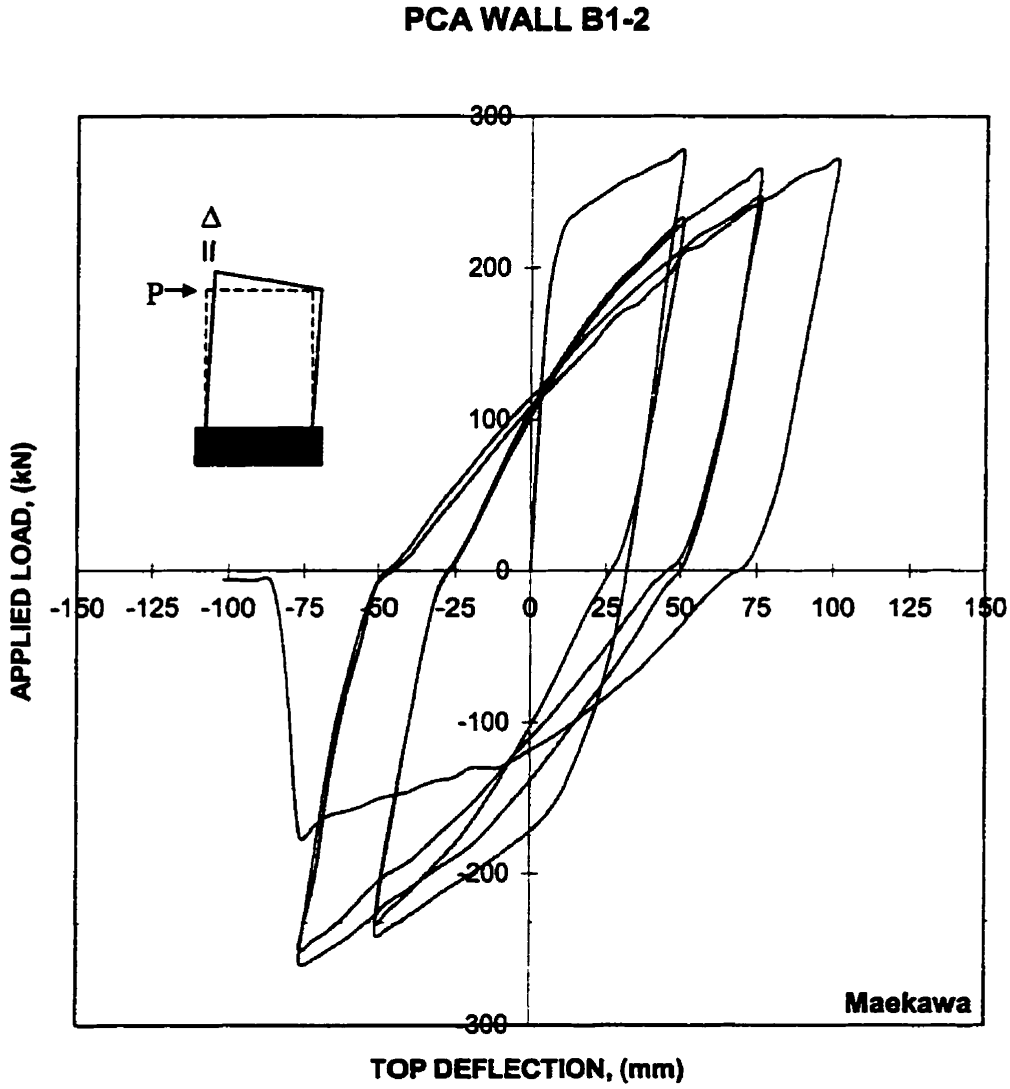

Figure 6.6 Analytical load-deformation response for PCA Wall B1-2 predicted by VecTor2

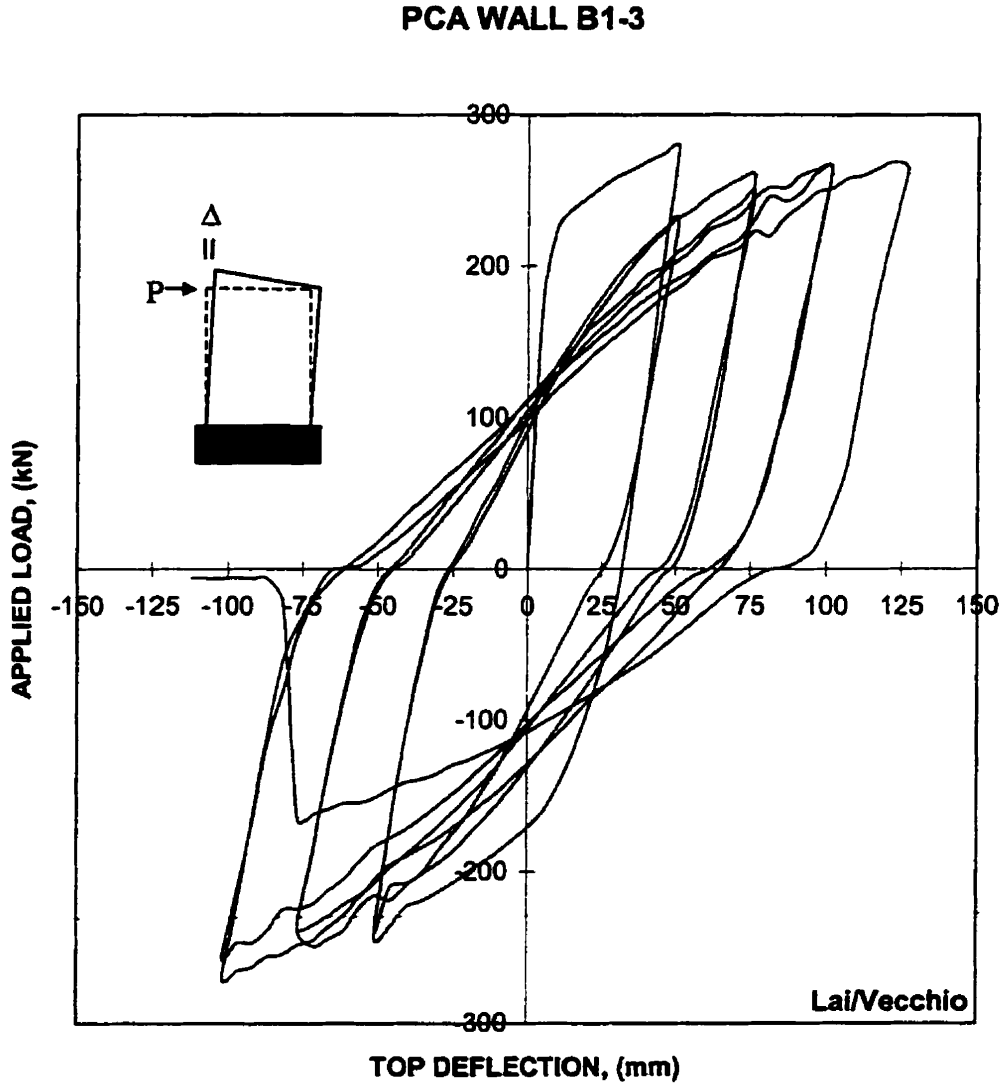

Figure 6.7 Analytical load-deformation response for PCA Wall B1-3 predicted by VecTor2

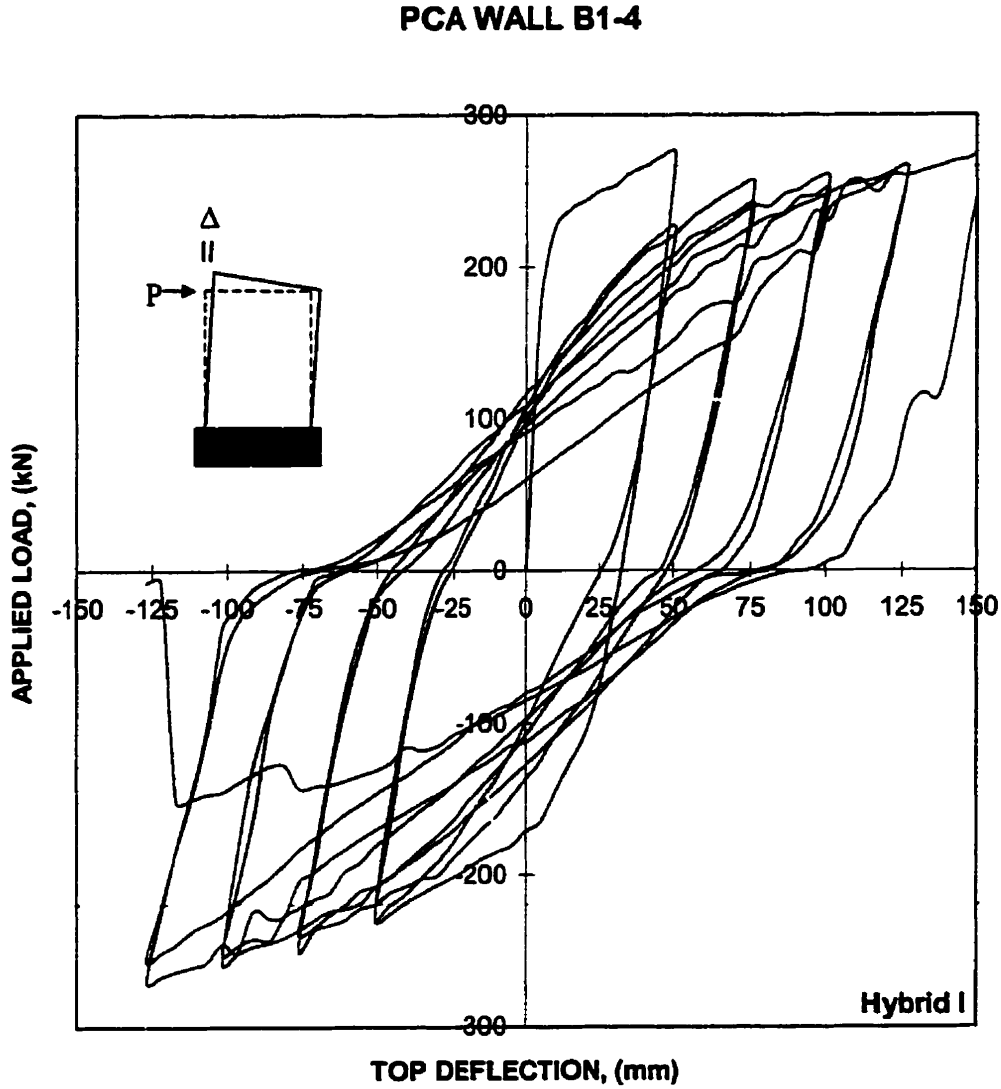

Figure 6.8 Analytical load-deformation response for PCA Wall B1-4 predicted by VecTor2

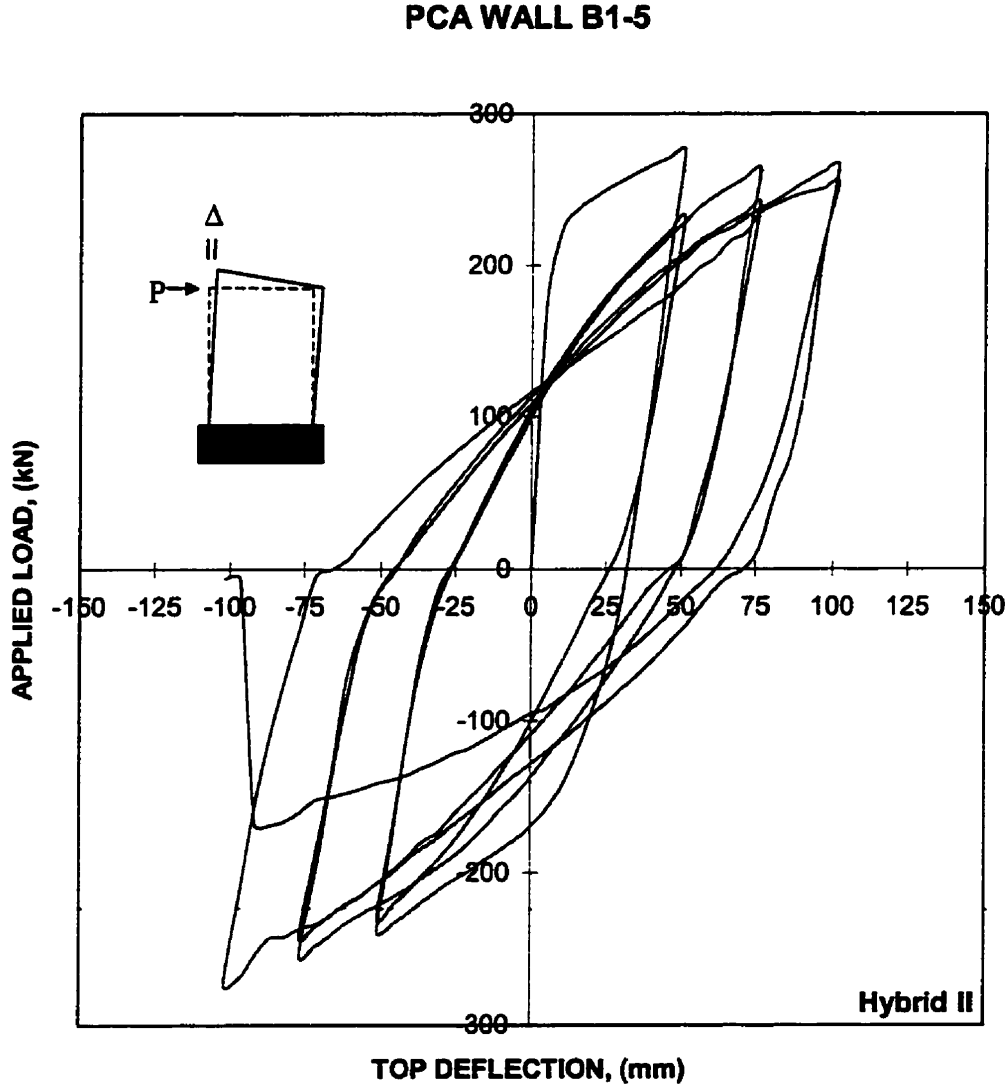

Figure 6.9 Analytical load-deformation response for PCA Wall B1-5 predicted by VecTor2

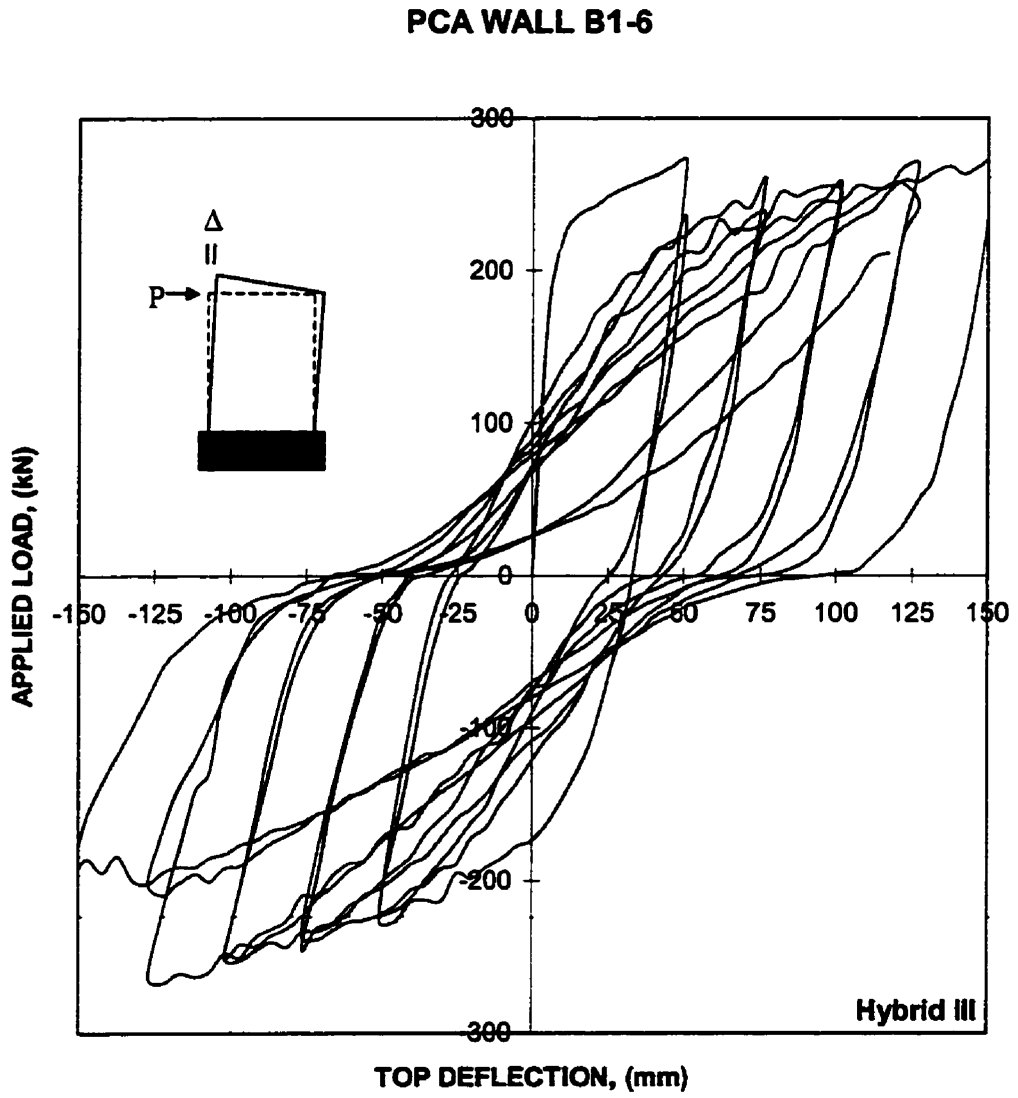

Figure 6.10 Analytical load-deformation response for PCA Wall B1-6 predicted by VecTor2

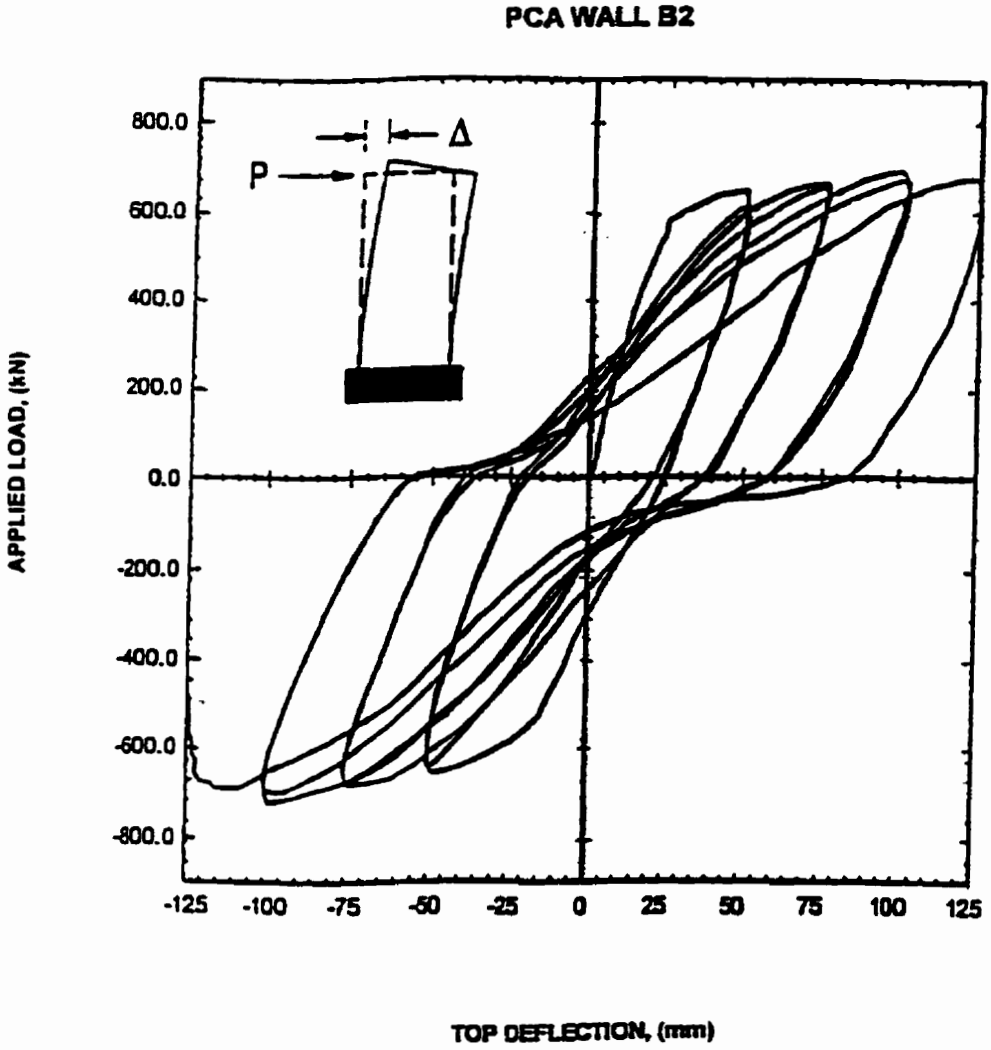

Figure 6.11 Experimental load-deformation response for PCA Wall B2

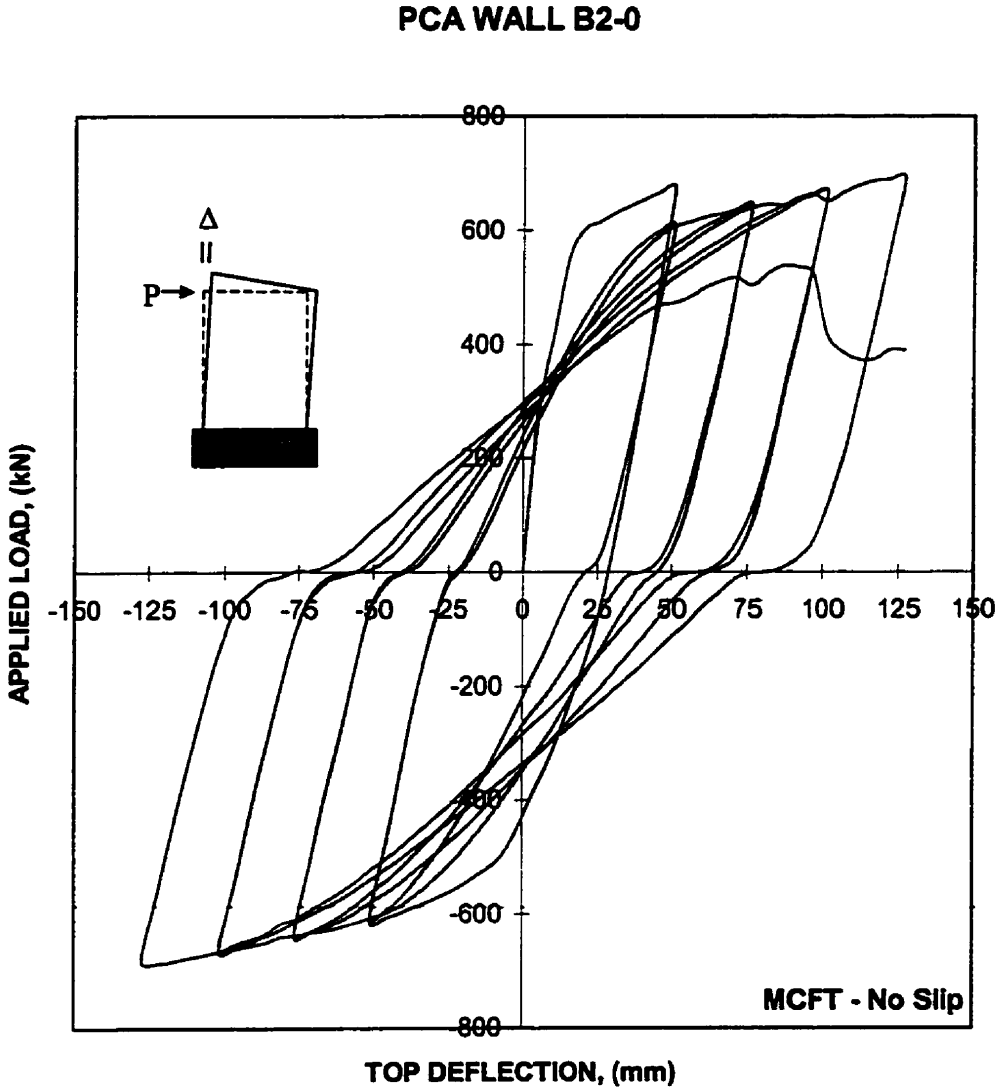

Figure 6.12 Analytical load-deformation response for PCA Wall B2-0 predicted by VecTor2

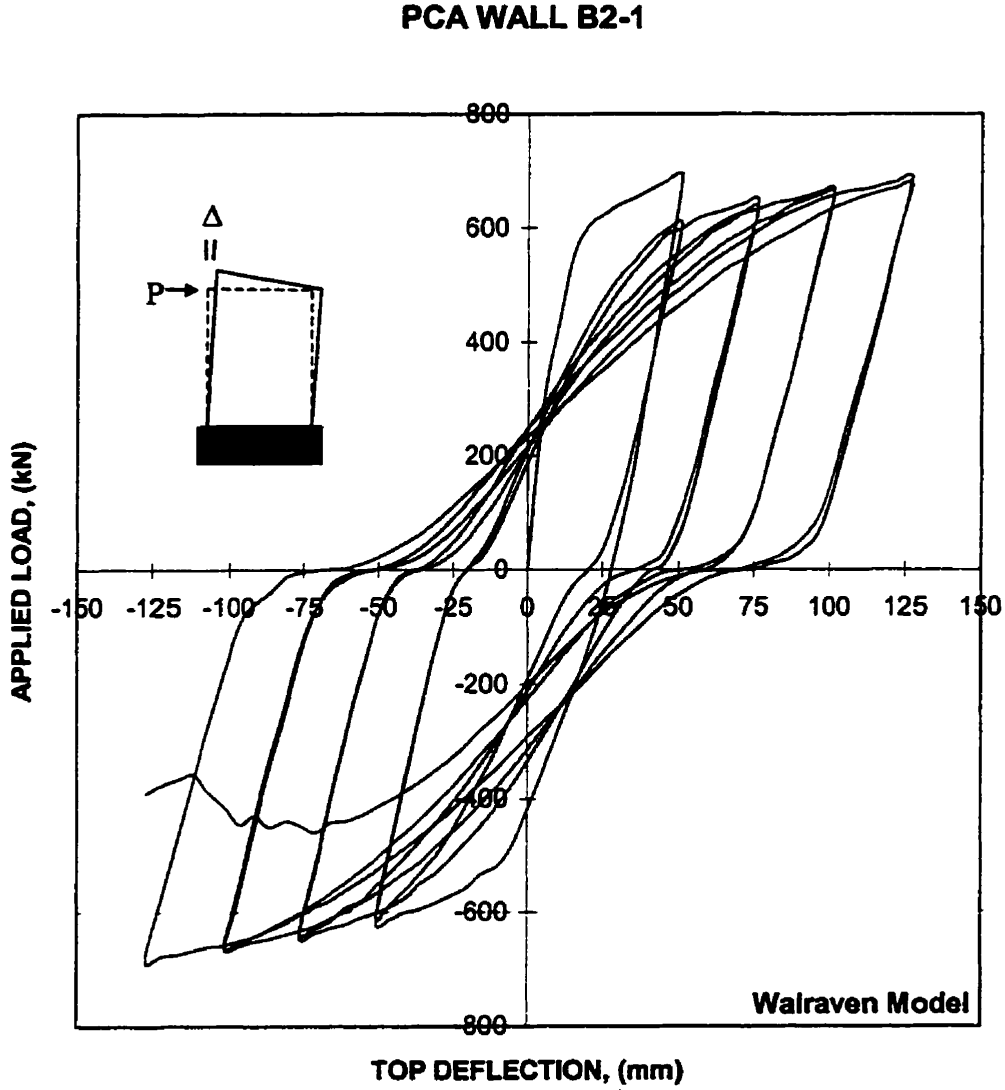

Figure 6.13 Analytical load-deformation response for PCA Wall B2-1 predicted by VecTor2

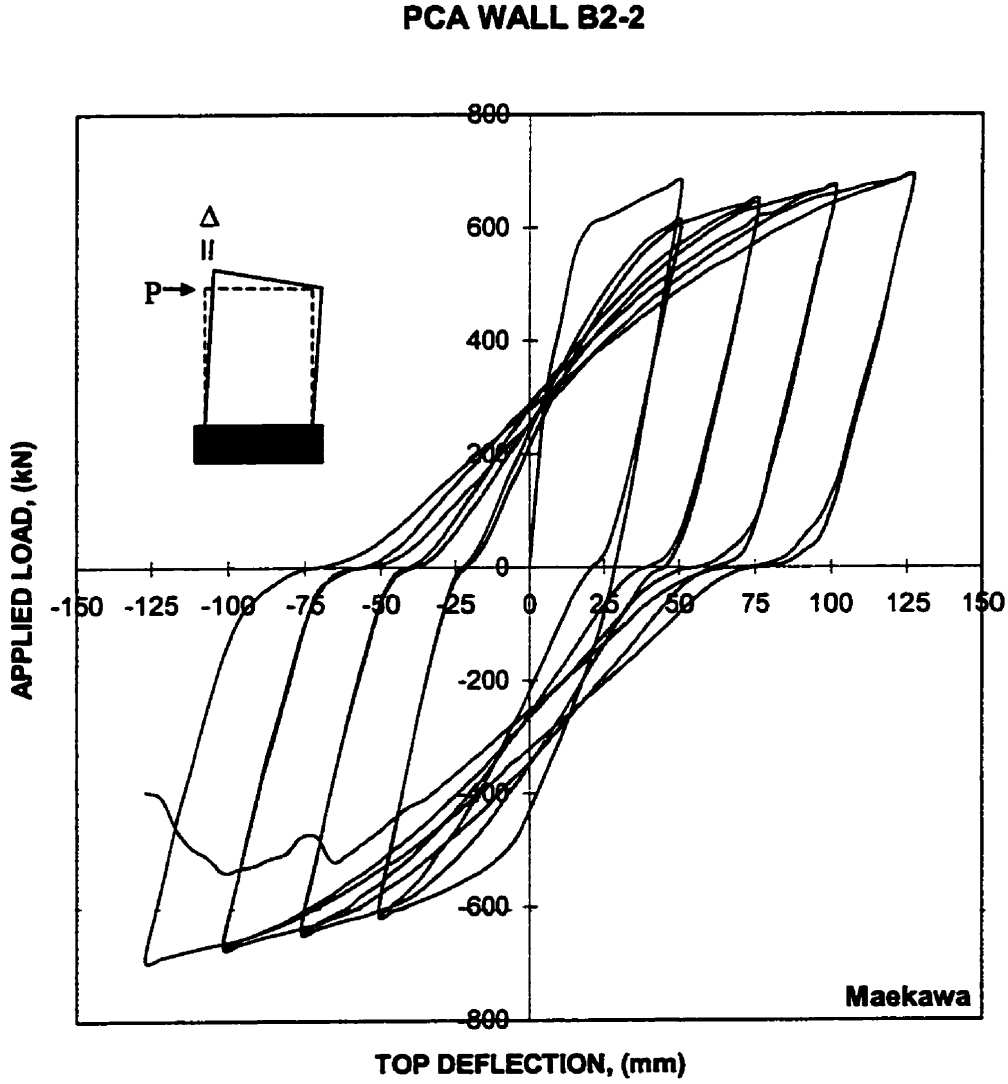

Figure 6.14 Analytical load-deformation response for PCA Wall B2-2 predicted by VecTor2

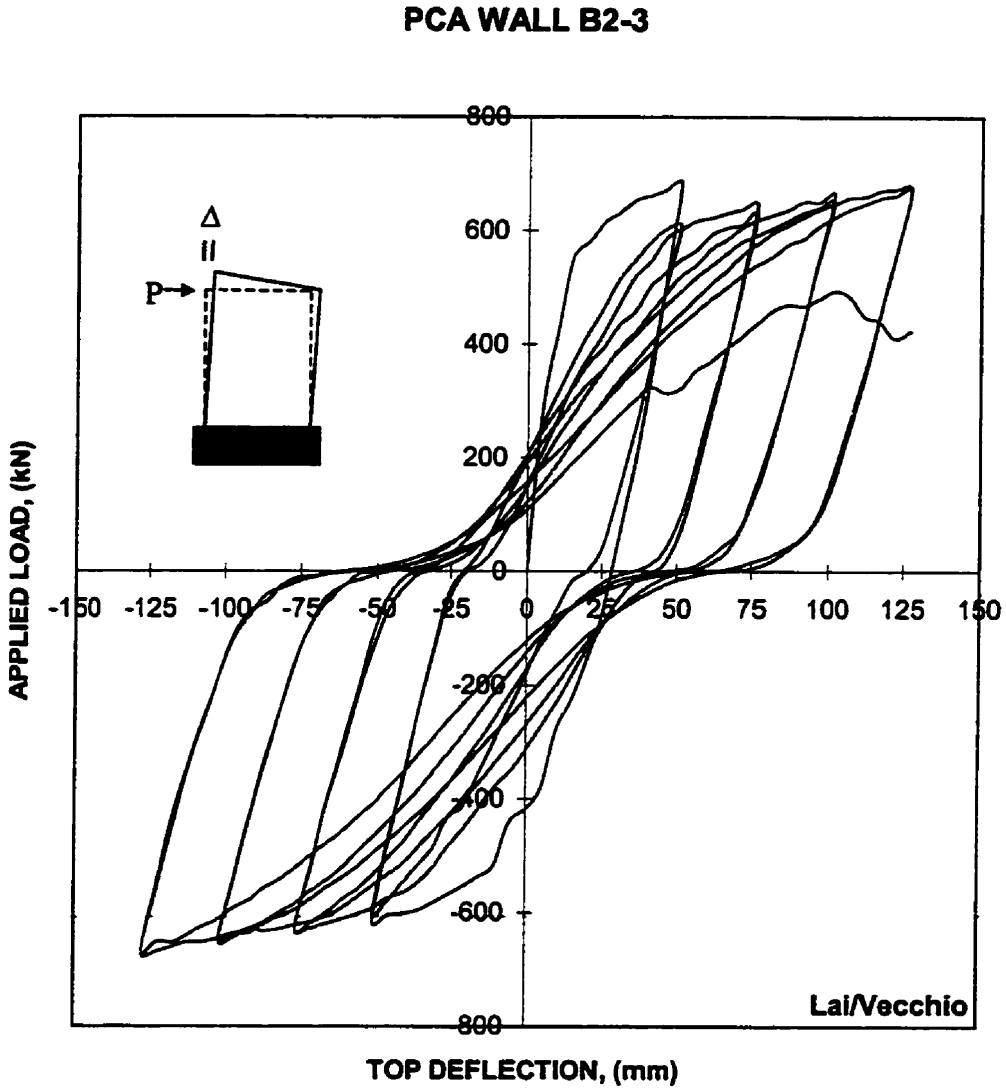

Figure 6.15 Analytical load-deformation response for PCA Wall B2-3 predicted by VecTor2

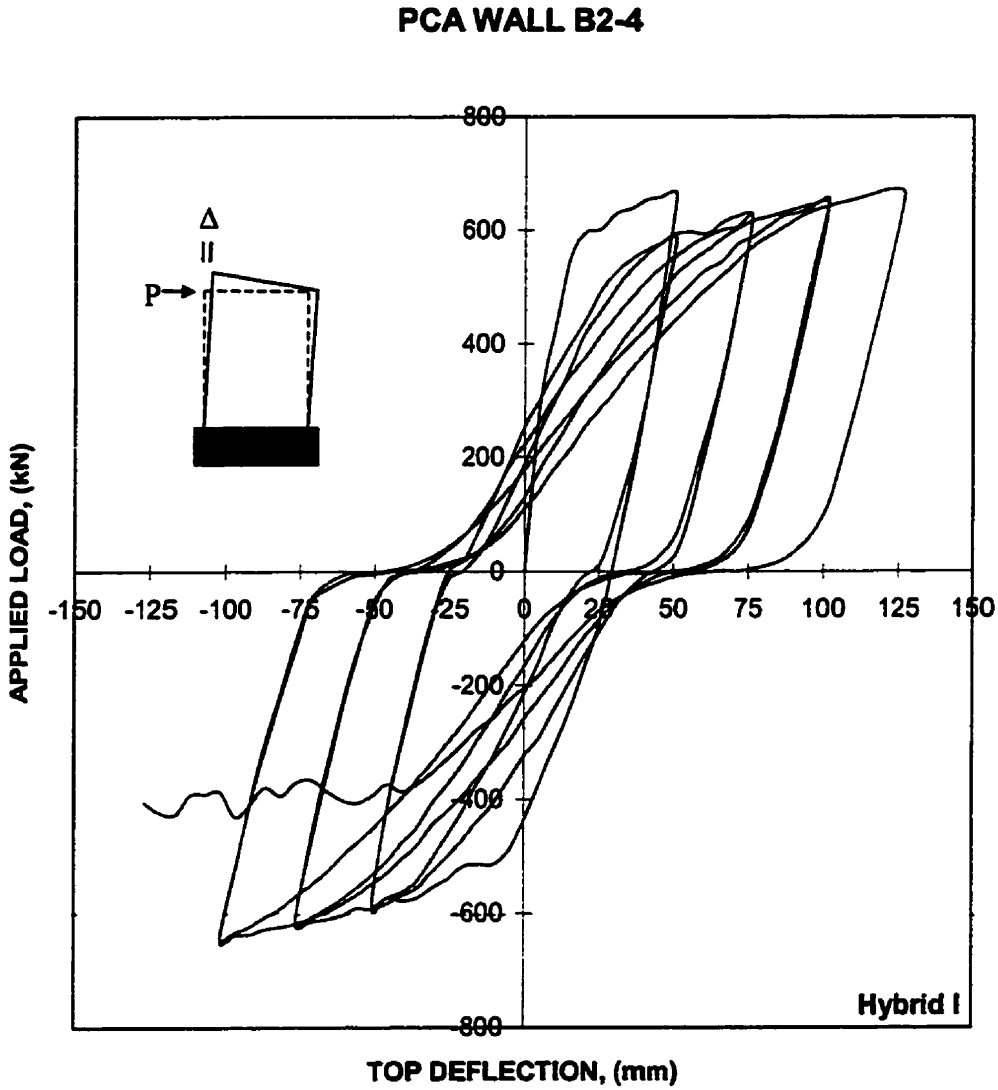

Figure 6.16 Analytical load-deformation response for PCA Wall B2-4 predicted by VecTor2

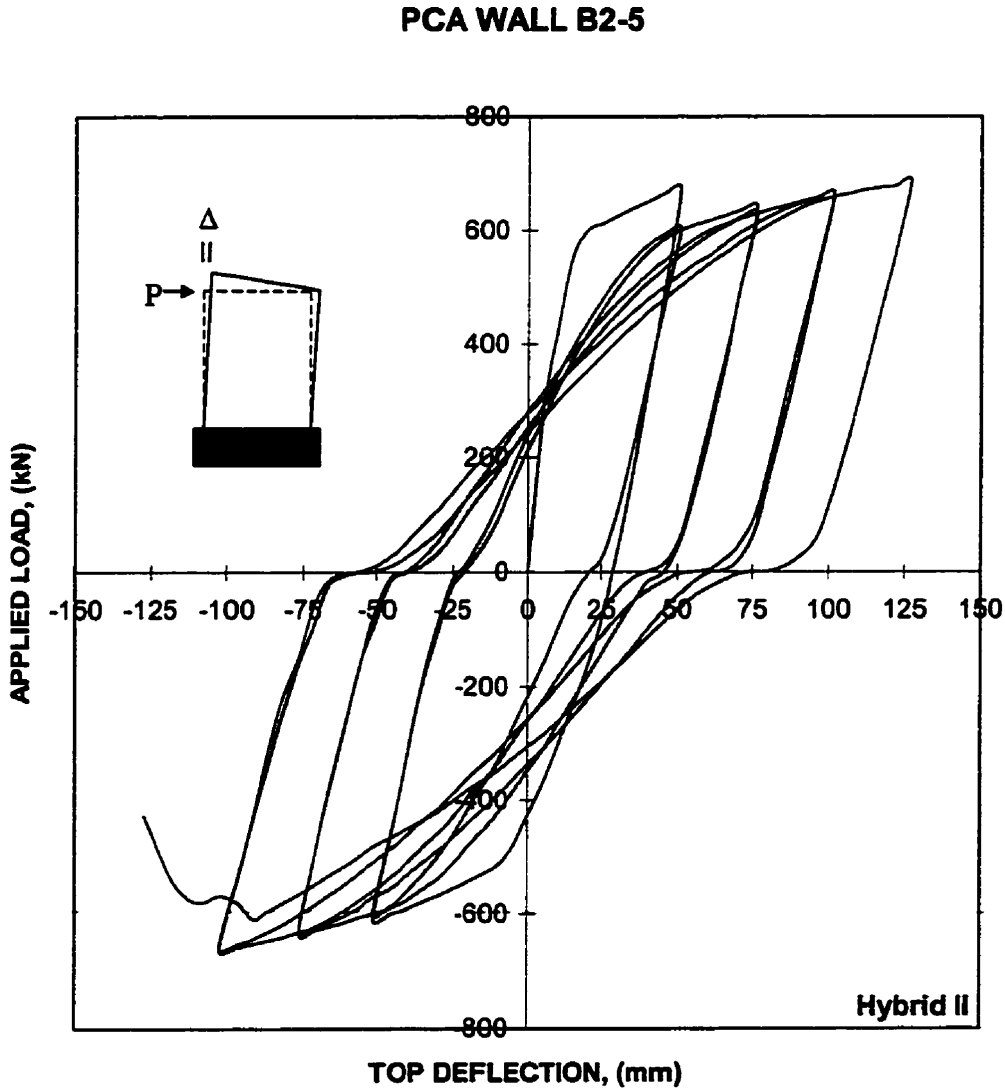

Figure 6.17 Analytical load-deformation response for PCA Wall B2-5 predicted by VecTor2

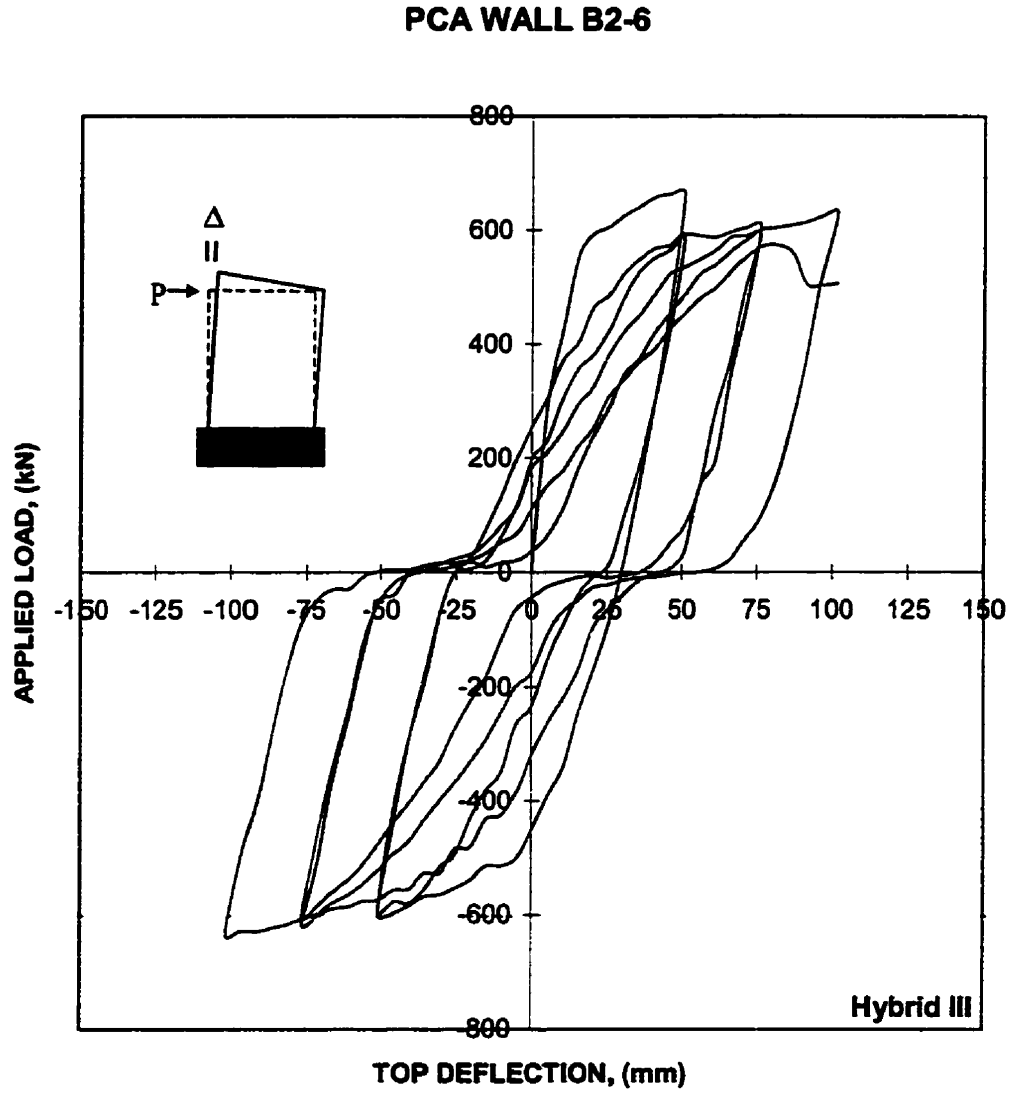

Figure 6.18 Analytical load-deformation response for PCA Wall B2-6 predicted by VecTor2

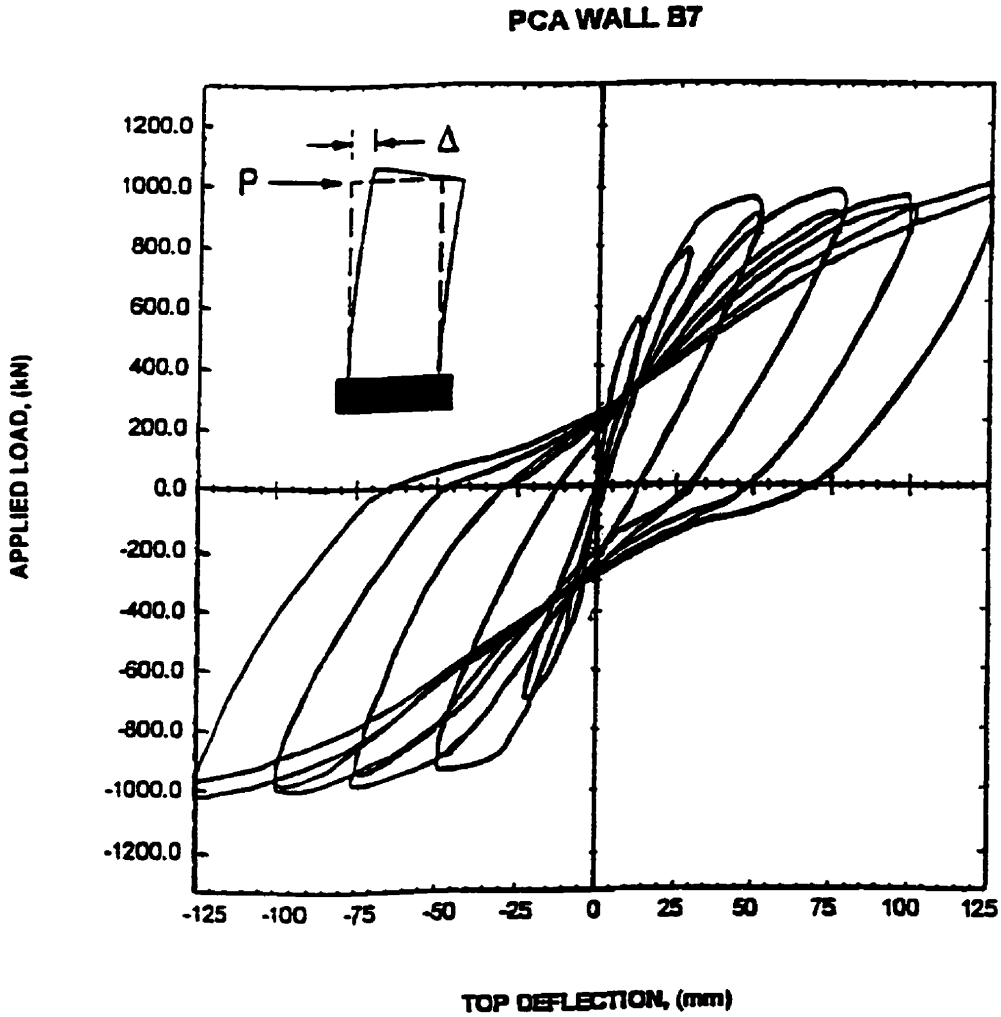

Figure 6.19 Experimental load-deformation response for PCA Wall B7

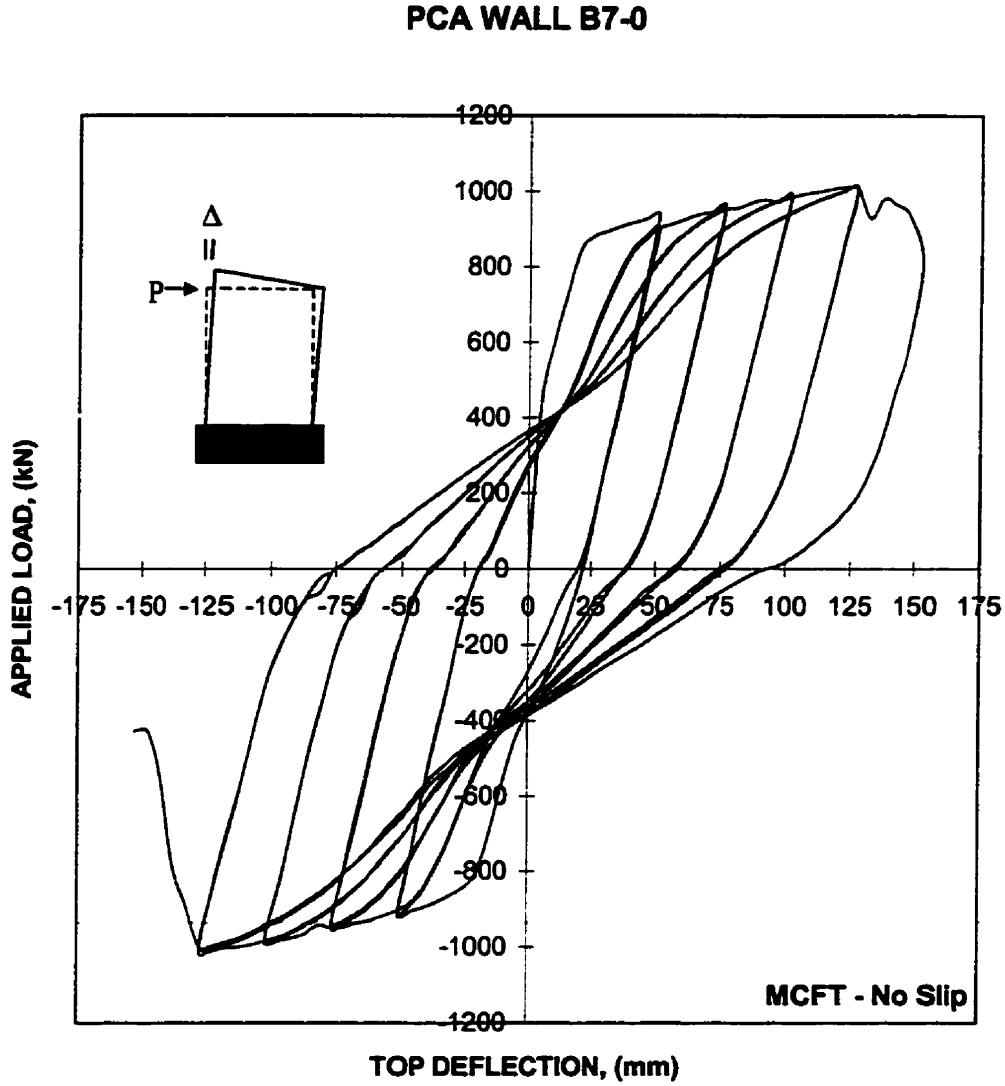

Figure 6.20 Analytical load-deformation response for PCA Wall B7-0 predicted by VecTor2

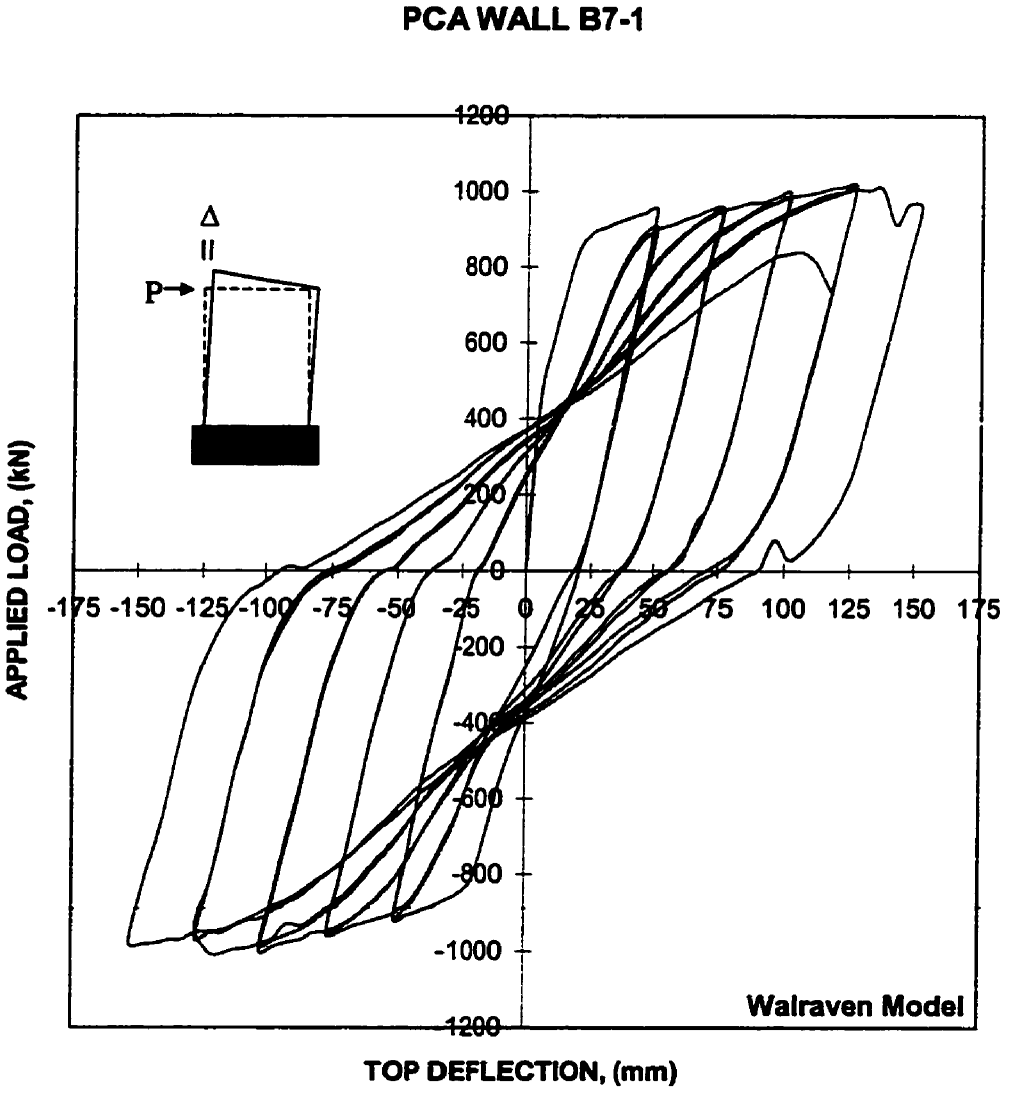

Figure 6.21 Analytical load-deformation response for PCA Wall B7-1 predicted by VecTor2

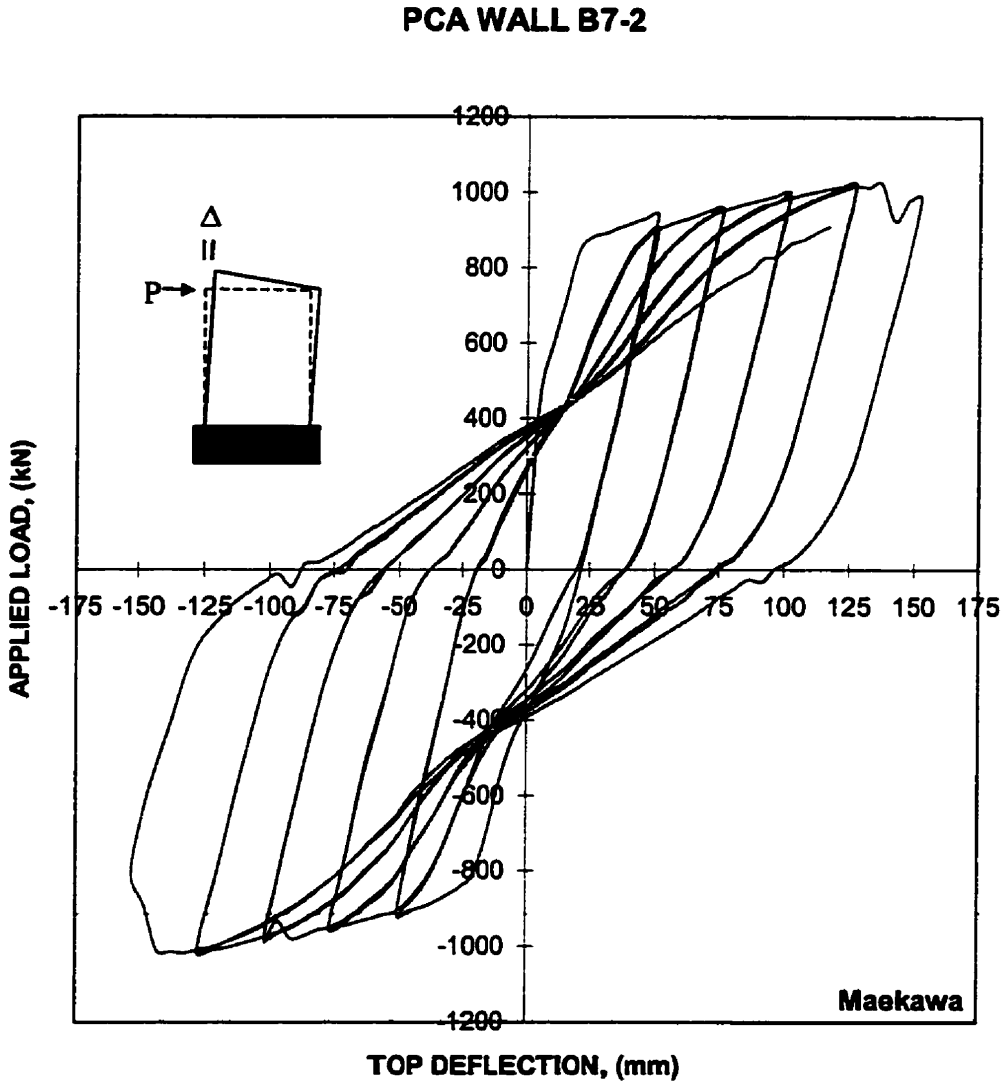

Figure 6.22 Analytical load-deformation response for PCA Wall B7-2 predicted by VecTor2

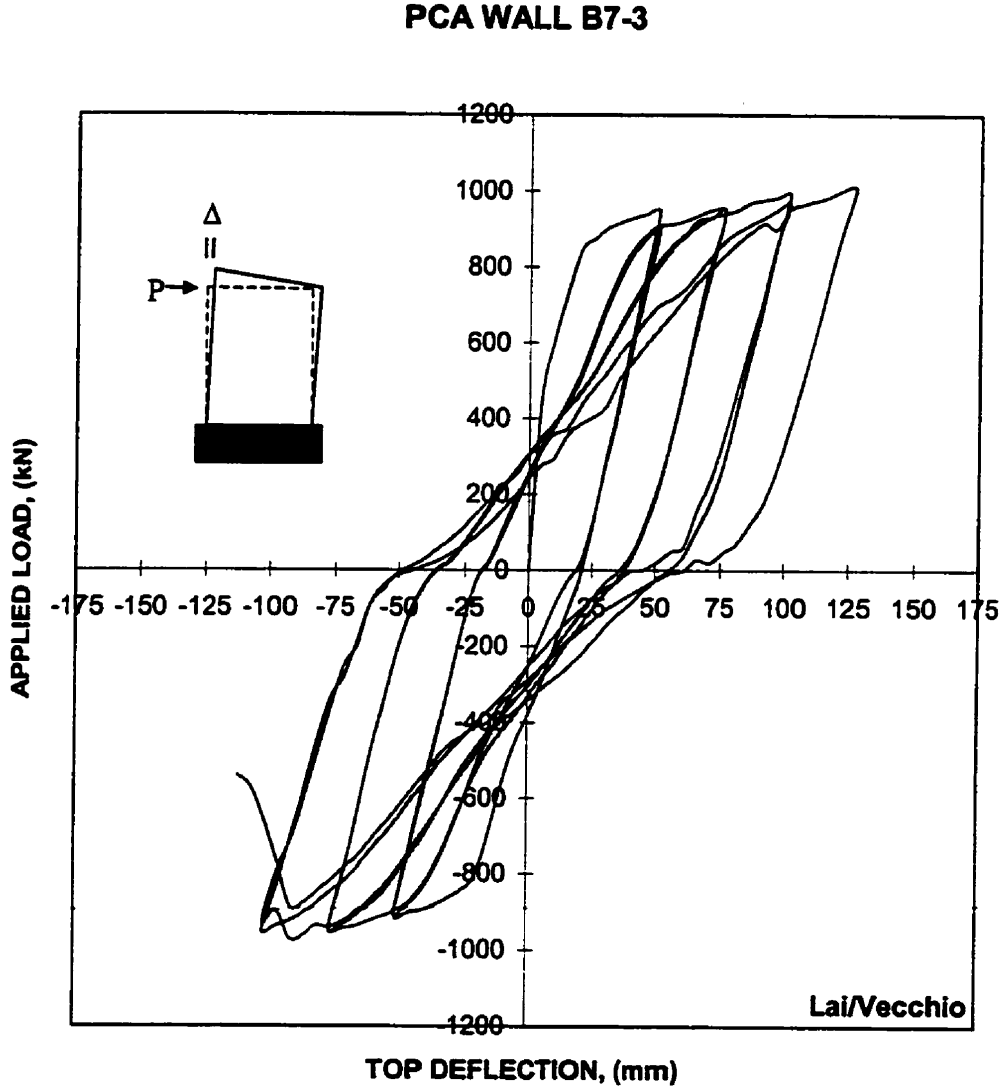

Figure 6.23 Analytical load-deformation response for PCA Wall B7-3 predicted by VecTor2

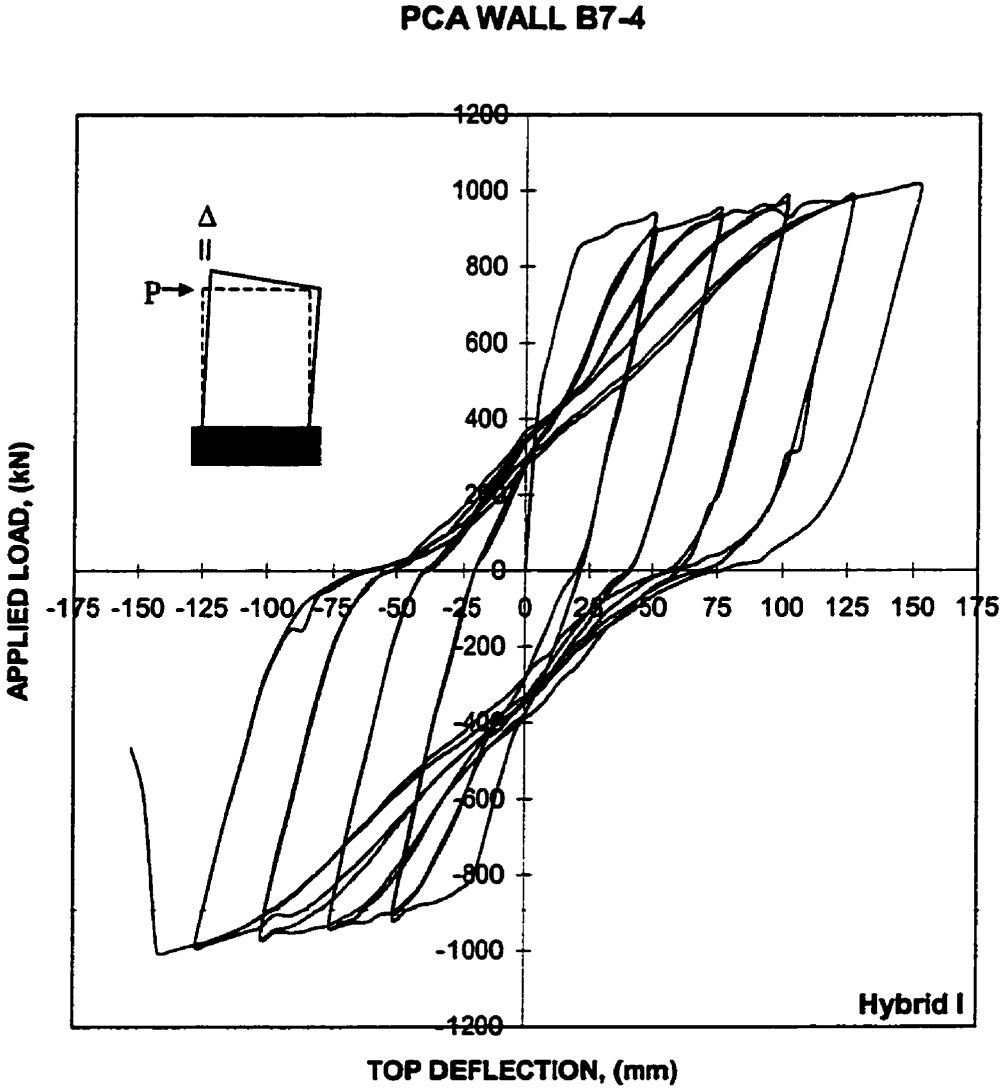

Figure 6.24 Analytical load-deformation response for PCA Wall B7-4 predicted by VecTor2

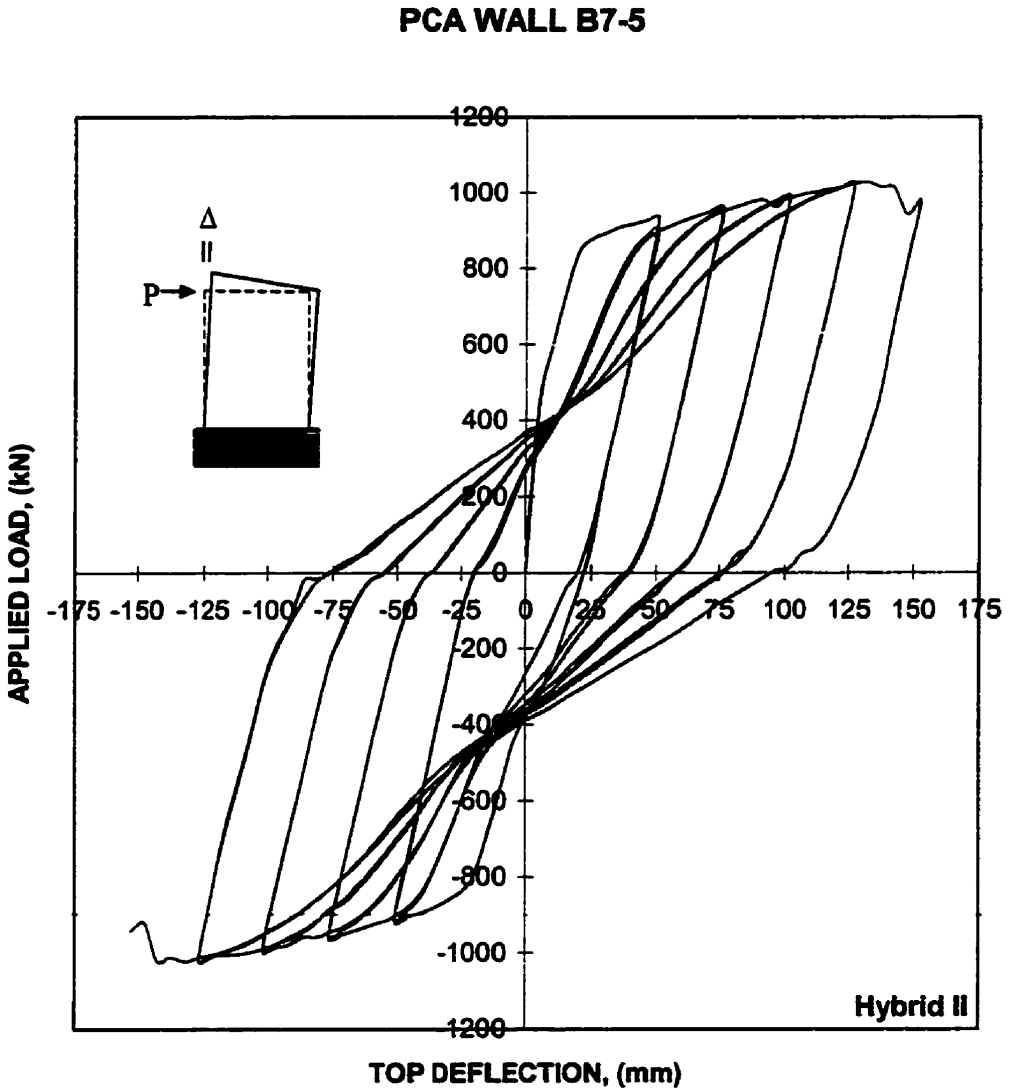

Figure 6.25 Analytical load-deformation response for PCA Wall B7-5 predicted by VecTor2

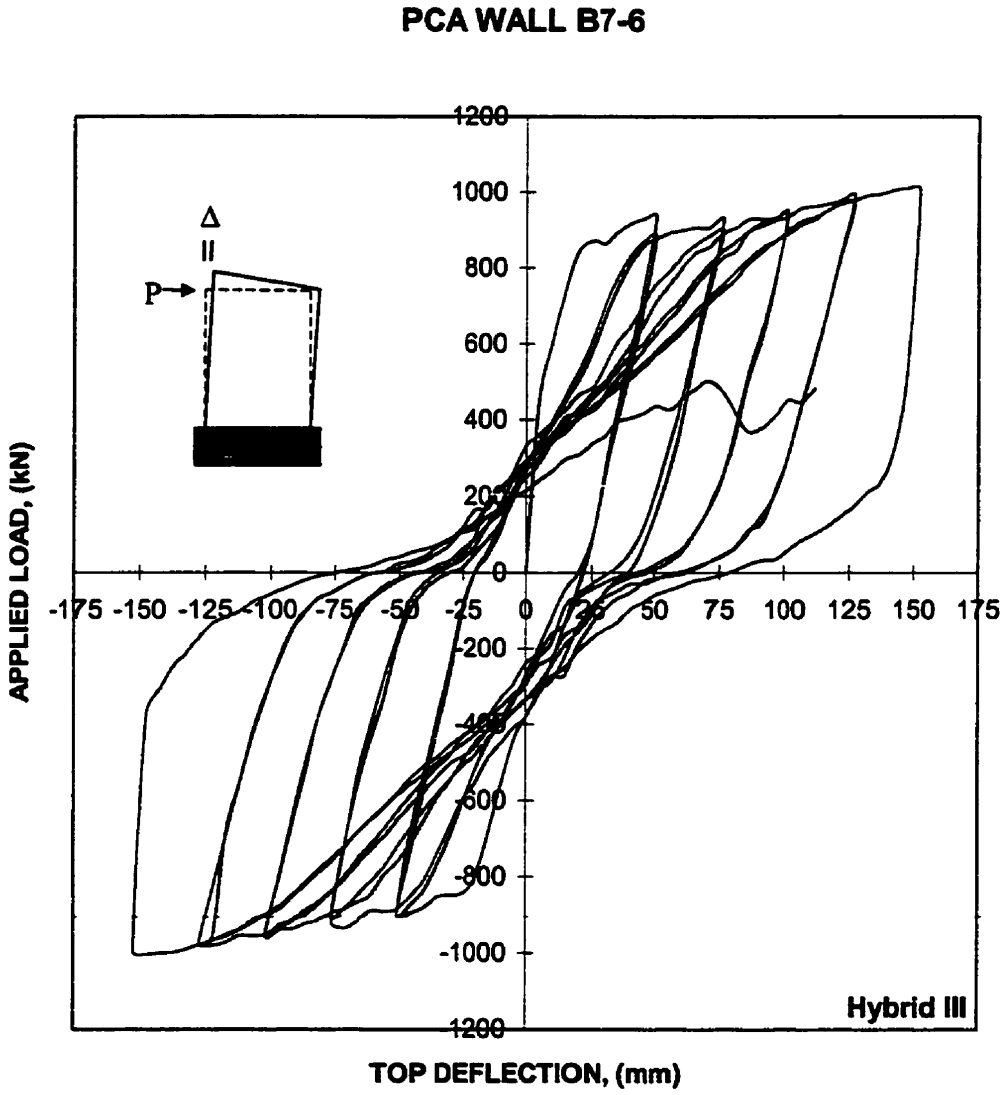

Figure 6.26 Analytical load-deformation response for PCA Wall B7-6 predicted by VecTor2

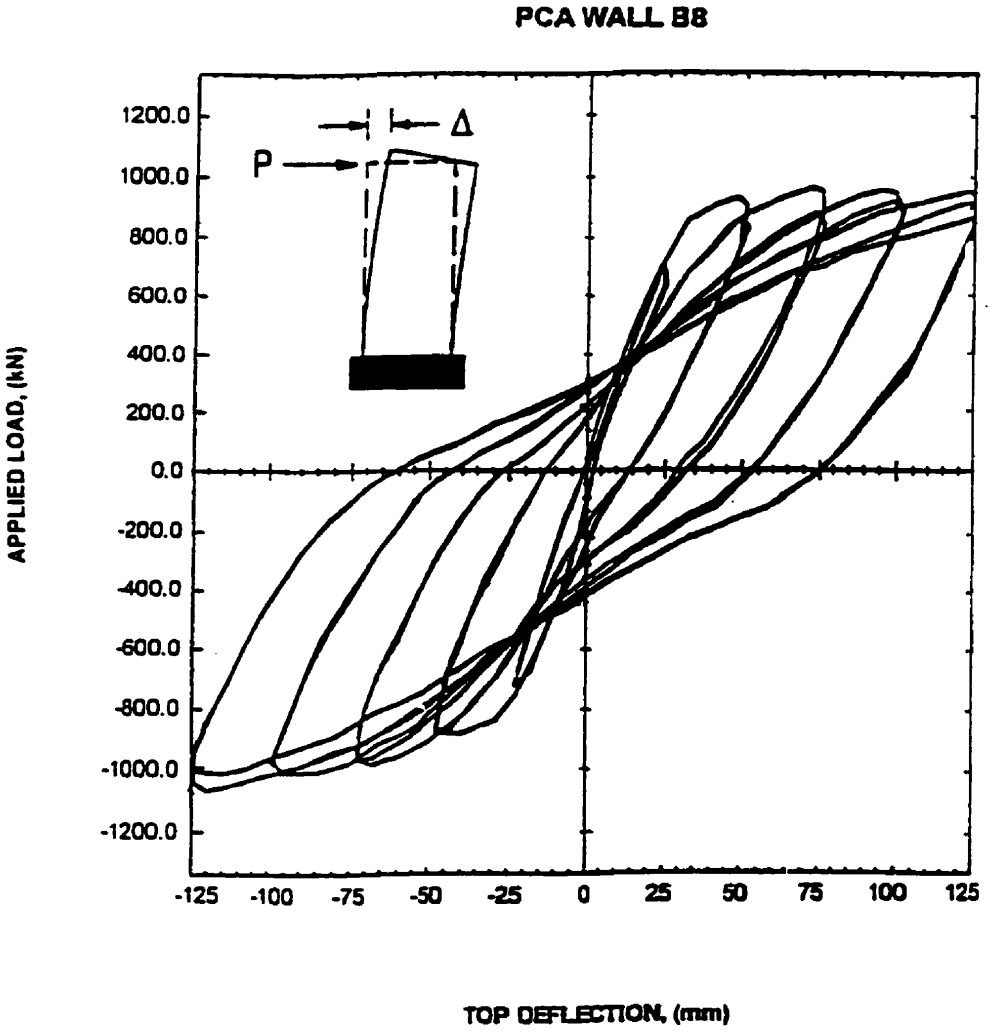

Figure 6.27 Experimental load-deformation response for PCA Wall B8

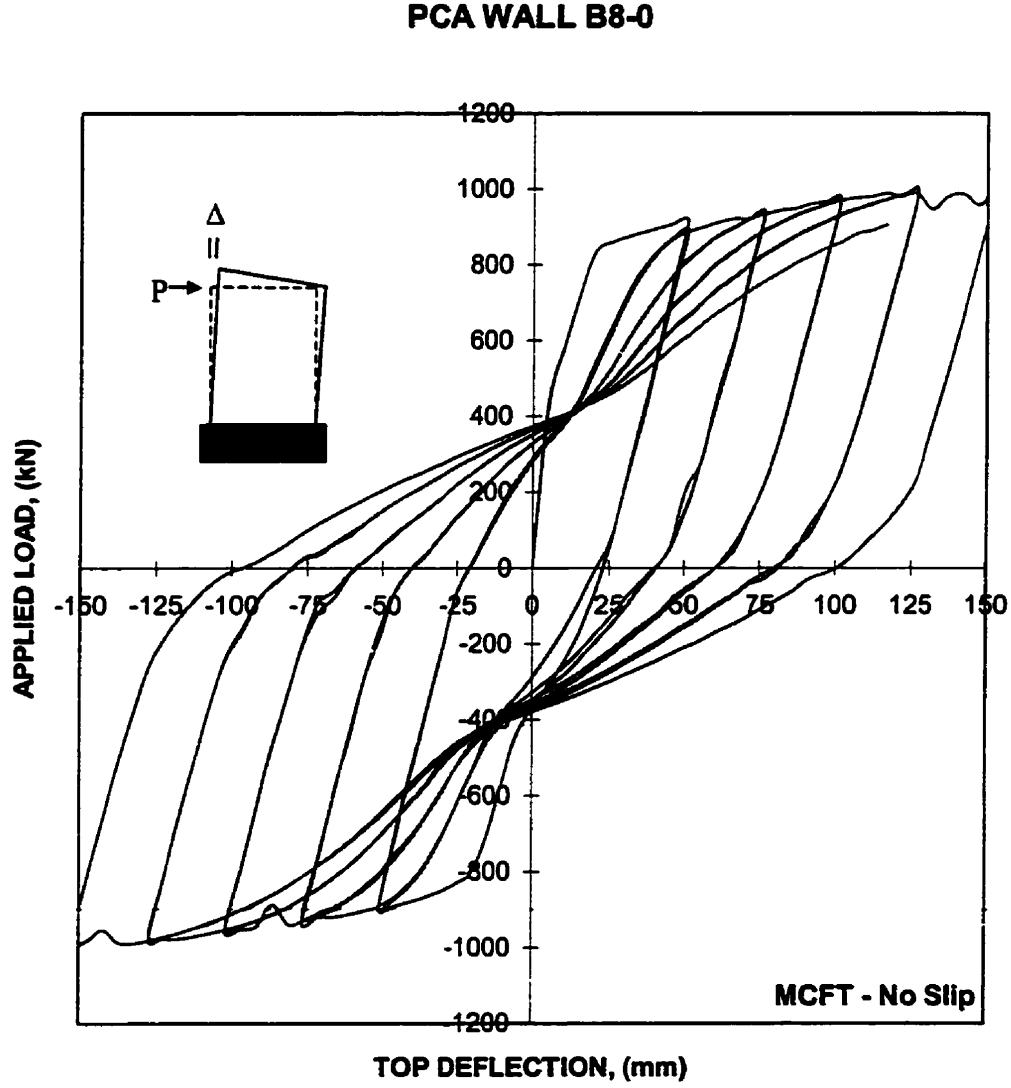

Figure 6.28 Analytical load-deformation response for PCA Wall B8-0 predicted by VecTor2

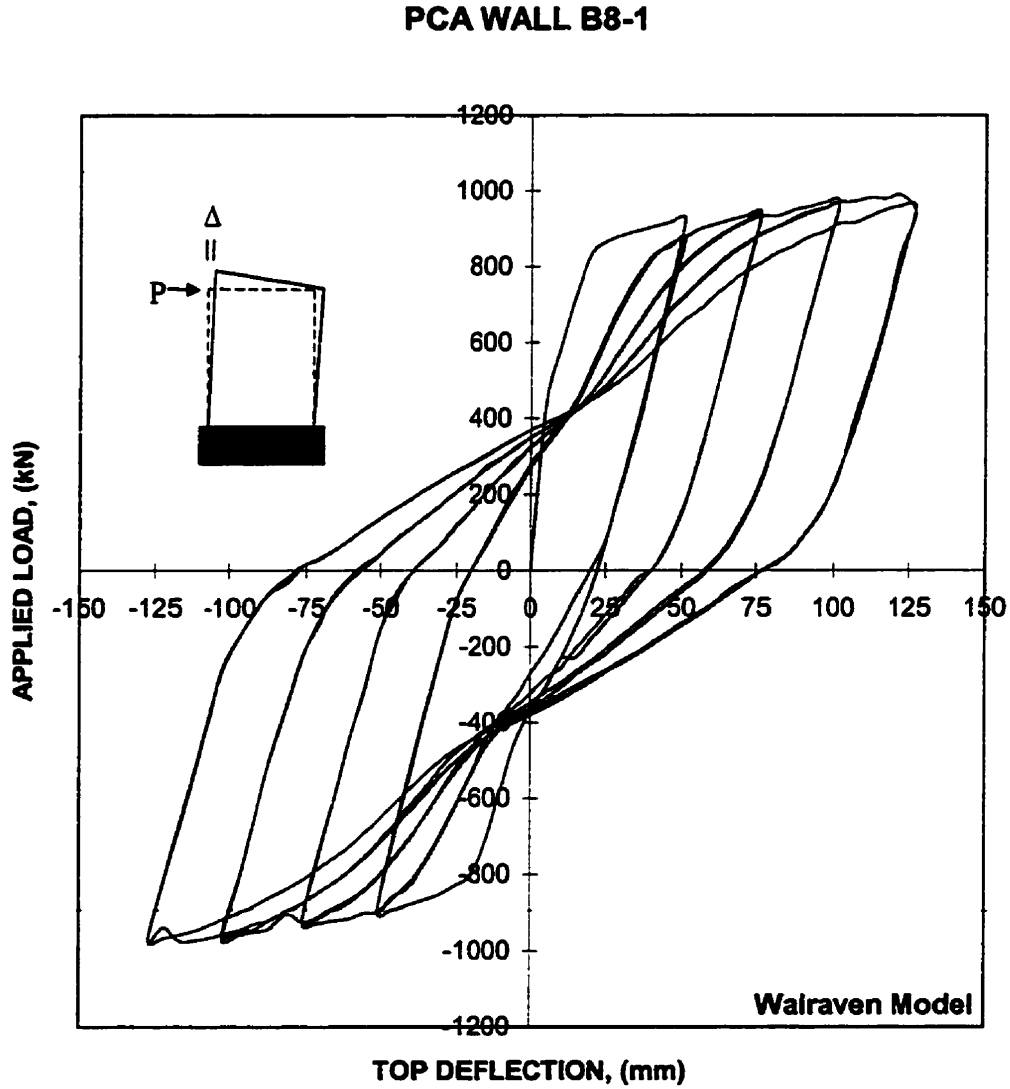

Figure 6.29 Analytical load-deformation response for PCA Wall B8-1 predicted by VecTor2

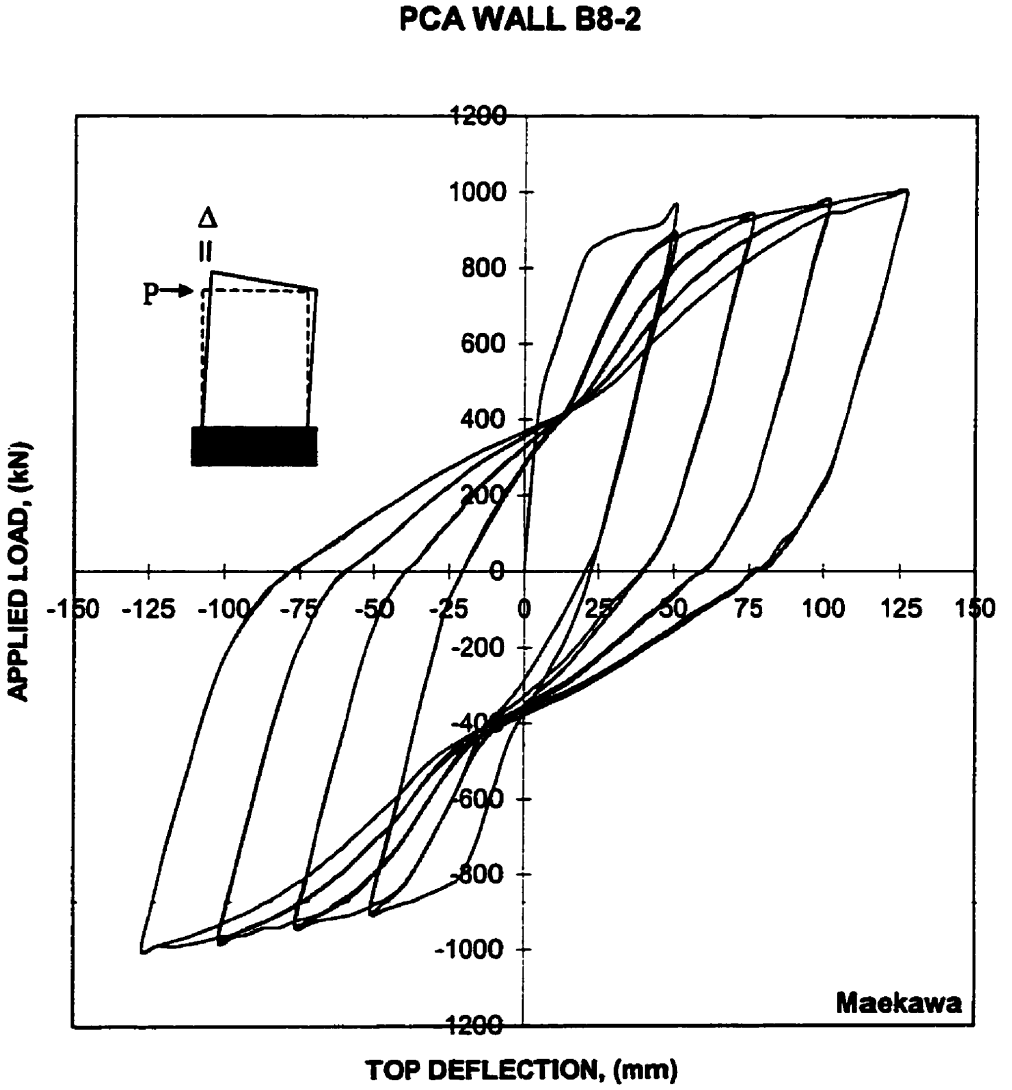

Figure 6.30 Analytical load-deformation response for PCA Wall B8-2 predicted by VecTor2

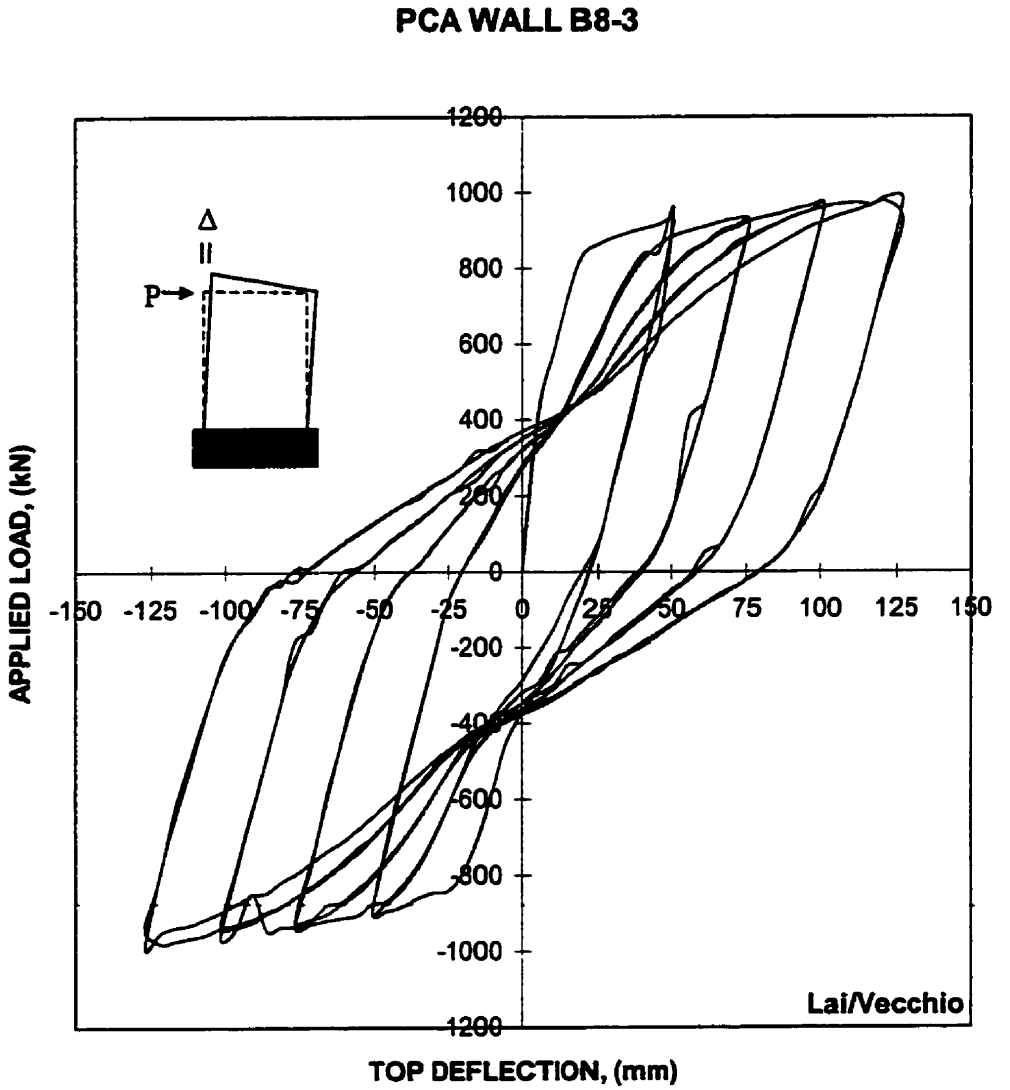

Figure 6.31 Analytical load-deformation response for PCA Wall B8-3 predicted by VecTor2

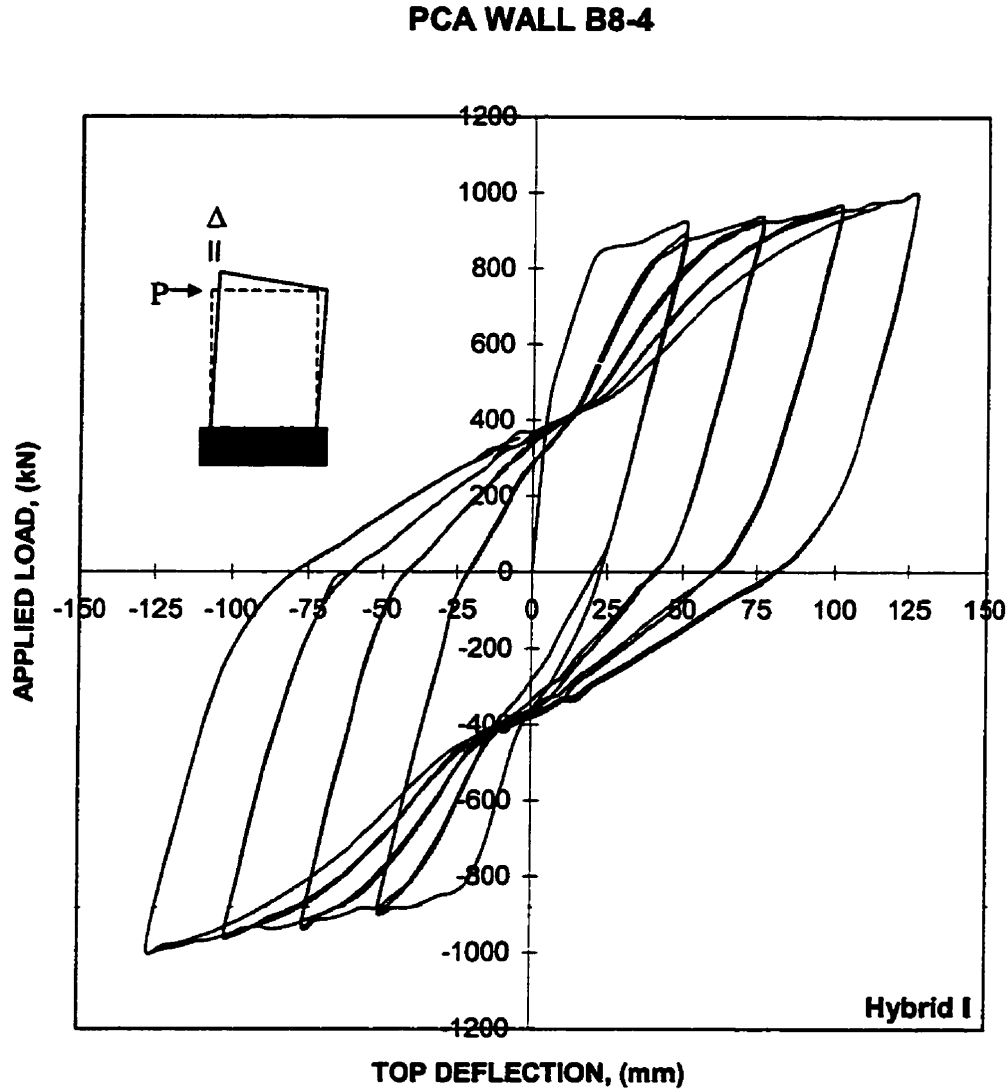

Figure 6.32 Analytical load-deformation response for PCA Wall B8-4 predicted by VecTor2

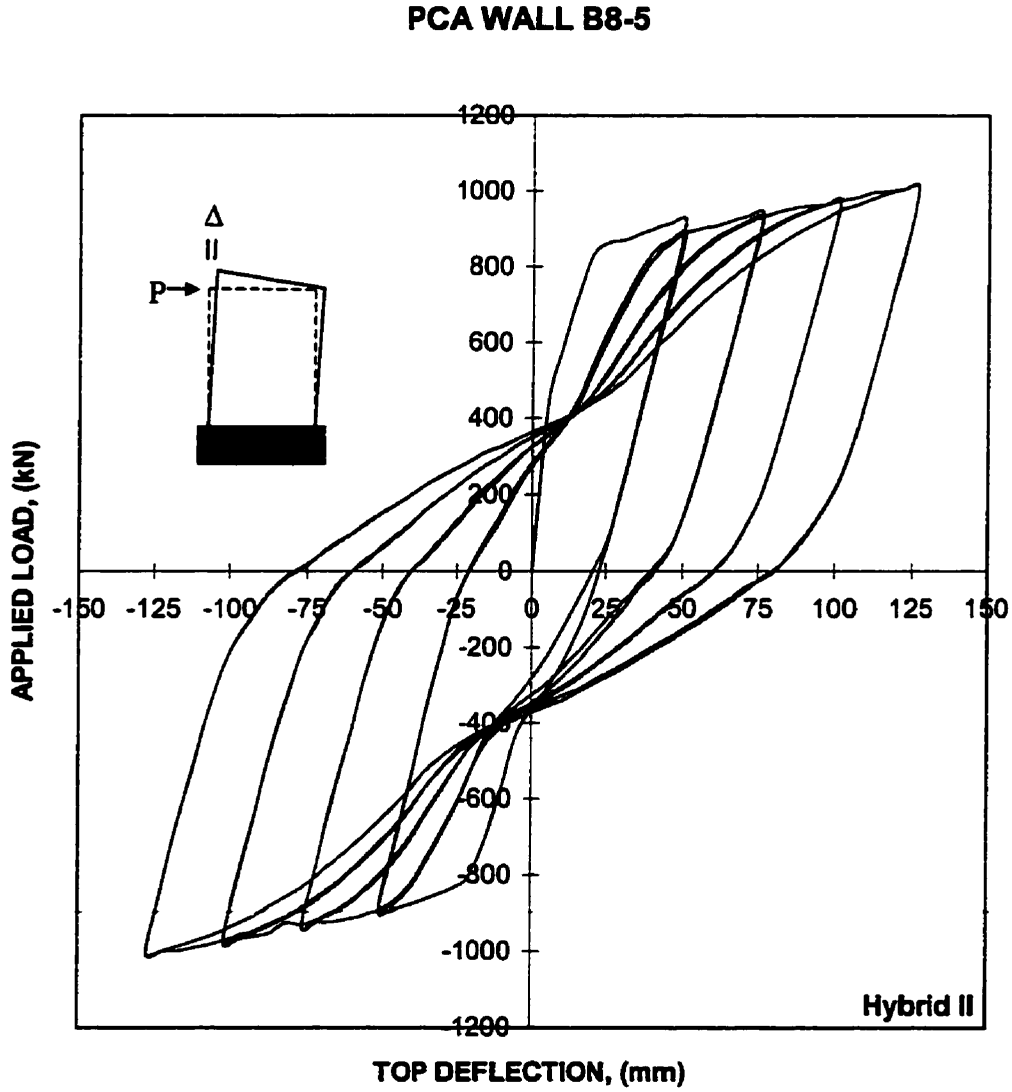

Figure 6.33 Analytical load-deformation response for PCA Wall B8-5 predicted by VecTor2

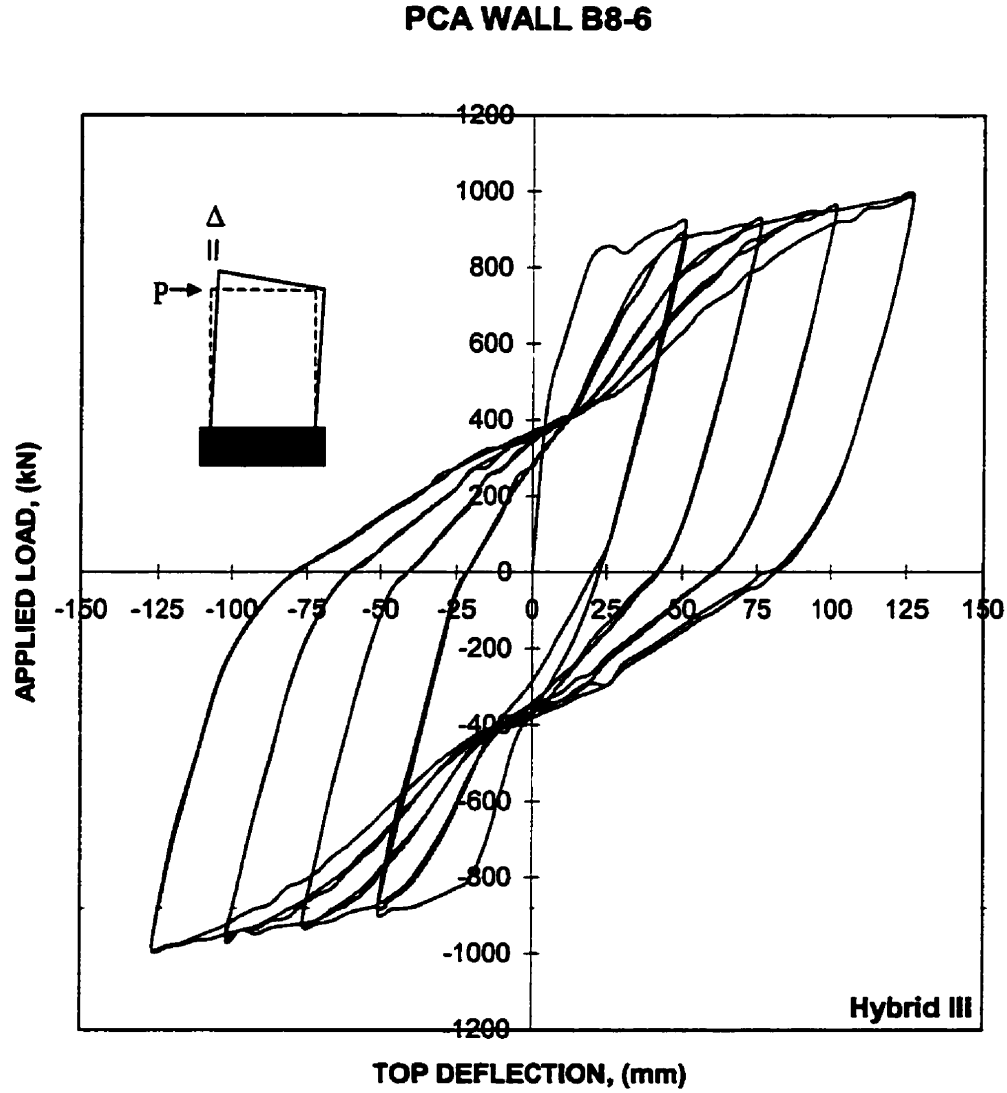

Figure 6.34 Analytical load-deformation response for PCA Wall B8-6 predicted by VecTor2

6.4 Ultimate Displacement and Strength Predictions

The maximum displacements predicted by VecTor2 are compared to the experimental values in Table 6.4. The results predicted with VecTor2 agreed very well in most models, with the hybrid formulation over-estimated the displacement by 25mm in most cases.

The predicted lateral load capacities are compared to the experimental values in Table 6.5. The analytical results are in very good agreement with the observed experimental values. The mean of F_{exp}/F_{pre} is 0.99 with a coefficient of variance of 1.88%. This demonstrates that VecTor2 is extremely accurate in predicting the ultimate strengths of shear walls.

The various slip distortion models did not have much influence on the ultimate load. However, the shape of the load-deformation plots and the failure modes were slightly different in each model. The hybrid models result in more instability in the analyses results.

Table 6.4 Maximum Displacement in millimetres (mm)

SPECIMEN	ANALYSIS MODELS							
	Exp.	MCFT	Maekawa	Walraven	Lai/Vecchio	Hybrid I	Hybrid II	Hybrid III
B1	100	125	100	100	125	150	100	150
B2	125	125	125	125	125	125	125	100
B7	125	150	150	150	125	150	150	150
B8	125	150	125	125	125	125	125	125

Table 6.5 Comparison of experimental ultimate strengths with analytical values

SPECIMEN	*ANALYSIS SERIES*	F_{exp} *(kN)*	F_{pre} *(kN)*	F_{exp}/F_{pre}
B1	B1-0	276	276	1.00
	B1-1	276	279	0.99
	B1-2	276	276	1.00
	B1-3	276	279	0.99
	B1-4	276	275	1.00
	B1-5	276	276	1.00
	B1-6	276	275	1.00
B2	B2-0	685	693	0.99
	B2-1	685	692	0.99
	B2-2	685	690	0.99
	B2-3	685	683	1.00
	B2-4	685	671	1.02
	B2-5	685	688	1.00
	B2-6	685	665	1.03
B7	B7-0	999	1011	0.99
	B7-1	999	1015	0.98
	B7-2	999	1024	0.98
	B7-3	999	1005	0.99
	B7-4	999	1012	0.99
	B7-5	999	1027	0.97
	B7-6	999	1010	0.99
B8	B8-0	959	999	0.96
	B8-1	959	988	0.97
	B8-2	959	1000	0.96
	B8-3	959	988	0.97
	B8-4	959	994	0.96
	B8-5	959	1012	0.95
	B8-6	959	990	0.97

Mean Value = 0.99

COV = 1.88%

6.5 Discussion of Results

In order to have confidence with the program VecTor2, and with the crack shear-slip models implemented within, experimental results must be compared with the analytical model. These experimental results should challenge the model to successfully predict responses under the same loading and restraint conditions.

The nonlinear finite element analyses, performed using VecTor2, predicted a correct failure mechanism for B2 when using the Walraven, Maekawa, Hybrid I, and Hybrid II (B2-1, B2-2, B2-4, B2-5) models. VecTor2 also predicted fairly accurate load-deformation responses and ultimate loads for all the walls analyzed. However, the failure mode of the other shear walls was not described in the literature, and therefore cannot be compared with the analytical values.

For PCA wall B1, the Walraven, Maekawa and Hybrid II models had the closest correlation in the shape of the hysteretic response curve compared to the experimental load-deformation response.

For PCA wall B7, the Lai/Vecchio model was the only model that captured the experimental load-deformation response. All the other models over-estimated the deflection by 25 mm.

For PCA wall B8, only the MCFT analysis over-estimated the deflection by 25 mm. All the other models have captured the load-deformation response fairly well.

In general, the analyses over-estimated the energy dissipation of the shear walls. It can be seen that the experimental results have a more pinched hysteresis loop than the analytical results.

It can be concluded that the behaviour is better modelled if slip is considered. The Walraven model seems to be more accurate and stable compared to the other models. The Hybrid formulation not only worsens the accuracy, but also results in more instability in the analyses results.

CHAPTER 7

Conclusions and Recommendations

7.1 Conclusions

A calculation procedure was developed for calculating crack shear stresses and crack shear displacements from the average strain measurements made on reinforced concrete panels subjected to known uniform edge stresses. The Vecchio panels (PV), Bhide panels (PB), Aspiotis panels (PHS and PA) and Kirschner panels (SE) were examined, and the crack shear stress and shear slip behaviours for these panels were determined. The experimental results gathered were compared against the behaviour predicted by crack shear-slip relations from widely recognized models developed by other researchers. The results from the test panels are in reasonably good agreement with the predictions of previously developed crack slip models, such as those of Walraven and Maekawa. Hence, the proposed method for calculating crack shear stresses and slip displacements in test panels is validated.

For many of the specimens considered in the correlation studies reported in this thesis, there is not much difference in the ultimate load calculated whether slip deformations are considered (DSFM) or whether they are ignored (MCFT). However, the ductility in the shear stress-strain response is better simulated if crack slips are

considered. Also, the mode of failure is better represented since, in addition to concrete strut crushing, the significant degree of sliding along the crack surfaces predicted to occur more closely corresponds to the actual observed failure mode. Hence, accounting for crack shear slip results in an improved simulation of response that generally goes beyond the marginal improvement seen in predicted ultimate load capacity.

The crack-slip constitutive model proposed herein produces comparable levels of accuracy to those obtained from the Walraven and Maekawa models. The proposed model combines features of the two other models, and gives marginally better results.

In the monotonic analysis, the accuracy of the proposed formulation was tested by examining correlations with the test results from panels, beams and shear walls. Accounting for crack shear slip results in improved predictions of the load-deformation response and ultimate load capacity of panels, beams and shear walls, relative to those obtained if crack shear slips are ignored (as in a fully rotating crack model).

In the cyclic analysis, it can be concluded that the behaviour is better modelled if slip is considered. The Walraven model seems to be more accurate and stable compared to the other models.

Good correlation in the crack shear slip data calculated from the test panels, compared to behaviour predicted by previously developed models (e.g. Walraven, Maekawa, Lai/Vecchio), suggests that the conceptual approach and constitutive models of the DSFM provide a reasonably accurate portrayal of the behaviour of cracked reinforced concrete elements.

The hybrid formulations are difficult to implement into finite element algorithms, while the Lai/Vecchio model is easily implemented. In the cyclic analysis, the hybrid formulations not only worsened the accuracy, but also results in more instability in the analyses results. Hence, it is recommended that hybrid formulations no longer be used.

Data from panel tests were re-examined to look for trends in the lag between principal stress and principal strain directions. The Vecchio panels (PV), Bhide panels (PB) and Aspiotis Panels (PHS and PA) were used for these analyses. The analyses showed a very scattered result. No strong correlation could be found between the rotational lag angle and the concrete/reinforcement material properties. As a rough

approximation, the constant lag θ^l can be taken as 5° for biaxially reinforced elements, 7.5° for uniaxially reinforced elements, and 10° for unreinforced elements.

7.2 Recommendations

Refinements to the current model are required to further improve accuracy and reduce the significant levels of scatter seen in the data. One deficiency that exists, and should be addressed, relates to the influence of strain hardening in the reinforcement across cracks. Currently, local strain hardening effects are not considered. In reality, the local strains in the reinforcement across the cracks can be several multiples of the average strain, depending primarily on the reinforcement ratio and bond characteristics, and can reach well into strain hardening behaviour. The higher local reinforcement stresses attained through strain hardening will, in turn, influence the calculation of shear stresses on the crack surfaces, and hence the calculation of crack shear slips. Thus, a rational and consistent approach that includes local strain hardening effects will likely result in an improved calculation of crack shear slip.

Allowances for a change in average crack spacing would also improve results, particularly at low and intermediate load levels. For the data analyses undertaken herein, aconstant crack spacing was assumed (50mm). This maybe one of the reason why no relationship was found between the change in stress/strain inclination.

For the successful operation of the program Vector2, it is essential that the program be well maintained and improved according to the developments in recent technologies and theories.

References

ADEGHE, L.N., 1986. "A finite element model for studying reinforced concrete detailing problems." Ph.D.Thesis, University of Toronto, pp. 264.

BAZANT, Z.P., and GAMBAROVA, P., 1980. "Rough Cracks in Reinforced Concrete", Journal of the Structural Division, ASCE, v.106, April, pp. 819-842.

BHIDE, S. B., and COLLINS, M.P., 1989. "Influence of Axial Tension on the Shear Capacity of Reinforced Concrete Members" American Concrete Institute Structural Journal, 86(5), pp. 570-581.

BRESLER, B., and SCORDELIS, A. C., 1963. "Shear Strength of Reinforced Concrete Beams" American Concrete Institute Journal, 60(1), pp. 51-74.

CEDOLIN, L., and DEI POLI S., 1977. "Finite Element Studies of Shear-Critical RC Beams", Journal of the Engineering Mechanics Division, ASCE, v.103, nEM3, June, pp. 523-537.

COOK, R.D., MALKUS, D.S., and PLESHA, M.E., 1989. Concepts and Applications of Finite Element Analysis, Third Edition, John Wiley and Sons, pp. 630.

DEI POLI, S., GAMBAROVA, P.G., and KARAKOC, C., 1987. "Aggregate Interlock Role in R.C. Thin-Webbed Beams in Shear", Journal of Structural Engineering, v113, n1, Jan., pp. 1-19.

FARDIS, M.N., and BUYUKOZTURK, O., 1979. "Shear Transfer Model for Reinforced Concrete". Journal of the Engineering Mechanics Division, ASCE, v105, nEM2, April, pp. 255-275.

FENWICK, R.C., and PAULAY T., 1968. "Mechanisms of Shear Resistance of Concrete Beams", Journal of the Structural Division, ASCE, v94, nST10, Oct., pp. 2325-2350.

HU, H.T., and SCHNOBRICH, W.C., 1990. "Nonlinear Analysis of Cracked Reinforced Concrete", ACI, v87, n2, Mar.-Apr., pp. 199-206.

KIRSCHNER, U., and COLLINS, M.P., 1986. "Investigating the Behaviour of Reinforced Concrete Shell Elements", University of Toronto, Civil Engineering Publication No. 86-09.

LEFAS, I. D., KOTSOVOS, M. D., and AMBRASEYS, N. N., 1990. "Behaviour of Reinforced Concrete Structural Walls: Strength, Deformation Characteristics, and Failure Mechanism." American Concrete Institute Structural Journal., 87(1), pp. 23-31.

OESTERLE, R.G. ET AL., 1976. "Earthquake-Resistant Structural Walls – Tests of Isolated Walls", Report to the National Science Foundation, Construction Technology Laboratories, Portland Cement Association, Skokie, Illinois, Nov, pp. 315.

OKAMURA, H., and MAEKAWA, K., 1991. "Nonlinear Analysis and Constitutive Models of Reinforced Concrete" University of Tokyo, ISBN 7655-1506-0, pp. 182.

PAULAY, T. and LOEBER, P.J., 1974. "Shear Transfer by Aggregate Interlock", Shear in Reinforced Concrete, Special Publication. SP-42, v1, ACI 1974, pp. 1-16.

PRISCO, M., and GAMBAROVA, P.G., 1995. "Comprehensive Model for Study of Shear in Thin-Webbed RC and PC Beams", Journal of Structural Engineering, v121, n12, Dec., pp. 1822-1831.

PODGORNIAK-STANIK, B., 1998. "The Influence of Concrete Strength, Distribution of Longitudinal Reinforcement, Amount of Transverse Reinforcement and Member Size on Shear Strength of Reinforced Concrete Members" M.A.Sc Thesis, Dept. of Civil Engineering, University of Toronto.

Soroushian, P., Obaseki, K., and Choi, K.B., 1988. "Analysis of Aggregate Interlock Behaviour at Cracks in Reinforced Concrete", Magazine of Concrete Research, v40, n142, March, pp. 43-49.

VECCHIO, F.J., LAI D., 2001. "Crack Shear-Slip in Reinforced Concrete Elements". Journal of Structural Engineering, ASCE, (in press).

VECCHIO, F.J, LAI D., SHIM W. and NG J., 2001. "Disturbed Stress Field Model for Reinforced Concrete: Validation". Journal of Structural Engineering. ASCE, 127(4), pp. 350-358.

VECCHIO, F.J., 2001. "Disturbed Stress Field Model for Reinforced Concrete: Implementation". Journal of Structural Engineering. ASCE, 127(1), pp 12-20.

VECCHIO, F.J., 2000. "Disturbed Stress Field Model for Reinforced Concrete: Formulation". Journal of Structural Engineering. ASCE, 126(9), pp 1070-1077.

VECCHIO, F.J., COLLINS, M.P., and ASPIOTOS, J., 1994. "High-Strength Concrete Elements Subjected to Shear", American Concrete Institute Structural Journal, 91(4), pp. 423-433.

VECCHIO, F.J., and COLLINS, M.P., 1993. "Compression Response of Cracked Reinforced Concrete", Journal of Structural Engineering, ASCE, 119(12), pp. 3590-3610.

VECCHIO, F.J., and COLLINS, M.P., 1989. "Predicting the Response of Reinforced Concrete Beams Subjected to Shear using the Modified Compression Field Theory." American Concrete Institute Structural Journal, Vol. 86, No. 3, pp. 258-267.

VECCHIO, F.J., and COLLINS, M.P., 1986. "The Modified Compression Field Theory for Reinforced Concrete Elements Subjected to Shear." American Concrete Institute Structural Journal, Vol. 83, No. 2, pp. 219-231.

VECCHIO, F.J., and COLLINS, M.P., 1982. "The Response of Reinforced Concrete to In-plane Shear and Normal Stresses." Publication No. 82-03, Department of Civil Engineering, University of Toronto, pp. 323.

WALRAVEN, J.C., 1995. "Shear Friction in High-Strength Concrete", Progress in Concrete Research, v4, TU Delft.

WALRAVEN, J.C., 1981. "Fundamental Analysis of Aggregate Interlock", Journal of Structural Engineering, ASCE, 107(11), pp. 2245-2270.

WALRAVEN, J.C., and REINHARDT, H.W., 1981. "Theory and Experiments on the Mechanical Behaviour of Cracks in Plain and Reinforced Concrete Subjected to Shear Loading", Concrete Mechanics – Part A, Heron, v26, n1A, CURVB Publishers, Netherlands, pp. 65.

YOSHIKAWA, H., WU, Z., and TANABE, T., 1989. "Analytical Model for Shear Slip of Cracked Concrete", Journal of Structural Engineering, v115, n4, April, pp. 771-788.

APPENDIX A

Panel I.D.	LS	f'_c (MPa)	E_o	f'_t (MPa)	ρ_x	ρ_y	f_{yx} (MPa)	f_{yy} (MPa)	v_{cr} (MPa)	v_u (MPa)	E_s (MPa)	s (mm)	θ_{init} (deg)
PV1	3 4 5 6 7	34.5	0.002200	1.94	0.01785	0.01680	483	483	2.21	8.02	200000	50	45
PV3	4 5 6	26.6	0.002300	1.70	0.00483	0.00483	662	662	1.66	3.07	200000	50	45
PV4	4 5 6 7 8	26.6	0.002500	1.70	0.10560	0.01056	242	242	1.79	2.89	200000	50	45
PV5	3 4 5 6 7	28.3	0.002500	1.76	0.00742	0.00742	621	621	1.73	4.24	200000	50	45
PV6	3 4 5 6 7 8	29.8	0.002500	1.80	0.01785	0.01785	266	266	2.00	4.55	200000	50	45
PV7	2 3 4 5 6 7	31.0	0.002500	1.84	0.01785	0.01785	453	453	1.93	6.81	200000	50	45
PV8	3 4 5 6 7	29.8	0.002500	1.80	0.02616	0.02616	462	462	1.73	6.67	200000	50	45
PV9	2 3 4 5 6 7	11.6	0.002800	1.12	0.01785	0.01785	455	455	1.38	3.74	200000	50	45
PV10	3 4 5 6 7 8	14.5	0.002700	1.26	0.01785	0.00999	276	276	1.86	3.97	200000	50	45
PV11	3 4 5 6 7 8 9	15.6	0.002600	1.30	0.01785	0.01306	235	235	1.66	3.56	200000	50	45
PV12	4 5 6	16.0	0.002500	1.32	0.01785	0.00446	469	269	1.73	3.13	200000	50	45

Panel I.D.	LS	f'_c (MPa)	E_o	f'_t (MPa)	ρ_x	ρ_y	f_{yx} (MPa)	f_{yy} (MPa)	v_{cr} (MPa)	v_u (MPa)	E_s (MPa)	s (mm)	θ_{init} (deg)
	7												
	8												
PV14	3	20.4	0.002230	1.49	0.01785	0.01785	455	455	1.93	5.24	200000	50	45
	4												
	5												
	6												
	7												
PV16	2	21.7	0.002000	1.54	0.00740	0.00740	255	255	2.07	2.14	200000	50	45
PV18	4	19.5	0.002000	1.46	0.01785	0.00315	431	412	2.00	3.04	200000	50	45
	5												
	6												
PV19	3	19.0	0.002150	1.44	0.01785	0.00713	458	299	2.07	3.95	200000	50	45
	4												
	5												
	6												
	7												
	8												
	9												
	10												
PV20	3	19.6	0.001800	1.46	0.01785	0.00885	460	297	2.21	4.26	200000	50	45
	4												
	5												
	6												
	7												
	8												
	9												
	10												
PV21	3	19.5	0.001800	1.46	0.01785	0.01296	458	302	2.35	5.03	200000	50	45
	4												
	5												
	6												
	7												
	8												
	9												
	10												
PV22	3	19.6	0.002000	1.46	0.01785	0.01524	458	420	2.42	6.07	200000	50	45
	4												
	5												
	6												
	7												
	8												
	9												
	10												
	11												
	12												
	13												
PV23	5	20.5	0.002000	1.49	0.01785	0.01785	518	518	3.73	8.87	200000	50	45
	6												
	7												
	8												
	9												
	10												
	11												
	12												
	13												
	14												
	15												

Panel I.D.	LS	f'_c (MPa)	E_o	f'_t (MPa)	ρ_x	ρ_y	f_{yx} (MPa)	f_{yy} (MPa)	v_{cr} (MPa)	v_u (MPa)	E_s (MPa)	s (mm)	θ_{init} (deg)
	16												
	17												
	18												
PV24	4	23.8	0.001900	1.61	0.01785	0.01785	492	492	4.97	7.94	200000	50	45
	5												
	6												
PV25	4	19.3	0.001800	1.45	0.01785	0.01785	466	466	4.14	9.12	200000	50	45
	5												
	6												
	7												
	8												
	9												
	10												
PV27	3	20.5	0.001900	1.49	0.01785	0.01785	442	442	2.04	6.35	200000	50	45
	4												
	5												
	6												
	7												
	8												
	9												
PV28	3	19.0	0.001850	1.44	0.01785	0.01785	483	483	1.66	5.80	200000	50	45
	4												
	5												
	6												
	7												
	8												
	9												
	10												
	11												
	12												
	13												
PV29	3	21.7	0.001800	1.54	0.01785	0.00885	441	324	2.21	5.87	200000	50	45
	4												
	5												
	6												
	7												
	8												
	9												
	10												
PB4	5	16.4	0.001875	1.92	0.01085	0.00000	423	0	0.81	1.16	200000	50	32
PB5	4	23.5	0.001780	2.08	0.01085	0.00000	415	0	0.78	2.64	200000	50	22
	5												
	7												
	8												
	9												
	10												
	11												
PB6	7	17.6	0.001860	1.81	0.01085	0.00000	425	0	0.85	1.15	200000	50	32
	8												
	9												
	10												
PB7	3	20.2	0.002150	2.19	0.01085	0.00000	425	0	-0.74	-0.86	200000	50	31
	4												
	5												
PB8	3	20.4	0.001950	1.98	0.01085	0.00000	425	0	-0.52	-0.80	200000	50	33
	4												
	5												

Panel I.D.	LS	f'_c (MPa)	E_o	f'_t (MPa)	ρ_x	ρ_y	f_{yx} (MPa)	f_{yy} (MPa)	v_{cr} (MPa)	v_u (MPa)	E_s (MPa)	s (mm)	θ_{init} (deg)
PB10	2 3 4 5 6 7	24.0	0.001875	2.37	0.01085	0.00000	433	0	-0.31	-0.56	200000	50	14
PB11	4	25.9	0.002025	2.97	0.01085	0.00000	433	0	-1.19	-1.27	200000	50	45
PB12	4	23.1	0.001538	2.93	0.01085	0.00000	433	0	-1.33	-1.53	200000	50	45
PB14	3 4 5 6 7	41.1	0.002813	3.43	0.02023	0.00000	489	0	-0.78	-1.54	200000	50	33
PB16	5 6 7 8 9	41.7	0.003225	2.76	0.02023	0.00000	502	0	-0.98	-1.42	200000	50	25
PB17	5 6 7 8 9 10	41.6	0.003075	3.02	0.02023	0.00000	502	0	-0.54	-1.22	200000	50	12
PB18	6 7 8	25.3	0.002230	2.35	0.02195	0.00000	402	0	-1.62	-1.72	200000	50	48
PB19	5 7 8	20.0	0.001913	2.34	0.02195	0.00000	402	0	-1.23	-1.28	200000	50	45
PB20	6 7 8 9 10	21.7	0.001888	2.56	0.02195	0.00000	424	0	-0.94	-1.42	200000	50	32
PB21	4 5 6 7 8 9	21.8	0.001800	2.47	0.02195	0.00000	402	0	-0.73	-1.42	200000	50	22
PB22	4 5 6 7 8	17.6	0.002025	1.86	0.02195	0.00000	433	0	-0.44	-1.03	200000	50	20
PB28	3 4 5 6 7 8	22.7	0.002013	2.45	0.00000	0.02195	0	426	0.84	1.53	200000	50	62
PB29	4 5 6 7 8	41.6	0.002600	3.16	0.02023	0.00000	496	0	-0.75	-1.49	200000	50	25

Panel I.D.	LS	f'_c (MPa)	E_o	f'_t (MPa)	ρ_x	ρ_y	f_{yx} (MPa)	f_{yy} (MPa)	v_{cr} (MPa)	v_u (MPa)	E_s (MPa)	s (mm)	θ_{init} (deg)
	9												
PB30	4	40.4	0.002600	3.19	0.02023	0.00000	496	0	-0.74	-1.48	200000	50	26
	5												
	6												
	7												
	8												
	9												
PB31	2	43.4	0.003000	3.71	0.02023	0.00000	496	0	-0.44	-1.15	200000	50	12
	3												
	4												
	5												
	6												
	7												
PB32	2	57.7	0.002550	4.12	0.02195	0.00000	415	0	-0.64	-1.49	200000	50	21
	3												
	4												
	5												
	6												
PHS1	5	72.2	0.002680	2.80	0.03230	0.00000	606	521	2.54	2.95	200000	50	45
PHS2	4	66.1	0.002480	2.68	0.03230	0.00410	606	521	1.94	6.66	200000	50	45
	5												
	6												
	7												
	8												
	9												
	10												
	11												
	12												
	13												
	14												
PHS3	3	58.4	0.002440	2.52	0.03230	0.00820	606	521	2.28	8.19	200000	50	45
	4												
	5												
	6												
	7												
	8												
	9												
	10												
	11												
	12												
	13												
PHS4	3	68.5	0.002600	2.73	0.03230	0.00820	606	521	2.39	6.91	200000	50	45
	4												
	5												
	6												
	7												
	8												
	9												
	10												
	11												
PHS5	3	52.1	0.002580	2.38	0.03230	0.00410	606	521	1.62	4.81	200000	50	45
	4												
	5												
	6												
	7												
	8												
	9												

Panel I.D.	LS	f'_c (MPa)	E_o	f'_t (MPa)	ρ_x	ρ_y	f_{yx} (MPa)	f_{yy} (MPa)	v_{cr} (MPa)	v_u (MPa)	E_s (MPa)	s (mm)	θ_{int} (deg)
PHS6	3	49.7	0.002250	2.33	0.03230	0.00410	606	521	2.25	9.89	200000	50	45
	4												
	5												
	6												
	7												
	8												
	9												
	10												
	11												
	12												
	13												
	14												
	15												
	16												
PHS7	3	53.6	0.002100	2.42	0.03230	0.00820	606	521	2.25	10.26	200000	50	45
	4												
	5												
	6												
	7												
	8												
	9												
	10												
	11												
	12												
	13												
PHS8	3	55.9	0.002170	2.47	0.03230	0.01240	606	521	2.15	10.84	200000	50	45
	4												
	5												
	6												
	7												
	8												
	9												
	10												
	11												
	12												
	13												
	14												
	15												
	16												
	17												
	18												
PHS9	3	56.0	0.002680	2.47	0.03230	0.00410	606	521	2.22	9.37	200000	50	45
	4												
	5												
	6												
	7												
	8												
	9												
	10												
	11												
	12												
	13												
PHS10	3	51.4	0.002450	2.37	0.03230	0.01240	606	521	2.13	8.58	200000	50	45
	4												
	5												
	6												
	7												

Panel I.D.	LS	f'_c (MPa)	E_o	f'_t (MPa)	p_x	p_y	f_{yx} (MPa)	f_{yy} (MPa)	v_{cr} (MPa)	v_u (MPa)	E_s (MPa)	s (mm)	θ_{init} (deg)
	8												
	9												
	10												
	11												
	12												
	13												
	14												
	15												
	16												
	17												
PA1	4	49.9	0.002090	2.33	0.01650	0.00820	522	522	2.19	6.34	200000	50	45
	5												
	6												
	7												
	8												
	9												
	10												
	11												
	12												
	13												
PA2	3	43.0	0.001990	2.16	0.01650	0.00820	522	522	1.88	6.22	200000	50	45
	4												
	5												
	6												
	7												
	8												
	9												
	10												
SE1	1	42.5	0.002540	2.15	0.02930	0.00978	492	479	—	—	200000	50	—
	2												
	3												
	4												
	5												
	6												
SE5	1	25.9	0.002400	1.68	0.02930	0.02930	492	492	—	—	200000	50	—
	2												
	3												
	4												
SE6	1	40.0	0.002500	2.09	0.02930	0.00326	492	479	—	—	200000	50	—
	2												
	3												
	4												
	5												
	6												
	7												
	8												
	9												
	10												

Panel I.D.	LS	σ_x (MPa)	σ_y (MPa)	τ_{xy} (MPa)	f_{sx} (MPa)	f_{sy} (MPa)	f_{c1} (MPa)	f_{c2} (MPa)	ε_x	ε_y	γ_{xy}	ε_{c1}
PV1	3	0.104	0.104	2.615	114.1	110.3	0.777	-4.457	0.000570	0.000551	0.001459	0.001281
	4	0.101	0.101	3.898	193.7	208.8	0.518	-7.280	0.000968	0.001043	0.002568	0.002271
	5	0.094	0.094	5.239	268.3	289.5	0.506	-9.972	0.001341	0.001447	0.003734	0.003244
	6	0.113	0.113	6.606	350.4	390.0	0.318	-12.897	0.001751	0.001949	0.005020	0.004341
	7	0.180	0.180	7.873	439.0	483.0	0.000	-15.748	0.002194	0.002504	0.006712	0.005671
PV3	4	-0.037	-0.037	2.033	182.2	167.4	1.152	-2.915	0.000910	0.000837	0.002222	0.001979
	5	-0.031	-0.031	2.676	352.9	366.0	0.909	-4.443	0.001763	0.001829	0.004389	0.003979
	6	-0.033	-0.033	3.019	445.6	485.8	0.739	-5.303	0.002227	0.002428	0.005622	0.005132
PV4	4	-0.055	-0.055	2.150	54.2	71.4	1.435	-2.870	0.000271	0.000357	0.000781	0.000710
	5	-0.062	-0.062	2.633	146.1	168.2	0.913	-4.357	0.000730	0.000841	0.001942	0.001781
	6	-0.151	-0.151	2.838	241.5	241.5	0.137	-5.539	0.002301	0.002633	0.005893	0.005582
	7	-0.207	-0.207	2.841	241.5	241.5	0.084	-5.598	0.004068	0.004663	0.010064	0.009708
	8	-0.051	-0.051	2.707	241.5	241.5	0.105	-5.309	0.005942	0.006615	0.014307	0.013867
PV5	3	-0.020	-0.020	2.185	191.2	171.5	0.821	-3.552	0.000956	0.000857	0.002175	0.002025
	4	0.002	0.002	2.697	262.6	237.2	0.846	-4.551	0.001312	0.001185	0.002997	0.002789
	5	0.007	0.007	2.947	303.3	298.4	0.722	-5.172	0.001516	0.001491	0.003836	0.003458
	6	0.008	0.008	3.683	405.7	426.4	0.604	-6.763	0.002028	0.002131	0.005270	0.004724
	7	0.003	0.003	4.168	498.3	514.0	0.415	-7.921	0.002490	0.002569	0.006621	0.005861
PV6	3	0.002	0.002	2.451	84.5	109.1	0.734	-4.188	0.000422	0.000545	0.001310	0.001143
	4	0.007	0.007	2.947	122.3	147.7	0.553	-5.358	0.000611	0.000738	0.001824	0.001594
	5	0.007	0.007	3.192	141.1	173.2	0.407	-6.003	0.000705	0.000865	0.002143	0.001871
	6	0.035	0.035	3.954	183.0	231.4	0.314	-7.642	0.000915	0.001156	0.003148	0.002760
	7	0.050	0.050	4.472	264.2	265.6	0.000	-8.944	0.001321	0.001546	0.004150	0.003676
	8	0.058	0.058	3.728	265.6	265.6	0.000	-7.456	0.007124	0.007288	0.018074	0.017499
PV7	2	-0.096	-0.096	1.976	41.9	39.4	1.155	-2.798	0.000209	0.000197	0.000495	0.000418
	3	-0.094	-0.094	2.601	123.1	114.1	0.391	-4.813	0.000615	0.000570	0.001399	0.001220
	4	-0.109	-0.109	3.732	216.6	194.5	-0.041	-7.516	0.001083	0.000972	0.002577	0.002212
	5	-0.085	-0.085	4.629	244.5	236.3	0.252	-9.006	0.001222	0.001181	0.003293	0.002809
	6	-0.167	-0.167	5.713	306.1	311.0	0.039	-11.388	0.001530	0.001554	0.004297	0.003626
	7	-0.179	-0.179	6.688	379.1	384.0	0.000	-13.377	0.001895	0.001919	0.005335	0.004449
PV8	3	-0.040	-0.040	2.605	73.0	72.2	0.665	-4.546	0.000365	0.000361	0.001097	0.000894
	4	-0.016	-0.016	3.733	123.9	122.3	0.497	-6.969	0.000619	0.000611	0.001871	0.001530
	5	-0.007	-0.007	4.721	162.5	161.3	0.480	-8.963	0.000812	0.000806	0.002548	0.002055
	6	0.028	0.028	5.699	203.9	210.5	0.308	-11.093	0.001019	0.001052	0.003345	0.002658
	7	-0.002	-0.002	6.662	258.9	273.3	0.000	-13.330	0.001294	0.001366	0.004363	0.003412
PV9	2	-0.074	-0.074	1.461	18.1	24.2	1.011	-1.913	0.000090	0.000121	0.000514	0.000358
	3	-0.067	-0.067	2.126	68.1	76.3	0.771	-3.483	0.000340	0.000381	0.001361	0.001006
	4	-0.041	-0.041	2.825	113.7	116.9	0.726	-4.925	0.000568	0.000584	0.002292	0.001676
	5	-0.009	-0.009	3.433	158.4	163.3	0.553	-6.313	0.000792	0.000816	0.003716	0.002599
	6	0.001	0.001	3.737	207.2	187.9	0.216	-7.267	0.001036	0.000939	0.005532	0.003596
	7	0.020	0.020	3.756	267.5	212.1	0.000	-7.577	0.001337	0.001060	0.008058	0.005120
PV10	3	-0.010	-0.010	2.048	43.1	70.6	1.300	-2.795	0.000215	0.000353	0.001055	0.000866
	4	-0.036	-0.036	2.782	89.9	147.7	1.207	-4.358	0.000449	0.000738	0.002028	0.001670
	5	-0.042	-0.042	3.498	138.7	265.9	0.891	-6.107	0.000693	0.001329	0.003276	0.002718
	6	-0.035	-0.035	3.800	169.5	276.0	0.876	-6.728	0.000847	0.001995	0.004531	0.003819
	7	-0.086	-0.086	3.968	196.9	276.0	0.764	-7.209	0.000984	0.003798	0.007310	0.006374
	8	-0.091	-0.091	3.669	175.6	276.0	0.637	-6.711	0.000878	0.006166	0.014465	0.011415
PV11	3	-0.014	-0.014	1.699	19.3	25.0	1.350	-2.049	0.000096	0.000125	0.000443	0.000322
	4	-0.017	-0.017	2.257	60.7	80.0	1.175	-3.338	0.000303	0.000400	0.001208	0.000954
	5	0.016	0.016	2.773	100.5	129.2	1.048	-4.498	0.000502	0.000646	0.001805	0.001461
	6	0.030	0.030	3.154	125.6	164.9	0.986	-5.322	0.000627	0.000824	0.002304	0.001860
	7	0.028	0.028	3.519	164.5	226.9	0.596	-6.441	0.000822	0.001134	0.003024	0.002475
	8	0.033	0.033	3.561	234.6	234.6	0.000	-7.210	0.001357	0.002352	0.005318	0.004389
	9	0.031	0.031	3.339	234.6	234.6	0.000	-6.772	0.001509	0.002780	0.006691	0.005235
PV12	4	-0.041	-0.041	2.089	78.8	151.4	1.039	-3.203	0.000394	0.000757	0.001500	0.001363
	5	-0.024	-0.024	2.461	110.8	251.1	0.925	-4.071	0.000554	0.001255	0.002272	0.002099
	6	-0.026	-0.026	2.804	141.6	269.1	0.992	-4.771	0.000707	0.002141	0.003364	0.003276

Panel I.D.	LS	σ_x (MPa)	σ_y (MPa)	τ_{xy} (MPa)	f_{sx} (MPa)	f_{sy} (MPa)	f_{c1} (MPa)	f_{c2} (MPa)	ε_x	ε_y	γ_{xy}	ε_{c1}
	7	-0.014	-0.014	3.134	185.9	269.1	1.034	-5.581	0.000929	0.005832	0.007388	0.007841
	8	-0.008	-0.008	3.091	157.1	269.1	1.182	-5.204	0.000785	0.012049	0.013311	0.015102
PV14	3	-0.006	-0.006	2.058	10.3	18.1	1.801	-2.318	0.000051	0.000090	0.000342	0.000241
	4	-0.014	-0.014	2.734	80.4	83.7	1.255	-4.213	0.000402	0.000418	0.001170	0.000976
	5	0.015	0.015	3.835	167.4	171.1	0.829	-6.841	0.000837	0.000855	0.002369	0.002011
	6	-0.019	-0.019	4.599	208.8	213.0	0.816	-8.383	0.001044	0.001064	0.002988	0.002528
	7	0.025	0.025	5.244	252.3	254.8	0.743	-9.745	0.001261	0.001273	0.003655	0.003063
PV16	2	-0.049	-0.049	2.107	186.7	207.6	0.600	-3.617	0.000933	0.001038	0.002463	0.002278
PV18	4	0.009	0.009	2.422	86.6	254.0	1.288	-3.614	0.000433	0.001269	0.001882	0.001882
	5	-0.026	-0.026	2.767	136.6	411.9	0.931	-4.719	0.000683	0.002819	0.003591	0.003869
	6	-0.132	-0.132	3.028	197.4	411.9	0.683	-5.769	0.000986	0.006925	0.007464	0.008756
PV19	3	0.016	0.016	2.075	18.1	40.2	1.787	-2.364	0.000090	0.000201	0.000443	0.000363
	4	-0.003	-0.003	2.451	51.3	97.2	1.646	-3.261	0.000256	0.000486	0.001013	0.000891
	5	-0.005	-0.005	2.820	73.0	141.1	1.665	-3.984	0.000365	0.000705	0.001451	0.001268
	6	-0.013	-0.013	3.133	109.6	233.5	1.313	-4.959	0.000547	0.001167	0.002181	0.001990
	7	-0.009	-0.009	3.481	143.2	299.5	1.132	-5.842	0.000716	0.001987	0.003359	0.003150
	8	-0.038	-0.038	3.723	186.7	299.5	0.999	-6.543	0.000933	0.003385	0.005040	0.004961
	9	-0.060	-0.060	3.867	206.4	299.5	0.975	-6.914	0.001031	0.005315	0.007167	0.007377
	10	-0.094	-0.094	3.955	230.6	299.5	0.857	-7.296	0.001152	0.008633	0.010509	0.011315
PV20	3	-0.039	-0.039	2.337	16.4	39.8	1.976	-2.699	0.000082	0.000199	0.000526	0.000399
	4	-0.027	-0.027	2.779	46.8	94.0	1.918	-3.640	0.000234	0.000470	0.001083	0.000910
	5	-0.033	-0.033	3.137	89.0	165.8	1.576	-4.699	0.000445	0.000828	0.001752	0.001537
	6	-0.032	-0.032	3.519	118.6	246.2	1.340	-5.699	0.000593	0.001230	0.002381	0.002135
	7	-0.041	-0.041	3.843	144.4	297.4	1.197	-6.489	0.000722	0.001770	0.003144	0.002906
	8	-0.069	-0.069	4.170	187.5	297.4	1.127	-7.243	0.000937	0.003131	0.004810	0.004703
	9	-0.040	-0.040	4.261	215.8	297.4	0.972	-7.637	0.001079	0.005100	0.007145	0.007208
	10	-0.011	-0.011	4.187	238.4	297.4	0.714	-7.815	0.001191	0.008542	0.011507	0.011747
PV21	3	-0.049	-0.049	2.523	23.0	30.0	2.075	-2.972	0.000115	0.000150	0.000499	0.000354
	4	-0.020	-0.020	3.081	78.4	98.1	1.727	-4.436	0.000392	0.000490	0.001325	0.001084
	5	-0.019	-0.019	3.512	107.5	137.5	1.643	-5.381	0.000537	0.000687	0.001795	0.001498
	6	-0.032	-0.032	3.855	123.5	170.3	1.618	-6.092	0.000617	0.000851	0.002215	0.001856
	7	-0.035	-0.035	4.211	151.0	223.6	1.380	-7.044	0.000755	0.001118	0.002734	0.002303
	8	-0.031	-0.031	4.574	187.1	302.2	0.924	-8.242	0.000935	0.001681	0.003638	0.003150
	9	-0.070	-0.070	4.891	232.6	302.2	0.787	-8.997	0.001163	0.003045	0.005472	0.004970
	10	-0.091	-0.091	5.029	272.4	302.2	0.570	-9.532	0.001362	0.005424	0.008656	0.008099
PV22	3	-0.039	-0.039	2.577	22.6	31.2	2.100	-2.100	0.000113	0.000156	0.000535	0.000389
	4	-0.033	-0.033	3.137	66.1	77.5	1.923	-1.923	0.000330	0.000388	0.001131	0.000895
	5	-0.028	-0.028	3.713	109.1	128.4	1.732	-1.732	0.000545	0.000642	0.001790	0.001462
	6	-0.026	-0.026	4.212	136.2	160.0	1.751	-1.751	0.000681	0.000800	0.002242	0.001845
	7	-0.022	-0.022	4.592	157.6	187.1	1.738	-1.738	0.000787	0.000935	0.002612	0.002160
	8	-0.022	-0.022	4.939	181.8	215.8	1.650	-1.650	0.000908	0.001079	0.002978	0.002464
	9	-0.031	-0.031	5.273	198.2	239.6	1.648	-1.648	0.000990	0.001198	0.003346	0.002752
	10	-0.013	-0.013	5.511	218.3	262.2	1.552	-1.552	0.001091	0.001310	0.003682	0.003026
	11	-0.009	-0.009	5.699	229.8	280.2	1.505	-1.505	0.001148	0.001401	0.003965	0.003240
	12	-0.014	-0.014	5.928	245.4	310.6	1.360	-1.360	0.001226	0.001552	0.004317	0.003516
	13	-0.018	-0.018	6.070	277.0	382.4	0.683	-0.683	0.001384	0.001911	0.005272	0.004230
PV23	5	-1.475	-1.475	3.731	13.5	11.5	2.032	-5.430	0.000068	0.000057	0.000645	0.000357
	6	-1.746	-1.746	4.428	20.1	20.1	2.323	-6.533	0.000100	0.000100	0.000880	0.000524
	7	-1.967	-1.967	4.991	42.7	43.9	2.251	-7.730	0.000213	0.000219	0.001337	0.000857
	8	-2.157	-2.157	5.474	62.0	68.9	2.149	-8.800	0.000310	0.000344	0.001733	0.001184
	9	-2.289	-2.289	5.808	72.6	82.1	2.140	-9.478	0.000363	0.000410	0.002060	0.001401
	10	-2.444	-2.444	6.204	89.9	102.2	2.047	-10.363	0.000449	0.000511	0.002422	0.001660
	11	-2.560	-2.560	6.517	102.6	113.2	2.031	-11.004	0.000513	0.000566	0.002774	0.001898
	12	-2.704	-2.704	6.863	110.4	127.2	2.041	-11.689	0.000552	0.000636	0.003126	0.002129
	13	-2.823	-2.823	7.185	128.4	144.0	1.932	-12.441	0.000642	0.000720	0.003510	0.002390
	14	-2.960	-2.960	7.525	136.2	158.0	1.942	-13.114	0.000681	0.000789	0.003953	0.002679
	15	-3.129	-3.129	7.945	147.7	175.2	1.937	-13.959	0.000738	0.000876	0.004543	0.003061

Panel I.D.	LS	σ_x (MPa)	σ_y (MPa)	τ_{xy} (MPa)	f_{cx} (MPa)	f_{cy} (MPa)	f_{c1} (MPa)	f_{c2} (MPa)	ε_x	ε_y	γ_{xy}	ε_{c1}
	16	-3.233	-3.233	8.208	161.3	189.2	1.852	-14.572	0.000806	0.000945	0.005125	0.003413
	17	-3.369	-3.369	8.563	172.3	210.5	1.784	-15.355	0.000861	0.001052	0.005913	0.003883
	18	-3.496	-3.496	8.876	188.3	229.8	1.657	-16.111	0.000941	0.001148	0.007458	0.004797
PV24	4	-4.480	-4.480	5.417	-25.8	-17.2	1.322	-9.514	-0.000129	-0.000086	0.000688	0.000224
	5	-5.226	-5.226	6.289	-27.1	-15.2	1.441	-11.138	-0.000135	-0.000076	0.000988	0.000391
	6	-5.574	-5.574	6.737	-23.8	-13.5	1.497	-11.978	-0.000119	-0.000068	0.001250	0.000539
PV25	4	-3.727	-3.727	5.485	-11.1	-5.7	1.908	-9.062	-0.000055	-0.000029	0.000855	0.000387
	5	-4.676	-4.676	6.851	5.3	16.8	1.979	-11.725	0.000027	0.000084	0.001607	0.000859
	6	-5.117	-5.117	7.512	19.3	34.9	1.912	-13.114	0.000096	0.000174	0.002228	0.001245
	7	-5.621	-5.621	8.234	27.9	53.3	1.891	-14.583	0.000139	0.000267	0.003111	0.001767
	8	-5.843	-5.843	8.440	50.1	72.2	1.508	-15.377	0.000250	0.000361	0.004015	0.002295
	9	-6.074	-6.074	8.735	50.9	74.3	1.547	-15.929	0.000254	0.000371	0.004687	0.002643
	10	-6.346	-6.346	9.125	61.1	78.4	1.535	-16.718	0.000306	0.000392	0.005509	0.002873
PV27	3	-0.030	-0.030	2.750	15.6	27.1	2.341	-3.163	0.000078	0.000135	0.000512	0.000342
	4	-0.028	-0.028	3.483	52.1	64.8	2.414	-4.556	0.000260	0.000324	0.001102	0.000820
	5	-0.043	-0.043	4.186	94.0	109.6	2.330	-6.047	0.000470	0.000547	0.001832	0.001413
	6	-0.037	-0.037	4.900	136.2	149.8	2.313	-7.490	0.000681	0.000748	0.002607	0.002002
	7	-0.029	-0.029	5.361	164.9	180.9	2.248	-8.479	0.000824	0.000904	0.003117	0.002396
	8	-0.026	-0.026	5.817	192.0	206.8	2.233	-9.404	0.000960	0.001033	0.003699	0.002825
	9	-0.032	-0.032	6.240	230.6	235.1	2.051	-10.428	0.001152	0.001175	0.004539	0.003418
PV28	3	0.630	0.630	2.068	39.8	37.7	2.006	-2.130	0.000199	0.000189	0.000651	0.000507
	4	0.878	0.878	2.743	99.7	102.2	1.819	-3.667	0.000498	0.000511	0.001504	0.001256
	5	1.065	1.065	3.282	143.2	145.7	1.768	-4.795	0.000716	0.000728	0.002118	0.001782
	6	1.213	1.213	3.773	182.6	180.5	1.745	-5.801	0.000912	0.000902	0.002684	0.002243
	7	1.316	1.316	4.124	206.0	209.7	1.730	-6.517	0.001029	0.001048	0.003078	0.002564
	8	1.428	1.428	4.449	231.4	237.2	1.695	-7.203	0.001156	0.001185	0.003512	0.002934
	9	1.533	1.533	4.786	260.5	261.8	1.658	-7.915	0.001302	0.001308	0.003962	0.003262
	10	1.649	1.649	5.123	291.7	292.5	0.000	-10.247	0.001458	0.001462	0.004524	0.003673
	11	1.708	1.708	5.315	312.7	311.8	0.000	-10.631	0.001562	0.001558	0.004938	0.003976
	12	1.753	1.753	5.457	331.5	329.9	0.000	-10.914	0.001657	0.001649	0.005348	0.004264
	13	1.796	1.796	5.611	345.1	343.8	0.000	-11.223	0.001724	0.001718	0.005802	0.004571
PV29	3	-0.053	-0.053	2.778	71.0	77.1	1.765	-3.821	0.000355	0.000385	0.001212	0.000988
	4	-0.056	-0.056	3.315	114.5	164.9	1.520	-5.135	0.000572	0.000824	0.002109	0.001782
	5	-0.056	-0.056	3.783	162.5	324.3	0.842	-6.724	0.000812	0.001694	0.003565	0.003140
	6	-0.361	-0.361	4.168	174.0	324.3	0.822	-7.518	0.000869	0.002135	0.004254	0.003795
	7	-0.709	-0.709	4.522	171.9	324.3	0.845	-8.201	0.000859	0.002331	0.004581	0.004050
	8	-1.058	-1.058	4.871	174.4	324.3	0.823	-8.922	0.000871	0.002493	0.005019	0.004371
	9	-1.395	-1.395	5.208	171.5	324.3	0.848	-9.569	0.000857	0.002686	0.005576	0.004765
	10	-1.765	-1.765	5.573	169.0	324.3	0.864	-10.262	0.000845	0.002924	0.006118	0.005190
PB4	5	0.993	-0.053	1.019	76.2	0.0	1.095	-0.983	0.000381	0.000455	0.000616	0.000723
PB5	4	0.849	-0.904	0.876	38.6	0.0	0.873	-1.346	0.000193	0.000037	0.000075	0.000266
	5	1.025	-1.087	1.056	60.7	0.0	0.933	-1.654	0.000303	0.000119	0.000119	0.000427
	7	0.998	-1.075	1.036	67.3	0.0	0.842	-1.648	0.000336	0.000107	0.000099	0.000438
	8	1.286	-1.343	1.315	107.9	0.0	0.902	-2.130	0.000539	0.000162	0.000546	0.000665
	9	1.601	-1.661	1.631	173.9	0.0	0.808	-2.754	0.000869	0.000308	0.001020	0.001119
	10	2.081	-2.149	2.115	262.5	0.0	0.782	-3.698	0.001312	0.000611	0.001880	0.001891
	11	1.498	-2.589	2.543	415.0	0.0	0.263	-4.857	0.002850	0.001811	0.004866	0.004710
PB6	7	0.923	-0.037	0.907	71.0	0.0	1.003	-0.886	0.000355	0.000326	0.000464	0.000535
	8	0.902	0.006	0.918	88.2	0.0	0.930	-0.979	0.000441	0.001487	0.001117	0.001689
	9	1.035	-0.057	1.027	116.5	0.0	0.924	-1.209	0.000582	0.001870	0.001618	0.002240
	10	1.073	-0.088	1.066	230.1	0.0	0.527	-2.039	0.001150	0.010935	0.007026	0.012034
PB7	3	1.580	-0.090	-0.835	158.3	0.0	0.745	-0.973	0.000792	0.001813	-0.002262	0.002551
	4	1.612	-0.103	-0.857	196.4	0.0	0.602	-1.224	0.000982	0.005694	-0.005451	0.007013
	5	1.489	-0.093	-0.791	196.9	0.0	0.500	-1.239	0.000984	0.010753	-0.008560	0.012284
PB8	3	1.959	-0.035	-0.677	139.4	0.0	0.966	-0.555	0.000697	0.000176	-0.000671	0.000871
	4	2.151	-0.016	-0.731	184.6	0.0	0.855	-0.722	0.000923	0.000746	-0.001247	0.001476
	5	2.274	-0.117	-0.795	268.6	0.0	0.505	-1.263	0.001343	0.005793	-0.004581	0.006727

Panel I.D.	LS	σ_x (MPa)	σ_y (MPa)	τ_{xy} (MPa)	f_{cx} (MPa)	f_{cy} (MPa)	f_{c1} (MPa)	f_{c2} (MPa)	ε_x	ε_y	γ_{xy}	ε_{c1}
PB10	2	1.751	-0.034	-0.312	55.0	0.0	1.249	-0.128	0.000275	0.000002	-0.000077	0.000298
	3	2.327	-0.037	-0.415	131.2	0.0	1.099	-0.233	0.000656	0.000045	-0.000308	0.000695
	4	2.946	-0.008	-0.494	212.4	0.0	0.962	-0.328	0.001062	0.000180	-0.000658	0.001170
	5	3.229	-0.043	-0.497	273.5	0.0	0.683	-0.465	0.001368	0.001919	-0.001945	0.002684
	6	3.210	-0.008	-0.529	305.5	0.0	0.538	-0.651	0.001528	0.005823	-0.004604	0.006859
	7	3.448	-0.020	-0.563	433.0	0.0	0.199	-1.469	0.002932	0.013324	-0.013780	0.016861
PB11	4	-0.001	-0.001	-1.191	-8.2	0.0	1.236	-1.148	-0.000041	0.008748	-0.012013	0.011732
PB12	4	0.027	0.227	-1.368	11.1	0.0	1.444	-1.310	0.000055	0.003541	-0.002626	0.004117
PB14	3	2.389	0.028	-0.781	2.5	0.0	2.583	-0.216	0.000012	0.000045	-0.000074	0.000118
	4	3.400	-0.022	-1.109	74.6	0.0	2.413	-0.545	0.000373	0.001126	-0.001252	0.001533
	5	3.683	0.023	-1.207	124.7	0.0	1.943	-0.759	0.000623	0.003964	-0.002717	0.004489
	6	4.270	0.034	-1.376	180.0	0.0	1.746	-1.084	0.000900	0.006664	-0.004441	0.007612
	7	4.622	-0.048	-1.508	274.4	0.0	1.083	-2.059	0.001372	0.014883	-0.009435	0.016828
PB16	5	2.338	-0.001	-1.169	60.8	0.0	1.934	-0.826	0.000304	0.000429	-0.000058	0.000716
	6	2.679	0.011	-1.334	136.0	0.0	1.428	-1.488	0.000680	0.003396	-0.003057	0.004141
	7	2.610	-0.061	-1.335	184.6	0.0	0.926	-2.111	0.000923	0.011995	-0.007548	0.013578
	8	2.749	-0.146	-1.448	253.5	0.0	0.600	-3.127	0.001268	0.023648	-0.011158	0.024580
	9	2.754	-0.134	-1.444	284.0	0.0	0.489	-3.614	0.001420	0.036708	-0.016149	0.037881
PB17	5	4.259	0.002	-0.726	134.0	0.0	1.840	-0.291	0.000670	0.000097	-0.000410	0.000745
	6	4.782	0.002	-0.808	184.0	0.0	1.510	-0.448	0.000920	0.000305	-0.000724	0.001094
	7	5.625	0.001	-0.934	252.6	0.0	1.242	-0.727	0.001263	0.001101	-0.001568	0.001974
	8	6.602	0.003	-1.100	321.6	0.0	1.162	-1.061	0.001608	0.002633	-0.003021	0.003723
	9	7.195	0.002	-1.202	420.3	0.0	0.719	-2.025	0.002101	0.005464	-0.005836	0.007177
	10	7.573	-0.085	-1.218	501.6	0.0	0.412	-3.071	0.002960	0.018050	-0.013742	0.020678
PB18	6	-0.070	-0.070	-1.656	44.9	0.0	1.207	-2.332	0.000224	0.006954	-0.003502	0.007426
	7	-0.062	-0.062	-1.665	54.6	0.0	1.197	-2.519	0.000273	0.015413	-0.006851	0.016177
	8	-0.096	-0.096	-1.648	85.5	0.0	1.119	-3.187	0.000427	0.019231	-0.007585	0.020977
PB19	5	1.270	0.050	-1.234	30.2	0.0	1.607	-0.950	0.000151	0.000129	-0.000353	0.000331
	7	1.270	-0.001	-1.233	109.1	0.0	0.798	-1.923	0.000545	0.008546	-0.004824	0.009208
	8	1.270	-0.001	-1.233	136.0	0.0	0.649	-2.364	0.000680	0.011724	-0.006491	0.012614
PB20	6	2.215	-0.030	-1.122	85.9	0.0	1.321	-1.022	0.000430	0.002602	-0.001702	0.002895
	7	2.263	0.041	-1.111	96.0	0.0	1.251	-1.055	0.000480	0.004876	-0.002560	0.005221
	8	2.514	0.044	-1.235	110.8	0.0	1.332	-1.205	0.000554	0.006630	-0.003455	0.007099
	9	2.711	0.050	-1.331	144.8	0.0	1.173	-1.591	0.000724	0.010069	-0.005232	0.010772
	10	2.871	0.056	-1.408	226.2	0.0	0.766	-2.804	0.001131	0.021993	-0.011065	0.023498
PB21	4	2.765	0.005	-0.895	87.1	0.0	1.467	-0.609	0.000435	0.000101	-0.000433	0.000563
	5	3.048	0.011	-0.998	108.2	0.0	1.438	-0.754	0.000541	0.000206	-0.000662	0.000771
	6	3.272	-0.014	-1.056	130.1	0.0	1.309	-0.907	0.000651	0.002199	-0.001632	0.002568
	7	3.683	0.006	-1.202	150.5	0.0	1.429	-1.044	0.000753	0.004224	-0.003134	0.004844
	8	4.067	0.021	-1.319	206.0	0.0	1.132	-1.566	0.001030	0.010501	-0.007622	0.011864
	9	4.323	-0.035	-1.381	237.1	0.0	0.996	-1.913	0.001186	0.018406	-0.013625	0.020788
PB22	4	3.693	0.017	-0.608	131.0	0.0	1.209	-0.373	0.000655	0.000108	-0.000494	0.000789
	5	4.510	0.022	-0.728	178.1	0.0	1.147	-0.525	0.000891	0.002057	-0.001621	0.002522
	6	5.332	0.027	-0.867	222.3	0.0	1.180	-0.702	0.001112	0.003843	-0.002695	0.004408
	7	6.143	0.051	-0.978	291.8	0.0	0.908	-1.119	0.001459	0.006908	-0.005267	0.008029
	8	6.383	0.039	-1.012	381.3	0.0	0.464	-2.412	0.001907	0.012074	-0.008903	0.013818
PB28	3	0.006	1.667	0.841	0.0	14.4	1.768	-0.411	0.000016	0.000072	0.000110	0.000125
	4	0.024	2.061	1.027	0.0	39.5	1.814	-0.597	0.000150	0.000198	0.000321	0.000331
	5	0.018	2.375	1.189	0.0	118.2	1.119	-1.321	0.000769	0.000591	0.001340	0.001350
	6	0.017	2.519	1.267	0.0	155.9	0.928	-1.814	0.002838	0.000780	0.002880	0.003538
	7	0.040	2.743	1.362	0.0	182.0	0.919	-2.131	0.005911	0.000910	0.004838	0.006900
	8	0.015	2.909	1.463	0.0	188.3	0.997	-2.207	0.011175	0.000941	0.007761	0.012500
PB29	4	1.956	-0.004	-0.980	40.6	0.0	1.724	-0.593	0.000203	0.000134	-0.000377	0.000319
	5	2.170	-0.031	-1.100	128.4	0.0	0.937	-1.395	0.000642	0.003030	-0.002711	0.003645
	6	2.444	-0.021	-1.233	156.8	0.0	0.957	-1.705	0.000784	0.004486	-0.003772	0.005283
	7	2.674	-0.024	-1.349	181.0	0.0	0.970	-1.982	0.000905	0.006901	-0.005385	0.007953
	8	2.818	-0.034	-1.426	199.9	0.0	0.960	-2.220	0.001000	0.009069	-0.006682	0.010287

Panel I.D.	LS	σ_x (MPa)	σ_y (MPa)	τ_{xy} (MPa)	f_{sx} (MPa)	f_{sy} (MPa)	f_{c1} (MPa)	f_{c2} (MPa)	ε_x	ε_y	γ_{xy}	ε_{c1}
	9	2.919	-0.055	-1.487	211.3	0.0	0.949	-2.358	0.001056	0.012662	-0.008513	0.014095
PB30	4	2.914	0.007	-0.984	173.7	0.0	0.751	-1.344	0.000868	0.004741	-0.003245	0.005300
	5	3.208	0.034	-1.069	188.7	0.0	0.840	-1.415	0.000943	0.007312	-0.004479	0.008028
	6	3.394	0.031	-1.127	206.8	0.0	0.830	-1.587	0.001034	0.009774	-0.005561	0.010603
	7	3.592	0.044	-1.197	220.6	0.0	0.877	-1.703	0.001103	0.011055	-0.006198	0.011973
	8	4.019	0.060	-1.334	256.9	0.0	0.916	-2.036	0.001285	0.012548	-0.007185	0.013622
	9	4.302	0.041	-1.431	299.3	0.0	0.840	-2.552	0.001497	0.016062	-0.009560	0.017558
PB31	2	2.557	0.028	-0.442	33.1	0.0	1.988	-0.074	0.000166	0.000205	-0.000017	0.000339
	3	3.659	0.024	-0.630	131.8	0.0	1.318	-0.302	0.000659	0.000435	-0.000592	0.000892
	4	4.579	0.023	-0.784	207.5	0.0	1.032	-0.627	0.001037	0.000837	-0.001262	0.001586
	5	5.214	0.031	-0.900	286.7	0.0	0.704	-1.259	0.001434	0.007669	-0.005079	0.008623
	6	5.780	0.016	-0.977	325.6	0.0	0.693	-1.484	0.001628	0.009599	-0.006330	0.010766
	7	6.415	0.024	-1.087	394.2	0.0	0.589	-2.124	0.001971	0.012738	-0.008434	0.014285
PB32	2	1.937	0.012	-0.642	19.0	0.0	1.774	-0.243	0.000095	0.000005	-0.000071	0.000142
	3	2.476	0.006	-0.824	54.6	0.0	1.737	-0.452	0.000273	0.000046	-0.000190	0.000311
	4	3.178	0.008	-1.046	132.5	0.0	1.261	-0.984	0.000663	0.000276	-0.000668	0.000837
	5	3.709	-0.038	-1.196	199.6	0.0	0.936	-1.644	0.000998	0.005973	-0.004001	0.006694
	6	4.238	0.038	-1.411	265.3	0.0	0.874	-2.421	0.001327	0.010826	-0.008478	0.013453
PHS1	5	0.012	0.012	2.746	23.6	0.0	2.403	-3.141	0.000109	0.000229	0.000452	0.000403
PHS2	4	-0.036	-0.036	2.537	3.6	5.2	2.433	-2.642	0.000017	0.000025	0.000172	0.000107
	5	-0.017	-0.017	3.025	12.2	17.0	2.780	-3.279	0.000057	0.000083	0.000271	0.000206
	6	-0.037	-0.037	3.295	88.3	192.9	1.593	-5.312	0.000409	0.000936	0.001480	0.001458
	7	-0.041	-0.041	3.792	115.1	288.6	1.506	-6.491	0.000534	0.001400	0.002059	0.002084
	8	-0.014	-0.014	4.037	135.5	364.7	1.336	-7.237	0.000628	0.001769	0.002524	0.002584
	9	0.005	0.005	4.495	176.5	509.9	0.953	-8.734	0.000818	0.002474	0.003401	0.003537
	10	-0.017	-0.017	4.841	192.4	521.2	1.060	-9.445	0.000892	0.002986	0.003979	0.004187
	11	-0.034	-0.034	5.043	207.2	521.2	1.085	-9.983	0.000960	0.003445	0.004424	0.004739
	12	0.019	0.019	5.295	229.6	521.2	1.159	-10.673	0.001064	0.004128	0.005092	0.005567
	13	-0.016	-0.016	5.684	256.3	521.2	1.236	-11.685	0.001188	0.005337	0.006215	0.006999
	14	0.020	0.020	6.186	300.7	521.2	1.349	-13.157	0.001393	0.007969	0.008510	0.010059
PHS3	3	0.004	0.004	2.995	26.2	26.0	2.486	-3.538	0.000121	0.000126	0.000475	0.000361
	4	0.024	0.024	3.480	80.6	117.7	1.815	-5.335	0.000373	0.000571	0.001275	0.001117
	5	0.013	0.013	3.986	117.0	202.4	1.418	-6.832	0.000542	0.000982	0.001895	0.001735
	6	0.003	0.003	4.499	139.5	254.3	1.367	-7.951	0.000646	0.001234	0.002287	0.002121
	7	0.025	0.025	4.978	164.1	312.5	1.256	-9.069	0.000760	0.001516	0.002737	0.002558
	8	0.020	0.020	5.489	184.8	362.9	1.237	-10.142	0.000857	0.001761	0.003138	0.002942
	9	-0.004	-0.004	6.006	204.0	413.6	1.220	-11.210	0.000946	0.002007	0.003549	0.003328
	10	-0.009	-0.009	6.518	230.7	472.8	1.086	-12.432	0.001069	0.002294	0.004003	0.003775
	11	-0.019	-0.019	7.031	252.8	521.2	1.057	-13.533	0.001171	0.002630	0.004526	0.004278
	12	-0.019	-0.019	7.529	313.4	521.2	0.860	-15.294	0.001452	0.003906	0.006065	0.005950
	13	-0.128	-0.128	8.098	347.8	521.2	0.932	-16.696	0.001612	0.005059	0.007368	0.007402
PHS4	3	0.648	0.648	2.782	66.5	93.6	2.056	-3.677	0.000308	0.000454	0.000899	0.000837
	4	0.784	0.784	3.272	119.1	181.2	1.596	-5.360	0.000552	0.000879	0.001609	0.001537
	5	0.913	0.913	3.772	147.6	279.0	1.356	-6.586	0.000684	0.001354	0.002203	0.002170
	6	1.056	1.056	4.252	171.0	325.1	1.447	-7.525	0.000793	0.001577	0.002650	0.002567
	7	1.177	1.177	4.758	202.2	386.1	1.376	-8.717	0.000937	0.001873	0.003125	0.003036
	8	1.301	1.301	5.279	239.6	459.6	1.187	-10.093	0.001111	0.002230	0.003640	0.003575
	9	1.420	1.420	5.774	269.5	521.2	1.115	-11.255	0.001249	0.002674	0.004207	0.004183
	10	1.532	1.532	6.183	306.0	521.2	1.242	-12.337	0.001418	0.003925	0.005444	0.005668
	11	1.582	1.582	6.435	334.0	521.2	1.263	-13.163	0.001548	0.005257	0.006714	0.007238
PHS5	3	0.470	0.470	2.032	12.4	4.3	2.302	-1.779	0.000057	0.000021	0.000240	0.000160
	4	0.590	0.590	2.540	63.3	154.3	1.888	-3.385	0.000293	0.000749	0.001291	0.001205
	5	0.721	0.721	3.027	119.6	327.4	1.397	-5.161	0.000554	0.001588	0.002455	0.002403
	6	0.851	0.851	3.531	152.7	496.9	1.182	-6.451	0.000708	0.002411	0.003407	0.003464
	7	0.976	0.976	4.022	204.0	521.2	1.210	-7.983	0.000945	0.004333	0.005247	0.005762
	8	1.029	1.029	4.228	222.9	521.2	1.289	-8.567	0.001033	0.005544	0.006350	0.007183
	9	1.099	1.099	4.446	248.8	521.2	1.348	-9.322	0.001153	0.007405	0.007784	0.009271

Panel I.D.	LS	σ_x (MPa)	σ_y (MPa)	τ_{xy} (MPa)	f_{sx} (MPa)	f_{sy} (MPa)	f_{c1} (MPa)	f_{c2} (MPa)	ε_x	ε_y	γ_{xy}	ε_{c1}
PHS6	3	-0.771	-0.771	2.833	5.9	4.5	1.959	-3.709	0.000027	0.000022	0.000265	0.000157
	4	-0.879	-0.879	3.315	12.0	9.3	2.228	-4.411	0.000055	0.000045	0.000376	0.000238
	5	-0.984	-0.984	3.790	43.9	63.8	2.011	-5.657	0.000203	0.000309	0.000877	0.000698
	6	-1.119	-1.119	4.313	72.5	136.2	1.835	-6.973	0.000336	0.000661	0.001441	0.001237
	7	-1.308	-1.308	4.883	93.5	206.5	1.761	-8.245	0.000434	0.001002	0.002024	0.001769
	8	-1.431	-1.431	5.364	129.3	273.1	1.499	-9.656	0.000599	0.001325	0.002466	0.002247
	9	-1.678	-1.678	6.000	149.5	348.8	1.428	-11.044	0.000693	0.001693	0.003026	0.002786
	10	-1.802	-1.802	6.486	168.5	397.8	1.422	-12.095	0.000781	0.001930	0.003407	0.003153
	11	-1.978	-1.978	7.044	191.1	456.4	1.365	-13.365	0.000886	0.002214	0.003841	0.003582
	12	-2.189	-2.189	7.617	208.4	521.2	1.333	-14.579	0.000966	0.002559	0.004361	0.004084
	13	-2.335	-2.335	8.149	233.8	521.2	1.408	-15.766	0.001084	0.003115	0.005100	0.004844
	14	-2.458	-2.458	8.643	262.7	521.2	1.438	-16.977	0.001218	0.003928	0.006051	0.005888
	15	-2.570	-2.570	9.134	298.1	521.2	1.420	-18.324	0.001381	0.005246	0.007549	0.007554
	16	-2.733	-2.733	9.661	323.6	521.2	1.490	-19.546	0.001500	0.007413	0.010133	0.010322
PHS7	3	-0.692	-0.692	2.759	4.1	1.3	1.996	-3.524	0.000019	0.000006	0.000215	0.000120
	4	-0.915	-0.915	3.539	22.1	21.0	2.191	-4.908	0.000103	0.000102	0.000465	0.000335
	5	-1.036	-1.036	4.216	70.2	121.0	1.598	-6.930	0.000325	0.000587	0.001272	0.001106
	6	-1.283	-1.283	5.039	102.6	185.8	1.416	-8.820	0.000476	0.000902	0.001863	0.001644
	7	-1.424	-1.424	5.744	129.8	246.0	1.317	-10.375	0.000602	0.001194	0.002384	0.002126
	8	-1.675	-1.675	6.551	159.1	302.1	1.202	-12.167	0.000737	0.001466	0.002917	0.002605
	9	-1.884	-1.884	7.331	181.2	351.9	1.227	-13.732	0.000840	0.001707	0.003371	0.003014
	10	-2.047	-2.047	8.058	210.1	413.6	1.100	-15.370	0.000973	0.002007	0.003906	0.003510
	11	-2.226	-2.226	8.750	236.7	473.2	0.961	-16.939	0.001097	0.002296	0.004445	0.003998
	12	-2.447	-2.447	9.574	259.9	521.2	1.012	-18.575	0.001205	0.002677	0.005050	0.004571
	13	-2.650	-2.650	10.261	285.3	521.2	1.160	-19.948	0.001322	0.003311	0.005851	0.005407
PHS8	3	-0.008	-0.008	2.757	7.8	6.1	2.586	-2.931	0.000036	0.000030	0.000284	0.000175
	4	-0.051	-0.051	3.554	46.5	71.3	2.323	-4.811	0.000215	0.000346	0.000896	0.000734
	5	-0.031	-0.031	4.286	97.0	152.7	1.786	-6.875	0.000450	0.000741	0.001612	0.001414
	6	-0.036	-0.036	5.042	133.4	220.8	1.544	-8.661	0.000618	0.001071	0.002190	0.001963
	7	-0.044	-0.044	5.804	155.2	274.5	1.607	-10.112	0.000719	0.001332	0.002707	0.002413
	8	-0.029	-0.029	6.535	181.5	321.7	1.646	-11.558	0.000841	0.001561	0.003192	0.002837
	9	-0.060	-0.060	7.320	212.7	379.4	1.552	-13.248	0.000986	0.001841	0.003710	0.003317
	10	-0.037	-0.037	8.046	246.0	447.2	1.352	-14.917	0.001140	0.002170	0.004267	0.003850
	11	-0.072	-0.072	8.589	279.5	498.5	1.030	-16.382	0.001295	0.002419	0.004716	0.004281
	12	-0.053	-0.053	9.069	305.0	521.2	1.016	-17.435	0.001413	0.002810	0.005240	0.004823
	13	-0.017	-0.017	9.534	332.8	521.2	1.148	-18.395	0.001542	0.003334	0.005956	0.005548
	14	-0.016	-0.016	9.990	353.9	521.2	1.331	-19.257	0.001640	0.004062	0.006891	0.006503
	15	-0.041	-0.041	10.276	376.6	521.2	1.309	-20.019	0.001745	0.004715	0.007638	0.007327
	16	-0.146	-0.146	10.457	397.6	521.2	1.134	-20.731	0.001843	0.005442	0.008422	0.008222
	17	-0.048	-0.048	10.455	404.4	521.2	1.152	-20.774	0.001874	0.006771	0.009801	0.009801
	18	-0.137	-0.137	10.652	428.9	521.2	0.980	-21.569	0.001988	0.007690	0.010767	0.010931
PHS9	3	-0.761	-0.761	2.822	-1.7	-1.0	2.091	-3.553	-0.000008	-0.000005	0.000163	0.000075
	4	-0.914	-0.914	3.541	18.6	34.7	2.262	-4.835	0.000086	0.000169	0.000451	0.000357
	5	-1.217	-1.217	4.396	86.6	199.1	1.482	-7.531	0.000401	0.000966	0.001720	0.001589
	6	-1.210	-1.210	4.975	135.1	325.7	1.140	-9.260	0.000626	0.001580	0.002638	0.002506
	7	-1.456	-1.456	5.765	161.2	399.7	1.156	-10.913	0.000747	0.001939	0.003194	0.003048
	8	-1.666	-1.666	6.535	193.8	505.6	1.030	-12.695	0.000898	0.002453	0.003964	0.003805
	9	-1.907	-1.907	7.351	233.2	521.2	1.088	-14.573	0.001081	0.003234	0.005073	0.004913
	10	-2.067	-2.067	7.870	256.7	521.2	1.169	-15.732	0.001190	0.003836	0.005869	0.005732
	11	-2.202	-2.202	8.395	281.8	521.2	1.267	-16.910	0.001306	0.004763	0.006882	0.006885
	12	-2.332	-2.332	8.843	300.9	521.2	1.361	-17.882	0.001395	0.006077	0.008294	0.008498
	13	-2.411	-2.411	9.162	325.3	521.2	1.339	-18.807	0.001508	0.007336	0.009602	0.010038
PHS10	3	0.579	0.579	2.546	20.0	30.9	2.613	-2.486	0.000093	0.000150	0.000461	0.000354
	4	0.741	0.741	3.007	64.4	115.2	2.011	-4.038	0.000298	0.000559	0.001147	0.001017
	5	0.869	0.869	3.506	98.1	161.9	1.835	-5.273	0.000455	0.000786	0.001611	0.001443
	6	0.990	0.990	4.011	127.8	214.9	1.671	-6.483	0.000592	0.001043	0.002075	0.001879
	7	1.126	1.126	4.506	154.5	259.4	1.616	-7.569	0.000716	0.001258	0.002483	0.002258

Panel I.D.	LS	σ_x (MPa)	σ_y (MPa)	τ_{xy} (MPa)	f_{cx} (MPa)	f_{cy} (MPa)	f_{c1} (MPa)	f_{c2} (MPa)	ε_x	ε_y	γ_{xy}	ε_{c1}
	8	1.247	1.247	5.005	173.0	299.3	1.690	-8.495	0.000802	0.001452	0.002903	0.002615
	9	1.363	1.363	5.510	202.0	248.0	1.562	-9.677	0.000936	0.001688	0.003324	0.003017
	10	1.492	1.492	6.010	227.3	394.4	1.510	-10.757	0.001053	0.001914	0.003751	0.003408
	11	1.607	1.607	6.516	254.3	455.1	1.320	-11.963	0.001179	0.002208	0.004272	0.003890
	12	1.734	1.734	7.010	288.5	521.2	0.998	-13.310	0.001337	0.002713	0.005009	0.004622
	13	1.860	1.860	7.485	321.5	521.2	1.174	-14.301	0.001490	0.003525	0.006042	0.005695
	14	1.934	1.934	7.742	247.8	521.2	1.187	-15.015	0.001612	0.004141	0.006791	0.006500
	15	1.986	1.986	8.009	366.6	521.2	1.283	-15.614	0.001699	0.004929	0.007685	0.007482
	16	2.063	2.063	8.248	386.1	521.2	1.374	-16.182	0.001789	0.005894	0.008773	0.008684
	17	2.135	2.135	8.582	430.1	521.2	1.308	-17.394	0.001993	0.008322	0.011339	0.011651
PA1	4	0.026	0.026	2.676	52.8	59.8	2.028	-3.337	0.000287	0.000325	0.000862	0.000737
	5	0.038	0.038	3.146	106.3	147.3	1.715	-4.601	0.000578	0.000801	0.001762	0.001577
	6	0.096	0.096	3.601	144.3	199.6	1.708	-5.533	0.000784	0.001085	0.002400	0.002144
	7	0.113	0.113	4.090	177.4	250.9	1.734	-6.492	0.000964	0.001363	0.002895	0.002625
	8	0.104	0.104	4.491	219.6	324.8	1.477	-7.556	0.001193	0.001765	0.003572	0.003288
	9	0.123	0.123	5.091	254.8	375.8	1.602	-8.641	0.001385	0.002042	0.004100	0.003789
	10	0.107	0.107	5.601	285.5	431.8	1.613	-9.650	0.001551	0.002347	0.004699	0.004332
	11	0.139	0.139	5.863	308.9	483.0	1.501	-10.280	0.001679	0.002625	0.005159	0.004774
	12	0.110	0.110	6.096	339.3	522.0	1.302	-10.961	0.001844	0.002955	0.005690	0.005299
	13	0.107	0.107	6.292	379.9	522.0	1.202	-11.538	0.002065	0.003502	0.006402	0.006064
PA2	3	-0.080	-0.080	2.584	101.6	132.9	1.138	-4.064	0.000552	0.000722	0.001500	0.001392
	4	-0.073	-0.073	3.091	131.4	187.0	1.183	-5.031	0.000714	0.001016	0.002050	0.001902
	5	-0.051	-0.051	3.810	176.9	260.6	1.251	-6.409	0.000961	0.001416	0.002827	0.002621
	6	-0.042	-0.042	4.539	223.2	339.1	1.288	-7.835	0.001213	0.001843	0.003598	0.003354
	7	-0.025	-0.025	5.028	251.6	392.8	1.338	-8.761	0.001367	0.002135	0.004146	0.003859
	8	-0.037	-0.037	5.538	284.9	460.1	1.283	-9.832	0.001549	0.002501	0.004780	0.004462
	9	-0.042	-0.042	6.031	334.9	522.0	1.118	-11.009	0.001820	0.003431	0.005990	0.005727
	10	-0.017	-0.017	6.155	385.9	522.0	0.902	-11.583	0.002097	0.004419	0.007170	0.007026
SE1	1	0.000	0.000	1.544	2.0	4.0	1.495	-1.593	0.000010	0.000020	0.000110	0.000070
	2	0.000	0.000	2.912	82.0	126.0	1.153	-4.788	0.000410	0.000630	0.001430	0.001250
	3	0.000	0.000	4.596	168.0	298.0	0.786	-8.623	0.000840	0.001490	0.003070	0.002730
	4	0.000	0.000	4.491	172.0	316.0	0.531	-8.661	0.000860	0.001580	0.003190	0.002850
	5	0.000	0.000	6.105	240.0	608.0	-0.360	-12.618	0.001200	0.003040	0.005330	0.004940
	6	0.000	0.000	6.772	256.0	1242.0	-2.665	-16.983	0.001280	0.006210	0.008750	0.008770
SE5	1	0.000	0.000	2.456	64.0	66.0	0.552	-4.361	0.000320	0.000330	0.001100	0.000880
	2	0.000	0.000	4.526	134.0	140.0	0.513	-8.541	0.000670	0.000700	0.002470	0.001920
	3	0.000	0.000	6.211	194.0	202.0	0.410	-12.013	0.000970	0.001010	0.004150	0.003070
	4	0.000	0.000	8.105	274.0	266.0	0.195	-16.017	0.001370	0.001330	0.018830	0.010770
SE6	1	0.000	0.000	1.298	18.0	18.0	1.026	-1.612	0.000090	0.000090	0.000080	0.000130
	2	0.000	0.000	2.105	40.0	50.0	1.497	-2.832	0.000200	0.000250	0.000320	0.000380
	3	0.000	0.000	2.456	12.0	68.0	2.170	-2.744	0.000060	0.000340	0.000630	0.000550
	4	0.000	0.000	0.000	-18.0	-4.0	0.527	0.013	-0.000090	-0.000020	0.000210	0.000060
	5	0.000	0.000	2.456	30.0	118.0	1.837	-3.100	0.000150	0.000590	0.001050	0.000940
	6	0.000	0.000	2.912	90.0	318.0	1.183	-4.857	0.000450	0.001590	0.002390	0.002350
	7	0.000	0.000	3.088	128.0	444.0	0.697	-5.894	0.000640	0.002220	0.003020	0.003140
	8	0.000	0.000	3.263	140.0	610.0	0.385	-6.475	0.000700	0.003050	0.003880	0.004140
	9	0.000	0.000	3.544	180.0	908.0	-0.389	-7.845	0.000900	0.004540	0.005180	0.005890
	10	0.000	0.000	3.754	148.0	1680.0	-1.109	-8.704	0.000740	0.008400	0.008330	0.010230

Panel I.D.	LS	ε_{c2}	θ_ε (deg)	θ_σ (deg)	γ_s	Δ^*_s	$\Delta\varepsilon_{1cr}$	ε_{scrx}	ε_{scry}	f_{scrx} (MPa)	f_{scry} (MPa)	f_{c1}^* (MPa)
PV1	3	-0.000178	44.630	46.003	-0.000070	-0.003503	0.000450	0.000787	0.000784	157.4	156.8	0.777
	4	-0.000298	45.842	44.815	0.000092	0.004579	0.000300	0.001119	0.001192	223.8	238.4	0.518
	5	-0.000492	45.812	44.798	0.000132	0.006616	0.000293	0.001488	0.001592	297.7	318.5	0.506
	6	-0.000683	46.103	44.357	0.000311	0.015531	0.000185	0.001846	0.002040	369.1	407.9	0.318
	7	-0.001048	46.324	44.495	0.000428	0.021413	0.000002	0.002195	0.002505	439.0	483.0	0.000
PV3	4	-0.000244	44.049	45.503	-0.000112	-0.005600	0.002385	0.002082	0.002051	416.3	410.1	1.152
	5	-0.000410	45.428	44.661	0.000118	0.005897	0.001884	0.002716	0.002760	543.3	552.0	0.909
	6	-0.000493	46.024	44.079	0.000382	0.019080	0.001530	0.003017	0.003169	603.4	633.7	0.739
PV4	4	-0.000076	48.145	43.789	0.000119	0.005946	0.000231	0.000391	0.000467	78.2	93.5	1.435
	5	-0.000164	46.631	43.728	0.000197	0.009854	0.000147	0.000807	0.000911	161.4	182.3	0.913
	6	-0.000321	46.613	45.000	0.000332	0.016600	0.000000	0.002301	0.002633	242.0	242.0	0.029
	7	-0.000374	46.690	45.000	0.000595	0.029750	0.000000	0.004068	0.004663	242.0	242.0	0.029
	8	-0.000456	46.345	45.000	0.000673	0.033650	0.000000	0.005942	0.006615	242.0	242.0	0.029
PV5	3	-0.000153	43.705	45.958	-0.000172	-0.008583	0.001106	0.001490	0.001428	298.1	285.7	0.821
	4	-0.000211	43.786	46.002	-0.000232	-0.011586	0.001141	0.001862	0.001775	372.5	355.1	0.846
	5	-0.000378	44.816	45.178	-0.000049	-0.002442	0.000975	0.002000	0.001981	400.0	396.3	0.722
	6	-0.000547	45.562	44.403	0.000213	0.010640	0.000815	0.002444	0.002530	488.8	506.0	0.604
	7	-0.000761	45.341	44.598	0.000172	0.008595	0.000562	0.002775	0.002846	555.0	569.2	0.415
PV6	3	-0.000173	47.683	42.439	0.000239	0.011973	0.000409	0.000645	0.000731	128.9	146.2	0.734
	4	-0.000234	46.994	42.797	0.000267	0.013338	0.000309	0.000777	0.000881	155.5	176.1	0.553
	5	-0.000278	47.135	42.444	0.000350	0.017516	0.000228	0.000829	0.000969	165.8	193.7	0.407
	6	-0.000397	47.197	41.882	0.000582	0.029076	0.000175	0.001012	0.001234	202.4	246.8	0.314
	7	-0.000480	46.555	44.919	0.000237	0.011837	-0.000004	0.001319	0.001544	263.8	266.0	0.000
	8	-0.000576	45.260	45.000	0.000164	0.008200	0.000000	0.007124	0.007288	266.0	266.0	0.007
PV7	2	-0.000077	44.295	45.318	-0.000017	-0.000875	0.000647	0.000529	0.000524	105.8	104.9	1.155
	3	-0.000180	44.082	45.887	-0.000088	-0.004414	0.000220	0.000722	0.000683	144.3	136.7	0.391
	4	-0.000367	43.773	46.516	-0.000247	-0.012358	-0.000022	0.001072	0.000960	214.5	192.0	-0.041
	5	-0.000484	44.643	45.453	-0.000093	-0.004653	0.000142	0.001292	0.001253	258.4	250.6	0.252
	6	-0.000670	45.164	44.780	0.000057	0.002850	0.000023	0.001542	0.001566	308.4	313.1	0.039
	7	-0.000886	45.132	44.812	0.000059	0.002950	0.000001	0.001896	0.001920	379.2	383.9	0.000
PV8	3	-0.000203	44.893	45.118	-0.000009	-0.000426	0.000254	0.000492	0.000489	98.3	97.7	0.665
	4	-0.000341	44.874	45.165	-0.000019	-0.000939	0.000191	0.000714	0.000707	142.8	141.4	0.497
	5	-0.000493	44.931	45.098	-0.000015	-0.000736	0.000184	0.000904	0.000899	180.8	179.7	0.480
	6	-0.000688	45.281	44.568	0.000083	0.004172	0.000119	0.001079	0.001110	215.8	222.1	0.308
	7	-0.000951	45.471	44.193	0.000195	0.009743	0.000001	0.001295	0.001366	258.9	273.3	0.000
PV9	2	-0.000157	46.712	43.924	0.000050	0.002514	0.000566	0.000384	0.000393	76.7	78.7	1.011
	3	-0.000356	45.862	44.013	0.000088	0.004393	0.000432	0.000564	0.000590	112.7	118.0	0.771
	4	-0.000616	45.205	44.703	0.000040	0.001988	0.000408	0.000774	0.000786	154.8	157.1	0.726
	5	-0.001117	45.190	44.633	0.000072	0.003580	0.000310	0.000949	0.000969	189.8	193.8	0.553
	6	-0.001937	44.502	46.318	-0.000351	-0.017566	0.000121	0.001094	0.001002	218.8	200.5	0.216
	7	-0.002943	44.017	48.749	-0.001326	-0.066307	0.000001	0.001337	0.001061	267.5	212.1	0.000
PV10	3	-0.000197	48.710	45.448	0.000121	0.006074	0.000943	0.000679	0.000832	135.8	166.3	1.300
	4	-0.000378	49.056	45.661	0.000242	0.012107	0.000879	0.000878	0.001188	175.7	237.5	1.207
	5	-0.000619	50.490	44.261	0.000720	0.036014	0.000897	0.001153	0.001766	230.7	276.0	0.891
	6	-0.000856	52.109	46.008	0.000988	0.049395	0.001055	0.001356	0.002541	271.2	276.0	0.876
	7	-0.001459	55.524	47.729	0.002106	0.105297	0.075000	0.034917	0.044865	276.0	276.0	0.639
	8	-0.003986	55.040	46.472	0.004538	0.226905	0.000793	0.001254	0.006583	250.8	276.0	0.637
PV11	3	-0.000123	46.851	45.146	0.000027	0.001337	0.000875	0.000531	0.000565	106.3	113.0	1.350
	4	-0.000257	47.282	45.248	0.000087	0.004327	0.000763	0.000681	0.000785	136.2	156.9	1.175
	5	-0.000349	47.273	45.550	0.000109	0.005466	0.000682	0.000837	0.000994	167.3	198.8	1.048
	6	-0.000453	47.441	45.395	0.000165	0.008261	0.000642	0.000944	0.001150	188.7	229.9	0.986
	7	-0.000565	47.942	44.893	0.000323	0.016165	0.000605	0.001126	0.001435	225.1	235.0	0.596
	8	-0.001021	50.289	49.483	0.000154	0.007702	0.000000	0.001357	0.002352	235.0	235.0	0.006
	9	-0.001575	50.360	49.776	0.000143	0.007153	0.000000	0.001509	0.002780	235.0	235.0	0.006
PV12	4	-0.000180	51.800	49.960	0.000099	0.004958	0.001196	0.000889	0.001458	177.8	269.0	1.039
	5	-0.000279	53.577	49.938	0.000301	0.015046	0.001434	0.001148	0.002095	229.6	269.0	0.925
	6	-0.000380	56.539	51.652	0.000621	0.031070	0.001878	0.001430	0.003296	286.0	269.0	0.992

Panel I.D.	LS	ε_{c2}	θ_s (deg)	θ_σ (deg)	γ_s	Δ^*_s	$\Delta\varepsilon_{1cr}$	ε_{ecrx}	ε_{ecry}	f_{ecrx} (MPa)	f_{ecry} (MPa)	f_{c1}^* (MPa)
	7	-0.001027	61.784	54.332	0.002281	0.114043	**0.002508**	0.001782	0.007487	356.3	269.0	1.034
	8	-0.002335	65.119	52.275	0.007559	0.377935	**0.002364**	0.001670	0.013528	334.0	269.0	1.182
PV14	3	-0.000104	48.246	44.032	0.000051	0.002527	**0.001009**	0.000572	0.000577	114.5	115.5	1.801
	4	-0.000194	45.402	44.693	0.000029	0.001427	**0.000703**	0.000758	0.000766	151.5	153.2	1.255
	5	-0.000358	45.223	44.754	0.000038	0.001917	**0.000465**	0.001071	0.001085	214.3	217.1	0.829
	6	-0.000460	45.197	44.772	0.000044	0.002189	**0.000458**	0.001275	0.001291	255.0	258.2	0.816
	7	-0.000592	45.096	44.880	0.000027	0.001365	**0.000418**	0.001471	0.001481	294.1	296.2	0.743
PV16	2	0.000187	46.215	43.947	0.000195	0.009772	**0.075000**	0.039811	0.037160	255.0	255.0	0.431
PV18	4	-0.000178	56.984	49.373	0.000540	0.027006	**0.001560**	0.001095	0.002168	218.9	412.0	1.288
	5	-0.000310	60.376	50.827	0.001367	0.068329	**0.001638**	0.001336	0.003803	267.3	412.0	0.931
	6	-0.000782	64.253	55.088	0.003000	0.150010	**0.001786**	0.001571	0.008126	314.2	412.0	0.683
PV19	3	-0.000094	52.006	45.245	0.000107	0.005360	**0.001442**	0.000805	0.000928	161.0	185.6	1.787
	4	-0.000148	51.387	46.298	0.000184	0.009194	**0.001369**	0.000909	0.001201	181.9	240.3	1.646
	5	-0.000223	51.599	46.509	0.000263	0.013157	**0.001392**	0.001025	0.001438	204.9	287.6	1.665
	6	-0.000277	52.925	46.329	0.000518	0.025910	**0.001319**	0.001176	0.001857	235.2	299.0	1.313
	7	-0.000441	55.366	46.730	0.001066	0.053298	**0.001439**	0.001392	0.002750	278.4	299.0	1.132
	8	-0.000644	57.973	49.567	0.001621	0.081042	**0.001586**	0.001600	0.004304	320.0	299.0	0.999
	9	-0.000972	60.433	50.662	0.002793	0.139666	**0.001698**	0.001713	0.006331	342.6	299.0	0.975
	10	-0.001584	62.722	52.030	0.004704	0.235192	**0.001682**	0.001789	0.009679	357.8	299.0	0.857
PV20	3	-0.000140	51.259	44.637	0.000124	0.006183	**0.001467**	0.000825	0.000923	165.0	184.7	1.976
	4	-0.000198	51.144	45.017	0.000235	0.011768	**0.001437**	0.000952	0.001189	190.4	237.8	1.918
	5	-0.000257	51.173	45.558	0.000349	0.017440	**0.001196**	0.001032	0.001438	206.3	287.6	1.576
	6	-0.000330	52.496	44.747	0.000658	0.032900	**0.001230**	0.001213	0.001840	242.7	297.0	1.340
	7	-0.000408	54.216	44.799	0.001070	0.053502	**0.001324**	0.001389	0.002428	277.8	297.0	1.197
	8	-0.000585	57.259	47.451	0.001775	0.088748	**0.001513**	0.001629	0.003952	325.8	297.0	1.127
	9	-0.000991	59.685	49.076	0.002967	0.148361	**0.001482**	0.001715	0.005946	343.0	297.0	0.972
	10	-0.001907	61.286	50.486	0.005027	0.251325	**0.001226**	0.001687	0.009272	337.5	297.0	0.714
PV21	3	-0.000146	46.985	45.125	0.000033	0.001641	**0.001349**	0.000786	0.000827	157.3	165.5	2.075
	4	-0.000244	47.124	45.595	0.000070	0.003523	**0.001128**	0.000945	0.001066	188.9	213.2	1.727
	5	-0.000303	47.383	45.561	0.000115	0.005741	**0.001074**	0.001063	0.001234	212.7	246.9	1.643
	6	-0.000372	48.012	44.992	0.000235	0.011731	**0.001051**	0.001143	0.001376	228.6	275.3	1.618
	7	-0.000455	48.781	44.310	0.000429	0.021437	**0.000945**	0.001239	0.001579	247.7	302.0	1.380
	8	-0.000564	50.797	43.195	0.000974	0.048679	**0.000918**	0.001423	0.002111	284.6	302.0	0.924
	9	-0.000817	54.492	45.691	0.001749	0.087474	**0.000927**	0.001616	0.003520	323.1	302.0	0.787
	10	-0.001463	57.569	47.687	0.003233	0.161673	**0.000779**	0.001715	0.005850	343.0	302.0	0.570
PV22	3	-0.000148	47.297	44.598	0.000051	0.002525	**0.001266**	0.000755	0.000780	151.0	156.0	2.100
	4	-0.000238	46.452	44.988	0.000058	0.002924	**0.001162**	0.000911	0.000969	182.3	193.8	1.923
	5	-0.000331	46.540	44.965	0.000099	0.004959	**0.001047**	0.001069	0.001165	213.8	233.0	1.732
	6	-0.000400	46.518	44.976	0.000121	0.006044	**0.001058**	0.001211	0.001329	242.1	265.7	1.751
	7	-0.000456	46.618	44.878	0.000159	0.007956	**0.001051**	0.001315	0.001458	263.0	291.7	1.738
	8	-0.000519	46.636	44.871	0.000184	0.009220	**0.000998**	0.001409	0.001576	281.8	315.1	1.650
	9	-0.000601	46.771	44.690	0.000244	0.012210	**0.000995**	0.001493	0.001690	298.6	338.1	1.648
	10	-0.000663	46.705	44.742	0.000252	0.012608	**0.000938**	0.001564	0.001775	312.9	355.0	1.552
	11	-0.000733	46.820	44.574	0.000312	0.015597	**0.000908**	0.001609	0.001848	321.8	369.7	1.505
	12	-0.000813	47.159	44.145	0.000455	0.022734	**0.000819**	0.001648	0.001949	329.6	389.9	1.360
	13	-0.001068	47.854	42.917	0.000909	0.045430	**0.000408**	0.001603	0.002100	320.6	420.0	0.683
PV23	5	-0.000288	44.546	44.141	0.000008	0.000417	**0.001137**	0.000654	0.000609	130.7	121.7	2.032
	6	-0.000356	45.000	45.000	0.000000	0.000000	**0.001302**	0.000751	0.000751	150.2	150.2	2.323
	7	-0.000480	45.132	44.937	0.000009	0.000447	**0.001262**	0.000845	0.000849	169.1	169.7	2.251
	8	-0.000549	45.576	44.674	0.000054	0.002686	**0.001204**	0.000919	0.000939	183.8	187.9	2.149
	9	-0.000660	45.656	44.585	0.000077	0.003842	**0.001199**	0.000971	0.001001	194.2	200.2	2.140
	10	-0.000763	45.727	44.493	0.000105	0.005243	**0.001147**	0.001033	0.001074	206.5	214.9	2.047
	11	-0.000876	45.550	44.582	0.000093	0.004673	**0.001138**	0.001090	0.001126	218.0	225.3	2.031
	12	-0.000999	45.770	44.373	0.000152	0.007620	**0.001143**	0.001136	0.001195	227.2	239.0	2.041
	13	-0.001121	45.636	44.445	0.000146	0.007299	**0.001082**	0.001193	0.001250	238.7	250.1	1.932
	14	-0.001275	45.787	44.261	0.000210	0.010496	**0.001088**	0.001239	0.001319	247.8	263.8	1.942
	15	-0.001484	45.866	44.116	0.000278	0.013905	**0.001085**	0.001297	0.001402	259.4	280.3	1.937

Panel I.D.	LS	ε_{c2}	θ_e (deg)	θ_α (deg)	γ_s	Δ^*_s	$\Delta\varepsilon_{1cr}$	ε_{sccx}	ε_{sccy}	f_{sccx} (MPa)	f_{sccy} (MPa)	f_{c1}^* (MPa)
	16	-0.001714	45.779	44.131	0.000294	0.014719	0.001038	0.001341	0.001448	268.2	289.7	1.852
	17	-0.002034	45.924	43.861	0.000426	0.021294	0.000999	0.001380	0.001532	276.1	306.3	1.784
	18	-0.002664	45.795	43.807	0.000517	0.025865	0.000928	0.001424	0.001593	284.9	318.6	1.657
PV24	4	-0.000465	46.790	44.593	0.000053	0.002638	0.000740	0.000246	0.000279	49.3	55.8	1.322
	5	-0.000598	46.723	44.516	0.000076	0.003784	0.000807	0.000275	0.000320	55.0	64.1	1.441
	6	-0.000712	46.174	44.611	0.000068	0.003398	0.000839	0.000306	0.000346	61.2	69.2	1.497
PV25	4	-0.000468	45.893	44.751	0.000033	0.001672	0.001069	0.000484	0.000501	96.8	100.2	1.908
	5	-0.000749	46.023	44.571	0.000081	0.004053	0.001108	0.000589	0.000630	117.9	125.9	1.979
	6	-0.000985	46.001	44.469	0.000119	0.005964	0.001072	0.000642	0.000700	128.4	140.0	1.912
	7	-0.001347	46.170	44.210	0.000214	0.010687	0.001059	0.000683	0.000782	136.6	156.3	1.891
	8	-0.001721	45.790	44.329	0.000205	0.010250	0.000845	0.000682	0.000774	136.5	154.7	1.508
	9	-0.002046	45.714	44.316	0.000229	0.011443	0.000867	0.000698	0.000794	139.6	158.8	1.547
	10	-0.002637	45.446	44.517	0.000179	0.008943	0.000859	0.000743	0.000814	148.6	162.9	1.535
PV27	3	-0.000173	48.188	43.932	0.000076	0.003802	0.001310	0.000757	0.000766	151.5	153.1	2.341
	4	-0.000284	46.649	44.067	0.000100	0.004992	0.001351	0.000958	0.000978	191.5	195.5	2.414
	5	-0.000420	46.218	44.048	0.000138	0.006891	0.001305	0.001144	0.001178	228.8	235.5	2.330
	6	-0.000606	45.743	44.294	0.000131	0.006561	0.001296	0.001345	0.001380	269.0	276.0	2.313
	7	-0.000722	45.735	44.237	0.000163	0.008149	0.001259	0.001471	0.001517	294.1	303.4	2.248
	8	-0.000874	45.572	44.351	0.000157	0.007839	0.001251	0.001600	0.001644	320.0	328.9	2.233
	9	-0.001121	45.142	44.815	0.000052	0.002616	0.001150	0.001731	0.001747	346.2	349.3	2.051
PV28	3	-0.000143	44.549	45.254	-0.000016	-0.000789	0.001123	0.000756	0.000756	151.1	151.1	2.006
	4	-0.000246	45.234	44.771	0.000025	0.001251	0.001019	0.001012	0.001017	202.4	203.3	1.819
	5	-0.000336	45.166	44.808	0.000026	0.001310	0.000991	0.001215	0.001220	243.0	244.0	1.768
	6	-0.000441	44.891	45.139	-0.000023	-0.001151	0.000979	0.001399	0.001394	279.8	278.8	1.745
	7	-0.000514	45.172	44.771	0.000044	0.002180	0.000971	0.001518	0.001529	303.6	305.9	1.730
	8	-0.000578	45.234	44.670	0.000069	0.003473	0.000951	0.001637	0.001655	327.4	331.0	1.695
	9	-0.000700	45.045	44.934	0.000015	0.000756	0.000930	0.001768	0.001772	353.6	354.4	1.658
	10	-0.000851	45.026	44.959	0.000010	0.000524	0.000001	0.001459	0.001462	291.7	292.5	0.000
	11	-0.000962	44.976	45.040	-0.000011	-0.000545	0.000002	0.001563	0.001559	312.6	311.9	0.000
	12	-0.001084	44.956	45.077	-0.000022	-0.001119	0.000001	0.001657	0.001650	331.5	329.9	0.000
	13	-0.001230	44.970	45.056	-0.000017	-0.000867	0.000002	0.001725	0.001719	345.0	343.9	0.000
PV29	3	-0.000225	45.727	48.002	-0.000097	-0.004847	0.001406	0.000985	0.001162	196.9	232.3	1.765
	4	-0.000342	48.409	47.516	0.000066	0.003302	0.001201	0.001120	0.001477	224.0	295.5	1.520
	5	-0.000532	51.946	45.115	0.000868	0.043384	0.000954	0.001287	0.002173	257.4	324.0	0.842
	6	-0.000643	53.280	45.809	0.001145	0.057269	0.000979	0.001345	0.002638	268.9	324.0	0.822
	7	-0.000762	53.908	45.629	0.001371	0.068554	0.000992	0.001344	0.002838	268.9	324.0	0.845
	8	-0.000904	53.954	45.713	0.001497	0.074830	0.000973	0.001346	0.002992	269.1	324.0	0.823
	9	-0.001104	54.079	45.526	0.001726	0.086316	0.000989	0.001342	0.003189	268.4	324.0	0.848
	10	-0.001271	54.385	45.379	0.001998	0.099894	0.000996	0.001336	0.003428	267.3	324.0	0.864
PB4	5	0.000043	50.666	42.019	0.000138	0.006879	0.001657	0.001295	0.001197	259.1	0.0	1.095
PB5	4	-0.000091	24.860	26.682	-0.000080	-0.004021	0.000631	0.000697	0.000164	139.3	0.0	0.873
	5	-0.000106	22.638	28.101	-0.000087	-0.004335	0.000711	0.000856	0.000277	171.2	0.0	0.933
	7	-0.000108	23.367	28.826	-0.000140	-0.007025	0.000659	0.000842	0.000260	168.4	0.0	0.842
	8	-0.000075	23.754	30.743	-0.000071	-0.003531	0.000762	0.001102	0.000361	220.4	0.0	0.902
	9	-0.000075	30.550	33.717	-0.000127	-0.006331	0.000778	0.001408	0.000548	281.5	0.0	0.808
	10	-0.000136	35.418	36.069	-0.000091	-0.004528	0.000845	0.001864	0.000904	372.8	0.0	0.782
	11	-0.000281	39.177	41.725	-0.000477	-0.023858	0.000000	0.002850	0.001811	415.0	0.0	0.000
PB6	7	0.000018	43.811	42.205	0.000016	0.000817	0.001535	0.001197	0.001019	239.4	0.0	1.003
	8	0.000136	66.550	45.871	0.001012	0.050578	0.001823	0.001325	0.002426	265.0	0.0	0.930
	9	0.000144	64.482	47.226	0.001159	0.057926	0.002003	0.001506	0.002949	301.1	0.0	0.924
	10	-0.000017	72.155	60.330	0.004834	0.241714	0.075000	0.019527	0.067558	425.0	0.0	0.518
PB7	3	0.000057	57.116	45.767	0.001081	0.054059	0.001449	0.001497	0.002557	299.4	0.0	0.745
	4	-0.000195	65.424	51.368	0.005798	0.289889	0.001827	0.001694	0.006809	338.8	0.0	0.602
	5	-0.000706	69.395	53.938	0.011925	0.596247	0.001920	0.001649	0.012007	329.8	0.0	0.500
PB8	3	-0.000001	28.010	36.306	-0.000698	-0.034886	0.001056	0.001383	0.000546	276.5	0.0	0.966
	4	0.000179	41.407	42.211	-0.000297	-0.014869	0.001309	0.001641	0.001337	328.2	0.0	0.855
	5	0.000331	67.029	53.150	0.005557	0.277843	0.001799	0.001990	0.006945	398.0	0.0	0.505

Panel I.D.	LS	ε_{c2}	θ_s (deg)	θ_σ (deg)	γ_s	Δ^*_s	$\Delta\varepsilon_{1cr}$	ε_{scrx}	ε_{scry}	f_{scrx} (MPa)	f_{scry} (MPa)	f_{c1}^* (MPa)
PB10	2	-0.000015	45.829	16.544	-0.000214	-0.010678	0.000681	0.000901	0.000057	180.2	0.0	1.249
	3	0.000003	15.676	24.365	-0.000662	-0.033120	0.000736	0.001266	0.000170	253.3	0.0	1.099
	4	0.000055	19.722	31.347	-0.001086	-0.054279	0.000834	0.001670	0.000406	334.0	0.0	0.962
	5	0.000606	52.545	38.057	0.000068	0.003406	0.000818	0.001875	0.002230	375.1	0.0	0.683
	6	0.000547	66.393	47.073	0.004617	0.230831	0.001152	0.002062	0.006440	412.4	0.0	0.538
	7	-0.000407	63.493	68.780	0.017182	0.859107	0.000000	0.002932	0.013324	433.0	0.0	0.000
PB11	4	-0.003157	63.071	43.930	0.008334	0.416714	0.002117	0.001057	0.009767	211.4	0.0	1.236
PB12	4	-0.000259	71.552	48.341	0.003768	0.188394	0.003410	0.001561	0.005444	312.3	0.0	1.444
PB14	3	-0.000034	52.475	17.318	-0.000042	-0.002106	0.000769	0.000713	0.000113	142.6	0.0	2.583
	4	0.000045	60.010	25.111	-0.000222	-0.011117	0.000887	0.001101	0.001286	220.1	0.0	2.413
	5	0.000175	70.338	32.718	0.001909	0.095457	0.000959	0.001302	0.004244	260.4	0.0	1.943
	6	0.000323	71.243	38.973	0.004709	0.235474	0.001182	0.001614	0.007131	322.8	0.0	1.746
	7	0.000283	72.667	53.140	0.015614	0.780709	0.002067	0.002116	0.016206	423.1	0.0	1.083
PB16	5	-0.000016	54.978	33.945	0.000094	0.004699	0.001009	0.000998	0.000744	199.7	0.0	1.934
	6	0.000017	65.726	45.748	0.002795	0.139744	0.001488	0.001405	0.004160	281.0	0.0	1.428
	7	0.000082	72.737	54.669	0.012947	0.647339	0.002046	0.001607	0.013357	321.5	0.0	0.926
	8	-0.000474	76.724	63.006	0.024663	1.233172	0.003492	0.001987	0.026421	397.5	0.0	0.600
	9	-0.000973	77.702	66.788	0.036697	1.834827	0.005008	0.002198	0.040938	439.6	0.0	0.489
PB17	5	0.000022	18.976	21.901	-0.000693	-0.034626	0.000614	0.001198	0.000182	239.7	0.0	1.840
	6	0.000104	25.793	28.906	-0.000906	-0.045308	0.000635	0.001407	0.000453	281.4	0.0	1.510
	7	0.000355	41.772	37.570	-0.000559	-0.027935	0.000778	0.001752	0.001390	350.4	0.0	1.242
	8	0.000510	54.143	43.808	0.000898	0.044922	0.001059	0.002159	0.003140	431.9	0.0	1.162
	9	0.000430	59.904	59.219	0.005736	0.286817	0.075000	0.021743	0.060822	502.0	0.0	0.433
	10	0.000263	68.824	67.807	0.020376	1.018796	0.000000	0.002960	0.018050	502.0	0.0	0.001
PB18	6	-0.000200	76.062	52.882	0.007428	0.371414	0.002074	0.000979	0.008273	195.9	0.0	1.207
	7	-0.000461	77.772	53.938	0.016512	0.825603	0.002271	0.001060	0.016897	212.0	0.0	1.197
	8	0.000475	79.060	56.188	0.020276	1.013782	0.002660	0.001251	0.021067	250.1	0.0	1.119
PB19	5	-0.000092	46.727	38.777	-0.000098	-0.004878	0.000991	0.000753	0.000518	150.7	0.0	1.607
	7	-0.000139	74.421	57.142	0.009277	0.463849	0.002099	0.001163	0.010027	232.6	0.0	0.798
	8	-0.000199	74.754	62.282	0.012777	0.638859	0.003159	0.001363	0.014199	272.7	0.0	0.649
PB20	6	0.000124	70.609	40.729	0.001895	0.094755	0.000912	0.000954	0.002990	190.7	0.0	1.321
	7	0.000131	74.808	43.626	0.004268	0.213411	0.001038	0.001024	0.005370	204.8	0.0	1.251
	8	0.000107	75.145	44.570	0.006023	0.301173	0.001178	0.001152	0.007210	230.3	0.0	1.332
	9	0.000059	75.344	50.289	0.010147	0.507332	0.001604	0.001379	0.011018	275.7	0.0	1.173
	10	-0.000121	76.033	63.334	0.023341	1.167069	0.004301	0.001997	0.025428	399.4	0.0	0.766
PB21	4	-0.000023	29.754	33.527	-0.000476	-0.023819	0.000692	0.000916	0.000312	183.2	0.0	1.467
	5	-0.000014	33.465	36.578	-0.000512	-0.025623	0.000787	0.001049	0.000486	209.8	0.0	1.438
	6	0.000291	66.252	39.560	0.001212	0.060606	0.000843	0.001152	0.002541	230.5	0.0	1.309
	7	0.000152	68.816	40.729	0.002967	0.148350	0.000986	0.001319	0.004644	263.9	0.0	1.429
	8	-0.000300	70.558	50.035	0.010658	0.532891	0.001515	0.001655	0.011391	331.0	0.0	1.132
	9	-0.001176	70.813	53.407	0.020425	1.021254	0.001795	0.001824	0.019563	364.8	0.0	0.996
PB22	4	0.000036	23.325	31.187	-0.000714	-0.035685	0.000514	0.001031	0.000246	206.2	0.0	1.209
	5	0.000487	62.404	35.555	0.000578	0.028920	0.000596	0.001285	0.002258	257.1	0.0	1.147
	6	0.000550	67.511	38.826	0.002092	0.104575	0.000729	0.001555	0.004130	310.9	0.0	1.180
	7	0.000439	67.938	49.344	0.006182	0.309104	0.001148	0.001946	0.007569	389.3	0.0	0.908
	8	0.000297	69.381	67.255	0.013492	0.674584	0.075000	0.013118	0.075863	433.0	0.0	0.170
PB28	3	-0.000038	32.371	63.802	-0.000023	-0.001138	0.000621	0.000137	0.000572	0.0	114.4	1.768
	4	-0.000009	45.391	59.201	-0.000110	-0.005523	0.000758	0.000349	0.000758	0.0	151.5	1.814
	5	-0.000009	40.946	42.257	-0.000049	-0.002454	0.001247	0.001452	0.001155	0.0	231.0	1.119
	6	-0.000028	27.029	35.366	-0.000992	-0.049618	0.001882	0.004090	0.001411	0.0	282.1	0.928
	7	-0.000068	22.088	32.625	-0.002516	-0.125807	0.002478	0.007669	0.001630	0.0	326.0	0.919
	8	-0.000353	18.625	33.719	-0.006473	-0.323649	0.002393	0.012831	0.001678	0.0	335.7	0.997
PB29	4	-0.000112	41.727	30.625	-0.000242	-0.012091	0.000777	0.000778	0.000336	155.6	0.0	1.724
	5	0.000008	65.723	49.697	0.002798	0.139924	0.001323	0.001195	0.003799	239.1	0.0	0.937
	6	-0.000028	67.264	52.406	0.004543	0.227164	0.001707	0.001419	0.005558	283.9	0.0	0.957
	7	-0.000130	69.046	54.239	0.007394	0.369680	0.002056	0.001607	0.008255	321.4	0.0	0.970
	8	-0.000210	70.194	55.685	0.009949	0.497454	0.002348	0.001746	0.010671	349.2	0.0	0.960

Panel I.D.	LS	ε_{c2}	θ_ε (deg)	θ_σ (deg)	γ_s	Δ^*_s	$\Delta\varepsilon_{1cr}$	ε_{scrx}	ε_{scry}	f_{scrx} (MPa)	f_{scry} (MPa)	f_{c1}^* (MPa)
	9	-0.000315	71.871	56.336	0.013991	0.699527	0.002485	0.001820	0.014384	363.9	0.0	0.949
PB30	4	0.000245	69.962	53.262	0.004636	0.231799	0.001451	0.001387	0.005673	277.4	0.0	0.751
	5	0.000240	72.417	53.199	0.007374	0.368720	0.001613	0.001522	0.008346	304.4	0.0	0.840
	6	0.000243	73.752	54.823	0.010101	0.505044	0.001862	0.001652	0.011018	330.4	0.0	0.830
	7	0.000246	74.026	55.318	0.011498	0.574891	0.002067	0.001772	0.012453	354.5	0.0	0.877
	8	0.000258	73.716	57.356	0.013235	0.661764	0.002673	0.002063	0.014443	412.6	0.0	0.916
	9	0.000132	73.350	60.902	0.017416	0.870821	0.003711	0.002375	0.018895	474.9	0.0	0.840
PB31	2	0.000057	56.128	12.939	0.000002	0.000086	0.000544	0.000683	0.000232	136.6	0.0	1.988
	3	0.000221	37.887	27.046	-0.000529	-0.026432	0.000518	0.001070	0.000542	213.9	0.0	1.318
	4	0.000281	41.316	38.929	-0.000461	-0.023048	0.000697	0.001459	0.001112	291.8	0.0	1.032
	5	0.000576	70.414	53.864	0.007485	0.374273	0.001438	0.001934	0.008607	386.8	0.0	0.704
	6	0.000583	70.775	55.790	0.009740	0.487022	0.001715	0.002170	0.010772	434.0	0.0	0.693
	7	0.000605	70.968	62.665	0.013661	0.683067	0.075000	0.017785	0.071924	496.0	0.0	0.434
PB32	2	-0.000042	45.534	21.415	-0.000113	-0.005663	0.000538	0.000561	0.000077	112.3	0.0	1.774
	3	-0.000017	29.973	28.274	-0.000294	-0.014707	0.000658	0.000783	0.000194	156.6	0.0	1.737
	4	0.000038	31.804	41.865	-0.000458	-0.022882	0.000933	0.001181	0.000692	236.1	0.0	1.261
	5	0.000289	70.460	51.797	0.005776	0.288801	0.001457	0.001555	0.006873	311.0	0.0	0.936
	6	0.000559	69.442	59.579	0.012426	0.621296	0.075000	0.020556	0.066597	415.0	0.0	0.842
PHS1	5	-0.000065	52.401	48.948	0.000057	0.002838	0.002020	0.000980	0.001378	196.1	275.6	2.403
PHS2	4	-0.000065	46.414	45.537	0.000005	0.000239	0.001378	0.000693	0.000727	138.7	145.4	2.433
	5	-0.000066	47.746	46.537	0.000011	0.000572	0.001669	0.000847	0.000962	169.3	192.4	2.780
	6	-0.000113	54.796	53.689	0.000061	0.003045	0.001476	0.000926	0.001894	185.3	378.8	1.593
	7	-0.000150	56.413	54.245	0.000168	0.008415	0.001462	0.001033	0.002363	206.7	472.6	1.506
	8	-0.000186	57.166	54.822	0.000226	0.011304	0.001425	0.001101	0.002721	220.2	521.0	1.336
	9	-0.000245	57.983	55.938	0.000270	0.013477	0.001655	0.001337	0.003610	267.5	521.0	0.953
	10	-0.000309	58.879	56.418	0.000386	0.019282	0.001983	0.001499	0.004362	299.7	521.0	1.060
	11	-0.000335	59.656	57.154	0.000444	0.022180	0.002201	0.001607	0.004998	321.5	521.0	1.085
	12	-0.000375	60.520	58.245	0.000471	0.023554	0.002643	0.001796	0.006039	359.2	521.0	1.159
	13	-0.000474	61.864	59.191	0.000696	0.034800	0.003139	0.002011	0.007653	402.3	521.0	1.236
	14	-0.000696	63.847	60.738	0.001165	0.058249	0.004122	0.002378	0.011106	475.6	521.0	1.349
PHS3	3	-0.000114	45.284	48.018	-0.000045	-0.002249	0.001404	0.000749	0.000902	149.8	180.4	2.486
	4	-0.000173	49.402	51.620	-0.000099	-0.004964	0.001207	0.000838	0.001313	167.7	262.6	1.815
	5	-0.000210	51.532	52.448	-0.000062	-0.003096	0.001009	0.000917	0.001616	183.3	323.2	1.418
	6	-0.000241	52.200	52.527	-0.000026	-0.001309	0.000995	0.001014	0.001861	202.9	372.2	1.367
	7	-0.000281	52.719	52.687	0.000003	0.000166	0.000947	0.001108	0.002115	221.6	423.1	1.256
	8	-0.000324	53.036	52.628	0.000046	0.002322	0.000949	0.001206	0.002360	241.3	472.0	1.237
	9	-0.000376	53.325	52.455	0.000112	0.005606	0.000949	0.001299	0.002604	259.7	520.8	1.220
	10	-0.000412	53.505	52.667	0.000123	0.006141	0.001186	0.001505	0.003044	301.1	521.0	1.086
	11	-0.000477	53.932	52.731	0.000200	0.009978	0.001471	0.001710	0.003562	342.1	521.0	1.057
	12	-0.000592	56.012	55.613	0.000092	0.004585	0.001671	0.001985	0.005044	397.0	521.0	0.860
	13	-0.000732	57.536	56.627	0.000258	0.012902	0.001997	0.002216	0.006452	443.3	521.0	0.932
PHS4	3	-0.000074	49.600	51.974	-0.000075	-0.003750	0.001364	0.000826	0.001301	165.1	260.1	2.056
	4	-0.000106	50.750	54.915	-0.000238	-0.011911	0.001193	0.000946	0.001678	189.2	335.5	1.596
	5	-0.000132	53.451	54.103	-0.000052	-0.002592	0.001034	0.001040	0.002033	207.9	406.6	1.356
	6	-0.000197	53.248	54.289	-0.000101	-0.005057	0.001119	0.001174	0.002314	234.8	462.9	1.447
	7	-0.000226	53.338	54.736	-0.000159	-0.007962	0.001111	0.001307	0.002614	261.5	521.0	1.376
	8	-0.000234	53.545	55.307	-0.000234	-0.011709	0.001517	0.001603	0.003256	320.5	521.0	1.187
	9	-0.000259	54.358	55.498	-0.000177	-0.008850	0.001986	0.001886	0.004023	377.3	521.0	1.115
	10	-0.000325	57.362	57.203	0.000034	0.001676	0.002618	0.002186	0.005775	437.2	521.0	1.242
	11	-0.000433	59.459	58.425	0.000277	0.013836	0.003050	0.002384	0.007470	476.8	521.0	1.263
PHS5	3	-0.000082	40.687	47.683	-0.000058	-0.002914	0.001473	0.000725	0.000827	145.0	165.3	2.302
	4	-0.000163	54.714	52.765	0.000094	0.004685	0.001636	0.000892	0.001786	178.4	357.1	1.888
	5	-0.000260	56.421	56.308	0.000010	0.000521	0.001529	0.001024	0.002646	204.9	521.0	1.397
	6	-0.000345	58.279	56.149	0.000283	0.014148	0.001971	0.001319	0.003770	263.9	521.0	1.182
	7	-0.000484	61.424	59.479	0.000424	0.021199	0.003108	0.001746	0.006639	349.3	521.0	1.210
	8	-0.000606	62.695	60.453	0.000609	0.030447	0.003711	0.001935	0.008352	387.1	521.0	1.289
	9	-0.000713	64.386	61.778	0.000907	0.045373	0.004581	0.002177	0.010962	435.5	521.0	1.348

Panel I.D.	LS	ε_{c2}	θ_s (deg)	θ_σ (deg)	γ_s	Δ^*_s	$\Delta\varepsilon_{1cr}$	ε_{scrx}	ε_{scry}	f_{scrx} (MPa)	f_{scry} (MPa)	f_{c1}^* (MPa)
PHS6	3	-0.000108	44.423	45.865	-0.000013	-0.000650	0.001132	0.000576	0.000605	115.2	121.1	1.959
	4	-0.000138	44.225	46.503	-0.000030	-0.001485	0.001338	0.000689	0.000749	137.8	149.8	2.228
	5	-0.000185	48.450	49.663	-0.000038	-0.001876	0.001460	0.000815	0.001157	163.0	231.5	2.011
	6	-0.000240	51.353	50.841	0.000026	0.001325	0.001445	0.000912	0.001530	182.5	306.0	1.835
	7	-0.000333	52.845	51.277	0.000114	0.005724	0.001440	0.000997	0.001878	199.5	375.7	1.761
	8	-0.000323	53.201	52.950	0.000023	0.001132	0.001378	0.001099	0.002203	219.8	440.5	1.499
	9	-0.000401	54.141	52.906	0.000138	0.006882	0.001334	0.001178	0.002542	235.6	508.3	1.428
	10	-0.000442	54.323	53.184	0.000142	0.007116	0.001489	0.001316	0.002884	263.2	521.0	1.422
	11	-0.000482	54.538	53.490	0.000148	0.007420	0.001671	0.001478	0.003294	295.5	521.0	1.365
	12	-0.000559	55.034	53.391	0.000266	0.013300	0.001846	0.001622	0.003748	324.5	521.0	1.333
	13	-0.000646	55.859	54.189	0.000319	0.015973	0.002109	0.001806	0.004502	361.2	521.0	1.408
	14	-0.000742	57.065	55.084	0.000458	0.022881	0.002367	0.001993	0.005519	398.7	521.0	1.438
	15	-0.000927	58.556	56.147	0.000712	0.035615	0.002636	0.002199	0.007064	439.8	521.0	1.420
	16	-0.001410	60.133	56.643	0.001426	0.071278	0.002915	0.002381	0.009447	476.3	521.0	1.490
PHS7	3	-0.000095	43.306	45.634	-0.000018	-0.000888	0.001015	0.000515	0.000525	103.0	104.9	1.996
	4	-0.000130	44.956	47.193	-0.000037	-0.001828	0.001196	0.000655	0.000746	131.1	149.2	2.191
	5	-0.000193	50.806	49.304	0.000069	0.003433	0.000987	0.000744	0.001154	148.9	230.8	1.598
	6	-0.000267	51.440	50.036	0.000094	0.004681	0.000925	0.000858	0.001445	171.5	289.1	1.416
	7	-0.000331	51.971	50.362	0.000138	0.006903	0.000896	0.000967	0.001725	193.3	345.1	1.317
	8	-0.000402	52.011	50.741	0.000134	0.006688	0.000859	0.001081	0.001981	216.2	396.2	1.202
	9	-0.000467	52.217	50.719	0.000181	0.009064	0.000891	0.001197	0.002241	239.4	448.2	1.227
	10	-0.000530	52.406	50.946	0.000207	0.010345	0.000841	0.001307	0.002514	261.4	502.9	1.100
	11	-0.000605	52.547	51.072	0.000237	0.011854	0.000938	0.001467	0.002864	293.5	521.0	0.961
	12	-0.000689	53.129	51.073	0.000377	0.018826	0.001246	0.001697	0.003431	339.4	521.0	1.012
	13	-0.000773	54.389	51.767	0.000565	0.028225	0.001498	0.001896	0.004235	379.1	521.0	1.160
PHS8	3	-0.000109	44.319	45.922	-0.000015	-0.000757	0.001195	0.000614	0.000647	122.8	129.3	2.586
	4	-0.000172	49.146	47.481	0.000053	0.002650	0.001149	0.000740	0.000970	147.9	194.0	2.323
	5	-0.000224	50.117	49.119	0.000057	0.002851	0.000960	0.000861	0.001290	172.2	257.9	1.786
	6	-0.000273	50.846	49.424	0.000111	0.005538	0.000870	0.000986	0.001573	197.2	314.6	1.544
	7	-0.000362	51.374	48.946	0.000236	0.011775	0.000910	0.001111	0.001849	222.3	369.8	1.607
	8	-0.000435	51.354	49.080	0.000260	0.012982	0.000950	0.001249	0.002104	249.7	420.7	1.646
	9	-0.000490	51.488	49.209	0.000303	0.015133	0.000927	0.001382	0.002372	276.3	474.5	1.552
	10	-0.000540	51.786	49.240	0.000390	0.019475	0.000916	0.001530	0.002695	306.1	521.0	1.352
	11	-0.000567	51.699	49.702	0.000338	0.016916	0.001012	0.001718	0.003008	343.7	521.0	1.030
	12	-0.000600	52.461	50.288	0.000412	0.020576	0.001219	0.001911	0.003531	382.1	521.0	1.016
	13	-0.000672	53.369	51.334	0.000442	0.022111	0.001481	0.002120	0.004237	424.0	521.0	1.148
	14	-0.000801	54.684	51.982	0.000688	0.034377	0.001775	0.002313	0.005164	462.7	521.0	1.331
	15	-0.000867	55.621	52.752	0.000820	0.041012	0.001889	0.002437	0.005912	487.4	521.0	1.309
	16	-0.000937	56.571	53.481	0.000985	0.049271	0.001811	0.002484	0.006612	496.9	521.0	1.134
	17	-0.001156	58.274	53.758	0.001720	0.086006	0.001886	0.002533	0.007998	506.6	521.0	1.152
	18	-0.001253	58.953	54.564	0.001859	0.092953	0.001810	0.002596	0.008892	519.3	521.0	0.980
PHS9	3	-0.000088	45.534	44.740	0.000004	0.000224	0.001132	0.000563	0.000556	112.6	111.2	2.091
	4	-0.000102	50.164	46.857	0.000054	0.002681	0.001390	0.000736	0.000909	147.2	181.8	2.262
	5	-0.000222	54.081	51.352	0.000173	0.008646	0.001225	0.000879	0.001713	175.8	342.6	1.482
	6	-0.000300	54.939	53.467	0.000144	0.007213	0.001110	0.001019	0.002296	203.8	459.3	1.140
	7	-0.000362	55.237	53.594	0.000195	0.009746	0.001207	0.001172	0.002721	234.5	521.0	1.156
	8	-0.000453	55.707	53.882	0.000271	0.013573	0.001472	0.001410	0.003414	281.9	521.0	1.030
	9	-0.000598	56.499	55.079	0.000273	0.013646	0.001829	0.001681	0.004464	336.1	521.0	1.088
	10	-0.000706	57.134	55.679	0.000327	0.016341	0.002086	0.001853	0.005259	370.6	521.0	1.169
	11	-0.000816	58.336	56.264	0.000556	0.027824	0.002396	0.002045	0.006420	409.0	521.0	1.267
	12	-0.001027	59.722	56.604	0.001035	0.051736	0.002659	0.002200	0.007930	440.1	521.0	1.361
	13	-0.001194	60.629	57.277	0.001311	0.065543	0.002835	0.002336	0.009342	467.3	521.0	1.339
PHS10	3	-0.000111	48.526	46.485	0.000033	0.001652	0.001235	0.000679	0.000800	135.7	159.9	2.613
	4	-0.000160	51.397	48.091	0.000136	0.006798	0.001028	0.000757	0.001128	151.3	225.7	2.011
	5	-0.000202	50.808	49.697	0.000064	0.003180	0.000998	0.000872	0.001366	174.5	273.2	1.835
	6	-0.000244	51.127	50.162	0.000072	0.003591	0.000944	0.000980	0.001600	195.9	319.9	1.671
	7	-0.000284	51.162	50.566	0.000052	0.002620	0.000941	0.001096	0.001819	219.2	363.9	1.616

Panel I.D.	LS	ε_{c2}	θ_ε (deg)	θ_σ (deg)	γ_s	Δ^*_s	$\Delta\varepsilon_{1cr}$	ε_{scrx}	ε_{scry}	f_{scrx} (MPa)	f_{scry} (MPa)	f_{c1}^* (MPa)
	8	-0.000361	51.313	50.309	0.000104	0.005198	0.000988	0.001205	0.002037	241.0	407.4	1.690
	9	-0.000392	51.374	50.670	0.000084	0.004186	0.000564	0.001163	0.002026	232.5	405.1	1.562
	10	-0.000441	51.459	50.760	0.000095	0.004727	0.000940	0.001429	0.002478	285.8	495.6	1.510
	11	-0.000504	51.775	50.579	0.000183	0.009143	0.001022	0.001591	0.002818	318.2	521.0	1.320
	12	-0.000572	52.681	50.752	0.000349	0.017469	0.001229	0.001829	0.003450	365.8	521.0	0.998
	13	-0.000680	54.306	52.338	0.000438	0.021892	0.001621	0.002095	0.004541	419.0	521.0	1.174
	14	-0.000747	55.215	53.561	0.000418	0.020880	0.000421	0.001761	0.004414	352.1	521.0	1.187
	15	-0.000854	56.398	54.277	0.000617	0.030838	0.002104	0.002416	0.006316	483.3	521.0	1.283
	16	-0.001002	57.535	55.005	0.000855	0.042761	0.002399	0.002578	0.007504	515.6	521.0	1.374
	17	-0.001335	59.584	56.702	0.001304	0.065215	0.002755	0.002823	0.010247	564.7	521.0	1.308
PA1	4	-0.000126	46.261	47.035	-0.000023	-0.001164	0.001666	0.001061	0.001217	212.2	243.4	2.028
	5	-0.000199	48.608	47.477	0.000070	0.003500	0.001354	0.001196	0.001536	239.3	307.3	1.715
	6	-0.000275	48.571	47.947	0.000053	0.002648	0.001321	0.001377	0.001814	275.4	362.7	1.708
	7	-0.000297	48.928	48.034	0.000091	0.004537	0.001311	0.001550	0.002088	310.0	417.5	1.734
	8	-0.000329	49.547	48.051	0.000189	0.009453	0.001042	0.001658	0.002341	331.7	468.2	1.477
	9	-0.000363	49.558	48.144	0.000204	0.010200	0.001182	0.001911	0.002698	382.3	522.0	1.602
	10	-0.000434	49.802	47.980	0.000304	0.015189	0.001542	0.002242	0.003198	448.4	522.0	1.613
	11	-0.000471	50.196	47.767	0.000444	0.022204	0.001670	0.002433	0.003540	486.7	522.0	1.501
	12	-0.000299	50.526	48.084	0.000493	0.024661	0.001650	0.002580	0.003869	516.1	522.0	1.302
	13	-0.000497	51.325	49.490	0.000420	0.021005	0.075000	0.033712	0.046855	522.0	522.0	0.989
PA2	3	-0.000118	48.234	48.239	0.000000	-0.000016	0.000882	0.000943	0.001213	188.7	242.6	1.138
	4	-0.000171	49.193	47.931	0.000091	0.004552	0.000882	0.001110	0.001502	222.0	300.4	1.183
	5	-0.000243	49.571	47.929	0.000164	0.008205	0.000890	0.001361	0.001907	272.2	381.3	1.251
	6	-0.000298	49.967	47.836	0.000271	0.013566	0.000868	0.001604	0.002320	320.8	463.9	1.288
	7	-0.000357	50.243	47.643	0.000383	0.019139	0.000877	0.001765	0.002614	353.0	522.0	1.338
	8	-0.000412	50.633	47.396	0.000549	0.027468	0.001184	0.002091	0.003142	418.3	522.0	1.283
	9	-0.000476	52.524	47.949	0.000987	0.049348	0.001359	0.002430	0.004181	486.0	522.0	1.118
	10	-0.000510	53.973	49.810	0.001091	0.054557	0.001173	0.002586	0.005104	517.1	522.0	0.902
SE1	1	-0.000040	47.900	44.819	0.000011	0.000535	0.000760	0.000393	0.000398	78.5	79.5	1.495
	2	-0.000200	49.300	39.319	0.000497	0.024869	0.000478	0.000696	0.000822	139.2	164.4	1.153
	3	-0.000400	51.000	38.839	0.001290	0.064507	0.000320	0.001034	0.001616	206.8	323.2	0.786
	4	-0.000410	51.300	38.879	0.001380	0.069004	0.000216	0.000991	0.001665	198.2	333.0	0.531
	5	-0.000700	54.600	42.459	0.002305	0.115242	0.000124	0.001267	0.003096	253.5	479.0	-0.360
	6	-0.001280	59.700	35.533	0.007502	0.375119	-0.000056	0.001243	0.006191	248.6	479.0	-2.665
SE5	1	-0.000220	45.400	44.658	0.000023	0.001156	0.000188	0.000415	0.000423	83.1	84.6	0.552
	2	-0.000550	45.300	44.444	0.000078	0.003898	0.000175	0.000759	0.000786	151.8	157.2	0.513
	3	-0.001080	45.300	44.459	0.000118	0.005915	0.000140	0.001041	0.001079	208.3	215.7	0.410
	4	-0.008070	44.900	44.586	0.000232	0.011613	0.000067	0.001404	0.001363	280.8	272.6	0.195
SE6	1	0.000050	46.700	39.884	0.000014	0.000711	0.000479	0.000372	0.000287	74.4	57.4	1.026
	2	0.000060	50.100	38.262	0.000123	0.006160	0.000645	0.000597	0.000497	119.5	99.4	1.497
	3	-0.000150	57.400	44.242	0.000297	0.014828	0.001278	0.000716	0.000962	143.2	192.4	2.170
	4	-0.000160	54.500	0.000	0.000210	0.010500	0.000090	0.000000	-0.000020	0.0	-4.0	0.527
	5	-0.000200	56.300	42.127	0.000543	0.027146	0.000964	0.000680	0.001024	136.1	204.8	1.837
	6	-0.000300	57.700	37.318	0.001732	0.086623	0.000487	0.000758	0.001769	151.5	353.8	1.183
	7	-0.000270	58.800	34.774	0.002536	0.126782	0.000255	0.000812	0.002303	162.3	460.6	0.697
	8	-0.000400	60.600	36.028	0.003431	0.171552	0.000212	0.000839	0.003123	167.8	479.0	0.385
	9	-0.000450	62.500	35.960	0.005068	0.253394	0.000037	0.000924	0.004553	184.9	479.0	-0.389
	10	-0.001090	66.300	40.682	0.008824	0.441197	0.000286	0.000905	0.008522	180.9	479.0	-1.109

Panel I.D.	LS	f_{c1}^{*}-f_{c1} (MPa)	v_{ci} (MPa)	w (mm)	f_{cc} (MPa)	Δ^{t}_{s}	v_{cimax}	v_{ci}/v_{cimax}	Δ^{o}_{s}/w	v_{ci}/f'_{c}	$v_{ci}/f'^{2/3}_{c}$	$\Delta^{o}_{s}/\Delta^{t}_{s}$	v_{ci}	Δ^{t}_{s}	$\Delta^{o}_{s}/\Delta^{t}_{s}$
						Walraven - Model A							Maekawa		
PV1	3	0.000	-0.004	0.064	41.4	0.000	15.912	0.000	-0.055	0.000	-0.001	71.249	0.088	0.001	-3.579
	4	0.000	0.020	0.114	41.4	0.000	14.160	0.001	0.040	0.001	0.003	10.825	-0.005	0.004	1.075
	5	0.000	0.019	0.162	41.4	0.001	12.777	0.001	0.041	0.001	0.003	12.070	-0.018	0.006	1.060
	6	0.000	0.017	0.217	41.4	0.001	11.509	0.001	0.072	0.000	0.003	24.344	-0.132	0.008	1.871
	7	0.000	0.000	0.284	41.4	0.000	10.273	0.000	0.076	0.000	0.000	—	-0.139	0.000	—
PV3	4	0.000	-0.021	0.099	31.9	0.000	12.851	-0.002	-0.057	-0.001	-0.004	11.736	0.015	0.004	-1.409
	5	0.000	0.011	0.199	31.9	0.000	10.448	0.001	0.030	0.000	0.002	13.196	-0.021	0.006	0.933
	6	0.000	0.024	0.257	31.9	0.001	9.431	0.003	0.074	0.001	0.005	14.864	-0.073	0.013	1.480
PV4	4	0.000	1.152	0.036	31.9	0.012	15.047	0.077	0.168	0.043	0.223	0.510	3.634	0.010	0.582
	5	0.000	0.731	0.089	31.9	0.015	13.150	0.056	0.111	0.027	0.142	0.638	7.551	0.022	0.456
	6	-0.108	0.024	0.279	31.9	0.001	9.086	0.003	0.059	0.001	0.005	11.895	11.500	0.014	1.162
	7	-0.055	0.024	0.485	31.9	0.003	6.804	0.003	0.061	0.001	0.005	11.615	11.500	0.029	1.035
	8	-0.076	0.024	0.693	31.9	0.004	5.429	0.004	0.049	0.001	0.005	8.080	11.500	0.046	0.732
PV5	3	0.000	-0.027	0.101	34.0	-0.001	13.185	-0.002	-0.085	-0.001	-0.005	14.146	0.046	0.005	-1.870
	4	0.000	-0.030	0.139	34.0	-0.001	12.126	-0.002	-0.083	-0.001	-0.006	13.280	0.065	0.007	-1.680
	5	0.000	-0.004	0.173	34.0	0.000	11.328	0.000	-0.014	0.000	-0.001	16.599	0.014	0.003	-0.740
	6	0.000	0.013	0.236	34.0	0.001	10.075	0.001	0.045	0.000	0.002	17.193	-0.064	0.008	1.255
	7	0.000	0.005	0.293	34.0	0.000	9.164	0.001	0.029	0.000	0.001	26.584	-0.053	0.007	1.199
PV6	3	0.000	0.065	0.057	35.8	0.001	15.049	0.004	0.210	0.002	0.012	13.635	-0.154	0.004	3.183
	4	0.000	0.042	0.080	35.8	0.001	14.232	0.003	0.167	0.001	0.008	17.839	-0.184	0.004	3.067
	5	0.000	0.037	0.094	35.8	0.001	13.773	0.003	0.187	0.001	0.007	23.464	-0.248	0.005	3.610
	6	0.000	0.035	0.138	35.8	0.001	12.481	0.003	0.211	0.001	0.006	29.167	-0.394	0.007	3.948
	7	0.000	-0.007	0.184	35.8	0.000	11.381	-0.001	0.064	0.000	-0.001	—	-0.020	0.005	2.574
	8	0.007	0.000	0.875	35.8	0.000	4.884	0.000	0.009	0.000	0.000	—	0.000	0.000	—
PV7	2	0.000	-0.014	0.021	37.2	0.000	16.908	-0.001	-0.042	0.000	-0.002	10.607	0.009	0.001	-1.469
	3	0.000	-0.012	0.061	37.2	0.000	15.200	-0.001	-0.072	0.000	-0.002	26.289	0.068	0.002	-2.559
	4	0.000	0.003	0.111	37.2	0.000	13.511	0.000	-0.112	0.000	0.001	—	0.200	0.002	-7.496
	5	0.000	-0.004	0.140	37.2	0.000	12.664	0.000	-0.033	0.000	-0.001	41.859	0.069	0.003	-1.861
	6	0.000	0.001	0.181	37.2	0.000	11.664	0.000	0.016	0.000	0.000	67.525	-0.043	0.002	1.542
	7	0.000	0.001	0.222	37.2	0.000	10.804	0.000	0.013	0.000	0.000	76.981	-0.043	0.002	1.445
PV8	3	0.000	-0.003	0.045	35.8	0.000	15.541	0.000	-0.010	0.000	-0.001	13.962	0.008	0.001	-0.718
	4	0.000	-0.003	0.077	35.8	0.000	14.342	0.000	-0.012	0.000	-0.001	19.062	0.018	0.001	-0.866
	5	0.000	-0.002	0.103	35.8	0.000	13.484	0.000	-0.007	0.000	0.000	20.400	0.014	0.001	-0.647
	6	0.000	0.005	0.133	35.8	0.000	12.617	0.000	0.031	0.000	0.001	32.744	-0.082	0.003	1.629
	7	0.000	0.000	0.171	35.8	0.000	11.677	0.000	0.057	0.000	0.000	—	-0.188	0.000	22.749
PV9	2	0.000	0.037	0.018	13.9	0.000	10.431	0.004	0.140	0.003	0.011	6.666	-0.017	0.001	2.353
	3	0.000	0.027	0.050	13.9	0.001	9.556	0.003	0.087	0.002	0.008	7.251	-0.047	0.003	1.654
	4	0.000	0.008	0.084	13.9	0.000	8.793	0.001	0.024	0.001	0.002	7.668	-0.021	0.002	0.810
	5	0.000	0.008	0.130	13.9	0.000	7.921	0.001	0.028	0.001	0.002	9.060	-0.036	0.004	0.867
	6	0.000	-0.009	0.180	13.9	-0.001	7.156	-0.001	-0.098	-0.001	-0.003	29.639	0.163	0.006	-2.745
	7	0.000	0.000	0.256	13.9	0.000	6.234	0.000	-0.259	0.000	0.000	—	0.490	0.002	—
PV10	3	0.000	0.349	0.043	17.4	0.006	10.881	0.032	0.140	0.024	0.092	0.978	0.381	0.008	0.771
	4	0.000	0.317	0.084	17.4	0.010	9.838	0.032	0.145	0.022	0.083	1.269	0.381	0.015	0.795
	5	0.000	0.770	0.136	17.4	0.035	8.745	0.088	0.265	0.053	0.202	1.034	0.680	0.042	0.853
	6	0.000	0.907	0.191	17.4	0.055	7.831	0.116	0.259	0.063	0.238	0.894	1.041	0.069	0.715
	7	-0.125	0.703	0.319	17.4	0.069	6.303	0.112	0.330	0.048	0.185	1.521	1.080	0.113	0.933
	8	0.000	0.671	0.571	17.4	0.124	4.550	0.147	0.398	0.046	0.176	1.824	0.859	0.237	0.956
PV11	3	0.000	0.202	0.016	18.7	0.002	12.158	0.017	0.083	0.013	0.051	0.837	0.211	0.002	0.639
	4	0.000	0.172	0.048	18.7	0.003	11.156	0.015	0.091	0.011	0.043	1.373	0.191	0.006	0.726
	5	0.000	0.142	0.073	18.7	0.004	10.465	0.014	0.075	0.009	0.036	1.487	0.196	0.009	0.637
	6	0.000	0.139	0.093	18.7	0.004	9.978	0.014	0.089	0.009	0.035	1.889	0.183	0.011	0.747
	7	0.000	0.488	0.124	18.7	0.020	9.310	0.052	0.131	0.031	0.124	0.828	0.475	0.029	0.555
	8	0.006	0.001	0.219	18.7	0.000	7.706	0.000	0.035	0.000	0.000	—	0.556	0.002	3.167
	9	0.006	0.001	0.262	18.7	0.000	7.160	0.000	0.027	0.000	0.000	97.032	0.555	0.003	2.379
PV12	4	0.000	0.612	0.068	19.2	0.015	10.727	0.057	0.073	0.038	0.153	0.337	0.972	0.017	0.296
	5	0.000	1.005	0.105	19.2	0.034	9.831	0.102	0.143	0.063	0.251	0.437	1.428	0.035	0.425
	6	0.000	1.254	0.164	19.2	0.063	8.673	0.145	0.190	0.078	0.314	0.494	1.900	0.067	0.461

Panel I.D.	LS	$f_{ct}^{*}-f_{ct}$ (MPa)	v_{ci} (MPa)	w (mm)	f_{cc} (MPa)	Δ_s^t	v_{cimax}	v_{ci}/v_{cimax}	Δ_g^e/w	v_{ci}/f'_c	$v_{ci}/f'^{2/3}_c$	Δ_g^e/Δ_s^t	v_{ci}	Δ_s^t	Δ_g^e/Δ_s^t
						Walraven - Model A							Maekawa		
	7	0.000	1.441	0.392	19.2	0.166	5.953	0.242	0.291	0.090	0.360	0.687	2.445	0.222	0.515
	8	0.000	1.529	0.755	19.2	0.393	3.972	0.385	0.501	0.096	0.382	0.963	2.305	0.597	0.633
PV14	3	0.000	0.061	0.012	24.5	0.000	14.065	0.004	0.210	0.003	0.013	7.774	-0.009	0.001	3.182
	4	0.000	0.014	0.049	24.5	0.000	12.721	0.001	0.029	0.001	0.003	6.336	-0.015	0.002	0.870
	5	0.000	0.008	0.101	24.5	0.000	11.213	0.001	0.019	0.000	0.002	8.482	-0.025	0.003	0.713
	6	0.000	0.008	0.126	24.5	0.000	10.586	0.001	0.017	0.000	0.002	7.719	-0.029	0.004	0.618
	7	0.000	0.004	0.153	24.5	0.000	10.007	0.000	0.009	0.000	0.001	8.421	-0.018	0.003	0.445
PV16	2	-0.169	0.077	0.114	26.0	0.002	11.221	0.007	0.086	0.004	0.017	4.215	0.000	0.009	1.030
PV18	4	0.000	0.921	0.094	23.4	0.025	11.127	0.083	0.287	0.047	0.209	1.066	1.290	0.028	0.955
	5	0.000	1.142	0.193	23.4	0.059	9.038	0.126	0.353	0.059	0.259	1.167	1.701	0.074	0.929
	6	0.000	0.978	0.438	23.4	0.113	6.184	0.158	0.343	0.050	0.222	1.323	2.023	0.190	0.790
PV19	3	0.000	0.757	0.018	22.8	0.006	13.340	0.057	0.295	0.040	0.174	0.926	0.775	0.004	1.204
	4	0.000	0.655	0.045	22.8	0.010	12.414	0.053	0.206	0.034	0.150	0.916	0.766	0.011	0.875
	5	0.000	0.654	0.063	22.8	0.013	11.828	0.055	0.208	0.034	0.150	0.991	0.803	0.015	0.858
	6	0.000	0.886	0.100	22.8	0.026	10.847	0.082	0.260	0.047	0.203	0.997	1.032	0.030	0.873
	7	0.000	1.206	0.158	22.8	0.052	9.572	0.126	0.338	0.063	0.277	1.018	1.416	0.060	0.891
	8	0.000	1.177	0.248	22.8	0.077	8.087	0.145	0.327	0.062	0.270	1.049	1.768	0.102	0.792
	9	0.000	1.194	0.369	22.8	0.117	6.701	0.178	0.379	0.063	0.274	1.197	1.953	0.172	0.813
	10	0.000	1.103	0.566	22.8	0.176	5.238	0.211	0.416	0.058	0.253	1.335	2.063	0.292	0.805
PV20	3	0.000	0.685	0.020	23.5	0.006	13.480	0.051	0.310	0.035	0.155	1.120	0.655	0.005	1.339
	4	0.000	0.646	0.046	23.5	0.010	12.577	0.051	0.259	0.033	0.146	1.194	0.647	0.011	1.112
	5	0.000	0.508	0.077	23.5	0.012	11.622	0.044	0.227	0.026	0.115	1.479	0.569	0.016	1.061
	6	0.000	0.883	0.107	23.5	0.027	10.837	0.081	0.308	0.045	0.199	1.224	0.852	0.032	1.035
	7	0.000	1.192	0.145	23.5	0.047	9.968	0.120	0.368	0.061	0.269	1.133	1.165	0.054	0.999
	8	0.000	1.232	0.235	23.5	0.075	8.400	0.147	0.377	0.063	0.278	1.177	1.588	0.097	0.910
	9	0.000	1.125	0.360	23.5	0.105	6.889	0.163	0.412	0.057	0.254	1.410	1.729	0.159	0.932
	10	0.000	0.870	0.587	23.5	0.143	5.195	0.167	0.428	0.044	0.197	1.753	1.667	0.263	0.954
PV21	3	0.000	0.321	0.018	23.4	0.002	13.532	0.024	0.093	0.016	0.073	0.694	0.332	0.003	0.595
	4	0.000	0.240	0.054	23.4	0.004	12.265	0.020	0.065	0.012	0.054	0.833	0.304	0.008	0.460
	5	0.000	0.230	0.075	23.4	0.005	11.647	0.020	0.077	0.012	0.052	1.095	0.298	0.011	0.540
	6	0.000	0.257	0.093	23.4	0.007	11.161	0.023	0.126	0.013	0.058	1.677	0.256	0.014	0.823
	7	0.000	0.355	0.115	23.4	0.012	10.608	0.033	0.186	0.018	0.080	1.853	0.254	0.021	1.000
	8	0.000	0.870	0.158	23.4	0.037	9.697	0.090	0.309	0.045	0.197	1.312	0.582	0.049	0.985
	9	0.000	0.809	0.249	23.4	0.052	8.187	0.099	0.352	0.041	0.183	1.671	0.927	0.082	1.063
	10	0.000	0.629	0.405	23.4	0.067	6.458	0.097	0.399	0.032	0.142	2.417	1.100	0.133	1.215
PV22	3	0.000	0.195	0.019	23.5	0.002	13.499	0.014	0.130	0.010	0.044	1.642	0.159	0.002	1.073
	4	0.000	0.151	0.045	23.5	0.002	12.602	0.012	0.065	0.008	0.034	1.287	0.150	0.005	0.594
	5	0.000	0.138	0.073	23.5	0.003	11.728	0.012	0.068	0.007	0.031	1.614	0.133	0.008	0.622
	6	0.000	0.140	0.092	23.5	0.004	11.204	0.012	0.066	0.007	0.032	1.606	0.136	0.010	0.583
	7	0.000	0.144	0.108	23.5	0.004	10.806	0.013	0.074	0.007	0.032	1.802	0.124	0.013	0.635
	8	0.000	0.136	0.123	23.5	0.005	10.448	0.013	0.075	0.007	0.031	1.975	0.114	0.014	0.652
	9	0.000	0.146	0.138	23.5	0.006	10.131	0.014	0.089	0.007	0.033	2.214	0.089	0.017	0.734
	10	0.000	0.137	0.151	23.5	0.006	9.846	0.014	0.083	0.007	0.031	2.242	0.087	0.018	0.701
	11	0.000	0.139	0.162	23.5	0.006	9.634	0.014	0.096	0.007	0.031	2.573	0.055	0.020	0.795
	12	0.000	0.147	0.176	23.5	0.007	9.374	0.016	0.129	0.008	0.033	3.299	-0.029	0.022	1.024
	13	0.000	0.102	0.212	23.5	0.006	8.763	0.012	0.215	0.005	0.023	8.015	-0.338	0.023	1.977
PV23	5	0.000	0.063	0.018	24.6	0.000	13.868	0.005	0.023	0.003	0.014	0.928	0.080	0.001	0.347
	6	0.000	0.000	0.026	24.6	0.000	13.548	0.000	0.000	0.000	0.000	—	0.000	0.000	—
	7	0.000	0.005	0.043	24.6	0.000	12.953	0.000	0.010	0.000	0.001	6.391	-0.006	0.001	0.533
	8	0.000	0.025	0.059	24.6	0.000	12.417	0.002	0.045	0.001	0.006	5.809	-0.036	0.003	1.003
	9	0.000	0.032	0.070	24.6	0.001	12.085	0.003	0.055	0.002	0.007	5.768	-0.053	0.004	1.066
	10	0.000	0.035	0.083	24.6	0.001	11.711	0.003	0.063	0.002	0.008	6.189	-0.074	0.005	1.148
	11	0.000	0.030	0.095	24.6	0.001	11.388	0.003	0.049	0.001	0.007	5.892	-0.065	0.005	0.964
	12	0.000	0.045	0.106	24.6	0.001	11.090	0.004	0.072	0.002	0.010	5.793	-0.105	0.007	1.126
	13	0.000	0.037	0.120	24.6	0.001	10.772	0.003	0.061	0.002	0.008	6.006	-0.102	0.007	1.035
	14	0.000	0.052	0.134	24.6	0.002	10.441	0.005	0.078	0.003	0.011	5.649	-0.143	0.009	1.109
	15	0.000	0.059	0.153	24.6	0.002	10.033	0.006	0.091	0.003	0.013	5.878	-0.187	0.012	1.183

Panel I.D.	LS	$f_{ct}^{*}-f_{ct}$ (MPa)	v_{ci} (MPa)	w (mm)	f_{cc} (MPa)	Δ^{t}_{s}	v_{cimax}	v_{ci}/v_{cimax}	Δ^{e}_{s}/w	v_{ci}/f'_{c}	$v_{ci}/f'^{1/3}_{c}$	$\Delta^{e}_{s}/\Delta^{t}_{s}$	v_{ci}	Δ^{t}_{s}	$\Delta^{e}_{s}/\Delta^{t}_{s}$
						Walraven - Model A							Maekawa		
	16	0.000	0.057	0.171	24.6	0.003	9.684	0.006	0.086	0.003	0.013	5.824	-0.192	0.013	1.120
	17	0.000	0.071	0.194	24.6	0.004	9.255	0.008	0.110	0.003	0.016	6.045	-0.270	0.017	1.249
	18	0.000	0.070	0.240	24.6	0.004	8.520	0.008	0.108	0.003	0.015	6.120	-0.300	0.022	1.187
PV24	4	0.000	0.019	0.011	28.6	0.000	15.229	0.001	0.236	0.001	0.004	30.882	-0.058	0.000	6.705
	5	0.000	0.025	0.020	28.6	0.000	14.871	0.002	0.194	0.001	0.005	21.634	-0.081	0.001	4.697
	6	0.000	0.021	0.027	28.6	0.000	14.568	0.001	0.126	0.001	0.004	18.048	-0.071	0.001	3.301
PV25	4	0.000	0.018	0.019	23.1	0.000	13.382	0.001	0.086	0.001	0.004	11.428	-0.030	0.001	2.330
	5	0.000	0.031	0.043	23.1	0.000	12.548	0.002	0.094	0.002	0.007	9.002	-0.072	0.002	1.912
	6	0.000	0.035	0.062	23.1	0.001	11.940	0.003	0.096	0.002	0.008	8.490	-0.104	0.003	1.756
	7	0.000	0.050	0.088	23.1	0.001	11.205	0.004	0.121	0.003	0.011	8.068	-0.176	0.006	1.801
	8	0.000	0.034	0.115	23.1	0.001	10.549	0.003	0.089	0.002	0.008	9.093	-0.163	0.007	1.561
	9	0.000	0.037	0.132	23.1	0.001	10.157	0.004	0.087	0.002	0.008	8.386	-0.172	0.008	1.433
	10	0.000	0.027	0.144	23.1	0.001	9.913	0.003	0.062	0.001	0.006	8.424	-0.128	0.007	1.197
PV27	3	0.000	0.088	0.017	24.6	0.001	13.898	0.006	0.222	0.004	0.019	6.219	-0.015	0.001	2.785
	4	0.000	0.078	0.041	24.6	0.001	13.016	0.006	0.122	0.004	0.017	4.716	-0.036	0.003	1.572
	5	0.000	0.079	0.071	24.6	0.002	12.067	0.007	0.098	0.004	0.017	4.142	-0.060	0.006	1.201
	6	0.000	0.059	0.100	24.6	0.002	11.252	0.005	0.066	0.003	0.013	3.988	-0.063	0.007	0.905
	7	0.000	0.060	0.120	24.6	0.002	10.765	0.006	0.068	0.003	0.013	4.182	-0.083	0.009	0.910
	8	0.000	0.052	0.141	24.6	0.002	10.281	0.005	0.055	0.003	0.012	3.991	-0.080	0.010	0.776
	9	0.000	0.012	0.171	24.6	0.001	9.680	0.001	0.015	0.001	0.003	4.769	-0.028	0.006	0.428
PV28	3	0.000	-0.019	0.025	22.8	0.000	13.074	-0.001	-0.031	-0.001	-0.004	4.275	0.000	0.001	-0.823
	4	0.000	0.014	0.063	22.8	0.000	11.846	0.001	0.020	0.001	0.003	4.552	-0.009	0.002	0.586
	5	0.000	0.013	0.089	22.8	0.000	11.113	0.001	0.015	0.001	0.003	3.841	-0.010	0.003	0.434
	6	0.000	-0.009	0.112	22.8	0.000	10.541	-0.001	-0.010	0.000	-0.002	3.790	0.009	0.003	-0.344
	7	0.000	0.013	0.128	22.8	0.000	10.176	0.001	0.017	0.001	0.003	4.635	-0.020	0.005	0.476
	8	0.000	0.020	0.147	22.8	0.001	9.786	0.002	0.024	0.001	0.004	4.353	-0.032	0.007	0.529
	9	0.000	0.005	0.163	22.8	0.000	9.464	0.000	0.005	0.000	0.001	3.582	-0.007	0.004	0.208
	10	0.000	0.000	0.184	22.8	0.000	9.090	0.000	0.003	0.000	0.000	—	-0.007	0.000	5.379
	11	0.000	-0.001	0.199	22.8	0.000	8.832	0.000	-0.003	0.000	0.000	11.342	0.007	0.002	-0.272
	12	0.000	0.000	0.213	22.8	0.000	8.601	0.000	-0.005	0.000	0.000	—	0.014	0.000	-7.026
	13	0.000	-0.001	0.229	22.8	0.000	8.367	0.000	-0.004	0.000	0.000	15.827	0.011	0.002	-0.366
PV29	3	0.000	0.434	0.049	26.0	0.007	13.100	0.033	-0.098	0.020	0.093	-0.735	0.725	0.009	-0.530
	4	0.000	0.398	0.089	26.0	0.010	11.876	0.034	0.037	0.018	0.085	0.340	0.689	0.017	0.199
	5	0.000	0.848	0.157	26.0	0.034	10.240	0.083	0.276	0.039	0.182	1.293	0.863	0.047	0.920
	6	0.000	0.848	0.190	26.0	0.040	9.602	0.088	0.302	0.039	0.182	1.440	0.966	0.059	0.970
	7	0.000	0.866	0.203	26.0	0.043	9.374	0.092	0.339	0.040	0.186	1.590	0.966	0.065	1.061
	8	0.000	0.846	0.219	26.0	0.045	9.103	0.093	0.342	0.039	0.182	1.655	0.968	0.070	1.069
	9	0.000	0.866	0.238	26.0	0.050	8.791	0.099	0.362	0.040	0.186	1.720	0.962	0.079	1.096
	10	0.000	0.878	0.260	26.0	0.055	8.477	0.104	0.385	0.040	0.189	1.809	0.951	0.088	1.132
PB4	5	0.000	0.987	0.036	19.7	0.014	11.794	0.084	0.190	0.060	0.244	0.487	1.398	0.011	0.630
PB5	4	0.000	0.439	0.013	28.2	0.002	15.042	0.029	-0.302	0.019	0.091	-1.754	0.607	0.002	-1.744
	5	0.000	0.498	0.021	28.2	0.004	14.703	0.034	-0.203	0.021	0.103	-1.162	0.772	0.004	-1.084
	7	0.000	0.463	0.022	28.2	0.004	14.680	0.032	-0.321	0.020	0.096	-1.986	0.772	0.004	-1.777
	8	0.000	0.536	0.033	28.2	0.006	14.229	0.038	-0.106	0.023	0.111	-0.625	1.051	0.007	-0.537
	9	0.000	0.539	0.056	28.2	0.009	13.404	0.040	-0.113	0.023	0.111	-0.741	1.410	0.011	-0.553
	10	0.000	0.570	0.095	28.2	0.014	12.202	0.047	-0.048	0.024	0.117	-0.328	1.925	0.021	-0.216
	11	-0.263	0.000	0.236	28.2	0.000	9.192	0.000	-0.101	0.000	0.000	—	2.237	0.000	—
PB6	7	0.000	0.910	0.027	21.2	0.010	12.545	0.073	0.031	0.052	0.217	0.083	1.293	0.007	0.109
	8	0.000	0.959	0.084	21.2	0.026	10.823	0.089	0.599	0.054	0.228	1.962	1.437	0.026	1.921
	9	0.000	0.999	0.112	21.2	0.034	10.157	0.098	0.517	0.057	0.238	1.706	1.629	0.037	1.566
	10	-0.009	0.910	0.602	21.2	0.164	4.852	0.187	0.402	0.052	0.217	1.478	1.983	0.289	0.836
PB7	3	0.000	0.765	0.128	24.3	0.027	10.518	0.073	0.424	0.038	0.170	2.039	1.624	0.036	1.513
	4	0.000	0.753	0.351	24.3	0.067	7.100	0.106	0.827	0.037	0.167	4.321	1.793	0.121	2.400
	5	0.000	0.687	0.614	24.3	0.118	5.130	0.134	0.971	0.034	0.153	5.056	1.703	0.241	2.470
PB8	3	0.000	0.710	0.044	24.4	0.010	12.885	0.055	-0.801	0.035	0.157	-3.421	1.432	0.011	-3.318
	4	0.000	0.776	0.074	24.4	0.017	11.933	0.065	-0.201	0.038	0.172	-0.876	1.772	0.019	-0.764
	5	0.000	0.674	0.336	24.4	0.057	7.272	0.093	0.826	0.033	0.149	4.853	2.073	0.107	2.585

Panel I.D.	LS	f_{ct}^{*}-f_{ct} (MPa)	v_{ci} (MPa)	w (mm)	f_{cc} (MPa)	Δ^{t}_{s}	v_{cimax}	v_{ci}/v_{cimax}	Δ^{e}_{s}/w	v_{ci}/f'_{c}	$v_{ci}/f'^{1/2}_{c}$	$\Delta^{e}_{s}/\Delta^{t}_{s}$	v_{ci}	Δ^{t}_{s}	$\Delta^{e}_{s}/\Delta^{t}_{s}$
						Walraven - Model A							Maekawa		
PB10	2	0.000	0.371	0.015	28.8	0.002	15.138	0.025	-0.717	0.015	0.076	-5.132	0.534	0.002	-4.521
	3	0.000	0.498	0.035	28.8	0.005	14.327	0.035	-0.953	0.021	0.102	-6.203	1.033	0.007	-5.024
	4	0.000	0.586	0.059	28.8	0.009	13.464	0.044	-0.928	0.024	0.120	-5.730	1.610	0.012	-4.350
	5	0.000	0.535	0.134	28.8	0.017	11.296	0.047	0.025	0.022	0.109	0.198	1.975	0.030	0.114
	6	0.000	0.578	0.343	28.8	0.045	7.822	0.074	0.673	0.024	0.118	5.127	2.232	0.097	2.382
	7	-0.199	0.000	0.843	28.8	0.000	4.504	0.000	1.019	0.000	0.000	—	1.585	0.000	—
PB11	4	0.000	1.191	0.587	31.1	0.167	5.976	0.199	0.710	0.046	0.234	2.500	1.146	0.293	1.424
PB12	4	0.000	1.623	0.206	27.7	0.079	9.602	0.169	0.915	0.070	0.338	2.395	1.683	0.093	2.029
PB14	3	0.000	0.805	0.006	49.3	0.002	20.323	0.040	-0.357	0.020	0.126	-1.397	0.820	0.001	-1.758
	4	0.000	1.131	0.077	49.3	0.015	16.837	0.067	-0.145	0.028	0.176	-0.739	1.711	0.021	-0.541
	5	0.000	1.248	0.224	49.3	0.043	12.396	0.101	0.425	0.030	0.195	2.239	2.395	0.075	1.271
	6	0.000	1.413	0.381	49.3	0.084	9.694	0.146	0.619	0.034	0.220	2.814	3.193	0.157	1.498
	7	0.000	1.445	0.841	49.3	0.276	5.900	0.245	0.928	0.035	0.225	2.833	4.108	0.479	1.629
PB16	5	0.000	1.302	0.036	50.0	0.009	18.824	0.069	0.131	0.031	0.202	0.502	1.871	0.010	0.482
	6	0.000	1.466	0.207	50.0	0.046	12.886	0.114	0.675	0.035	0.227	3.050	2.841	0.074	1.884
	7	0.000	1.306	0.679	50.0	0.167	6.894	0.189	0.954	0.031	0.202	3.887	3.068	0.328	1.972
	8	0.000	1.178	1.229	50.0	0.719	4.471	0.263	1.003	0.028	0.182	1.716	3.252	0.735	1.678
	9	0.000	1.140	1.894	50.0	-0.774	3.137	0.363	0.969	0.027	0.177	-2.371	3.221	1.431	1.282
PB17	5	0.000	0.740	0.037	49.9	0.005	18.728	0.039	-0.930	0.018	0.115	-6.302	1.678	0.008	-4.584
	6	0.000	0.834	0.055	49.9	0.008	17.892	0.047	-0.828	0.020	0.129	-5.410	2.409	0.012	-3.746
	7	0.000	0.955	0.099	49.9	0.016	16.080	0.059	-0.283	0.023	0.148	-1.799	3.425	0.025	-1.126
	8	0.000	1.115	0.186	49.9	0.032	13.386	0.083	0.241	0.027	0.173	1.421	4.364	0.056	0.801
	9	-0.286	0.727	0.359	49.9	0.040	10.058	0.072	0.799	0.017	0.113	7.184	4.465	0.100	2.863
	10	-0.411	0.003	1.034	49.9	0.001	5.101	0.001	0.985	0.000	0.000	—	3.552	0.025	41.310
PB18	6	0.000	1.595	0.371	30.4	0.131	7.706	0.207	1.000	0.063	0.317	2.845	2.069	0.190	1.958
	7	0.000	1.644	0.809	30.4	0.381	4.760	0.345	1.021	0.065	0.327	2.167	2.214	0.587	1.405
	8	0.000	1.671	1.049	30.4	0.661	3.935	0.425	0.967	0.066	0.332	1.535	2.538	0.901	1.125
PB19	5	0.000	1.291	0.017	24.0	0.009	13.749	0.094	-0.295	0.065	0.289	-0.548	1.615	0.005	-0.916
	7	0.000	1.236	0.460	24.0	0.149	6.085	0.203	1.007	0.062	0.276	3.103	2.327	0.232	1.996
	8	0.000	1.235	0.631	24.0	0.221	5.013	0.246	1.013	0.062	0.276	2.887	2.464	0.361	1.771
PB20	6	0.000	1.137	0.145	26.0	0.042	10.501	0.108	0.655	0.052	0.244	2.261	2.070	0.050	1.878
	7	0.000	1.192	0.261	26.0	0.075	8.455	0.141	0.818	0.055	0.256	2.830	2.245	0.106	2.018
	8	0.000	1.312	0.355	26.0	0.113	7.306	0.180	0.848	0.060	0.282	2.660	2.528	0.166	1.813
	9	0.000	1.412	0.539	26.0	0.197	5.771	0.245	0.942	0.065	0.303	2.580	2.975	0.307	1.655
	10	0.000	1.525	1.175	26.0	0.842	3.340	0.457	0.993	0.070	0.327	1.386	3.516	1.077	1.084
PB21	4	0.000	0.972	0.028	26.2	0.009	13.897	0.070	-0.846	0.045	0.208	-2.511	1.852	0.008	-3.086
	5	0.000	1.067	0.039	26.2	0.013	13.511	0.079	-0.665	0.049	0.229	-1.928	2.203	0.011	-2.270
	6	0.000	1.081	0.128	26.2	0.036	10.896	0.099	0.472	0.050	0.232	1.692	2.484	0.043	1.422
	7	0.000	1.230	0.242	26.2	0.072	8.751	0.141	0.613	0.056	0.264	2.055	2.864	0.098	1.514
	8	0.000	1.351	0.593	26.2	0.212	5.445	0.248	0.898	0.062	0.289	2.508	3.577	0.341	1.564
	9	0.000	1.341	1.039	26.2	0.543	3.678	0.365	0.983	0.062	0.287	1.880	3.833	0.788	1.297
PB22	4	0.000	0.732	0.039	21.1	0.011	12.110	0.060	-0.905	0.042	0.174	-3.329	2.005	0.010	-3.567
	5	0.000	0.820	0.126	21.1	0.031	9.839	0.083	0.229	0.047	0.195	0.937	2.669	0.038	0.761
	6	0.000	0.950	0.220	21.1	0.059	8.171	0.116	0.474	0.054	0.226	1.785	3.333	0.080	1.308
	7	0.000	1.057	0.401	21.1	0.118	6.164	0.172	0.770	0.060	0.252	2.612	4.223	0.183	1.692
	8	-0.294	0.405	0.691	21.1	0.088	4.427	0.091	0.976	0.023	0.096	7.694	3.389	0.219	3.079
PB28	3	0.000	-0.870	0.006	27.2	-0.003	15.088	-0.058	-0.182	-0.038	-0.183	0.431	-0.995	0.002	-0.736
	4	0.000	-1.081	0.017	27.2	-0.007	14.647	-0.074	-0.334	-0.048	-0.227	0.808	-1.463	0.005	-1.182
	5	0.000	-1.232	0.068	27.2	-0.023	12.797	-0.096	-0.036	-0.054	-0.259	0.106	-2.523	0.022	-0.111
	6	0.000	-1.307	0.177	27.2	-0.056	10.067	-0.130	-0.280	-0.058	-0.274	0.890	-2.923	0.068	-0.726
	7	0.000	-1.436	0.345	27.2	-0.117	7.581	-0.189	-0.365	-0.063	-0.301	1.077	-3.250	0.167	-0.754
	8	0.000	-1.494	0.625	27.2	-0.247	5.372	-0.278	-0.518	-0.066	-0.314	1.313	-3.402	0.388	-0.834
PB29	4	0.000	1.021	0.016	49.9	0.004	19.862	0.051	-0.758	0.025	0.158	-3.047	1.380	0.004	-3.257
	5	0.000	1.105	0.182	49.9	0.031	13.487	0.082	0.768	0.027	0.171	4.555	2.386	0.054	2.570
	6	0.000	1.243	0.264	49.9	0.049	11.646	0.107	0.860	0.030	0.193	4.601	2.776	0.091	2.488
	7	0.000	1.347	0.398	49.9	0.083	9.526	0.141	0.930	0.032	0.209	4.447	3.083	0.161	2.291
	8	0.000	1.407	0.514	49.9	0.119	8.219	0.171	0.967	0.034	0.218	4.163	3.289	0.234	2.128

Panel I.D.	LS	$f_{c1}^{*}-f_{c1}$ (MPa)	v_{ci} (MPa)	w (mm)	f_{cc} (MPa)	Δ_s^t	v_{cimax}	v_{ci}/v_{cimax}	Δ_g^*/w	v_{ci}/f'_c	$v_{ci}/f'^{2/3}_c$	Δ_g^*/Δ_s^t	v_{ci}	Δ_s^t	Δ_g^*/Δ_s^t
						Walraven - Model A							Maekawa		
	9	0.000	1.425	0.705	49.9	0.194	6.715	0.212	0.993	0.034	0.221	3.612	3.397	0.366	1.912
PB30	4	0.000	1.006	0.265	48.5	0.041	11.460	0.088	0.875	0.025	0.158	5.649	2.690	0.082	2.820
	5	0.000	1.123	0.401	48.5	0.072	9.340	0.120	0.919	0.028	0.177	5.146	2.953	0.148	2.485
	6	0.000	1.178	0.530	48.5	0.106	7.951	0.148	0.953	0.029	0.185	4.744	3.147	0.221	2.285
	7	0.000	1.267	0.599	48.5	0.136	7.369	0.172	0.960	0.031	0.199	4.229	3.356	0.273	2.107
	8	0.000	1.430	0.681	48.5	0.187	6.771	0.211	0.972	0.035	0.225	3.533	3.791	0.352	1.878
	9	0.000	1.509	0.878	48.5	0.318	5.673	0.266	0.992	0.037	0.237	2.735	4.082	0.529	1.648
PB31	2	0.000	0.457	0.017	52.1	0.002	20.230	0.023	0.005	0.011	0.069	0.048	0.603	0.003	0.034
	3	0.000	0.673	0.045	52.1	0.006	18.760	0.036	-0.593	0.016	0.102	-4.757	1.753	0.009	-3.073
	4	0.000	0.834	0.079	52.1	0.011	17.192	0.048	-0.291	0.019	0.127	-2.112	2.885	0.018	-1.288
	5	0.000	0.964	0.431	52.1	0.063	9.305	0.104	0.868	0.022	0.146	5.902	3.727	0.147	2.553
	6	0.000	1.019	0.538	52.1	0.089	8.164	0.125	0.905	0.023	0.155	5.457	4.082	0.203	2.395
	7	-0.155	0.840	0.714	52.1	0.114	6.796	0.124	0.956	0.019	0.128	6.015	4.093	0.268	2.546
PB32	2	0.000	0.696	0.007	69.2	0.001	23.996	0.029	-0.798	0.012	0.092	-5.012	0.838	0.001	-4.615
	3	0.000	0.934	0.016	69.2	0.003	23.419	0.040	-0.946	0.016	0.123	-5.417	1.434	0.003	-4.640
	4	0.000	1.130	0.042	69.2	0.007	21.788	0.052	-0.547	0.020	0.149	-3.275	2.576	0.010	-2.338
	5	0.000	1.189	0.335	69.2	0.046	12.272	0.097	0.863	0.021	0.157	6.216	3.318	0.110	2.634
	6	-0.032	1.435	0.673	69.2	0.142	8.160	0.176	0.924	0.025	0.189	4.361	3.977	0.311	2.000
PHS1	5	0.000	2.759	0.020	86.6	0.008	25.858	0.107	0.141	0.038	0.325	0.354	3.136	0.007	0.408
PHS2	4	0.000	1.893	0.005	79.3	0.002	25.815	0.073	0.045	0.029	0.233	0.107	1.941	0.002	0.159
	5	0.000	2.175	0.010	79.3	0.004	25.446	0.085	0.055	0.033	0.267	0.138	2.337	0.003	0.182
	6	0.000	1.131	0.073	79.3	0.010	21.549	0.052	0.042	0.017	0.139	0.315	2.115	0.017	0.178
	7	0.000	1.044	0.104	79.3	0.012	20.016	0.052	0.081	0.016	0.128	0.701	2.246	0.024	0.344
	8	0.000	0.986	0.129	79.3	0.014	18.940	0.052	0.087	0.015	0.121	0.828	2.343	0.030	0.373
	9	0.000	1.342	0.177	79.3	0.025	17.180	0.078	0.076	0.020	0.165	0.547	3.017	0.051	0.262
	10	0.000	1.598	0.209	79.3	0.034	16.155	0.099	0.092	0.024	0.197	0.561	3.477	0.069	0.278
	11	0.000	1.682	0.237	79.3	0.041	15.377	0.109	0.094	0.025	0.207	0.543	3.758	0.083	0.267
	12	0.000	1.874	0.278	79.3	0.054	14.341	0.131	0.085	0.028	0.231	0.440	4.236	0.108	0.218
	13	0.000	2.074	0.350	79.3	0.076	12.843	0.162	0.099	0.031	0.255	0.458	4.776	0.154	0.227
	14	0.000	2.409	0.503	79.3	0.138	10.501	0.229	0.116	0.036	0.296	0.421	5.639	0.274	0.212
PHS3	3	0.000	1.356	0.018	70.1	0.004	23.394	0.058	-0.125	0.023	0.177	-0.515	1.671	0.004	-0.502
	4	0.000	0.791	0.056	70.1	0.006	21.137	0.037	-0.089	0.014	0.104	-0.817	1.588	0.011	-0.451
	5	0.000	0.556	0.087	70.1	0.006	19.591	0.028	-0.036	0.010	0.073	-0.507	1.581	0.015	-0.209
	6	0.000	0.522	0.106	70.1	0.007	18.735	0.028	-0.012	0.009	0.068	-0.193	1.690	0.018	-0.073
	7	0.000	0.459	0.128	70.1	0.007	17.853	0.026	0.001	0.008	0.060	0.024	1.779	0.021	0.008
	8	0.000	0.448	0.147	70.1	0.008	17.143	0.026	0.016	0.008	0.059	0.300	1.893	0.024	0.096
	9	0.000	0.444	0.166	70.1	0.009	16.484	0.027	0.034	0.008	0.058	0.654	1.990	0.028	0.202
	10	0.000	0.905	0.189	70.1	0.020	15.782	0.057	0.033	0.016	0.118	0.313	2.629	0.047	0.132
	11	0.000	1.392	0.214	70.1	0.034	15.060	0.092	0.047	0.024	0.182	0.294	3.266	0.068	0.146
	12	0.000	1.259	0.298	70.1	0.043	13.072	0.096	0.015	0.022	0.165	0.107	3.985	0.097	0.047
	13	0.000	1.418	0.370	70.1	0.061	11.727	0.121	0.035	0.024	0.186	0.210	4.615	0.137	0.094
PHS4	3	0.000	0.883	0.042	82.2	0.005	23.740	0.037	-0.090	0.013	0.107	-0.797	1.553	0.008	-0.456
	4	0.000	0.471	0.077	82.2	0.004	21.727	0.022	-0.155	0.007	0.057	-2.926	1.581	0.011	-1.042
	5	0.000	0.428	0.109	82.2	0.005	20.179	0.021	-0.024	0.006	0.052	-0.525	1.606	0.016	-0.162
	6	0.000	0.441	0.128	82.2	0.006	19.316	0.023	-0.039	0.006	0.053	-0.859	1.796	0.020	-0.258
	7	0.000	0.381	0.152	82.2	0.006	18.387	0.021	-0.052	0.006	0.046	-1.350	1.967	0.022	-0.361
	8	0.000	0.987	0.179	82.2	0.018	17.424	0.057	-0.066	0.014	0.119	-0.660	2.846	0.044	-0.267
	9	0.000	1.625	0.209	82.2	0.034	16.452	0.099	-0.042	0.024	0.196	-0.261	3.694	0.069	-0.128
	10	0.000	1.930	0.283	82.2	0.055	14.479	0.133	0.006	0.028	0.233	0.031	4.485	0.111	0.015
	11	0.000	2.058	0.362	82.2	0.076	12.850	0.160	0.038	0.030	0.249	0.182	4.965	0.158	0.088
PHS5	3	0.000	1.803	0.008	62.5	0.003	22.742	0.079	-0.364	0.035	0.250	-0.836	1.993	0.002	-1.241
	4	0.000	1.390	0.060	62.5	0.013	19.742	0.070	0.078	0.027	0.193	0.375	2.070	0.017	0.283
	5	0.000	0.905	0.120	62.5	0.014	17.149	0.053	0.004	0.017	0.125	0.036	2.069	0.028	0.018
	6	0.000	1.615	0.173	62.5	0.036	15.362	0.105	0.082	0.031	0.224	0.397	2.955	0.059	0.238
	7	0.000	2.054	0.288	62.5	0.074	12.533	0.164	0.074	0.039	0.285	0.285	4.001	0.128	0.166
	8	0.000	2.276	0.359	62.5	0.105	11.251	0.202	0.085	0.044	0.315	0.291	4.447	0.181	0.168
	9	0.000	2.514	0.464	62.5	0.157	9.782	0.257	0.098	0.048	0.348	0.289	4.971	0.273	0.166

Panel I.D.	LS	$f_{ct}^{*}-f_{ct}$ (MPa)	v_{ci} (MPa)	w (mm)	f_{cc} (MPa)	Δ^{t}_{s}	v_{cimax}	v_{ci}/v_{cimax}	Δ^{e}_{s}/w	v_{ci}/f'_{c}	$v_{ci}/f'^{1/3}_{c}$	$\Delta^{e}_{s}/\Delta^{t}_{s}$	v_{ci}	Δ^{t}_{s}	$\Delta^{e}_{s}/\Delta^{t}_{s}$
						Walraven - Model A							Maekawa		
PHS6	3	0.000	1.527	0.008	59.6	0.003	22.222	0.069	-0.083	0.031	0.217	-0.215	1.612	0.002	-0.305
	4	0.000	1.741	0.012	59.6	0.005	21.963	0.079	-0.125	0.035	0.247	-0.316	1.915	0.003	-0.425
	5	0.000	1.559	0.035	59.6	0.010	20.601	0.076	-0.054	0.031	0.221	-0.197	2.129	0.010	-0.188
	6	0.000	1.398	0.062	59.6	0.013	19.204	0.073	0.021	0.028	0.198	0.099	2.272	0.017	0.076
	7	0.000	1.331	0.088	59.6	0.017	18.000	0.074	0.065	0.027	0.189	0.336	2.393	0.025	0.229
	8	0.000	1.076	0.112	59.6	0.017	17.041	0.063	0.010	0.022	0.153	0.067	2.546	0.029	0.039
	9	0.000	1.024	0.139	59.6	0.019	16.074	0.064	0.049	0.021	0.145	0.356	2.659	0.036	0.189
	10	0.000	1.225	0.158	59.6	0.026	15.476	0.079	0.045	0.025	0.174	0.276	3.053	0.046	0.154
	11	0.000	1.486	0.179	59.6	0.035	14.832	0.100	0.041	0.030	0.211	0.211	3.543	0.060	0.124
	12	0.000	1.796	0.204	59.6	0.048	14.142	0.127	0.065	0.036	0.255	0.277	3.995	0.078	0.171
	13	0.000	1.953	0.242	59.6	0.062	13.213	0.148	0.066	0.039	0.277	0.259	4.522	0.101	0.158
	14	0.000	2.062	0.294	59.6	0.079	12.118	0.170	0.078	0.041	0.292	0.288	5.041	0.133	0.172
	15	0.000	2.118	0.378	59.6	0.107	10.704	0.198	0.094	0.043	0.300	0.332	5.584	0.188	0.190
	16	0.000	2.265	0.516	59.6	0.169	8.965	0.253	0.138	0.046	0.321	0.422	6.084	0.300	0.238
PHS7	3	0.000	1.172	0.006	64.3	0.002	23.202	0.051	-0.148	0.022	0.160	-0.496	1.233	0.001	-0.641
	4	0.000	1.230	0.017	64.3	0.004	22.495	0.055	-0.109	0.023	0.168	-0.454	1.501	0.004	-0.454
	5	0.000	0.811	0.055	64.3	0.007	20.278	0.040	0.062	0.015	0.111	0.516	1.442	0.011	0.304
	6	0.000	0.679	0.082	64.3	0.008	18.973	0.036	0.057	0.013	0.093	0.610	1.561	0.016	0.296
	7	0.000	0.609	0.106	64.3	0.009	17.939	0.034	0.065	0.011	0.083	0.809	1.678	0.020	0.346
	8	0.000	0.526	0.130	64.3	0.009	17.017	0.031	0.051	0.010	0.072	0.762	1.830	0.023	0.287
	9	0.000	0.535	0.151	64.3	0.010	16.302	0.033	0.060	0.010	0.073	0.892	1.989	0.028	0.326
	10	0.000	0.453	0.176	64.3	0.010	15.511	0.029	0.059	0.008	0.062	1.048	2.113	0.030	0.340
	11	0.000	0.704	0.200	64.3	0.017	14.805	0.048	0.059	0.013	0.096	0.684	2.545	0.045	0.265
	12	0.000	1.255	0.229	64.3	0.035	14.053	0.089	0.082	0.023	0.171	0.536	3.270	0.072	0.263
	13	0.000	1.475	0.270	64.3	0.049	13.084	0.113	0.104	0.028	0.201	0.578	3.876	0.096	0.293
PHS8	3	0.000	1.093	0.009	67.1	0.002	23.506	0.046	-0.086	0.020	0.146	-0.356	1.181	0.002	-0.392
	4	0.000	0.874	0.037	67.1	0.005	21.742	0.040	0.072	0.016	0.117	0.528	1.182	0.008	0.353
	5	0.000	0.556	0.071	67.1	0.005	19.924	0.028	0.040	0.010	0.074	0.532	1.170	0.012	0.238
	6	0.000	0.444	0.098	67.1	0.006	18.664	0.024	0.056	0.008	0.059	0.986	1.220	0.015	0.361
	7	0.000	0.487	0.121	67.1	0.007	17.744	0.027	0.098	0.009	0.065	1.604	1.284	0.020	0.581
	8	0.000	0.483	0.142	67.1	0.008	16.956	0.028	0.092	0.009	0.065	1.549	1.411	0.024	0.535
	9	0.000	0.433	0.166	67.1	0.009	16.145	0.027	0.091	0.008	0.058	1.750	1.505	0.028	0.550
	10	0.000	0.507	0.193	67.1	0.012	15.331	0.033	0.101	0.009	0.068	1.674	1.694	0.036	0.547
	11	0.000	0.885	0.214	67.1	0.022	14.730	0.060	0.079	0.016	0.118	0.754	2.289	0.054	0.312
	12	0.000	1.227	0.241	67.1	0.035	14.038	0.087	0.085	0.022	0.164	0.589	2.891	0.075	0.276
	13	0.000	1.438	0.277	67.1	0.047	13.208	0.109	0.080	0.026	0.192	0.468	3.529	0.097	0.228
	14	0.000	1.706	0.325	67.1	0.066	12.254	0.139	0.106	0.031	0.228	0.519	4.117	0.131	0.263
	15	0.000	1.725	0.366	67.1	0.077	11.535	0.150	0.112	0.031	0.231	0.535	4.472	0.154	0.267
	16	0.000	1.535	0.411	67.1	0.078	10.844	0.142	0.120	0.027	0.205	0.631	4.586	0.167	0.295
	17	0.000	1.576	0.490	67.1	0.100	9.807	0.161	0.176	0.028	0.211	0.860	4.722	0.214	0.401
	18	0.000	1.381	0.547	67.1	0.102	9.179	0.150	0.170	0.025	0.185	0.913	4.872	0.230	0.404
PHS9	3	0.000	1.616	0.004	67.2	0.002	23.873	0.068	0.060	0.029	0.216	0.133	1.591	0.001	0.222
	4	0.000	1.770	0.018	67.2	0.006	22.921	0.077	0.150	0.032	0.237	0.458	2.000	0.005	0.519
	5	0.000	1.117	0.079	67.2	0.012	19.521	0.057	0.109	0.020	0.149	0.731	2.084	0.020	0.442
	6	0.000	0.800	0.125	67.2	0.012	17.580	0.045	0.058	0.014	0.107	0.580	2.249	0.027	0.264
	7	0.000	0.893	0.152	67.2	0.017	16.605	0.054	0.064	0.016	0.119	0.590	2.597	0.036	0.268
	8	0.000	1.325	0.190	67.2	0.030	15.410	0.086	0.071	0.024	0.177	0.453	3.319	0.058	0.233
	9	0.000	1.560	0.246	67.2	0.045	13.942	0.112	0.056	0.028	0.208	0.302	4.093	0.087	0.157
	10	0.000	1.714	0.287	67.2	0.058	13.025	0.132	0.057	0.031	0.229	0.281	4.580	0.112	0.146
	11	0.000	1.899	0.344	67.2	0.078	11.920	0.159	0.081	0.034	0.254	0.355	5.115	0.150	0.186
	12	0.000	2.066	0.425	67.2	0.109	10.657	0.194	0.122	0.037	0.276	0.474	5.551	0.208	0.248
	13	0.000	2.085	0.502	67.2	0.136	9.677	0.215	0.131	0.037	0.279	0.480	5.893	0.263	0.249
PHS10	3	0.000	1.067	0.018	61.7	0.004	21.969	0.049	0.093	0.021	0.149	0.438	1.199	0.004	0.413
	4	0.000	0.715	0.051	61.7	0.006	20.086	0.036	0.134	0.014	0.100	1.196	1.039	0.010	0.696
	5	0.000	0.536	0.072	61.7	0.006	19.037	0.028	0.044	0.010	0.075	0.563	1.109	0.012	0.259
	6	0.000	0.442	0.094	61.7	0.006	18.071	0.024	0.038	0.009	0.062	0.621	1.161	0.015	0.241
	7	0.000	0.389	0.113	61.7	0.006	17.308	0.022	0.023	0.008	0.054	0.441	1.259	0.017	0.153

Panel I.D.	LS	$f_{c1}^{*}-f_{c1}$ (MPa)	v_{ci} (MPa)	w (mm)	f_{cc} (MPa)	Δ_s^t	$v_{ci/max}$	$v_{ci}/v_{ci/max}$	Δ_s^e/w	v_{ci}/f'_c	$v_{ci}/f'^{2/3}_c$	Δ_s^e/Δ_s^t	v_{ci}	Δ_s^t	Δ_s^e/Δ_s^t
						Walraven - Model A							Maekawa		
	8	0.000	0.421	0.131	61.7	0.007	16.646	0.025	0.040	0.008	0.059	0.712	1.343	0.021	0.247
	9	0.000	-0.472	0.151	61.7	-0.009	15.959	-0.030	0.028	-0.009	-0.066	-0.451	1.219	0.026	0.159
	10	0.000	0.312	0.170	61.7	0.007	15.342	0.020	0.028	0.006	0.044	0.689	1.513	0.025	0.192
	11	0.000	0.611	0.195	61.7	0.015	14.645	0.042	0.047	0.012	0.085	0.602	1.872	0.041	0.225
	12	0.000	1.225	0.231	61.7	0.036	13.700	0.089	0.076	0.024	0.171	0.487	2.623	0.072	0.241
	13	0.000	1.525	0.285	61.7	0.055	12.515	0.122	0.077	0.030	0.213	0.397	3.421	0.106	0.206
	14	0.000	1.612	0.325	61.7	0.067	11.753	0.137	0.064	0.031	0.225	0.311	2.348	0.130	0.161
	15	0.000	1.788	0.374	61.7	0.087	10.940	0.163	0.082	0.035	0.249	0.354	4.337	0.165	0.186
	16	0.000	1.967	0.434	61.7	0.114	10.086	0.195	0.098	0.038	0.274	0.374	4.789	0.214	0.200
	17	0.000	1.996	0.583	61.7	0.172	8.457	0.236	0.112	0.039	0.278	0.379	5.405	0.324	0.201
PA1	4	0.000	0.561	0.037	59.9	0.004	20.534	0.027	-0.032	0.011	0.079	-0.328	0.751	0.006	-0.189
	5	0.000	0.440	0.079	59.9	0.005	18.454	0.024	0.044	0.009	0.062	0.686	0.712	0.012	0.284
	6	0.000	0.411	0.107	59.9	0.006	17.273	0.024	0.025	0.008	0.058	0.430	0.781	0.017	0.158
	7	0.000	0.409	0.131	59.9	0.007	16.384	0.025	0.035	0.008	0.058	0.622	0.841	0.021	0.216
	8	0.000	0.335	0.164	59.9	0.007	15.298	0.022	0.057	0.007	0.047	1.295	0.812	0.025	0.384
	9	0.000	0.450	0.189	59.9	0.011	14.569	0.031	0.054	0.009	0.064	0.913	1.008	0.034	0.302
	10	0.000	0.969	0.217	59.9	0.027	13.853	0.070	0.070	0.019	0.137	0.556	1.551	0.059	0.256
	11	0.000	1.301	0.239	59.9	0.040	13.320	0.098	0.093	0.026	0.184	0.551	1.866	0.079	0.283
	12	0.000	1.450	0.265	59.9	0.050	12.738	0.114	0.093	0.029	0.205	0.494	2.105	0.095	0.260
	13	-0.213	1.158	0.303	59.9	0.046	11.975	0.097	0.069	0.023	0.164	0.459	2.140	0.099	0.212
PA2	3	0.000	0.267	0.070	51.6	0.003	17.522	0.015	0.000	0.006	0.041	-0.005	0.558	0.009	-0.002
	4	0.000	0.281	0.095	51.6	0.004	16.485	0.017	0.048	0.007	0.043	1.057	0.597	0.013	0.364
	5	0.000	0.289	0.131	51.6	0.006	15.216	0.019	0.063	0.007	0.044	1.407	0.678	0.018	0.450
	6	0.000	0.292	0.168	51.6	0.007	14.108	0.021	0.081	0.007	0.045	1.851	0.741	0.024	0.556
	7	0.000	0.306	0.193	51.6	0.009	13.434	0.023	0.099	0.007	0.047	2.194	0.769	0.029	0.650
	8	0.000	0.844	0.223	51.6	0.028	12.710	0.066	0.123	0.020	0.129	0.994	1.306	0.059	0.462
	9	0.000	1.239	0.286	51.6	0.052	11.418	0.109	0.172	0.029	0.189	0.948	1.859	0.100	0.494
	10	0.000	1.068	0.351	51.6	0.056	10.338	0.103	0.155	0.025	0.163	0.978	2.096	0.119	0.458
SE1	1	0.000	0.751	0.004	51.0	0.001	20.813	0.036	0.153	0.018	0.115	0.574	0.761	0.001	0.789
	2	0.000	0.637	0.063	51.0	0.007	17.730	0.036	0.398	0.015	0.098	3.555	1.211	0.012	2.061
	3	0.000	0.435	0.137	51.0	0.009	14.952	0.029	0.473	0.010	0.067	7.032	1.416	0.024	2.730
	4	0.000	0.294	0.143	51.0	0.006	14.765	0.020	0.484	0.007	0.045	10.734	1.246	0.020	3.399
	5	0.000	0.825	0.247	51.0	0.030	12.117	0.068	0.467	0.019	0.127	3.824	1.366	0.067	1.726
	6	0.000	3.426	0.439	51.0	0.234	9.121	0.376	0.855	0.081	0.526	1.605	1.229	0.340	1.103
SE5	1	0.000	0.007	0.044	31.1	0.000	14.515	0.000	0.026	0.000	0.001	14.383	-0.023	0.001	1.234
	2	0.000	0.010	0.096	31.1	0.000	12.767	0.001	0.041	0.000	0.002	17.086	-0.078	0.003	1.453
	3	0.000	0.008	0.154	31.1	0.000	11.267	0.001	0.039	0.000	0.002	22.329	-0.109	0.004	1.470
	4	0.000	0.003	0.539	31.1	0.000	6.306	0.000	0.022	0.000	0.001	32.955	0.120	0.011	1.019
SE6	1	0.000	0.750	0.007	48.0	0.002	20.014	0.037	0.109	0.019	0.119	0.461	0.981	0.001	0.554
	2	0.000	1.054	0.019	48.0	0.005	19.309	0.055	0.324	0.026	0.167	1.276	1.544	0.005	1.349
	3	0.000	1.719	0.028	48.0	0.010	18.858	0.091	0.539	0.043	0.272	1.422	1.784	0.009	1.703
	4	0.000	0.000	0.003	48.0	0.000	20.221	0.000	3.500	0.000	0.000	—	0.000	0.000	—
	5	0.000	1.405	0.047	48.0	0.013	17.897	0.079	0.578	0.035	0.222	2.100	1.651	0.014	1.979
	6	0.000	0.813	0.118	48.0	0.016	15.114	0.054	0.737	0.020	0.129	5.478	1.585	0.028	3.092
	7	0.000	0.446	0.157	48.0	0.011	13.902	0.032	0.808	0.011	0.071	11.340	1.525	0.029	4.435
	8	0.000	0.590	0.207	48.0	0.019	12.622	0.047	0.829	0.015	0.093	8.993	1.596	0.046	3.741
	9	0.000	0.732	0.295	48.0	0.034	10.870	0.067	0.860	0.018	0.116	7.558	1.832	0.079	3.201
	10	0.000	2.412	0.512	48.0	0.209	8.086	0.298	0.863	0.060	0.381	2.107	1.848	0.334	1.323

Panel I.D.	LS	Δ^t_s	C_r	Δ^e_s/Δ^t_s	Δ_2	Δ^t_s	Δ^e_s/Δ^t_s	V_{co}	Δ^t_s	Δ^e_s/Δ^t_s	Δ_2	Δ^t_s	Δ^e_s/Δ^t_s
		Lal/Vec. - Model A			Lal/Vec. - Model B			Walraven - Model B			Lal/Vec. - Model C		
PV1	3	0.002	1	-2.177	0.042	—	—	1.380	0.018	-0.192	0.060	—	—
	4	0.006	1	0.811	0.060	0.005	1.014	1.380	0.030	0.154	0.089	0.007	0.682
	5	0.007	1	0.928	0.074	0.006	1.160	1.380	0.041	0.163	0.114	0.009	0.753
	6	0.008	1	1.860	0.087	0.007	2.325	1.380	0.053	0.293	0.140	0.011	1.453
	7	0.000	1	—	0.101	—	—	1.380	0.068	0.315	0.169	—	—
PV3	4	0.006	1	-0.941	0.059	—	—	1.064	0.024	-0.233	0.084	—	—
	5	0.007	1	0.837	0.089	0.006	1.047	1.064	0.046	0.129	0.134	0.009	0.694
	6	0.013	1	1.490	0.102	0.010	1.862	1.064	0.059	0.325	0.159	0.016	1.191
PV4	4	0.022	1	0.271	0.030	0.018	0.339	1.064	0.022	0.265	0.041	0.024	0.250
	5	0.034	1	0.293	0.056	0.027	0.366	1.064	0.038	0.260	0.078	0.038	0.260
	6	0.014	1	1.215	0.107	0.011	1.519	1.064	0.064	0.260	0.169	0.017	0.958
	7	0.022	1	1.370	0.147	0.017	1.713	1.064	0.117	0.254	0.261	0.031	0.961
	8	0.032	1	1.067	0.190	0.025	1.333	1.064	0.191	0.176	0.377	0.050	0.673
PV5	3	0.007	1	-1.280	0.059	—	—	1.132	0.025	-0.346	0.085	—	—
	4	0.009	1	-1.310	0.072	—	—	1.132	0.033	-0.356	0.105	—	—
	5	0.004	1	-0.633	0.081	—	—	1.132	0.040	-0.061	0.121	—	—
	6	0.009	1	1.233	0.096	0.007	1.541	1.132	0.055	0.195	0.150	0.011	0.987
	7	0.007	1	1.299	0.108	0.005	1.624	1.132	0.067	0.128	0.175	0.009	1.004
PV6	3	0.007	1	1.787	0.041	0.005	2.234	1.192	0.017	0.704	0.057	0.007	1.600
	4	0.007	1	1.941	0.050	0.005	2.426	1.192	0.022	0.611	0.071	0.008	1.710
	5	0.007	1	2.428	0.056	0.006	3.034	1.192	0.025	0.706	0.080	0.008	2.118
	6	0.009	1	3.105	0.070	0.007	3.881	1.192	0.035	0.842	0.104	0.011	2.627
	7	0.005	1	2.290	0.083	—	—	1.192	0.043	0.275	0.126	—	—
	8	0.000	1	—	0.241	0.000	—	1.192	0.294	0.028	0.536	0.000	—
PV7	2	0.001	1	-0.604	0.020	—	—	1.240	0.007	-0.119	0.028	—	—
	3	0.003	1	-1.485	0.042	—	—	1.240	0.017	-0.260	0.059	—	—
	4	0.002	1	-5.440	0.061	0.002	-6.800	1.240	0.028	-0.441	0.089	0.003	-4.661
	5	0.003	1	-1.490	0.070	—	—	1.240	0.034	-0.136	0.105	—	—
	6	0.002	1	1.377	0.081	0.002	1.721	1.240	0.043	0.066	0.124	0.003	1.124
	7	0.002	1	1.413	0.091	0.002	1.766	1.240	0.052	0.056	0.143	0.003	1.122
PV8	3	0.001	1	-0.371	0.035	—	—	1.192	0.013	-0.032	0.048	—	—
	4	0.002	1	-0.540	0.049	—	—	1.192	0.020	-0.046	0.069	—	—
	5	0.002	1	-0.451	0.059	—	—	1.192	0.026	-0.028	0.085	—	—
	6	0.003	1	1.261	0.069	0.003	1.577	1.192	0.033	0.128	0.101	0.004	1.071
	7	0.000	1	19.589	0.079	0.000	24.486	1.192	0.040	0.241	0.120	0.001	16.212
PV9	2	0.003	1	0.793	0.021	0.003	0.991	0.464	0.005	0.493	0.026	0.003	0.811
	3	0.006	1	0.764	0.044	0.005	0.955	0.464	0.011	0.393	0.054	0.006	0.768
	4	0.004	1	0.449	0.060	0.004	0.561	0.464	0.016	0.123	0.076	0.004	0.444
	5	0.006	1	0.575	0.078	0.005	0.719	0.464	0.023	0.153	0.101	0.006	0.556
	6	0.008	1	-2.107	0.094	—	—	0.464	0.030	-0.590	0.124	—	—
	7	0.002	1	—	0.112	—	—	0.464	0.042	-1.588	0.154	—	—
PV10	3	0.018	1	0.345	0.039	0.014	0.431	0.580	0.017	0.367	0.049	0.018	0.340
	4	0.027	1	0.448	0.059	0.022	0.560	0.580	0.027	0.448	0.077	0.028	0.432
	5	0.061	1	0.586	0.079	0.049	0.732	0.580	0.061	0.590	0.105	0.065	0.550
	6	0.086	1	0.572	0.095	0.069	0.715	0.580	0.091	0.545	0.131	0.095	0.522
	7	0.110	1	0.958	0.124	0.088	1.197	0.580	0.126	0.833	0.181	0.128	0.820
	8	0.175	1	1.293	0.169	0.140	1.617	0.580	0.232	0.978	0.276	0.230	0.987
PV11	3	0.006	1	0.214	0.019	0.005	0.267	0.624	0.007	0.205	0.024	0.006	0.213
	4	0.013	1	0.338	0.041	0.010	0.422	0.624	0.015	0.296	0.052	0.013	0.330
	5	0.016	1	0.344	0.054	0.013	0.431	0.624	0.020	0.276	0.070	0.016	0.332
	6	0.019	1	0.443	0.063	0.015	0.553	0.624	0.024	0.344	0.082	0.020	0.422
	7	0.044	1	0.369	0.074	0.035	0.462	0.624	0.044	0.364	0.099	0.047	0.346
	8	0.003	1	2.726	0.102	0.002	3.407	0.624	0.041	0.186	0.143	0.003	2.425
	9	0.003	1	2.229	0.112	0.003	2.786	0.624	0.049	0.147	0.160	0.004	1.941
PV12	4	0.032	1	0.156	0.052	0.025	0.195	0.640	0.030	0.165	0.067	0.033	0.151
	5	0.057	1	0.265	0.067	0.045	0.331	0.640	0.056	0.267	0.089	0.060	0.250
	6	0.089	1	0.348	0.087	0.071	0.435	0.640	0.095	0.327	0.119	0.098	0.317

Panel I.D.	LS	Δ^t_s	C_r	Δ^a_s/Δ^t_s	Δ_2	Δ^t_s	Δ^a_s/Δ^t_s	V_{co}	Δ^t_s	Δ^a_s/Δ^t_s	Δ_2	Δ^t_s	Δ^a_s/Δ^t_s
		Lai/Vec. - Model A			Lai/Vec. - Model B			Wallraven - Model B			Lai/Vec. - Model C		
	7	0.194	1	0.588	0.137	0.155	0.735	0.640	0.240	0.475	0.211	0.238	0.478
	8	0.403	1	0.937	0.204	0.323	1.171	0.640	0.557	0.679	0.368	0.583	0.649
PV14	3	0.002	1	1.020	0.015	0.002	1.275	0.816	0.005	0.539	0.019	0.003	0.988
	4	0.003	1	0.425	0.040	0.003	0.532	0.816	0.013	0.109	0.053	0.004	0.403
	5	0.004	1	0.453	0.063	0.003	0.567	0.816	0.023	0.083	0.086	0.005	0.416
	6	0.005	1	0.432	0.072	0.004	0.540	0.816	0.028	0.078	0.100	0.006	0.390
	7	0.004	1	0.337	0.081	0.003	0.422	0.816	0.033	0.041	0.114	0.005	0.300
PV16	2	0.014	1	0.697	0.067	0.011	0.871	0.868	0.028	0.345	0.093	0.016	0.628
PV18	4	0.046	1	0.587	0.061	0.037	0.734	0.780	0.047	0.577	0.083	0.050	0.544
	5	0.088	1	0.776	0.093	0.070	0.970	0.780	0.099	0.694	0.133	0.101	0.677
	6	0.155	1	0.965	0.143	0.124	1.207	0.780	0.204	0.736	0.234	0.203	0.740
PV19	3	0.013	1	0.428	0.020	0.010	0.536	0.760	0.012	0.462	0.026	0.013	0.417
	4	0.022	1	0.410	0.038	0.018	0.512	0.760	0.022	0.424	0.050	0.023	0.392
	5	0.029	1	0.453	0.048	0.023	0.567	0.760	0.029	0.459	0.063	0.031	0.429
	6	0.047	1	0.546	0.064	0.038	0.683	0.760	0.048	0.537	0.086	0.051	0.506
	7	0.079	1	0.676	0.083	0.063	0.845	0.760	0.085	0.625	0.116	0.088	0.605
	8	0.110	1	0.740	0.106	0.088	0.924	0.760	0.127	0.637	0.156	0.129	0.629
	9	0.152	1	0.916	0.131	0.122	1.146	0.760	0.191	0.732	0.205	0.191	0.731
	10	0.216	1	1.089	0.167	0.173	1.361	0.760	0.298	0.790	0.289	0.298	0.789
PV20	3	0.013	1	0.492	0.022	0.010	0.615	0.784	0.012	0.523	0.028	0.013	0.477
	4	0.022	1	0.527	0.038	0.018	0.659	0.784	0.022	0.539	0.050	0.023	0.502
	5	0.029	1	0.605	0.054	0.023	0.756	0.784	0.030	0.582	0.072	0.031	0.565
	6	0.049	1	0.670	0.066	0.039	0.837	0.784	0.051	0.648	0.090	0.054	0.615
	7	0.073	1	0.735	0.079	0.058	0.919	0.784	0.078	0.683	0.110	0.081	0.660
	8	0.107	1	0.833	0.103	0.085	1.041	0.784	0.123	0.719	0.151	0.125	0.710
	9	0.142	1	1.042	0.129	0.114	1.303	0.784	0.179	0.831	0.202	0.179	0.830
	10	0.192	1	1.309	0.171	0.154	1.636	0.784	0.273	0.922	0.300	0.269	0.933
PV21	3	0.008	1	0.211	0.020	0.006	0.264	0.780	0.008	0.202	0.026	0.008	0.205
	4	0.015	1	0.231	0.043	0.012	0.289	0.780	0.018	0.196	0.057	0.016	0.219
	5	0.019	1	0.305	0.053	0.015	0.381	0.780	0.023	0.249	0.071	0.020	0.285
	6	0.023	1	0.503	0.061	0.019	0.629	0.780	0.028	0.416	0.082	0.025	0.466
	7	0.032	1	0.667	0.069	0.026	0.833	0.780	0.037	0.580	0.094	0.035	0.609
	8	0.065	1	0.750	0.083	0.052	0.937	0.780	0.070	0.692	0.116	0.073	0.668
	9	0.088	1	0.998	0.106	0.070	1.247	0.780	0.103	0.851	0.156	0.104	0.845
	10	0.113	1	1.434	0.137	0.090	1.792	0.780	0.150	1.079	0.220	0.145	1.117
PV22	3	0.006	1	0.392	0.021	0.005	0.489	0.784	0.008	0.327	0.028	0.007	0.379
	4	0.010	1	0.280	0.038	0.008	0.350	0.784	0.014	0.208	0.050	0.011	0.267
	5	0.014	1	0.348	0.052	0.011	0.435	0.784	0.021	0.241	0.070	0.015	0.326
	6	0.017	1	0.356	0.060	0.014	0.445	0.784	0.025	0.243	0.082	0.018	0.330
	7	0.019	1	0.413	0.066	0.015	0.516	0.784	0.029	0.279	0.091	0.021	0.379
	8	0.021	1	0.447	0.072	0.016	0.559	0.784	0.032	0.292	0.099	0.023	0.407
	9	0.023	1	0.528	0.077	0.019	0.660	0.784	0.035	0.347	0.106	0.026	0.476
	10	0.024	1	0.525	0.081	0.019	0.657	0.784	0.038	0.334	0.113	0.027	0.470
	11	0.025	1	0.614	0.084	0.020	0.767	0.784	0.040	0.388	0.118	0.029	0.545
	12	0.028	1	0.820	0.088	0.022	1.025	0.784	0.044	0.521	0.125	0.031	0.723
	13	0.026	1	1.721	0.097	0.021	2.152	0.784	0.049	0.925	0.141	0.031	1.487
PV23	5	0.003	1	0.124	0.020	0.003	0.156	0.820	0.006	0.066	0.026	0.003	0.120
	6	0.000	1	—	0.026	0.000	—	0.820	0.008	0.000	0.034	0.000	—
	7	0.002	1	0.250	0.037	0.001	0.312	0.820	0.012	0.038	0.048	0.002	0.237
	8	0.005	1	0.524	0.045	0.004	0.656	0.820	0.015	0.174	0.060	0.005	0.493
	9	0.006	1	0.592	0.050	0.005	0.740	0.820	0.018	0.216	0.068	0.007	0.552
	10	0.008	1	0.679	0.056	0.006	0.849	0.820	0.021	0.256	0.076	0.008	0.629
	11	0.008	1	0.600	0.061	0.006	0.750	0.820	0.023	0.205	0.083	0.008	0.552
	12	0.010	1	0.734	0.065	0.008	0.917	0.820	0.025	0.299	0.090	0.011	0.669
	13	0.010	1	0.707	0.070	0.008	0.883	0.820	0.028	0.262	0.097	0.011	0.640
	14	0.013	1	0.794	0.075	0.011	0.993	0.820	0.031	0.336	0.104	0.015	0.713
	15	0.015	1	0.897	0.081	0.012	1.122	0.820	0.035	0.393	0.114	0.017	0.796

Panel I.D.	LS	Δ^t_s	C_T	Δ^e_s/Δ^t_s	Δ_2	Δ^t_s	Δ^e_s/Δ^t_s	V_{co}	Δ^t_s	Δ^e_s/Δ^t_s	Δ_2	Δ^t_s	Δ^e_s/Δ^t_s
		Lai/Vec. - Model A			Lai/Vec. - Model B			Walraven - Model B			Lai/Vec. - Model C		
	16	0.017	1	0.891	0.086	0.013	1.114	0.820	0.039	0.379	0.122	0.019	0.783
	17	0.020	1	1.053	0.092	0.016	1.317	0.820	0.044	0.481	0.133	0.023	0.913
	18	0.023	1	1.103	0.103	0.019	1.379	0.820	0.054	0.480	0.153	0.028	0.931
PV24	4	0.001	1	2.167	0.014	0.001	2.709	0.952	0.004	0.597	0.018	0.001	2.064
	5	0.002	1	1.780	0.021	0.002	2.225	0.952	0.007	0.558	0.027	0.002	1.685
	6	0.002	1	1.377	0.026	0.002	1.721	0.952	0.009	0.394	0.034	0.003	1.297
PV25	4	0.002	1	0.846	0.021	0.002	1.058	0.770	0.006	0.266	0.027	0.002	0.821
	5	0.005	1	0.887	0.037	0.004	1.108	0.770	0.012	0.343	0.048	0.005	0.848
	6	0.006	1	0.924	0.047	0.005	1.155	0.770	0.016	0.374	0.063	0.007	0.873
	7	0.010	1	1.079	0.059	0.008	1.348	0.770	0.022	0.495	0.079	0.011	1.003
	8	0.010	1	1.037	0.069	0.008	1.296	0.770	0.026	0.389	0.094	0.011	0.950
	9	0.011	1	1.010	0.075	0.009	1.262	0.770	0.030	0.384	0.103	0.013	0.915
	10	0.010	1	0.874	0.079	0.008	1.092	0.770	0.032	0.283	0.109	0.011	0.787
PV27	3	0.004	1	0.987	0.019	0.003	1.233	0.820	0.006	0.603	0.025	0.004	0.952
	4	0.007	1	0.726	0.036	0.005	0.908	0.820	0.012	0.408	0.047	0.007	0.690
	5	0.010	1	0.669	0.051	0.008	0.836	0.820	0.019	0.365	0.068	0.011	0.624
	6	0.011	1	0.575	0.063	0.009	0.719	0.820	0.025	0.267	0.086	0.012	0.527
	7	0.013	1	0.622	0.070	0.010	0.777	0.820	0.029	0.284	0.097	0.014	0.563
	8	0.014	1	0.568	0.077	0.011	0.710	0.820	0.033	0.240	0.108	0.015	0.508
	9	0.008	1	0.341	0.086	0.006	0.426	0.820	0.037	0.071	0.122	0.009	0.299
PV28	3	0.002	1	-0.323	0.026	—	—	0.760	0.007	-0.108	0.033	—	—
	4	0.004	1	0.309	0.048	0.003	0.386	0.760	0.016	0.080	0.063	0.004	0.292
	5	0.005	1	0.260	0.059	0.004	0.325	0.760	0.021	0.063	0.080	0.005	0.242
	6	0.005	1	-0.226	0.068	—	—	0.760	0.024	-0.047	0.093	—	—
	7	0.007	1	0.331	0.074	0.005	0.413	0.760	0.028	0.078	0.101	0.007	0.301
	8	0.009	1	0.389	0.080	0.007	0.486	0.760	0.032	0.109	0.111	0.010	0.350
	9	0.005	1	0.160	0.085	0.004	0.200	0.760	0.034	0.022	0.119	0.005	0.143
	10	0.000	1	4.370	0.090	0.000	5.463	0.760	0.038	0.014	0.128	0.000	3.852
	11	0.002	1	-0.229	0.094	—	—	0.760	0.041	-0.013	0.135	—	—
	12	0.000	1	-6.112	0.098	—	—	0.760	0.043	-0.026	0.141	—	—
	13	0.003	1	-0.329	0.102	—	—	0.760	0.046	-0.019	0.148	—	—
PV29	3	0.018	1	-0.263	0.040	0.015	-0.329	0.868	0.020	-0.245	0.053	0.020	-0.247
	4	0.027	1	0.122	0.058	0.022	0.153	0.868	0.031	0.107	0.079	0.030	0.112
	5	0.061	1	0.713	0.081	0.049	0.891	0.868	0.068	0.639	0.115	0.069	0.626
	6	0.070	1	0.817	0.090	0.056	1.022	0.868	0.080	0.712	0.131	0.081	0.704
	7	0.074	1	0.921	0.093	0.060	1.151	0.868	0.086	0.794	0.136	0.087	0.787
	8	0.078	1	0.961	0.097	0.062	1.202	0.868	0.092	0.817	0.144	0.092	0.814
	9	0.084	1	1.025	0.102	0.067	1.282	0.868	0.100	0.859	0.152	0.101	0.858
	10	0.091	1	1.103	0.107	0.072	1.378	0.868	0.110	0.910	0.161	0.110	0.911
PB4	5	0.026	1	0.270	0.034	0.020	0.337	0.656	0.024	0.293	0.043	0.026	0.264
PB5	4	0.007	1	-0.590	0.016	0.005	-0.738	0.940	0.007	-0.558	0.021	0.007	-0.562
	5	0.010	1	-0.421	0.022	0.008	-0.526	0.940	0.011	-0.403	0.029	0.011	-0.398
	7	0.010	1	-0.694	0.022	0.008	-0.868	0.940	0.011	-0.656	0.030	0.011	-0.657
	8	0.015	1	-0.238	0.030	0.012	-0.298	0.940	0.016	-0.227	0.040	0.016	-0.224
	9	0.022	1	-0.291	0.042	0.017	-0.364	0.940	0.023	-0.270	0.057	0.023	-0.269
	10	0.033	1	-0.138	0.059	0.026	-0.173	0.940	0.037	-0.124	0.082	0.036	-0.125
	11	0.000	1	—	0.100	0.000	—	0.940	0.051	-0.468	0.151	0.000	—
PB6	7	0.019	1	0.043	0.027	0.015	0.054	0.705	0.017	0.047	0.035	0.019	0.042
	8	0.045	1	1.115	0.058	0.036	1.394	0.705	0.045	1.130	0.077	0.048	1.051
	9	0.057	1	1.016	0.069	0.046	1.270	0.705	0.058	1.000	0.093	0.061	0.943
	10	0.210	1	1.153	0.174	0.168	1.442	0.705	0.290	0.832	0.301	0.289	0.835
PB7	3	0.051	1	1.059	0.073	0.041	1.324	0.810	0.055	0.991	0.101	0.057	0.956
	4	0.109	1	2.661	0.126	0.087	3.327	0.810	0.139	2.083	0.199	0.137	2.119
	5	0.173	1	3.443	0.176	0.139	4.304	0.810	0.257	2.320	0.315	0.248	2.406
PB8	3	0.022	1	-1.561	0.037	0.018	-1.951	0.814	0.022	-1.593	0.049	0.024	-1.483
	4	0.034	1	-0.432	0.052	0.028	-0.540	0.814	0.035	-0.427	0.070	0.037	-0.402
	5	0.099	1	2.814	0.124	0.079	3.518	0.814	0.126	2.197	0.193	0.123	2.255

Panel I.D.	LS	$\Delta^t_{2_c}$	C_r	$\Delta^e_2/\Delta^t_{2_c}$	Δ_2	$\Delta^t_{2_c}$	$\Delta^e_2/\Delta^t_{2_c}$	V_{co}	$\Delta^t_{2_c}$	$\Delta^e_2/\Delta^t_{2_c}$	Δ_2	$\Delta^t_{2_c}$	$\Delta^e_2/\Delta^t_{2_c}$
		Lal/Vec. - Model A			Lal/Vec. - Model B			Walraven - Model B			Lal/Vec. - Model C		
PB10	2	0.007	1	-1.587	0.017	0.005	-1.984	0.961	0.007	-1.430	0.022	0.007	-1.506
	3	0.015	1	-2.272	0.031	0.012	-2.840	0.961	0.016	-2.117	0.041	0.016	-2.127
	4	0.023	1	-2.338	0.044	0.019	-2.923	0.961	0.025	-2.171	0.059	0.025	-2.154
	5	0.040	1	0.084	0.073	0.032	0.105	0.961	0.048	0.071	0.103	0.046	0.074
	6	0.086	1	2.683	0.122	0.069	3.354	0.961	0.120	1.926	0.197	0.111	2.078
	7	0.000	1	—	0.230	0.000	—	0.961	0.246	3.495	0.476	0.000	—
PB11	4	0.209	1	1.998	0.167	0.167	2.497	1.036	0.312	1.337	0.312	0.311	1.338
PB12	4	0.105	1	1.795	0.093	0.084	2.244	0.922	0.123	1.527	0.138	0.124	1.516
PB14	3	0.004	1	-0.545	0.008	0.003	-0.681	1.644	0.005	-0.459	0.011	0.004	-0.485
	4	0.030	1	-0.370	0.045	0.024	-0.462	1.644	0.037	-0.301	0.067	0.036	-0.311
	5	0.071	1	1.347	0.085	0.057	1.684	1.644	0.099	0.966	0.141	0.094	1.013
	6	0.119	1	1.986	0.115	0.095	2.482	1.644	0.181	1.301	0.212	0.175	1.343
	7	0.320	1	2.437	0.225	0.256	3.046	1.644	0.589	1.325	0.539	0.613	1.273
PB16	5	0.018	1	0.255	0.027	0.015	0.319	1.668	0.021	0.220	0.039	0.021	0.221
	6	0.072	1	1.937	0.081	0.058	2.421	1.668	0.098	1.426	0.133	0.095	1.470
	7	0.213	1	3.046	0.176	0.170	3.808	1.668	0.379	1.707	0.388	0.376	1.723
	8	0.816	1	1.512	0.545	0.652	1.890	1.668	1.736	0.710	1.563	1.870	0.660
	9	-0.804	1	-2.281	-0.426	-0.643	-2.852	1.668	-1.906	-0.963	-1.558	-2.354	-0.779
PB17	5	0.014	1	-2.455	0.028	0.011	-3.069	1.664	0.018	-1.939	0.040	0.016	-2.125
	6	0.020	1	-2.281	0.036	0.016	-2.851	1.664	0.025	-1.806	0.053	0.023	-1.946
	7	0.033	1	-0.851	0.052	0.026	-1.063	1.664	0.043	-0.656	0.079	0.040	-0.701
	8	0.057	1	0.785	0.076	0.046	0.982	1.664	0.079	0.570	0.123	0.074	0.605
	9	0.077	1	3.721	0.110	0.062	4.651	1.664	0.131	2.184	0.202	0.113	2.545
	10	0.019	1	53.213	0.321	0.015	66.516	1.664	0.525	1.942	0.845	0.040	25.282
PB18	6	0.161	1	2.305	0.126	0.129	2.882	1.012	0.213	1.741	0.209	0.214	1.739
	7	0.401	1	2.061	0.221	0.320	2.576	1.012	0.616	1.341	0.455	0.661	1.249
	8	0.668	1	1.517	0.311	0.535	1.896	1.012	1.061	0.956	0.711	1.222	0.830
PB19	5	0.015	1	-0.320	0.019	0.012	-0.400	0.800	0.014	-0.339	0.024	0.016	-0.310
	7	0.186	1	2.497	0.147	0.149	3.121	0.800	0.246	1.884	0.244	0.246	1.883
	8	0.257	1	2.488	0.180	0.205	3.110	0.800	0.365	1.752	0.323	0.369	1.730
PB20	6	0.067	1	1.405	0.077	0.054	1.756	0.868	0.074	1.282	0.109	0.076	1.243
	7	0.108	1	1.970	0.107	0.087	2.462	0.868	0.130	1.638	0.162	0.131	1.627
	8	0.147	1	2.042	0.126	0.118	2.552	0.868	0.188	1.601	0.201	0.188	1.601
	9	0.229	1	2.218	0.161	0.183	2.773	0.868	0.317	1.598	0.282	0.321	1.583
	10	0.845	1	1.381	0.369	0.676	1.726	0.868	1.321	0.883	0.848	1.555	0.751
PB21	4	0.019	1	-1.281	0.027	0.015	-1.601	0.872	0.018	-1.324	0.036	0.020	-1.219
	5	0.025	1	-1.040	0.034	0.020	-1.300	0.872	0.024	-1.061	0.045	0.026	-0.983
	6	0.060	1	1.012	0.072	0.048	1.265	0.872	0.065	0.937	0.101	0.067	0.903
	7	0.104	1	1.429	0.103	0.083	1.786	0.872	0.123	1.203	0.154	0.124	1.192
	8	0.246	1	2.166	0.171	0.197	2.708	0.872	0.350	1.524	0.308	0.354	1.504
	9	0.564	1	1.810	0.298	0.451	2.263	0.872	0.896	1.139	0.651	0.986	1.035
PB22	4	0.022	1	-1.586	0.035	0.018	-1.983	0.704	0.021	-1.697	0.046	0.023	-1.536
	5	0.056	1	0.518	0.074	0.045	0.648	0.704	0.057	0.504	0.101	0.061	0.477
	6	0.091	1	1.144	0.101	0.073	1.430	0.704	0.102	1.025	0.144	0.105	0.999
	7	0.157	1	1.969	0.138	0.126	2.461	0.704	0.197	1.568	0.217	0.197	1.567
	8	0.152	1	4.434	0.192	0.122	5.543	0.704	0.240	2.808	0.344	0.218	3.088
PB28	3	0.006	1	-0.201	0.009	—	—	0.908	0.000	-9.835	0.012	—	—
	4	0.013	1	-0.423	0.019	—	—	0.908	-0.001	5.043	0.024	—	—
	5	0.039	1	-0.062	0.048	—	—	0.908	-0.006	0.402	0.065	—	—
	6	0.083	1	-0.598	0.086	—	—	0.908	-0.017	2.911	0.125	—	—
	7	0.149	1	-0.844	0.123	—	—	0.908	-0.043	2.932	0.197	—	—
	8	0.275	1	-1.177	0.177	—	—	0.908	-0.097	3.348	0.327	—	—
PB29	4	0.009	1	-1.345	0.015	0.007	-1.682	1.664	0.010	-1.158	0.022	0.010	-1.185
	5	0.056	1	2.498	0.075	0.045	3.123	1.664	0.077	1.818	0.121	0.072	1.931
	6	0.080	1	2.842	0.093	0.064	3.552	1.664	0.115	1.967	0.159	0.110	2.072
	7	0.119	1	3.099	0.118	0.095	3.873	1.664	0.186	1.989	0.220	0.179	2.068
	8	0.159	1	3.136	0.140	0.127	3.920	1.664	0.261	1.907	0.281	0.255	1.948

Panel I.D.	LS	Δ^t_s	C_r	Δ^e_s/Δ^t_s	Δ_2	Δ^t_s	Δ^e_s/Δ^t_s	V_{co}	Δ^t_s	Δ^e_s/Δ^t_s	Δ_2	Δ^t_s	Δ^e_s/Δ^t_s
		Lai/Vec. - Model A			Lai/Vec. - Model B			Wallraven - Model B			Lai/Vec. - Model C		
	9	0.237	1	2.954	0.183	0.189	3.692	1.664	0.420	1.666	0.409	0.424	1.649
PB30	4	0.072	1	3.197	0.093	0.058	3.997	1.616	0.107	2.168	0.159	0.099	2.344
	5	0.110	1	3.347	0.119	0.088	4.184	1.616	0.175	2.110	0.222	0.164	2.243
	6	0.150	1	3.370	0.144	0.120	4.213	1.616	0.253	2.000	0.290	0.242	2.090
	7	0.180	1	3.192	0.158	0.144	3.990	1.616	0.309	1.859	0.331	0.302	1.903
	8	0.229	1	2.884	0.177	0.184	3.605	1.616	0.399	1.659	0.389	0.403	1.644
	9	0.360	1	2.417	0.239	0.288	3.021	1.616	0.659	1.321	0.580	0.699	1.246
PB31	2	0.006	1	0.014	0.016	0.005	0.018	1.736	0.009	0.010	0.023	0.007	0.012
	3	0.015	1	-1.769	0.031	0.012	-2.212	1.736	0.020	-1.329	0.045	0.017	-1.512
	4	0.025	1	-0.907	0.045	0.020	-1.134	1.736	0.034	-0.685	0.068	0.031	-0.754
	5	0.104	1	3.597	0.122	0.083	4.496	1.736	0.178	2.107	0.237	0.161	2.326
	6	0.135	1	3.607	0.143	0.108	4.509	1.736	0.241	2.019	0.295	0.223	2.186
	7	0.172	1	3.960	0.184	0.138	4.950	1.736	0.348	1.962	0.418	0.314	2.174
PB32	2	0.003	1	-1.682	0.008	0.003	-2.103	2.308	0.005	-1.161	0.012	0.004	-1.420
	3	0.007	1	-2.120	0.014	0.006	-2.650	2.308	0.009	-1.561	0.020	0.008	-1.775
	4	0.016	1	-1.452	0.027	0.013	-1.815	2.308	0.021	-1.076	0.041	0.019	-1.187
	5	0.079	1	3.678	0.096	0.063	4.598	2.308	0.137	2.114	0.186	0.122	2.369
	6	0.187	1	3.320	0.162	0.150	4.150	2.308	0.372	1.672	0.391	0.361	1.719
PHS1	5	0.013	1	0.219	0.015	0.010	0.273	2.888	0.016	0.173	0.023	0.016	0.175
PHS2	4	0.004	1	0.056	0.006	0.003	0.070	2.644	0.005	0.045	0.009	0.005	0.046
	5	0.007	1	0.077	0.010	0.006	0.097	2.644	0.009	0.062	0.015	0.009	0.064
	6	0.022	1	0.140	0.037	0.017	0.176	2.644	0.032	0.094	0.059	0.028	0.109
	7	0.027	1	0.312	0.046	0.022	0.390	2.644	0.042	0.198	0.076	0.036	0.235
	8	0.031	1	0.368	0.052	0.025	0.460	2.644	0.050	0.225	0.089	0.042	0.271
	9	0.046	1	0.294	0.063	0.037	0.367	2.644	0.073	0.184	0.112	0.065	0.208
	10	0.058	1	0.335	0.069	0.046	0.419	2.644	0.091	0.211	0.126	0.084	0.230
	11	0.065	1	0.339	0.075	0.052	0.424	2.644	0.105	0.211	0.139	0.097	0.228
	12	0.079	1	0.296	0.082	0.064	0.371	2.644	0.129	0.182	0.158	0.122	0.193
	13	0.103	1	0.337	0.094	0.083	0.421	2.644	0.173	0.201	0.191	0.168	0.208
	14	0.164	1	0.354	0.120	0.132	0.443	2.644	0.290	0.201	0.272	0.297	0.196
PHS3	3	0.009	1	-0.241	0.015	0.007	-0.301	2.336	0.012	-0.189	0.023	0.011	-0.201
	4	0.016	1	-0.310	0.032	0.013	-0.388	2.336	0.024	-0.207	0.050	0.020	-0.250
	5	0.018	1	-0.168	0.043	0.015	-0.210	2.336	0.032	-0.097	0.069	0.023	-0.132
	6	0.021	1	-0.064	0.049	0.016	-0.079	2.336	0.037	-0.035	0.079	0.027	-0.049
	7	0.022	1	0.007	0.055	0.018	0.009	2.336	0.043	0.004	0.090	0.029	0.006
	8	0.024	1	0.096	0.059	0.019	0.120	2.336	0.048	0.048	0.100	0.033	0.071
	9	0.026	1	0.212	0.064	0.021	0.265	2.336	0.054	0.104	0.109	0.036	0.155
	10	0.042	1	0.145	0.068	0.034	0.182	2.336	0.070	0.087	0.119	0.059	0.105
	11	0.059	1	0.170	0.074	0.047	0.213	2.336	0.091	0.110	0.131	0.083	0.120
	12	0.073	1	0.063	0.089	0.058	0.079	2.336	0.122	0.037	0.169	0.110	0.042
	13	0.094	1	0.137	0.102	0.075	0.171	2.336	0.163	0.079	0.203	0.150	0.086
PHS4	3	0.012	1	-0.302	0.025	0.010	-0.377	2.740	0.019	-0.194	0.040	0.016	-0.239
	4	0.014	1	-0.852	0.038	0.011	-1.065	2.740	0.028	-0.429	0.061	0.018	-0.653
	5	0.017	1	-0.151	0.047	0.014	-0.189	2.740	0.037	-0.071	0.078	0.023	-0.113
	6	0.020	1	-0.257	0.052	0.016	-0.321	2.740	0.042	-0.119	0.088	0.027	-0.188
	7	0.021	1	-0.385	0.057	0.017	-0.481	2.740	0.048	-0.165	0.099	0.029	-0.276
	8	0.038	1	-0.305	0.063	0.031	-0.382	2.740	0.067	-0.175	0.112	0.055	-0.214
	9	0.057	1	-0.156	0.069	0.045	-0.195	2.740	0.091	-0.097	0.126	0.083	-0.106
	10	0.080	1	0.021	0.082	0.064	0.026	2.740	0.132	0.013	0.159	0.125	0.013
	11	0.104	1	0.134	0.095	0.083	0.167	2.740	0.177	0.078	0.196	0.171	0.081
PHS5	3	0.006	1	-0.452	0.009	0.005	-0.565	2.084	0.008	-0.388	0.013	0.008	-0.387
	4	0.024	1	0.192	0.036	0.020	0.240	2.084	0.031	0.150	0.054	0.030	0.157
	5	0.032	1	0.016	0.055	0.026	0.020	2.084	0.048	0.011	0.088	0.041	0.013
	6	0.058	1	0.244	0.068	0.046	0.305	2.084	0.082	0.173	0.114	0.078	0.181
	7	0.100	1	0.211	0.091	0.080	0.264	2.084	0.150	0.142	0.166	0.147	0.144
	8	0.130	1	0.234	0.103	0.104	0.292	2.084	0.200	0.152	0.199	0.201	0.152
	9	0.180	1	0.253	0.122	0.144	0.316	2.084	0.287	0.158	0.252	0.297	0.153

Panel I.D.	LS	Δ^t_s	C_T	Δ^e_p/Δ^t_s	Δ_2	Δ^t_s	Δ^e_p/Δ^t_s	V_{co}	Δ^t_s	Δ^e_p/Δ^t_s	Δ_2	Δ^t_s	Δ^e_p/Δ^t_s
		Lai/Vec. - Model A			Lai/Vec. - Model B			Wairaven - Model B			Lai/Vec. - Model C		
PHS6	3	0.006	1	-0.109	0.009	0.005	-0.136	1.988	0.007	-0.093	0.013	0.007	-0.094
	4	0.009	1	-0.171	0.012	0.007	-0.213	1.988	0.010	-0.148	0.017	0.010	-0.147
	5	0.018	1	-0.104	0.025	0.014	-0.131	1.988	0.022	-0.087	0.037	0.021	-0.088
	6	0.026	1	0.051	0.037	0.021	0.064	1.988	0.032	0.041	0.056	0.031	0.042
	7	0.033	1	0.176	0.046	0.026	0.220	1.988	0.042	0.135	0.072	0.040	0.142
	8	0.035	1	0.033	0.053	0.028	0.041	1.988	0.048	0.024	0.084	0.044	0.026
	9	0.040	1	0.174	0.061	0.032	0.218	1.988	0.057	0.121	0.098	0.051	0.134
	10	0.048	1	0.149	0.065	0.038	0.186	1.988	0.068	0.105	0.107	0.063	0.113
	11	0.059	1	0.127	0.070	0.047	0.158	1.988	0.082	0.090	0.117	0.078	0.095
	12	0.072	1	0.184	0.076	0.058	0.231	1.988	0.101	0.131	0.129	0.098	0.135
	13	0.087	1	0.184	0.083	0.069	0.230	1.988	0.124	0.128	0.146	0.122	0.131
	14	0.106	1	0.217	0.093	0.084	0.271	1.988	0.156	0.147	0.170	0.154	0.149
	15	0.134	1	0.265	0.108	0.108	0.331	1.988	0.208	0.171	0.209	0.207	0.172
	16	0.194	1	0.367	0.134	0.156	0.458	1.988	0.317	0.225	0.282	0.328	0.217
PHS7	3	0.004	1	-0.217	0.007	0.003	-0.272	2.144	0.005	-0.175	0.010	0.005	-0.186
	4	0.009	1	-0.207	0.015	0.007	-0.258	2.144	0.011	-0.166	0.022	0.010	-0.175
	5	0.017	1	0.202	0.033	0.014	0.253	2.144	0.024	0.142	0.051	0.021	0.165
	6	0.021	1	0.227	0.043	0.017	0.283	2.144	0.032	0.147	0.067	0.026	0.181
	7	0.024	1	0.293	0.050	0.019	0.366	2.144	0.039	0.179	0.080	0.030	0.229
	8	0.025	1	0.264	0.057	0.020	0.330	2.144	0.045	0.150	0.093	0.033	0.202
	9	0.029	1	0.318	0.062	0.023	0.397	2.144	0.051	0.178	0.103	0.038	0.240
	10	0.029	1	0.353	0.068	0.023	0.441	2.144	0.057	0.183	0.114	0.040	0.261
	11	0.041	1	0.291	0.073	0.033	0.364	2.144	0.070	0.169	0.126	0.056	0.211
	12	0.062	1	0.306	0.079	0.049	0.382	2.144	0.095	0.198	0.139	0.087	0.217
	13	0.077	1	0.366	0.087	0.062	0.457	2.144	0.120	0.236	0.158	0.112	0.251
PHS8	3	0.005	1	-0.150	0.009	0.004	-0.187	2.236	0.006	-0.117	0.014	0.006	-0.127
	4	0.013	1	0.208	0.025	0.010	0.260	2.236	0.018	0.149	0.038	0.015	0.171
	5	0.016	1	0.175	0.038	0.013	0.219	2.236	0.027	0.106	0.060	0.020	0.140
	6	0.018	1	0.301	0.047	0.015	0.376	2.236	0.034	0.163	0.075	0.024	0.235
	7	0.022	1	0.524	0.053	0.018	0.655	2.236	0.041	0.287	0.087	0.029	0.402
	8	0.025	1	0.515	0.059	0.020	0.644	2.236	0.047	0.275	0.098	0.033	0.388
	9	0.027	1	0.565	0.064	0.021	0.707	2.236	0.053	0.284	0.109	0.036	0.418
	10	0.033	1	0.599	0.070	0.026	0.749	2.236	0.063	0.310	0.122	0.045	0.433
	11	0.047	1	0.358	0.075	0.038	0.448	2.236	0.079	0.214	0.131	0.066	0.255
	12	0.062	1	0.333	0.080	0.049	0.416	2.236	0.099	0.209	0.144	0.089	0.231
	13	0.076	1	0.292	0.087	0.061	0.365	2.236	0.121	0.183	0.160	0.112	0.198
	14	0.096	1	0.359	0.095	0.077	0.449	2.236	0.153	0.224	0.182	0.146	0.235
	15	0.107	1	0.382	0.102	0.086	0.477	2.236	0.176	0.233	0.202	0.169	0.242
	16	0.112	1	0.440	0.110	0.090	0.550	2.236	0.192	0.257	0.224	0.182	0.271
	17	0.136	1	0.632	0.124	0.109	0.790	2.236	0.242	0.356	0.266	0.233	0.369
	18	0.142	1	0.653	0.135	0.114	0.816	2.236	0.267	0.349	0.300	0.253	0.368
PHS9	3	0.003	1	0.067	0.005	0.003	0.084	2.240	0.004	0.056	0.007	0.004	0.057
	4	0.011	1	0.245	0.015	0.009	0.306	2.240	0.013	0.202	0.023	0.013	0.205
	5	0.025	1	0.340	0.041	0.020	0.424	2.240	0.036	0.243	0.065	0.032	0.270
	6	0.030	1	0.242	0.055	0.024	0.302	2.240	0.047	0.153	0.089	0.039	0.185
	7	0.037	1	0.266	0.061	0.029	0.333	2.240	0.058	0.168	0.103	0.049	0.199
	8	0.053	1	0.254	0.070	0.043	0.317	2.240	0.081	0.168	0.120	0.074	0.184
	9	0.072	1	0.190	0.081	0.057	0.238	2.240	0.110	0.124	0.146	0.103	0.132
	10	0.086	1	0.190	0.088	0.069	0.238	2.240	0.134	0.122	0.164	0.128	0.128
	11	0.107	1	0.260	0.098	0.086	0.324	2.240	0.171	0.163	0.191	0.166	0.167
	12	0.138	1	0.375	0.113	0.110	0.469	2.240	0.227	0.227	0.231	0.226	0.228
	13	0.166	1	0.395	0.127	0.133	0.494	2.240	0.283	0.232	0.273	0.286	0.229
PHS10	3	0.009	1	0.188	0.016	0.007	0.236	2.056	0.011	0.150	0.023	0.010	0.160
	4	0.015	1	0.443	0.032	0.012	0.554	2.056	0.022	0.309	0.048	0.019	0.366
	5	0.017	1	0.186	0.040	0.014	0.233	2.056	0.027	0.117	0.062	0.021	0.151
	6	0.019	1	0.192	0.047	0.015	0.240	2.056	0.033	0.110	0.074	0.023	0.153
	7	0.020	1	0.131	0.053	0.016	0.163	2.056	0.037	0.070	0.084	0.026	0.102

Panel I.D.	LS	Δ^t_s	C_r	Δ^e_s/Δ^t_s	Δ_2	Δ^t_s	Δ^e_s/Δ^t_s	V_{co}	Δ^t_s	Δ^e_s/Δ^t_s	Δ_2	Δ^t_s	Δ^e_s/Δ^t_s
		Lai/Vec. - Model A			Lai/Vec. - Model B			Wallraven - Model B			Lai/Vec. - Model C		
	8	0.023	1	0.224	0.058	0.019	0.279	2.056	0.043	0.121	0.093	0.030	0.173
	9	0.027	1	0.153	0.063	—	—	2.056	0.031	0.134	0.103	—	—
	10	0.024	1	0.195	0.067	0.019	0.243	2.056	0.052	0.091	0.113	0.032	0.146
	11	0.038	1	0.241	0.073	0.030	0.301	2.056	0.066	0.138	0.124	0.052	0.177
	12	0.063	1	0.278	0.080	0.050	0.347	2.056	0.096	0.182	0.141	0.088	0.198
	13	0.084	1	0.260	0.090	0.067	0.325	2.056	0.129	0.169	0.165	0.123	0.178
	14	0.097	1	0.214	0.098	0.078	0.268	2.056	0.153	0.137	0.183	0.146	0.143
	15	0.118	1	0.262	0.107	0.094	0.327	2.056	0.187	0.165	0.207	0.183	0.169
	16	0.144	1	0.296	0.117	0.115	0.370	2.056	0.234	0.183	0.237	0.233	0.183
	17	0.203	1	0.321	0.146	0.162	0.402	2.056	0.350	0.186	0.323	0.360	0.181
PA1	4	0.011	1	-0.107	0.026	0.009	-0.133	1.996	0.016	-0.072	0.039	0.013	-0.090
	5	0.017	1	0.209	0.043	0.013	0.261	1.996	0.028	0.124	0.066	0.021	0.170
	6	0.020	1	0.131	0.052	0.016	0.164	1.996	0.036	0.073	0.082	0.026	0.104
	7	0.023	1	0.194	0.058	0.019	0.243	1.996	0.043	0.106	0.094	0.030	0.151
	8	0.025	1	0.379	0.067	0.020	0.474	1.996	0.051	0.186	0.110	0.033	0.287
	9	0.032	1	0.316	0.072	0.026	0.395	1.996	0.061	0.168	0.122	0.044	0.234
	10	0.054	1	0.284	0.078	0.043	0.354	1.996	0.084	0.182	0.134	0.074	0.206
	11	0.068	1	0.327	0.083	0.054	0.409	1.996	0.102	0.217	0.144	0.095	0.234
	12	0.079	1	0.314	0.088	0.063	0.393	1.996	0.119	0.208	0.156	0.112	0.220
	13	0.077	1	0.271	0.095	0.062	0.339	1.996	0.125	0.168	0.174	0.114	0.185
PA2	3	0.013	1	-0.001	0.042	0.010	-0.002	1.720	0.024	-0.001	0.062	0.015	-0.001
	4	0.017	1	0.274	0.051	0.013	0.342	1.720	0.031	0.148	0.077	0.020	0.225
	5	0.021	1	0.384	0.061	0.017	0.480	1.720	0.040	0.203	0.096	0.027	0.307
	6	0.026	1	0.527	0.071	0.021	0.659	1.720	0.050	0.269	0.114	0.033	0.409
	7	0.029	1	0.654	0.077	0.023	0.818	1.720	0.058	0.331	0.126	0.038	0.499
	8	0.056	1	0.495	0.083	0.044	0.619	1.720	0.084	0.327	0.140	0.074	0.369
	9	0.084	1	0.590	0.096	0.067	0.737	1.720	0.124	0.397	0.168	0.117	0.420
	10	0.092	1	0.595	0.108	0.073	0.744	1.720	0.146	0.374	0.198	0.134	0.406
SE1	1	0.002	1	0.214	0.005	0.002	0.268	1.700	0.003	0.176	0.007	0.003	0.190
	2	0.019	1	1.323	0.039	0.015	1.654	1.700	0.026	0.969	0.058	0.022	1.118
	3	0.027	1	2.364	0.063	0.022	2.955	1.700	0.045	1.433	0.099	0.034	1.884
	4	0.023	1	2.997	0.065	0.018	3.746	1.700	0.044	1.581	0.102	0.029	2.378
	5	0.060	1	1.927	0.089	0.048	2.408	1.700	0.092	1.250	0.151	0.081	1.415
	6	0.241	1	1.554	0.124	0.193	1.943	1.700	0.350	1.072	0.240	0.373	1.006
SE5	1	0.002	1	0.612	0.035	0.002	0.765	1.036	0.013	0.091	0.048	0.002	0.564
	2	0.004	1	0.954	0.059	0.003	1.192	1.036	0.024	0.163	0.082	0.005	0.848
	3	0.005	1	1.170	0.077	0.004	1.462	1.036	0.036	0.166	0.113	0.006	1.002
	4	0.008	1	1.394	0.158	0.007	1.742	1.036	0.130	0.089	0.287	0.012	0.956
SE6	1	0.004	1	0.175	0.008	0.003	0.219	1.600	0.005	0.147	0.012	0.005	0.156
	2	0.011	1	0.580	0.018	0.008	0.725	1.600	0.012	0.507	0.025	0.012	0.513
	3	0.018	1	0.818	0.023	0.014	1.023	1.600	0.020	0.736	0.033	0.021	0.718
	4	0.000	1	—	0.005	0.000	—	1.600	0.002	5.648	0.007	0.000	—
	5	0.024	1	1.130	0.033	0.019	1.413	1.600	0.028	0.982	0.048	0.028	0.976
	6	0.035	1	2.472	0.059	0.028	3.090	1.600	0.047	1.846	0.090	0.043	2.021
	7	0.032	1	3.997	0.070	0.025	4.996	1.600	0.051	2.472	0.110	0.040	3.171
	8	0.045	1	3.798	0.082	0.036	4.747	1.600	0.071	2.424	0.133	0.059	2.906
	9	0.067	1	3.789	0.100	0.053	4.736	1.600	0.107	2.373	0.173	0.093	2.728
	10	0.229	1	1.928	0.140	0.183	2.410	1.600	0.348	1.267	0.279	0.364	1.212